Spatial Formation Control

by

Iman Fadakar

A thesis
presented to the University of Waterloo
in fulfillment of the
thesis requirement for the degree of
Doctor of Philosophy
in
Mechanical and Mechatronics Engineering

Waterloo, Ontario, Canada, 2015

Author's Declaration

I hereby declare that I am the sole author of this thesis. This is a true copy of the thesis, including any required final revisions, as accepted by my examiners.

I understand that my thesis may be made electronically available to the public.

Abstract

In this thesis, we study robust spatial formation control from several aspects. First, we study robust adaptive attitude synchronization for a network of rigid body agents using various attitude error functions defined on SO(3). Our results are particularly useful for networks with large initial attitude difference. We devise an adaptive geometric approach to cope with situations where the inertia matrices are not available for measurement. We use the Frobenius norm as a measure for the difference between the actual values of inertia matrices and their estimated values, to construct the individual adaptive laws of the agents. Compared to the previous methods for synchronization on SO(3) such as those which are based on quaternions, our proposed approach does not contain any attitude representation ambiguity. As the final part of our studies from the attitude synchronization aspect, we analyze robustness to external disturbances and unmodeled dynamics, and propose a method to attenuate such effects. Simulation results illustrate the effectiveness of the proposed approach.

In the next part of the thesis, we study the distributed localization of the extremum point of unknown quadratic functions representing various physical or artificial signal potential fields. It is assumed that the value of such functions can be measured at each instant. Using high pass filtering of the measured signals, a linear parametric model is obtained for system identification. For design purposes, we add a consensus term to modify the identification subsystem. Next, we analyze the exponential convergence of the proposed estimation scheme using algebraic graph theory. In addition, we derive a distributed identifiability condition and use it for the construction of distributed extremum seeking control laws. In particular, we show that for a network of connected agents, if each agent contains a portion of the dithering signals, it is still possible to drive the system states to the extremum point provided that the distributed identifiability condition is satisfied.

In the final part of this research, several robust control problems for general linear time invariant multi-agent systems are studied. We consider the robust consensus problem in the presence of unknown Lipschitz nonlinearities and polytopic uncertainties in the model of each agent. Next, this problem is solved in the presence of external disturbances. A set of control laws is proposed for the network to attain the consensus task and under the zero initial condition, achieves the desired H-infinity performance. We show that by implementing the modified versions of these control laws, it is possible to perform two-time scales formation control.

Acknowledgments

I would like to express my deep appreciation to my supervisors, Prof. Jan Huissoon and Prof. Baris Fidan, for their valuable guidance, patience, support and constant encouragement during my research.

I also wish to thank my committee members, Prof. John McPhee, Prof. Howard Li, Prof. Amir Khajepour, Prof. Steven Waslander, for reviewing and improving my thesis.

I also want to thank my friends, Saeid Khosravani and Ehsan Hashemi for all their support and encouragement during my studies at University of Waterloo.

Dedication

To my mother and father.

Table of Contents

List of Figures

List of Abbreviations

ES	Extremum seeking
HJB	Hamilton-Jacobi-Bellman
LMI	Linear matrix inequality
LQG	Linear quadratic Gaussian
LQR	Linear quadratic regulator
LTI	Linear time invariant
MAS	Multi agent system
NES	Newton based extremum seeking
PE	Persistence of excitation
PID	Proportional-integral-derivative
RDE	Riccati difference equation
RHC	Receding horizon control
SAR	Synthetic aperture radars
SDP	Semi definite programming
SO(3)	Special orthogonal group
SLAM	Simultaneous localization and mapping
UAV	Unmanned aerial vehicle

List of Symbols

$A(\rho), B, B_1, C$	Constant matrices of the general linear dynamics
a_{ij}	Entries of the adjacency matrix
$D_i(\cdot)$	Measured signal of each agent
E_j	j^{th} error vector of the network
e_i	error vector of the i^{th} agent
e_R	Attitude error vector
$F(\cdot)$	Function of the field
H	Hessian matrix of the field
$\hat{I}_i, \hat{J}_i$	Estimation of the inertia matrix
$\tilde{I}_i, \tilde{J}_i$	Estimation errors
I_i, J_i	Inertia matrix
k_2, K	Consensus gain matrices
L	Laplacian matrix of the network
$\bar{M}$	Upper bound of the 2-norm of the inertia matrix
$\underline{M}$	Lower bound of the 2-norm of the inertia matrix
$M_i(\cdot)$	Inertia matrix for the i^{th} Lagrangian agent
n_i	Normal vector to the trajectories of the i^{th} agent

R	Average of the positions of the agents in the network
R_i	Rotation matrix of the i^{th} agent
r_i	Location of the i^{th} vehicle
$S_i(t), M_i(t)$	Vectors of the dithering signals
t_i	Tangent vector to the trajectories of the i^{th} agent
u_c	Steering law for the chaser agent
u_i	Input of the i^{th} agent
u_k, M	Input moment
v_j	j^{th} eigenvector of the the Laplacian matrix
x_i	State of the i^{th} agent
Z	Stack vector of the performance variables
z_i	Performance variable of the i^{th} agent
γ	H_∞ performance
δ_i	Disturbance vector which is affecting the i^{th} agent
ϵ	Scaling parameter
$\tilde{\theta}, \tilde{\eta}$	Estimation error vectors
$\hat{\theta}, \hat{\eta}$	Estimation of the agents
θ^*	Location of the extremum
θ	State of the sensor agent
θ_i	Heading angle of the i^{th} vehicle
$\lambda_{min}(A)$	Minimum eigenvalue of the matrix A
$\lambda_{max}(A)$	Maximum eigenvalue of the matrix A
λ_i	i^{th} eigenvalue of the Laplacian matrix
Ξ	Stack vector of the unknown parameters of the field

ξ_i	State of the i^{th} agent high pass filter
ρ^*	Location of the source
ρ	Stack vector of uncertainties
σ_{si}	Switching parameter for the i^{th} agent
Φ	Stack vector of the measured signals of the linear parametric model
Ω_d, ω_r	Desired angular velocity
Ω_i^r	Angular velocity error vector
ω_i	Disturbance which is affecting the i^{th} agent
$[A]^\wedge, \overset{\triangle}{A}$	Hat map
$[\cdot]^\vee$	Vee map
$\otimes$	Kronecker product
$\|\cdot\|_F$	Frobenius norm
$\dot{\tilde{V}}$	Generalized derivative of the V
$[A]^+$	Pseudoinverse of the matrix A
$grad(f)$	Gradient of the function $f(\cdot)$
SYM(A)	Symmetric part of the matrix A
$tr(A)$	Trace of the matrix A

Chapter 1

Introduction

Over the past decade, analyzing multi agent systems (MASs) has been one of the centers of interest in control and optimization theory. The main reason for this growing popularity can be attributed to the various practical applications of MASs, e.g. formation control of aerial vehicles, attitude synchronization of multiple satellites, distributed resource allocation and identification, distributed power management, etc. From a practical standpoint, controlling an MAS can be a challenging task due to the difficulties for controlling each individual agent, being augmented with the complexities arising from the communication between agents in the network such as packet loss and different network connection protocols. From a theoretical point of view, for designing and analyzing a distributed control law for an MAS, several theories ranging from control and optimization to algebraic graph theory are used in a unified framework to model the individual agents and their connections.

In general, MASs can be designed to be robust to the failure of one or a group of agents. This provides the MASs with extra flexibility to perform a particular task using less time

and resources. For example, in [2], it is shown that if two aircraft maintain a particular relative distance with respect to each other during a transportation mission, the magnitude of the drag forces on the follower aircraft will be reduced up to 15-20%. The followers must be located in the wake of the tip vortices of the lead aircraft. The reason for such a significant reduction lies in aerodynamic theory, where it can be shown that the aforementioned tip vortices act as "turbulators" and delay the separation of the flow from the aerodynamic surfaces of the follower agents.

Among the many problems which have been considered in the field of MASs, the consensus and synchronization tasks have received particular attention due to the fact that many of the practical problems in MASs can be converted to these tasks using appropriate transformations. For instance, by defining some offsets, the formation control problem can be interpreted as a consensus problem. The rendezvous problem can also be solved using zero offsets. In these problems, the individual robot control laws are typically derived by calculating the gradient of a particular potential function which measures the amount of 'disagreement' in the robotic network. The main structure of the corresponding consensus laws is directly related to the relative positions of the agents and the average locations of the neighboring agents. At each time step, these average positions act as desired positions for the agents. However, it is not always possible to treat the consensus problem with this methodology. One example is the attitude synchronization problem, where the intrinsic nature of $SO(3)$, which is the set of all possible rotations in $\mathbb{R}^3$, does not permit us to construct a continuous feedback control law that globally stabilizes the attitude of a rigid body on it. In order to cope with such difficulties, several methods have been proposed, such as using quaternions as coordinate charts on $SO(3)$ for representing the attitude of a rigid body and some geometric approaches.

Both the quaternion based and geometric approaches have their own capabilities and weak-

nesses. For example, quaternions double cover the rotation manifold of a rigid body, and hence they cause ambiguities in representation of the attitude of a rigid body, but they are easy to work with. Geometric methods, on the other hand, give more insight about the nature of the system and enable us to follow a systematic control design. Also, for quaternions, usually metrics for calculating the attitude differences between the agents are not optimal in the sense that they usually measure extra or less error since there is not any injective map between the elements of $SO(3)$ and quaternions. In the geometric control methods, by choosing an appropriate error function on the configuration manifold of the system, the error vectors and corresponding control laws are constructed. Following this procedure, the control laws become independent of any charts, and for implementation one can use both Euler angles and quaternions.

In the third chapter of this thesis, we consider the attitude synchronization problem for multiple agents that is studied in [3], [4], [5] using an appropriate error function which measures the amount of "disagreement" between the attitudes of the agents. This task has many applications in astronomy and defense systems. For example, the problem of imaging using multiple synthetic aperture radars (SAR) can be expressed as the attitude synchronization problem. Another practical application of the attitude synchronization problem is satellite formation control for on-orbit assembly tasks or interferometry missions.

In order to achieve the consensus task among multiple mechanical agents, the information of agents' inertial properties is required. However, in many practical situations the exact values of these properties might not be available or be time-varying. In this regard, chapter 3 can be divided in to two parts. In sections 3.2.3-3.3.5, the main goal is to design a set of adaptive control laws, one for each agent, that synchronize agents' attitudes and steer their angular velocities to a common desired value. It is clear that this problem in its very nature can be expressed as a consensus problem. The main difference between this prob-

lem and previous synchronization problems is the fact that the attitude synchronization problem is required to be solved on a general nonlinear manifold instead of a vector space and hence the control laws must be defined in a way that could take such a difference into account [6],[7].

In section 3.4.2, we consider the attitude control problem in the presence of time-varying input dependent inertias. A geometric framework is used to solve this problem.

In chapter 4 we study the distributed extremum seeking task. This problem has been studied extensively in the adaptive control literature due to its vast applications for automatic tuning of various electrical and mechanical components. Compared to classical adaptive control problems where the desired objectives, i.e. set points, tracking paths, etc. are known a priori, in an extremum seeking task, the control goals are not directly available. However, it is assumed that partial information regarding the objectives is available through measurements. The exact values of the objectives, e.g. set points, must be computed via online filtering of the received signals.

It is widely known that the main condition for successful adaptive identification is sufficient information richness of the input of the identification model. If the objectives of the control task are known and fixed, it can be shown that, in order to fulfill the regulation or tracking control problem, it is not necessary to satisfy the persistence of excitation(PE) at all times. In other words, successful identification of the parameters of the model is not compulsory for obtaining the control goals. In extremum seeking problems, the input of the system must be designed in a way that the PE condition will be satisfied during the control period. This requirement violates the control objectives such as regulation. However, in many practical situations, it is possible to add several small dithering signals to the inputs of the models to assure that the PE condition is satisfied and at the same time the final deviation from the control objective is restricted to a small neighborhood of

the regulation point.

The objectives which are discussed in chapter 4 can be divided into Localization and Extremum Seeking tasks. For the distributed localization problem, we added a consensus term to the identification dynamics of individual agents to enhance the identifiability of the network. Further, we study the convergence behavior of the proposed method. Next, we design a two time scales identification scheme where on the fast time scale the agents reach consensus about the estimated values of the unknown target and on the slow time scale the network as a whole converges to the actual values of the parameters.

In MASs, uncertainties and external disturbances can affect both the agents' dynamics and their information exchange process. For example, the communication links between the agents can be constructed or deleted based on the relative distance of the agents. Also, wireless communication devices can be subject to packet dropping and data loss issues. In the first part of chapter 5, we consider the effects of polytopic uncertainties on the agents' dynamics and design a set of control laws to achieve the consensus task. In the second part of this chapter, an H_∞ consensus problem is considered in the presence of polytopic uncertainties and unknown Lipschitz nonlinearities. Finally, we study the two time scales formation control problem which is a direct consequence of the robustness results.

1.1 Summary of the Main Contributions

- In chapter 3, we designed a set of novel coordinate independent adaptive control laws to synchronize the attitudes of multiple rigid body agents with connected communication topology. The convergence analysis of the proposed control laws is further extended to the case which the dynamics of each agent is affected by bounded disturbance torques. An adaptive σ-modification technique is used to increase the

robustness of the control laws.

- In chapter 4, a novel distributed adaptive source localization algorithm is designed based on the results of [1]. A collective condition for ensuring the exponential convergence of the estimation system is obtained and it is used in the context of localization problems to find a distributed identifiability condition for the extremum seeking problem. We showed that for a network of connected agents, if each agent contains a portion of the dithering signals, it is still possible to drive the system states to the extremum point, provided that the distributed identifiability condition is satisfied.

- In chapter 5, the robust consensus problem for a network of agents with general linear dynamics is considered where it is assumed that the uncertainties inside the structure of the linear model belong to a set of known polytopes. Using this additional information, a novel H_∞ consensus controller is designed to fulfill the objective of the robust consensus task.

Chapter 2

Literature Review

Studying the behavior of MASs is inspired by the motions of groups of animals in nature. Examples of such behavior are the movement of flocks of birds and migration of a school of fish. In [8] three simple laws are proposed to model the flocking behavior of a group of mobile agents in three dimensions. These laws include: "Flock Centering" which can be described as the tendency of individual agents to remain close to nearby flock mates, "Obstacle Avoidance" which can characterize how the agents move within the flock such that they avoid collision between themselves. The third law is "Velocity Matching" which describes the intention of nearby agents to match their respective velocity vectors. In [9] a mathematical model for a "Velocity Matching" law is proposed in the context of studying the phase transition for systems which consist of several self-driven agents with constant speed. It is assumed that at each time step, agents move in the average direction of the motion of their respective neighbors added with a zero mean noise. The collective behavior of agents and phase transition is studied for different numbers of agents and noise. The "Escape Panic" behavior in a group of humans who are trapped within a closed area with

few exits can also be modeled using similar methods described in [8]. This is done in [10] where in addition to modeling, several optimal strategies are proposed to avoid the perilous movement of a group of trapped human beings. In [11] several potential functions are proposed to build a flocking control law which can subsume the previous three laws.

The consensus problem for a network of single integrators is first considered in the seminal paper [12] by Olfati-Saber and Murray. This problem has received a great deal of attention during the past decade due to the fact that many tasks in the field of MASs such as attitude synchronization and flocking can be converted to his problem. The communication graph of the network is assumed to be directed and for the case of a balanced graph [1] a simple set of linear control laws is proposed to achieve the consensus task. Using several tools from algebraic graph theory and matrix analysis, the properties of the communication graph of the network are embedded in to a single Laplacian matrix. Also, several conclusions regarding the convergence properties of the control algorithms are obtained through analysis of the spectral properties of the Laplacian matrix based on the Gershgorin circle theorem [13]. It is shown that the convergence rate of the consensus algorithm is directly related to the second smallest eigenvalue of the Laplacian matrix, i.e. $\lambda_2(L)$. Furthermore, the stability of the control algorithms is investigated in the presence of switching topology and time-delays in the communication channels. It is proved that there exists a trade-off between robustness of the network with respect to time-delays and the performance of the consensus task.

Optimizing the convergence properties of the consensus problem is crucial for achieving better performance in MASs. In [14], the problem of finding the fastest averaging consensus algorithm is considered for undirected graphs. The authors transformed this problem to the task of finding the solution for a semidefinite program which can be solved effi-

[1] Graphs for which the number of in-degree and out-degree of each vertex in the graph are equal

ciently using existing algorithms [14]. First, they defined two convergence criteria for the consensus problem where the first is related to the asymptotic convergence for a large number of time steps. The second is based on the amount of convergence at each time step. It has been shown that these two problems can be cast as spectral radius and norm minimization, respectively. In [15], the problem of maximizing the $\lambda_2(L)$ for the Laplacian matrix of weighted undirected graphs is studied in detail. It is assumed that the weight of each edge in the graph is a function of the relative distance between the vertices which are located at both ends of the edge. Several functions are used to model the signals which are received at vertices in the communication graph and a modified SDP[2]-based method is used to solve the problem.

The conditions for asymptotic consensus which are presented in [12] are further relaxed in [16] where it is proved that if the union of the communication graph of the network over specific periods contains a spanning tree, then the asymptotic consensus can be achieved. The authors also proved that for a nonnegative matrix where its row sums are positive and equal to each other, the value of the row sum is an eigenvalue of the matrix which corresponds to the consensus eigenvector. This result is then directly used to prove the stability of the proposed consensus algorithm. In [17], the consensus problem over random Erdos Renye graphs [3] is considered. The asymptotic convergence of the stochastic consensus problem is studied using the notion of stochastic stability [18]. Interestingly, it is found that unlike the deterministic case where a union of the network communication graph is required to be connected over a specific period of time, in the probabilistic case, the random graph implicitly contains such a connectivity feature. Another example of the consensus problem for random graphs is investigated in [19] where the random graph is

[2]Semi Definite Program

[3]In Erdos Renye graphs, the probability of a link existing between any pair of vertices is equal to a pre specified value.

generated through a process called "Random Rewiring" of the edges of the initial graph. For this specific type of random graph, it is found that while it is possible to dramatically increase the $\lambda_2(L)$ of the Laplacian matrix of the network using rewiring, the $\lambda_{max}(L)$ of the graph will not change significantly and hence, the robustness of the network to the time delays will not be affected.

In [20], the problem of finding the optimal control laws for the consensus task has been discussed. In the first step of design, the authors assumed that the network topology is a complete graph. After obtaining the classical LQR[4] solution for such a graph, only the control gains associated with the edges in the initial communication graph will be applied to the agents. The asymptotic convergence of this method is studied for the case of finite strings and lattice graphs. Also, the effects of increasing the local and cooperation gains are investigated in depth through simulations. In [21], it is mathematically proved that to solve the global optimal consensus problem for a MAS, full knowledge of the agents is required. The authors further proved that for any valid Laplacian matrix, there exists an optimal performance index which can be associated with the network topology. In [22] a receding horizon control strategy for MASs is suggested where each agent tries to optimize its own local objective function. These local costs will be designed in a way that the MAS collectively attains a common objective. The authors made the assumption that each agent, prior to updating its own state, sends and receives the information regarding the most recent calculated optimal path with the neighboring agents in a synchronous fashion. The stability of the proposed algorithm is then studied based on two requirements which are related to the speed of the receding horizon updates and the deviation of the calculated optimal trajectory which is obtained from the processor of each agents and the received trajectory from the neighboring agents. In [23], a semi-decentralized optimal control ap-

[4]Linear Quadratic Control

proach is proposed for the minimization of the local costs in MASs. The authors provided a modified Hamilton-Jacobi-Bellman (HJB) for MASs which incorporates the concept of multi-level control. The control law for each agent is partitioned into local and global parts. The global part defines the relation between the control law of each agent and the information which is received from the neighboring agents. This part is modeled with a simple linear combination of the neighbors' states. Using such simplification, a solution to the HJB equation is obtained. In addition to control design, the robustness of the proposed methods is also studied in the presence of faulty agents inside the network. In [24], a game theoretic approach is suggested for the consensus problem where the communication constraints between agents are modeled as Linear Matrix Inequalities (LMIs). Additional convex constraints are also added to enhance the stability of the method. The RHC consensus task for multiple general linear dynamics is analyzed in [25] where several sufficient conditions are provided for the LTI[5] dynamics, based on the Riccati Difference Equation (RDE). Compared to the results of [22], the proposed algorithm only requires each agent at each time step to receive the neighbors' current states. A distributed optimal control strategy is designed in [26] for the MASs with directed communication topologies. For the special case where the Laplacian matrix of the network has a diagonal Jordan form, it is shown that the global distributed optimal control problem always has a feasible solution. In [27], the constrained optimal consensus problem for time varying net work communication graphs is considered. To solve the constrained problem, the gradient of the disagreement function in [12] is projected onto the set of the constraints for each agents. The authors further studied the relation between their proposed method and the alternating projection method with adaptive weights.

In [28], the controllability problem for the leader-follower MASs is studied. The leaders'

[5]Linear Time Invariant

inputs were regarded as the main inputs of the dynamical system which consists of all agents' dynamics. The case of the line graph is considered as the benchmark example. It is also shown that enhancing the connectivity of the network communication graph does not necessarily lead to controllability of the system. These results are further extended to more general cases using a graph theoretic perspective in [29]. It is proved that if none of the eigenvectors of the Laplacian matrix has a zero component then the controllability of the network does not depend on the choice of leader. The authors also investigated the relation between the symmetries in network topology and controllability using the notion of leader symmetry. They proved that if the network is leader symmetric then it is uncontrollable. For the case of multiple leaders, a necessary condition is derived based on the equitable partitions of the topology of the network.

In [30], the formation control problem for multiple autonomous vehicles is discussed using the double integrator model for agents. The authors used distance based structural potential functions to define the cost of formation. These functions are built based on the physical distance between the vertices of a rigid graph. The classical Hamiltonian mechanics theory is then used to derive the equations of motion and control laws. In addition, it is shown that if the initial velocities of agents belong to a particular set, then the collision avoidance between the agents is guaranteed. Finally, sigmoid functions are utilized to propose bounded control laws for agents. The flocking problem with partially available information is formulated in [11]. Three types of agents are defined to model leaders, followers and obstacles in the workspace. A formation potential function is designed which acts as a repulsive function at close distance and attractive at long range. The gradients of such functions are then used to construct the control laws. In the proximity of the obstacles, each agent projects its velocity and positions on the nearby obstacles to find the states of imaginary agents which are considered on the surface of the obstacles. The states

of these fictitious agents are then used inside the potential functions to find the control law which guarantees collision avoidance. Using such a framework, the compression and fragmentation of a network of vehicles are shown with the help of simulations. In [31], the behavior which is observed in [9] is mathematically proved using the properties of stochastic matrices.

The algebraic graph theory is used in [32] to model the formation control problem on undirected graphs. A Nyquist test is provided based on the spectral properties of the Laplacian matrix to analyze the stability and robustness of the network. The authors used general LTI dynamics to model the autonomous vehicles. In [33], the leader to formation stability concept is presented. This idea closely resembles the notion of input to state stability [34]. The authors used tree graphs to model the topology of the network and used the properties of class-$\mathcal{K}$ functions to compute the L_2 gain of the formation. Further, they generalized the results to nonholonomic vehicles using the bearing and distance measurements. Finally, the formation gains for different graph architectures are obtained and it is concluded that the parallel graph structure offers more stable and robust formation. In [35], a vision based formation control law is proposed for nonholonomic vehicles. For obtaining the experimental results, each agent is equipped with an omnidirectional camera and various formation strategies are tested in the presence of obstacles in the the robots' workspace. The idea of using virtual leaders as a tool for steering a swarm of holonomic vehicles is studied in [36]. Beside proving the asymptotic stability of the formation control laws, the authors investigated the robustness of the network to loss of one or more agents for fulfilling the formation task.

The problem of attaining formation for the case in which the states of the leader are only partially available to some of the followers is considered in [37]. A Lyapunov function which contains the costs of estimation and formation is used to analyze the convergence of

the algorithm. With the help of Young's inequality, the lower bounds for formation control and observer gains were obtained and it is shown that they are related to the spectral properties of the Laplacian matrix of the network.

In [38], the formation control of nonholonomic vehicles is studied using the Lie group setting. Using a coordinate independent representation of agents' kinematics, it is shown that for the case of fixed forward velocity, there exist two equilibrium points which are related to flocking and cyclic pursuit. This idea is further extended to three dimensions using the notion of natural Frenet frames. Compared to the two dimensional case, it is founded that the agents can also perform the helical formation. The stability analysis is performed for the formation of two vehicles. In [39], the cyclic pursuit problem for $n \geq 2$ number of agents is studied in detail. The authors used the definition of circulant matrices to represent the relative agents' dynamics. The stability analysis is done using the linearization method. In [40], several necessary and sufficient conditions for the formation control of nonholonomic vehicles is presented. It is shown that the rendezvous problem is solvable if and only if the network communication graph contains a globally reachable agent. Next, it is proved that such condition can be satisfied if the Laplacian matrix has the zero as its simple eigenvalue. Furthermore, the line formation is considered and it is verified that such a formation is attainable if and only if the network topology contains at most two disjoint and closed sets of agents. The rendezvous problem is further investigated in [41] for multiple unicycles using several tools from nonsmooth analysis theory. The authors devised a set of control laws which guarantee the connectivity maintenance of the network for completion of the rendezvous task.

In [42], the distributed optimal formation control problem is considered using the dual decomposition methods. The upper bound of the duality gap between the primal and dual problem is also computed. The authors extended their results to the case of agent with

nonlinear dynamics. The nonlinear model predictive control is used in [43] to solve the optimal formation tracking problem for multiple nonholonomic vehicles. The optimization problem is solved based on a splitting method which has the capability to be used for real time implementation. In [44], a sequential linear programming method is proposed to solve the formation control problem with guaranteed collision avoidance. The latter is achieved via convexification of the collision constraints where each agent tries to find the optimal trajectory within a convex polygon which is built using the position of its neighbors.

In [45] a formation control law is designed using a PDE-based approach. The discretized linear reaction-advection PDE is used to find the control laws of agents. The stability of several formation profiles are studied using a modified Lyapunov functional.

A formation control methodology is suggested in [46] that ensures the formation stability of the network in addition to tracking the desired path. The authors used the notion of graph rigidity and relative distance measurements to design the formation control laws. In [47], the authors have proposed a decomposition method to separate the dynamics of formation shape from the general maneuvers of the swarm. The formation shape is defined based on the relative position vectors of the neighbors of each agent. Using such an approach, an energy based framework is developed for the purpose of control design. In [48], this idea is further extended to the flocking problem on balanced graphs. It is shown that for the case of inertial agents a poor choice of formation control gains can cause unstable behaviors which can be aggravated in the presence of cycles in the communication graph of the network. In [49], the previous idea is used for a network of quadrotors. The motion constraints of these robots greatly increase the complexity of the control design procedure. The authors used a constructive method based on energy-like Lyapunov functions. Furthermore, a formation tracking control law is introduced to ensure that the center of mass of the swarm will track the desired path in a stable fashion. A set of control laws are suggested in [50] for time

scale separation of the formation objectives. In this approach, the swarm first reaches the formation shape in the fast time scale while its center of mass tracks the predefined path on the slow time scale. The latter is particularly useful for situations in which the agents should protect a high valued moving target. Singular perturbation theory is then utilized to tune the speed of each subsystem. The collision avoidance between the agents is also guaranteed through a similar approach as in [51]. In [52], the formation control on SE(3) is considered for rigid graphs. It is mentioned that the quadratic function which is built based on the difference between the relative distance of the neighboring agents and their respective desired values, has undesired equilibrium points which are stable. In order to solve this issue, the authors proposed a quadratic majorization technique to convexify the main potential function. It is shown that this function only poses the formation shape as its equilibrium point. Furthermore, the formation control problem is formulated using a set of linear equations. The solution to this problem is obtained using a modified distributed Jacobi method. The robustness of the network to communication failure and external noise is also studied. In [53], a distributed model predictive control is developed for the formation task using online alternating direction of multipliers. The information exchange between agents is modeled using a set of constraints. The proposed algorithm is implemented on different graph topologies.

In [54], the coverage control problem for a network of holonomic and nonholonomic vehicles is considered. A cost function is introduced to measure the optimality of the locations of the agents in a domain in which the distribution of an event can be measured locally using the attached sensors. Using the authors proposed method, each agent move toward the centroid of the Voronoi cells which are built based on the locations of the near-by agents. A modified Voronoi tessellation is used in [55] to solve the coverage control task in the presence of pre-specified constraints on the amount of area which each agent can observe

during the execution of the task. This algorithm is particularly useful for the case of a heterogeneous network where many types of agents with different capabilities are used to fulfill the mission.

In [56], the spacecraft formation control is considered for high inclination orbits. A two points boundary value problem is generated from the Hamilton-Jacobi optimality conditions. Using the expansion of the Hamiltonian of the network in terms of known functions, the previous problem is solved. The authors used the famous Clohessy-Wiltshire equations of motion to represent relative spacecrafts' dynamics. The formation flying problem for multiple telescopes around the L_2 liberation point of earth-sun system is presented in [57]. It is reported that at such points, less interference from the astronomical objects will affect the data acquisition systems. In [58], the formation control along elliptic orbits is considered and a modified version of Tschaunor-Hempd is used to represent the relative dynamics. A formation keeping methodology is proposed in [59] for a network of satellites which are subjected to J_2 perturbation effects. The authors further studied the effect of drag forces which result from the movement of the swarm in low earth orbits on the formation performance. Several impulsive control strategies are proposed to reject the aforementioned disturbances.

In [60], the Extremum Seeking(ES) problem for general nonlinear dynamics is studied in detail. Using several convexity assumptions on the profile of the reference to out-put map, the exponential stability of the averaged system is proved via linearization. The main idea of this paper is to add multiple harmonic signals (associated with the number of unknowns) at the input of the nonlinear system. The gradient of the unknown map is then extracted using a combination of high and low pass filters. With the help of this method, the dynamical system on the fast time scale "Oscillates" to extract information and on the slow time scale steers itself toward the optimum location. Using the Tikhonov theorem [34], the

stability of the whole system is concluded from the exponential convergence of the averaged system. In [61], an ES method is proposed which besides obtaining the gradient of the unknown map, has the capability to estimate higher order derivatives of the measurement field. In [62], the previous idea is utilized to design a Newton-based Extremum seeking (NES) approach. In this framework, the harmonic signals which are used to estimate the gradient of the measurement field are multiplied with out-put measurements and passed through a set of integrators to obtain the components of the Hessian matrix of the field. Since the calculation of such a matrix might produce singularities, additional filtering is used to ensure well-posedness of the resulting signals. The authors further demonstrated through several simulations that compared to gradient based ES methods, the convergence rate of the online optimization problem can be greatly improved. In [63], the same authors presented the stochastic version of this algorithm. The performance of the ES task is heavily dependent on the choice of the perturbation signals which are added to the input of the dynamical systems.

It is shown in [64] that in addition to the frequencies and amplitudes of the dither signals, their shapes also play an important role in the convergence of the ES algorithm. The authors reported that for the special case of small oscillation, the best convergence speed between all the waves with similar frequency and amplitude belongs to square wave signals. In [63], the authors used the ES idea for the source seeking problem. The physical field which is caused by the source is modeled as a quadratic functions with unknown constants. It is assumed that the mobile robot can only measure the value of this field at its position. A nonholonomic vehicle model is used for the purpose of stability analysis. The perturbation signal is added to the forward velocity of the vehicle while its angular speed kept at constant value. It is shown that the robot can be steered locally to a neighborhood of the source position. The size of such neighborhood is inversely proportional to the magnitude

of the dither signals. The draw-back of this method comes from the fact that changing the forward velocity of a nonholonomic agent will produce nonsmooth trajectories. In [65], the dither signal is added to the angular velocity of a nonholonomic vehicle for the purpose of gradient extraction. Using this method, the mobile robot can follow a very smooth trajectory toward the source location. The authors made an assumption that the measurement sensor is located in front of the center of the vehicle. The logic behind this idea is to increase the range of movement of the sensor for acquiring information from a larger portion of the field of interest. Furthermore, the possibility of placing the measurement sensor at the center of vehicle is investigated, however, it is shown that such a placement requires the use of a derivative block in the demodulation part of the ES algorithm. In [66], the three dimensional source seeking problem is considered for fixed wing UAVs. Two ES demodulation loops are used for yaw and pitch steering. The authors proved that the robot will eventually rotate around the source point. The radius of such a circle is shown to be inversely proportional to to the distance of the measurement sensor to the center of vehicle. A distributed ES scheme is devised in [67] based on partial differential equations. The main goal of the proposed approach is to disperse the agents in a way that the swarm density will be higher around the source point. The authors assumed that the vehicles are capable of measuring their relative distance. In [68], the formation control problem is formulated as an ES problem. The authors treat the formation shape as the Nash equilibrium of the network and by adding dither signals to the forward velocities of the agents the formation objective is attained.

In [1], an adaptive source localization scheme is suggested which is robust to slow drifts of the source position. The authors assumed that the seeking robot can measure its distance to the target. Using a high pass filter a linear parameter model is obtained where the components of the source locations are treated as unknown coefficients. Based on classical

adaptive control theory, the robustness of the proposed algorithm is studied. In [69], the distributed localization and control is considered for a network of underwater vehicles. It is assumed that each agent shares its information regarding the profile of the field, with its neighbors. The control laws of the vehicles are then designed to ensure that the centroid of the swarm will move in the direction of the gradient of the estimated field. In [70], the distributed detectability condition for a network of observers is presented. Satisfaction of this condition plays a fundamental role in the convergence proof of distributed H_∞ and H_2 filters since both method use modified output injections in their structures. The authors considered the Simultaneous Localization and Mapping(SLAM) problem as a benchmark to present their framework. The results were also generalized to the graphs which cannot be spanned by a tree. In [71] a distributed H_∞ filter is devised using the vector Lyapunov functions. The observer gains were obtained as a solution of a set of LMI constraints. In order to solve theses LMIs distributively, a gradient based algorithm is used. In [72], a distributed Kalman filter is designed for the purpose of estimating the states of a linear time-varying system. The computational complexity of obtaining the local Kalman gains is also calculated. In [73], a distributed parameter identification problem is studied for a network of sensors. To prove the main convergence results, the authors expanded the measurement errors in terms of the eigenvectors of the Laplacian matrix of network.

The attitude control problem is considered in [74] using the unit quaternion representation of the attitude kinematics. Several attitude error vectors are constructed on SO(3) and used for the design of tracking control laws. The robustness of the proposed approach is then investigated with the help of input to state stability analysis. Furthermore, the results extended to the case where the inertia tensor is not available for tracking. In [75] the disturbance rejection properties of the previous result is studied in detail.

In some practical situations, the attitude control objective must be obtained while it is

guaranteed that the attitude of the robot will not enter to a pre specified set to protect the onboard sensors from direct exposure to radiations. In [29], the attitude control problem in the presence of convex attitude constraints is considered. To facilitate the convergence proofs, several barrier functions are used to take in to account the costs of the constraints inside the Lyapunov function which are used for stability analysis.

It is easy to show that the unit quaternions double cover the SO(3). This indicates that for each physical attitude, there exist two unit quaternions. The former can cause redundant motion of the rigid body. In [76] a switching quaternion representation is designed to solve these redundancy issues. The authors used a nonsmooth Lyapunov function to determine the switching position. The robustness of the proposed method with respect to small measurement noise is also analyzed and a hysteresis based approach is suggested to reject such disturbances.

Control of a Vertical Take off and Landing(VTOL) aircraft is a challenging task since the coupling between the rotational and translational dynamics are highly intricate and nonlinear. In [77], a multi level control structure is designed for position control of such aircraft. Using their approach, the VTOL aircraft in the fast time scale adjusts its orientation to generate the required translation control force. The stability analysis of the proposed method is performed using singular perturbation theory and it is determined explicitly that to what extent the attitude controller should be faster than the translational one. Tracking control of UAVs is also a challenging task. This is due to the fact that these robots are under actuated. In another words, they have less number of actuators than their degree of freedom. The translational and rotational dynamics of these robots are highly nonlinear and coupled. It is possible to use simple PID or LQG controllers for very simple maneuvers which do not involve large rotations, however, for ensuring the global stability of VTOL-UAVs the full nonlinear model must be taken into account in

the control design procedure which naturally leads to nonlinear feedback control laws [78]. Also, since these robots are generally have unstable zero dynamics the exact input-output linearization method cannot be used because such techniques require a minimum phase system [34]. However, the possibility of designing an approximate input-output linearization is studied in [79]. Another nonlinear control method which has been extensively used for controlling UAVs is Backstepping [80]. This is achieved by modeling the dynamics of UAVs as a cascade system using suitable change of coordinates. In this regard, quadrotors orientation and thrust is used as a control variable to stabilize the vehicle position and in the next step the attitude controller is designed using Lyapunov stability analysis. In [81], authors proposed a globally stable control law for VTOL-UAVs which is based on using quaternion representation for both attitude kinematics and dynamics. They have formulated two stages in the control problems. In the first part a globally stable control law is designed for the translational dynamics while treating the effects of the rotational part as a perturbation term. In the next step, the effects of the previous perturbation is eliminated with the help of additional term in the attitude control laws. Performing such a multistage design, requires smooth extraction of the attitude reference trajectory since the time derivative this signal will be used in the attitude control design for tracking problem. This is achieved with the algorithm which is first proposed in [82].

2.1 Contributions to Literature

The main contributions of this thesis, considering the relevant literature, as reviewed in this chapter, can be summarized as follows

2.1.1 Attitude Synchronization

In chapter 3, several robust adaptive attitude synchronization problems are studied for a network of rigid body agents. Compared to [83],[5],[4], a coordinate independent approach is used to obtain both the estimation and adaptive control laws from a single Lyapunov function. Next, we modified the attitude synchronization control laws using the optimal norm on SO(3) which is first introduced in [84]. The adaptive estimation law for each agent is designed locally in the sense that the estimation dynamic of each agent is independent of the estimation error of the neighboring agents. We further focused on the local adaptive control design for each agent and construct a set of adaptive laws which can ensure the convergence of the tracking error system for the cases in which the inertia tensors of agents are time varying.

2.1.2 Distributed Localization and Extremum Seeking

In chapter 4, we designed a distributed adaptive source localization algorithm based on the results of [1]. Compared to the adaptive attitude synchronization task, here the unknown parameters (coordinates of the source) are assumed to be global and therefore, the local adaptive estimation laws are built based on the states of each agents and its neighbors' estimators. We derived a collective condition for ensuring the exponential convergence of the estimation system. We later used the localization results including a distributed identifiability condition for the extremum seeking problem. In particular, we showed that for a network of connected agents, if each agent contains a portion of the dithering signals, it is still possible to drive the system states to the extremum point, provided that the distributed identifiability condition is satisfied.

2.1.3 Robust Formation Control

In chapter 5, we considered the robust consensus problem for a network of agents with general linear dynamics. Compared to [85], it is further assumed that the uncertainties inside the structure of the linear model belong to a set of known polytopes. Using this additional information, an H_∞ consensus controller is designed to achieve the robust consensus task.

Chapter 3

Attitude Synchronization

3.1 Preliminaries

3.1.1 Graph Theoretical Modeling of Rigid Body Networks

We use graph theory notions for representing the network topology of a group of rigid bodies. Here, we state the theorems and definitions in abridged form and refer to [86] for full versions of these theorems. We represent a network of m rigid body agents by a directed graph $G = (V, \varepsilon)$ of order m, which consists of a vertex set V of m elements and another set of edges, $\varepsilon \subset V \times V$. We index the elements of the vertex set with $\{1, ..., m\}$. A graph is called undirected if $(j, i) \in \varepsilon$ whenever $(i, j) \in \varepsilon$. A weighted graph is a triplet $D = (V, \varepsilon, A)$ where A stands for weighted adjacency matrix which has the following properties: for each i, j in the index set the entry $a_{ij} = a_{ji} = 1$ if $(i, j) \in \varepsilon$, and $a_{ij} = 0$ otherwise. Furthermore, we assume that $a_{ii} = 0$ for all vertices.

3.1.2 Rotation Group $SO(3)$

$SO(3)$ denotes the set of all orthogonal matrices in $\mathbb{R}^{3\times3}$ whose determinants are equal to 1. $so(3)$ denotes the Lie algebra of $SO(3)$ and is defined as follows:

$$so(3) = \left\{O \in \mathbb{R}^{3\times3} | O^T = -O\right\}$$

The mapping $[\cdot]^\wedge : \mathbb{R}^3 \to so(3)$ is called the *hat map* and is defined as

$$x = [x_1, x_2, x_3]^T \in \mathbb{R}^3, [x]^\wedge = \begin{bmatrix} 0 & -x_3 & x_2 \\ x_3 & 0 & -x_1 \\ -x_2 & x_1 & 0 \end{bmatrix} \tag{3.1}$$

Another useful map in this context is *vee map* $[\cdot]^\vee : so(3) \to \mathbb{R}^3$, which is the inverse of hat map. These maps have the following important characteristics [84]:

$$[a]^\wedge b = a \times b = -b \times a = -[b]^\wedge a \tag{3.2}$$

$$tr\left[Q[a]^\wedge\right] = \frac{1}{2} tr\left[[a]^\wedge \left(Q - Q^T\right)\right] = [a]^T \left(Q^T - Q\right)^\vee \tag{3.3}$$

for all $a, b \in \mathbb{R}^3$ and $Q \in \mathbb{R}^{3\times3}$.

Computing the gradient of a function on $SO(3)$ has a crucial importance in stability analysis since in the context of rigid body dynamics, the Lyapunov functions are usually defined on the general manifold of the system. It is shown in [87] that if $V(R) = tr\left[R^T A\right]$ where $A \in \mathbb{R}^{3\times3}$ and $R \in SO(3)$, then the gradient of V on $SO(3)$ satisfies

$$\nabla V_{SO(3)} = \frac{1}{2} R\left[R^T A - A^T R\right].$$

Due to discontinuities in some of the functions which will be defined in Section 3.3.1, we need to use the following generalized derivative notion in place of the regular derivative: Given a dynamical system $\dot{x} = f(x(t), t)$ and a function $V(x(t), t)$, the generalized

derivative of V is defined as [88]:

$$\dot{\tilde{V}}(x(t),t) = \bigcap_{\zeta \in \partial V(x(t),t)} \zeta^T \begin{pmatrix} K[f](x(t),t) \\ 1 \end{pmatrix},$$

∂V and $K[f]$ are expressed by

$$\partial V = co\left\{\lim \nabla V(x,t) | (\psi,\sigma) \to (x,t), (\psi,\sigma) \notin \chi\right\}$$
$$K[f](x) = co\left\{\lim f(\beta) | \beta \to x, \beta \notin \chi\right\}$$

where χ is the set of points where the gradient of V does not exist. Note that χ has a measure zero, and co represents convex closure.

3.1.3 Rigid Body Dynamics

The attitude of a general rigid body evolves on the nonlinear manifold $SO(3)$. This group represents the set of all possible rotations in $\mathbb{R}^{3\times3}$. Suppose that we have m rigid bodies whose rotation matrices with respect to an inertial frame are expressed by $R_k \in SO(3)$, $k \in \{1, ..., m\}$. Then, the equations of motion of each agent can be expressed as follows:

$$J_k \dot{\Omega}_k = [J_k \Omega_k]^\wedge \Omega_k + u_k \tag{3.4}$$
$$\dot{R}_k = R_k [\Omega_k]^\wedge \tag{3.5}$$

where $J_k = diag(J_{k1}, J_{k2}, J_{k3})$ denotes the inertia matrix of the k^{th} agent, and J_{k1}, J_{k2}, J_{k3} are principal moments of inertia, and without loss of generality we assume that $J_{k1} \leq J_{k2} \leq J_{k3}$. $u_k \in \mathbb{R}^3$ is the control input and $\Omega_k \in \mathbb{R}^3$ is the angular velocity vector of this agent. From (3.4) and (3.5), it is clear that these vectors are defined in body frame coordinates. The components of these vectors in inertial coordinate frame can be easily obtained by left multiplication of them by the rotation matrix. The model (3.4),(3.5) has been widely

used in control theory to represent the attitude dynamics of a fully actuated vehicle which can be modeled as a rigid body. A more accurate model can be obtained, for the vehicles operating in the presence of external fields (such as wind or water) by adding a damping term which is directly related to the angular velocity of the vehicle.

3.2 Problem Definition and Approach

3.2.1 Problems

The attitude synchronization problems we consider in this chapter can be formulated as follows.

Problem 3.1(Nominal Synchronization Problem) Consider a network of m rigid body agents (Fig. 3.1) whose dynamics are governed by (3.4),(3.5), Design a set of control laws that asymptotically synchronizes the attitudes of the agents in the network, i.e.

$$\Omega_1 = \Omega_2 = \cdots = \Omega_m = \Omega_d$$
$$R_1 = \cdots = R_m$$

where Ω_d is the reference angular velocity.

It should be noted that Ω_d is not a time-varying tracking signal. In fact, it is a constant signal which is for the ideal model of rigid bodies is equal to $\Omega_d = [0\ 0\ 1]^T$, The main purpose of this signal is to increase the stability of the rigid bodies at the synchronized state since from classical mechanics it is known that rotation around the axis with largest moment of inertia is a stable equilibrium of (3.4) and (3.5). Many spacecraft are working based on this technique to enhance the stability of their motion.

Problem 3.2 Consider *Problem 3.1*, but additionally assume that the values of inertia

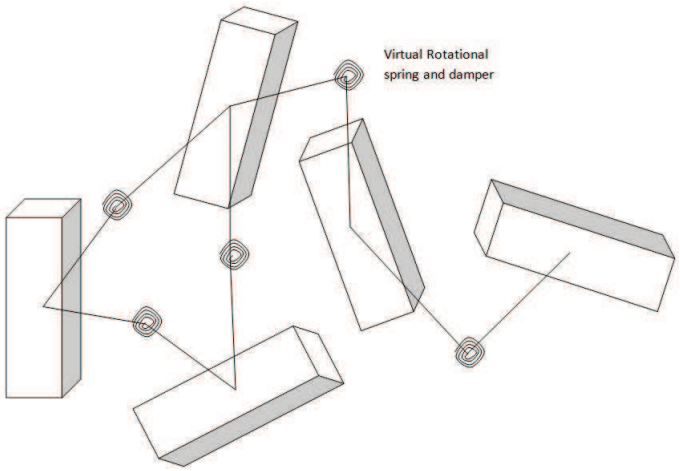

Figure 3.1: A typical rigid body network.

matrices J_k are not available for measurement. Perform task of *Problem 3.1.*

Problem 3.3 Consider *Problem 3.2* and suppose that there exist a bounded disturbance or unmodeled dynamics in the input channels, which is formulated by adding an uncertainty term δ_k to the right hand side of (3.4), each entry $\delta_{k,i}$ of which satisfies $\|\delta_{k,i}\| \leq \Delta_{k,i},\ i \in \{1, 2, 3\}$ for known positive upper bounds $\Delta_{k,i}$. Perform task of Problem 3.1,

We address Problems 3.1 3.2, and 3.3 in the following sections. Before that, first, we formulate the kinematic synchronization problem on a general manifold and analyze the main strategy which is used in this chapter to achieve the consensus task for dynamics agents from the kinematic controllers.

3.2.2 Kinematic Synchronization

In the context of MASs, the consensus problem for a network of agents has been studied in depth based on vector spaces and the relation between the stability properties of the system and the connectivity of the network was established during the past decade. The

main element of these algorithms is the Laplacian matrix of the graph of the network. This matrix has all the required information regarding the communication graph of the network for computing control laws for each agent. In order to extend these results from vector spaces to manifolds several methods have been proposed in [87] and [83]. The natural way to perform this generalization is to embed the configuration manifold of the system in $\mathbb{R}^d$ as in [87]. In order to formally define this algorithm, consider a general manifold $\mathcal{M}^n$ together with a function $f : \mathcal{M}^n \to \mathbb{R}$ which is defined as follows:

$$f = \eta \sum_{i=1}^{n} \sum_{j=1}^{n} a_{ij} tr\left[x_j^T x_k\right], \qquad \eta > 0 \tag{3.6}$$

where η is a positive constant and we assumed that $x_i \in \mathbb{R}^{n\times n}$ to facilitate the construction of this function on rotation manifold for the next sections. Next, consider the following algorithm [87]:

$$\dot{x}_i = -\beta \left[grad(f)\right]_{\mathcal{M},k}, \qquad k \in 1, \cdots, n \tag{3.7}$$

where $\beta > 0$ is a positive constant. The subscript $\mathcal{M}, k$ implies that this operation performed on the manifold $\mathcal{M}$ along trajectory of x_k. It is shown in [89] that, using this algorithm for the network of agents will result in asymptotic stability of the synchronization task, however, this algorithm will not guarantee that this convergence occurs in finite time. In order to assure that the finite time convergence, it is possible to use the nonsmooth algorithms which are proposed in [90].

In order to extend the results of kinematic synchronization to the dynamic case, we can use the backstepping method [34]. Consider a simple kinematic equation $\dot{x} = u$, which can be stabilized by $u = g(x)$. The latter suggests that there exists a Lyapunov function $f(\cdot) > 0$ which its time derivative is negative definite, i.e., $\nabla f \cdot g(x) < 0$. Next, consider

the following system:

$$\dot{x} = z$$
$$\dot{z} = u \tag{3.8}$$

In order to stabilize the previous system (3.8), consider the following Lyapunov function ($z^{'} = z - g(x)$):

$$V = f + \frac{1}{2}(z - g(x))^2 \tag{3.9}$$

The time derivative of the Lyapunov function (3.9) will be as follows:

$$\dot{V} = \frac{\partial f}{\partial x} z + (u - \frac{\partial g}{\partial x}) z^{'} \tag{3.10}$$

Then, by choosing the following input:

$$u = \frac{\partial g}{\partial x}\dot{x} - \frac{\partial f}{\partial x} - k z^{'} \tag{3.11}$$

The time derivative of (3.9) will become:

$$\dot{V} = \frac{\partial f}{\partial x} g(x) - k z^{'2} < 0 \tag{3.12}$$

which ensures the asymptotic stability of the (3.9). In the next section, we use this idea to propose a dynamic controller on $SO(3)$.

3.2.3 Adaptive Attitude Synchronization

The main goal of this section is to solve Problem 3.2 for a network of m agents. We will find a set of control inputs for the agents to synchronize their attitudes while having a synchronized velocity, Ω_d. In general, for stabilization problems, we do not need to

have the value of the agent's inertia matrix but for tracking purpose we need to have this information to design the control laws. In this section, we propose an adaptive control law for this problem based on the results of [87] as follows:

$$u_k = -\left[\hat{J}_k\Omega_k\right]^{\wedge}\Omega_k + \hat{J}_k\dot{F}_k + \mu\left(F_k - \Omega_k + \Omega_d\right) \tag{3.13}$$

where, $F_k = \alpha\sum_{j=1}^{m} a_{jk}\left[R_k^T R_j - R_j^T R_k\right]^{\vee}, k = 1, \cdots, m, \alpha \geq 0$. μ is a positive constant and $\hat{J}_k$ is the estimate of inertia matrix of the k^{th} agent and a_{jk} is the (j,k) element of the adjacency matrix. In order to design an adaptive law for obtaining $\hat{J}_k$, we consider the modified version of the Lyapunov function proposed in [87]:$(l > 0)$

$$\begin{aligned} V = &\frac{-1}{2}\sum_{k=1}^{m}\sum_{j=1}^{m} a_{jk} tr\left(R_k^T R_j\right) + \sum_{k=1}^{m}\frac{1}{2d_k}\left\|J_k - \hat{J}_k\right\|_F^2 \\ &+ \frac{l}{2}\sum_{k=1}^{m}\left(\Omega_k^r - F_k\right)^T J_k\left(\Omega_k^r - F_k\right), \end{aligned} \tag{3.14}$$

where $l, d_k, k \in \{1, \cdots, m\}$, are positive constants and $\Omega_k^r = \Omega_k - \Omega_d$. $\|\cdot\|_F$ denotes the Frobenius norm. In fact, the values of d_k are acting as tuning gains of the adaptation laws and can be changed to enhance the performance of the adaptation process. Next, we compute the time derivative of the Lyapunov function (3.14) as follows:

$$\begin{aligned} \dot{V} = &\frac{-1}{\alpha}\sum_{k=1}^{m} tr\left(-\left[F_k\right]^{\wedge}\left[\Omega_k\right]^{\wedge}\right) + \sum_{k=1}^{m}\frac{1}{d_k} tr\left[\tilde{J}_k\dot{\tilde{J}}_k\right] \\ &+ l\sum_{k=1}^{m}\left(\Omega_k^r - F_k\right)^T\left(J_k\dot{\Omega}_k^r - J_k\dot{F}_k\right) \end{aligned} \tag{3.15}$$

where $\tilde{J}_k = J_k - \hat{J}_k$. Using the fact that $tr\left(-\left[a\right]^{\wedge}\left[b\right]^{\wedge}\right) = 2a^T b$ for $a, b \in \mathbb{R}^3$ and the kinematic equations (3.4),(3.5), we have:

$$\begin{aligned} \dot{V} = &\frac{-2}{\alpha}\sum_{k=1}^{m} F_k^T\Omega_k + \sum_{k=1}^{m}\frac{1}{d_k} tr\left[\tilde{J}_k\dot{\tilde{J}}_k\right] \\ &+ l\sum_{k=1}^{m}\left(\Omega_k^r - F_k\right)^T\left(\left[J_k\Omega_k\right]^{\wedge}\Omega_k + u_k - J_k\dot{F}_k\right) \end{aligned} \tag{3.16}$$

Next, we put (3.13) into (3.16):

$$\begin{aligned}\dot{V} = &\frac{-2}{\alpha}\sum_{k=1}^{m} F_k^T \Omega_K + \sum_{k=1}^{m} \frac{1}{d_k} tr\left[\tilde{J}_k \dot{\tilde{J}}_k\right] \\ &+ l\sum_{k=1}^{m} \left(\Omega_k^r - F_k\right)^T \left([J_k\Omega_k]^\wedge \Omega_k - \left[\hat{J}_k\Omega_k\right]^\wedge \Omega_k + \hat{J}_k\dot{F}_k\right. \\ &\left. + \mu\left(F_k - \Omega_k + \Omega_d\right) - J_k\dot{F}_k\right) \end{aligned} \tag{3.17}$$

Here, we can see the main rationale for using the Frobenius norm in the structure of the Lyapunov function (3.14). This particular norm enables us to design adaptation laws for each agent by combining the second and third term in (3.17). We rearrange (3.17) as follows:

$$\begin{aligned}\dot{V} = &l\sum_{k=1}^{m} \left(\Omega_k^r - F_k\right)^T \left(\left[\tilde{J}_k\Omega_k\right]^\wedge \Omega_k + \mu(F_k - \Omega_k + \Omega_d)\right. \\ &\left. - \tilde{J}_k\dot{F}_k\right) + \frac{-2}{\alpha}\sum_{k=1}^{m} F_k^T\Omega_k + \sum_{k=1}^{m}\frac{1}{d_k} tr\left[\tilde{J}_k\dot{\tilde{J}}_k\right] \end{aligned} \tag{3.18}$$

Next, using the identities $a \cdot b = tr(ab^T)$ and $a \cdot (b \times c) = b \cdot (c \times a) = c \cdot (a \times b)$, for $a, b, c \in \mathbb{R}^3$, we have

$$\begin{aligned}\dot{V} = &l\mu\sum_{k=1}^{m}(\Omega_k^r - F_k)^T(F_k - \Omega_k + \Omega_d) \\ &\sum_{k=1}^{m} tr\left[\tilde{J}_k\left(\frac{1}{d_k}\dot{\tilde{J}}_k - \dot{F}_k(\Omega_k^r - F_k)^T - \Omega_k((\Omega_k^r - F_k)\times\Omega_k)^T\right)\right] \\ &\frac{-2}{\alpha}\sum_{k=1}^{m} F_k^T\Omega_k \end{aligned} \tag{3.19}$$

Choosing the adaptation laws as:

$$\dot{\tilde{J}}_k = d_k\left[\dot{F}_k(\Omega_k^r - F_k)^T + \Omega_k((\Omega_k^r - F_k)\times\Omega_k)^T\right] \tag{3.20}$$

and using (3.20) in (3.19), after simplification, (3.19) will become as follows:

$$\dot{V} = \sum_{k=1}^{m} -\left(-\mu l - \frac{1}{\alpha}\right) \|\Omega_k^r - F_k\|^2 - \frac{1}{\alpha}\left(\|\Omega_k^r\|^2 + \|F_k\|^2\right) - \frac{2}{\alpha} F_k^T \Omega_d \tag{3.21}$$

The summation over the last term of (3.21) is equal to zero. Using this fact and choosing μ in a way that $\mu l \geq \frac{1}{\alpha}$, we can conclude that the time derivative of (3.14) is negative semi definite. From this, it is possible to deduce that $\Omega_k^r, F_k, \tilde{J}_k$ are belonging to L_∞. From the fact that the Lyapunov function (3.14) is lower bounded and its time derivative is non increasing, we can find that it has a finite limit i.e. $\lim_{t\to\infty} V(t) = V_\infty$. From (3.4) and (3.5), we can conclude that $\dot{\Omega}_k^r, \dot{F}_k \in L_\infty$. Furthermore, using (3.21), we can write:

$$\begin{aligned}
&\dot{V} \leq -\frac{1}{\alpha} \sum_{k=1}^{m} \left(\|\Omega_k^r\|^2 + \|F_k\|^2\right) \\
&\Rightarrow -\alpha \int_0^\infty \dot{V}\ dt \geq \sum_{k=1}^{m} \int_0^\infty \|\Omega_k^r\|^2\ dt + \int_0^\infty \|F_k\|^2\ dt \\
&\Rightarrow \alpha(V(0) - V_\infty) \geq \sum_{k=1}^{m} \|\Omega_k^r\|_2^2 + \|F_k\|_2^2
\end{aligned} \tag{3.22}$$

So we can deduce that $\Omega_k^r, F_k \in L_2$. By applying Barbalat's Lemma [91] we will have $\Omega_k^r \to 0, F_k \to 0$.

Remark 3.1 For solving the previous problem, we did not assume any reference signal for the rotation matrix, and the consensus will be achieved on the general manifold of the system. In order to perform the previous task in the presence of such a reference signal, by considering a tree like topology for the network communication graph, it is possible to consider a virtual leader with a fixed angular velocity Ω_d and desired rotation matrix $R_d(t)$. Next, using the same procedure we can prove the stability results.

3.2.4 Robust Adaptive Control

In this section, we consider the Problem 3.3. In fact, we want to design a more robust control law for the previous task. In the past approach, we assumed that the system is perfect and there is no external noise in the input. However, in aeronautic applications a small noise caused by unmodeled dynamics or from the external sources can lead to a catastrophic failure. In order to handle these types of noises, we need to modify our previous approach. Agents dynamic models for this case were discussed in section 3.2.3. As stated before, first we assume that the upper bound for these vectors are known i.e $\|\delta_k\| \leq \Delta_k$. We use Lyapunov function (3.14) to analyze this problem. The time derivative of this Lyapunov function in this case takes the following form:

$$\dot{V} = l\sum_{k=1}^{m}(\Omega_k^r - F_k)^T([J_k\Omega_k]^\wedge \Omega_k + u_k + \delta_k - J_k\dot{F}_k)$$
$$\frac{-2}{\alpha}\sum_{k=1}^{m}F_k^T\Omega_k + \sum_{k=1}^{m}\frac{1}{d_k}tr\left[\tilde{J}_k\dot{\tilde{J}}_k\right] \tag{3.23}$$

we need to devise a method to suppress the effects of noises on the dynamics of each of agents for achieving the attitude synchronization task. The latter can be done by adding an extra term to the control law (3.13) which is related to the upper bound on the noise vector. Our proposed control law for this case is as follows:

$$u_k = -\left[\hat{J}_k\Omega_k\right]^\wedge \Omega_k + \hat{J}_k\frac{d}{dt}F_k$$
$$+\mu(F_k - \Omega_k + \Omega_d) - \frac{\Delta_k^2(\Omega_k^r - F_k)}{\Delta_k\|\Omega_k^r - F_k\| + \epsilon_k} \tag{3.24}$$
$$\dot{\hat{J}}_k = d_k[\dot{F}_k(\Omega_k^r - F_k)^T$$
$$\Omega_k((\Omega_k^r - F_k)\times\Omega_k)^T - 2\sigma_k\hat{J}_k] \tag{3.25}$$

where σ_k and ϵ_k are design parameters. (3.24) and (3.25) have an extra term compared to equations (3.13) and (3.20). The main purpose of these terms is to confine the trajectories

of the system to a small neighborhood of the origin by choosing sufficiently small values for σ_k and ϵ_k. By choosing such values for these parameters, we will increase the control effort and hence, there is a tradeoff between increasing the efficiency of the synchronization task and the amount of control effort. After the insertion of (3.24) and (3.25) in (3.23), we reach to

$$\begin{aligned}\dot{V} = &\sum_{k=1}^{m} -\left(\mu l - \frac{1}{\alpha}\right)\|\Omega_k^r - F_k\|^2 - \frac{1}{\alpha}\left(\|\Omega_k^r\|^2 + \|F_k\|^2\right) \\ &+ (\Omega_k^r - F_k)^T\left(\delta_k - \frac{\Delta_k^2(\Omega_k^r - F_k)}{\Delta_k\|\Omega_k^r - F_k\| + \epsilon_k}\right) \\ &\sigma_k tr[\tilde{J}_k\hat{J}_k] \end{aligned} \tag{3.26}$$

since $\|\delta_k\| \leq \Delta_k$, we can find that:

$$\begin{aligned}\dot{V} \leq &\sum_{k=1}^{m} -\left(\mu l - \frac{1}{\alpha}\right)\|\Omega_k^r - F_k\|^2 - \frac{1}{\alpha}(\|\Omega_k^r\|^2 + \|F_k\|^2) \\ &\sigma_k tr[\tilde{J}_k\hat{J}_k] + \epsilon_k \end{aligned} \tag{3.27}$$

Next, we need to find some bounds for the $\sum_{k=1}^{m}\sigma_k tr[\tilde{J}_k\hat{J}_k]$ term. Here, we use the approach from [92]:

$$\begin{aligned}&\sum_{k=1}^{m}\sigma_k tr[\tilde{J}_k\hat{J}_k] = \sum_{k=1}^{m}\sigma_k tr[\tilde{J}_k(J_k - \tilde{J}_k)] \\ &= \sum_{k=1}^{m}\sigma_k(-\tilde{J}_{k,ii}^2 + \tilde{J}_{k,ij}J_{k,ji}) \leq \sum_{k=1}^{m}\sigma_k\left(-\frac{\tilde{J}_{k,ii}^2}{2} + \frac{J_{k,ij}^2}{2}\right) \\ &= \sum_{k=1}^{m}\frac{-\sigma_k}{2}tr[\tilde{J}_k^2] + \frac{\sigma_k}{2}tr[J_k^2] \\ &= \sum_{k=1}^{m}\frac{-\sigma_k}{2}\left\|\tilde{J}_k\right\|_F^2 + \frac{\sigma_k}{2}\|J_k\|_F^2 \end{aligned} \tag{3.28}$$

where we used summation convention for brevity, we need to assume that the values of the maximum eigenvalues $\lambda_{k,M}$ of the inertia matrices of agents are known. This assumption is

not restrictive since we can easily approximate these values. Using this assumption, (3.28) results in:

$$\sum_{k=1}^{m} \sigma_k tr[\tilde{J}_k J_k] \leq \sum_{k=1}^{m} \frac{-\sigma_k}{2} \left\| \tilde{J}_k \right\|_F^2 + \frac{3\sigma_k}{2} \lambda_{K,M}^2 \tag{3.29}$$

then we can write (3.27) as follows:

$$\begin{aligned} \dot{V} \leq \sum_{k=1}^{m} & - \left(\mu l - \frac{1}{\alpha} \right) \|\Omega_k^r - F_k\|^2 - \frac{1}{\alpha} (\|\Omega_k^r\|^2 + \|F_k\|^2) \\ & \frac{-\sigma_k}{2} \left\| \tilde{J}_k \right\|_F^2 + \frac{3\sigma_k}{2} \lambda_{K,M}^2 + \epsilon_k \end{aligned} \tag{3.30}$$

we can conclude that if the following condition holds:

$$\begin{aligned} \sum_{k=1}^{m} & \left(\mu l - \frac{1}{\alpha} \right) \|\Omega_k^r - F_k\|^2 + \frac{1}{\alpha} (\|\Omega_k^r\|^2 + \|F_k\|^2) \\ & + \frac{\sigma_k}{2} \left\| \tilde{J}_k \right\|_F^2 \geq \sum_{k=1}^{m} \left(\frac{3\sigma_k}{2} \lambda_{K,M}^2 + \epsilon_k \right) \geq \beta \end{aligned} \tag{3.31}$$

then $\dot{V} \leq 0$. Here we can see the fact that by choosing sufficiently small ϵ_k and σ_k for each agent in the network we can 'trap' the trajectories of the system in to a small neighborhood around the origin.

In the next scenario, we assume that the upper bound for each element of the δ_k is known, i.e. $\|\delta_{k,i}\| \leq \Delta_{k,i}$, $i \in \{1, 2, 3\}$. The modified input for this case is as follows

$$u_k = - \left[\hat{J}_k \Omega_k \right]^{\wedge} \Omega_k + \hat{J}_k \frac{d}{dt} F_k$$

$$\mu(F_k - \Omega_k + \Omega_d) - P_k \tag{3.32}$$

$$\dot{\hat{J}}_k = d_k [\dot{F}_k (\Omega_k^r - F_k)^T + \Omega_k ((\Omega_k^r - F_k) \times \Omega_k)^T] \tag{3.33}$$

where the i^{th} element of P_k is as follows:

$$P_{k,i} = -\Delta_{k,i} sign(\Omega_k^r - F_k)_i \tag{3.34}$$

then, we can find that by using (3.32) and (3.33) the time derivative of the Lyapunov function (3.14) results in:

$$\dot{V} \leq \sum_{k=1}^{m} - \left(\mu l - \frac{1}{\alpha}\right) \|\Omega_k^r - F_k\|^2 - \frac{1}{\alpha}(\|\Omega_k^r\|^2 + \|F_k\|^2) \tag{3.35}$$

The rest of stability proof can be carried forward based on the method which is used in section 3.2.3

3.3 Attitude Synchronization with Optimal Norm

In this section, we analyze the different norm definitions which can be used to measure the amount of "disagreement" for the attitude synchronization problem of a rigid body network.

3.3.1 Error Functions on $SO(3)$ and Norm Definitions

An error function acts as an artificial potential energy of the network. In fact, we can imagine this function as a potential energy of the network where agents are connected to each other via imaginary rotational springs as depicted in Fig. 3.1. As we will discuss later, this function can also be used to build error vectors between attitudes of the agents in the network. These error vectors are used in the feedback control laws of the network. For instance, in [87] and [5], the following function has been used for a typical network:

$$V_p = \sum_{i=1}^{m} \sum_{j=1}^{m} a_{ji} tr[I_{3\times 3} - R_i^T R_j] \tag{3.36}$$

If the agents in the network are in a synchronized state, then this function will be equal to zero. In other words, this function measures the total "disagreement" in the network.

In order to better understand the structure of (3.36), consider an individual term

$$V_{ij} = \frac{1}{2} tr\left[I_{3\times 3} - R_i^T R_j\right] \tag{3.37}$$

The attitude error vector corresponding to (3.37) is as follows:

$$e_R = \frac{1}{2}\left(R_i^T R_j - R_j^T R_i\right)^\vee, \tag{3.38}$$

The structure of the synchronization control laws presented in [83], [87], [5] are directly related to this error vector. (3.38) can be derived by computing the gradient of (3.37) on $SO(3)$. In order to study the characteristics of (3.38), without loss of generality, we assume that $R_i = I$, and substitute in (3.38), leading to

$$e_R = \frac{1}{2}\left(R_j - R_j^T\right)^\vee \tag{3.39}$$

We can use the Rodrigues formula to expand R_j as follows:

$$R_j = e^{\omega^\wedge \theta} = I + \frac{\omega^\wedge}{\|\omega\|}\sin\left(\|\omega\|\,\theta\right) + \frac{(\omega^\wedge)^2}{\|\omega\|^2}\left(1 - \cos\left(\|\omega\|\,\theta\right)\right)$$
$$R_j^T = e^{-\omega^\wedge \theta} = I - \frac{\omega^\wedge}{\|\omega\|}\sin\left(\|\omega\|\,\theta\right) + \frac{(\omega^\wedge)^2}{\|\omega\|^2}\left(1 - \cos\left(\|\omega\|\,\theta\right)\right)$$

If $\|\omega\| = 1$, θ represents the angle of rotation about the axis ω. We can easily observe that

$$\left(R_j - R_j^T\right)^\vee = \frac{2}{\|\omega\|}\sin\left(\|\omega\|\,\theta\right)\omega \tag{3.40}$$

Since $\|\omega\| = 1$, (3.40) indicates that the error vector is related to the angle between the current and desired attitude position which is $\theta = 0$ for $R_i = I$.

The main drawback of using error function (3.37) is as follows: From $\theta = 0$ to $\theta = \frac{\pi}{2}$ the norm of error vector increases, which is desirable; but from $\theta = \frac{\pi}{2}$ to $\theta = \pi$ it decreases, which is undesirable. Using (3.36), the controller needs to put extra effort for attitude synchronization since the methodology for finding the attitude error will weight the actual

difference in attitude positions differently from 0 to $\frac{\pi}{2}$ and from $\frac{\pi}{2}$ to π.

Next, we study an alternative function which monotonically increases with the difference in attitude positions of agents. One such function is introduced in [84] for tracking a reference signal on $SO(3)$. Here, we use the following modified version of this function

$$V_{ij} = 2 - \sqrt{1 + tr[R_i^T R_j]}, \quad V_p = \sum_{i=1}^{m} \sum_{j=1}^{m} a_{ij} V_{ij} \tag{3.41}$$

The error vector for (3.41) can be derived as

$$e_{ij} = \frac{1}{2\sqrt{1 + tr\left[R_j^T R_i\right]}} \left(R_j^T R_i - R_i^T R_j\right)^\vee \tag{3.42}$$

Again, using Rodrigues formula, we find that for $Q = R_j^T R_k = e^{\omega_1^\wedge \theta_1}$, (3.42) becomes:

$$\|e_{ij}\| = \sin \frac{\|\omega_1\| \, \theta_1}{2} \tag{3.43}$$

It is clear that unlike the error function (3.37), the error function (3.41) monotonically increases from 0 to π. In [93], it is also shown that, (3.41) is actually the viscosity solution to the Hamilton-Jacobi-Bellman equation for the optimal control problem on $SO(3)$ with the cost function:

$$\mathbb{H} = \frac{1}{2} \int_0^\infty tr[I_{3\times 3} - R(t)] + \Omega^T(t)\Omega(t) \; dt \tag{3.44}$$

where $\dot{R} = R\Omega^\wedge$. We can show that the relative kinematics of two agents can also be converted to this optimal control problem using the method which is first proposed in [38]. Consider two agents in the network with kinematics (3.5). If these agents have the same attitudes then $R_i^{-1} R_j = I$. In this regard, consider the following change of variable:

$$R = R_i^{-1} R_j \Rightarrow \; \dot{R} = R_i^{-1} R_j \left[\Omega_j^\wedge - R^{-1} \hat{\Omega}_i^\wedge R^{-1}\right] \tag{3.45}$$

By denoting $\left[\Omega_j^\wedge - R^{-1}\hat{\Omega}_i^\wedge R^{-1}\right]$ as $\Omega_{ij}^\wedge$, (3.45) indicates that the attitude synchronization of two agents can be seen as an optimal control problem with the cost function (3.44).
In this chapter, we use the following potential function to measure the amount of "disagreement" in the network and design the control laws

$$V_p = \sum_{k=1}^{m}\sum_{j=1}^{m} a_{jk}\left(2 - \sqrt{1 + tr[R_k^T R_j]}\right) \tag{3.46}$$

3.3.2 Synchronization Scheme Design

In this section, we revisit *Problem 3.1* for a network of rigid body agents. We use the optimal norm introduced in Section 3.3.1 for analysis and control design. Consider a network consisting of m rigid bodies with dynamic equations (3.4), (3.5). These rigid bodies can be spacecraft, ground robots, a network of satellites in the earth orbit, or an array of radio telescopes. We propose the following control law for the attitude synchronization task of *Problem 3.1*:

$$u_k = -\left[J_k\Omega_k\right]^\wedge \Omega_k + J_k N_k + \mu\left(M_k - \Omega_k + \Omega_d\right), \tag{3.47}$$

where

$$M_k = \alpha\sum_{j=1}^{m} M_{jk}, \quad N_k = \alpha\sum_{j=1}^{m} N_{jk} \;\; \alpha > 0$$

$$M_{jk} = \begin{cases} \frac{a_{jk}}{2\sqrt{1+tr[R_k^T R_j]}}\left[R_k^T R_j - R_j^T R_k\right]^\vee & if\ tr[R_j^T R_k] \neq -1 \\ a_{jk}\left[R_k^T R_j - R_j^T R_k\right]^\vee & otherwise \end{cases}$$

$$N_{jk} = \begin{cases} \frac{d}{dt}\left(\frac{a_{jk}}{2\sqrt{1+tr[R_k^T R_j]}}\left[R_k^T R_j - R_j^T R_k\right]^\vee\right) & if\ tr[R_j^T R_k] \neq -1 \\ \frac{d}{dt}\left(a_{jk}\left[R_k^T R_j - R_j^T R_k\right]^\vee\right) & otherwise \end{cases}$$

μ and α are positive constants and as we will show later, they can be adjusted to achieve better stability results.

Remark 3.2: $N_{jk} = \dot{M}_{jk}$ does not hold, because of the discontinuous nature of M_{jk} laws. In order to study the stability properties of the previous algorithm we use the Lyapunov function

$$V = V_p + \frac{l}{2}\sum_{k=1}^{m}(\Omega_k^r - G_k)^T J_k(\Omega_k^r - G_k) \tag{3.48}$$

where l is a positive constant and $\Omega_k^r = \Omega_k - \Omega_d$. G_k is defined as:

$$G_k = \sum_{j=1}^{m} G_{jk} = \sum_{j=1}^{m} \frac{\alpha a_{jk}}{2\sqrt{1 + tr[R_k^T R_j]}} \left[R_k^T R_j - R_j^T R_k\right]^\vee$$

The main difference between our proposed Lyapunov function and the one proposed in [87] is in the first term of (3.48). This term measures the artificial potential energy related to the attitude differences of the rigid bodies in the network. As we mentioned earlier, it is possible to consider this function as a potential energy of the network where agents are connected to each other via imaginary rotational springs as depicted in Fig. 3.1.

It is clear that this function is positive definite for the attitude synchronization equilibrium since $tr[R_k^T R_j] \leq 3$. Next, we compute the generalized time derivative [88] of V:

$$\begin{aligned}\dot{\tilde{V}} &= \frac{1}{2}\sum_{k=1}^{m}\sum_{j=1}^{m}\frac{-a_{jk}tr[\dot{R}_k^T R_j + R_k^T \dot{R}_j]}{2\sqrt{1 + tr[R_k^T R_j]}} \\ &+ l\sum_{k=1}^{m}(\Omega_k^r - G_k)^T(J_k\dot{\Omega}_k^r - J_k\dot{G}_k)\end{aligned} \tag{3.49}$$

If $tr[R_k^T R_j] = -1$, we need to use the limits of G_k and $\dot{G}_k$. , existence and boundedness of which are established in [84]. Substituting (3.4) and (3.5), we reach

$$\begin{aligned}\dot{\tilde{V}} &= \frac{1}{2}\sum_{k=1}^{m}\sum_{j=1}^{m}\frac{-a_{jk}tr[-\Omega_k^\wedge R_k^T R_j + R_k^T R_j \Omega_j^\wedge]}{2\sqrt{1 + tr[R_k^T R_j]}} \\ &+ l\sum_{k=1}^{m}(\Omega_k^r - G_k)^T([J_k\Omega_k]^\wedge \Omega_k + u_k - J_k\dot{G}_k)\end{aligned} \tag{3.50}$$

Using the fact $tr[A^T] = tr[A]$ and tweaking the indices j and k, (3.50) can be rewritten as

$$\begin{aligned}\dot{\tilde{V}} &= \frac{1}{2}\sum_{k=1}^{m}\sum_{j=1}^{m}\frac{-a_{jk}tr[R_k^T R_j \Omega_j^\wedge]}{\sqrt{1+tr[R_k^T R_j]}} \\ &+ l\sum_{k=1}^{m}(\Omega_k^r - G_k)^T([J_k\Omega_k]^\wedge \Omega_k + u_k - J_k\dot{G}_k) \end{aligned} \tag{3.51}$$

Using the control law (3.47) for agents, (3.51) becomes

$$\begin{aligned}\dot{\tilde{V}} &= \frac{1}{2}\sum_{k=1}^{m}\sum_{j=1}^{m}\frac{-a_{jk}tr[R_k^T R_j \Omega_j^\wedge]}{\sqrt{1+tr[R_k^T R_j]}} \\ &+ l\sum_{k=1}^{m}(\Omega_k^r - G_k)^T(J_k(N_k - \dot{G}_k) + \mu(M_k - \Omega_k + \Omega_d))) \end{aligned} \tag{3.52}$$

Using the facts $\lim_{R_i\to R_j} M_{ik} = G_{jk}$ and $\lim_{R_i\to R_j} N_{ik} = \dot{G}_{jk}$, (3.52) can be expressed as

$$\begin{aligned}\dot{\tilde{V}} &= \frac{1}{2}\sum_{k=1}^{m}\sum_{j=1}^{m}\frac{-a_{jk}tr[R_k^T R_j \Omega_j^\wedge]}{\sqrt{1+tr[R_k^T R_j]}} \\ &- \mu l\sum_{k=1}^{m}(\Omega_k^r - G_k)^T(\Omega_k^r - G_k) \end{aligned} \tag{3.53}$$

Substituting (3.3) in (3.53), we obtain

$$\begin{aligned}\dot{\tilde{V}} &= \frac{1}{2}\sum_{k=1}^{m}\sum_{j=1}^{m}\frac{-a_{jk}\Omega_j^T\left[R_j^T R_k - R_k^T R_j\right]^\vee}{\sqrt{1+tr[R_k^T R_j]}} \\ &- \mu l\sum_{k=1}^{m}(\Omega_k^r - G_k)^T(\Omega_k^r - G_k), \end{aligned} \tag{3.54}$$

which, using the definition of G_k and changing the index, turns into

$$\dot{\tilde{V}} = \frac{-1}{\alpha}\sum_{k=1}^{m} G_k^T\Omega_k - \mu l\sum_{k=1}^{m}(\Omega_k^r - G_k)^T(\Omega_k^r - G_k) \tag{3.55}$$

Adding and subtracting $\sum_{k=1}^{m} G_k\Omega_d$, we obtain

$$\begin{aligned}\dot{\tilde{V}} &= \sum_{k=1}^{m}\left(-\left(\mu l - \frac{1}{2\alpha}\right)\|\Omega_k^r - G_k\|^2 - \frac{1}{2\alpha}\left(\|\Omega_k^r\|^2 + \|G_k\|^2\right)\right. \\ &- \left.\frac{1}{\alpha}G_k^T\Omega_d\right) \end{aligned} \tag{3.56}$$

Since

$$\frac{a_{jk}}{\sqrt{1+tr[R_k^T R_j]}}(R_k^T R_j - R_j^T R_k)^\vee = \frac{-a_{kj}}{\sqrt{1+tr[R_j^T R_k]}}(R_j^T R_k - R_k^T R_j)^\vee,$$

the summation over the last term in (3.56) is equal to zero and we deduce that $\dot{\tilde{V}} \leq 0$, and $\dot{\tilde{V}} < 0$ for $\|\Omega_k^r\| \neq 0$ and $\|G_k\| \neq 0$ for $\mu l \geq \frac{1}{2\alpha}$. Comparing to the results of [87],[83], it is clear that we can choose smaller value of μ for stabilization. Now, we are in position to invoke LaSalle-Yoshizawa Theorem for nonsmooth systems(Corollary 2 in [88]) and conclude that the equilibrium of the system is asymptotically stable, i.e. $G_k \to 0$ and $\Omega_k^r \to 0, k \in \{1, \cdots, m\}$.

Theorem 3.1: Consider *Problem 3.1* for a network of m rigid bodies with dynamics (3.4) and (3.5). For $\mu l \geq \frac{1}{2\alpha}$, the control law (3.47) asymptotically synchronizes the attitudes of the agents of the network.

Remark 3.3: Since the control algorithm (3.47) is a backstepping-type controller, we can regard α and μ as control gains for different steps of backstepping method. It is also clear that choosing high value for α enables us to use smaller μ in (3.47). This particular relation between the gains is directly related to the optimal norm (3.46) which appears in the structure of the Lyapunov function (3.48). The latter property is also observed in stability analysis of general mechanical systems. For instance, consider a simple spring-mass-damper, where the rate of change of the mechanical energy (Lyapunov function for the system) depends only on the value of the damper coefficient. However, in [94], authors proposed a Lyapunov function for studying the input to state stability of the system whose time derivative depends on both of the system gains and can be used for robust stability analysis.

3.3.3 Performance Analysis

In this section, we analyze and compare the performance of control algorithm (3.47) with the results in [87]. As mentioned in Section 3.3.1, the norm of the error vector (3.38) is directly related to the sine of the angle between the two neighboring agents while the norm of the error vector (3.42) is proportional to the sine of the half of this angle. If there exists a large physical difference $\theta = \pi - \epsilon$, where $\epsilon \geq 0$ is small, between the attitudes of the agents, then the error vector (3.38) tends to zero despite this large difference. This issue can be solved by using the error vector (3.42). In order to study the effects of this issue on the performance of the synchronization task we start with an example of consensus problem in two dimensional Euclidean space. In this regard, consider a network of holonomic agents with kinematics $\dot{x}_i = u_{ix},\ \dot{y}_i = u_{iy},\ i \in \{1, \cdots, n\}$. This network can reach the state of consensus using the algorithms proposed in [95]. We consider two special cases as follows:

$$\begin{aligned} u_{ix,1} &= -\sum_{j \in N_i} \sin\left(x_i - x_j\right), \quad u_{ix,2} = -\sum_{j \in N_i} \sin\left(\frac{x_i - x_j}{2}\right) \\ u_{iy,1} &= -\sum_{j \in N_i} \sin\left(y_i - y_j\right), \quad u_{iy,2} = -\sum_{j \in N_i} \sin\left(\frac{y_i - y_j}{2}\right) \end{aligned} \tag{3.57}$$

Suppose that a network of four agents, with the communication graph depicted in Fig. 3.2, is released from the following initial condition, where $\epsilon_{ix}, \epsilon_{iy} << 1$:

$$X(0) = [\epsilon_{1x}, \epsilon_{2x}, \pi - \epsilon_{3x}, \pi - \epsilon_{4x}],\ Y(0) = [\epsilon_{1y}, \pi - \epsilon_{2y}, \pi - \epsilon_{3y}, \epsilon_{4y}] \tag{3.58}$$

We can analyze the stability of the distributed algorithm (3.57) for this network using the method proposed in [95] and the Lyapunov function

$$V = \zeta_x^T \zeta_x + \zeta_y^T \zeta_y, X = \alpha \mathbf{1}_n + \zeta_x,\ Y = \beta \mathbf{1}_n + \zeta_y,\ \alpha, \beta > 0. \tag{3.59}$$

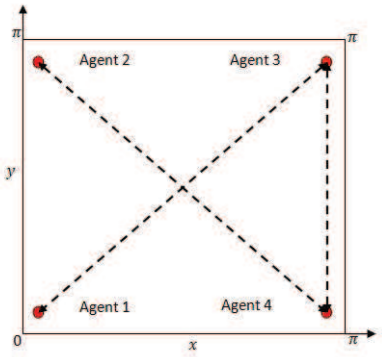

Figure 3.2: The initial network configuration for control algorithms (3.57).

where $X = [x_1, \cdots, x_n]^T$ and $Y = [y_1, \cdots, y_n]^T$. Then for the previous algorithms, we have

$$\dot{V}_1 = -\sum_i \sum_{j \in N_i} (\zeta_{ix} - \zeta_{jx}) \sin(\zeta_{ix} - \zeta_{jx}), \ \dot{V}_2 = -\sum_i \sum_{j \in N_i} (\zeta_{ix} - \zeta_{jx}) \sin\left(\frac{\zeta_{ix} - \zeta_{jx}}{2}\right), \tag{3.60}$$

hence, we can write

$$\dot{V}_1(0) = -\pi(\sin(\epsilon_1 + \epsilon_3) + \sin(\epsilon_2 + \epsilon_4)) + O(\epsilon^2), \ \dot{V}_2(0) = -\pi + O(\epsilon), \tag{3.61}$$

which clearly shows the huge difference between the decreasing rates of the Lyapunov function (3.59) using the previous control methods in the beginning of the control task. From (3.60), we can deduce that this situation continues until the relative positions between agents decrease. In particular, in the context of attitude synchronization, consider two agents in the network with the disagreement function (3.41). The time derivative of (3.41) is

$$\frac{dV_{ij}}{dt} = \frac{-1}{2\sqrt{1 + tr[R_j^T R_i]}} tr[R_j^T R_i \hat{\Omega}_i - \hat{\Omega}_j R_j^T R_i]. \tag{3.62}$$

Using (3.3), this can be rewritten as:

$$\frac{dV_{ij}}{dt} = \frac{-1}{2\sqrt{1+tr[R_j^T R_i]}}\left[-\Omega_i^T(R_j^T R_i - R_i^T R_j)^\vee - \Omega_j^T(R_i^T R_j - R_j^T R_i)^\vee\right] \tag{3.63}$$

Next, if we choose the kinematic controllers

$$\Omega_i = \frac{-1}{2\sqrt{1+tr[R_j^T R_i]}}[R_j^T R_i - R_i^T R_j]^\vee, \quad \Omega_j = \frac{-1}{2\sqrt{1+tr[R_i^T R_j]}}[R_i^T R_j - R_j^T R_i]^\vee \tag{3.64}$$

then (3.63) becomes:

$$\frac{dV_{ij}}{dt} = \frac{-1}{2(1+tr[R_j^T R_i)}\left\|[R_j^T R_i - R_i^T R_j]^\vee\right\|^2 \approx \sin^2(\frac{\theta_{ij}}{2}). \tag{3.65}$$

On the other hand, if we used the error vector (3.38) to design the kinematic controllers [87],[83]

$$\Omega_i = [R_j^T R_i - R_i^T R_j]^\vee, \quad \Omega_j = [R_i^T R_j - R_j^T R_i]^\vee$$

then, we can write

$$\frac{dV_{ij}}{dt} = \frac{-1}{2\sqrt{1+tr[R_j^T R_i}}\left\|[R_j^T R_i - R_i^T R_j]^\vee\right\|^2 \approx \sin(\frac{\theta_{ij}}{2})\sin(\theta_{ij}). \tag{3.66}$$

From (3.66), it is clear that in the presence of large angular difference ($\theta_{ij} = \pi - \epsilon, 0 < \epsilon << 1$), V_{ij} will decrease much faster with (3.64). The latter problem is aggravated in the situations where the communication graph of the network compels the agents with large attitude differences to become neighbors. One of such situations is depicted in Fig. 3.3, where 4 agents with huge difference in attitude positions are communicating via a line graph topology which is popular in attitude synchronization problems [96, 97, 5].

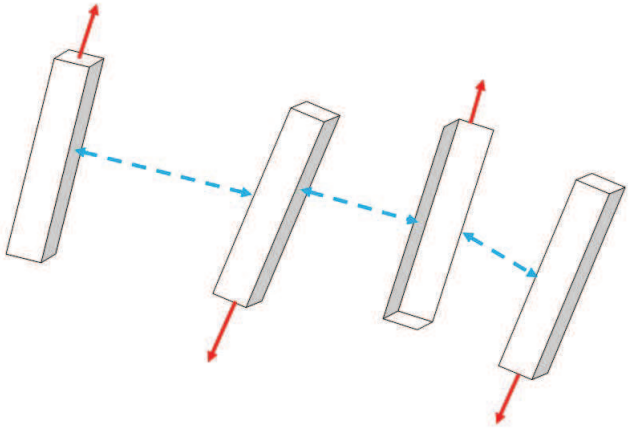

Figure 3.3: Network of rigid bodies with large attitude differences with line graph topology.

3.3.4 Adaptive Attitude Synchronization with Optimal Norm

In the previous section, we assumed that the values of the principal moments of inertia were available for the purpose of control design. This assumption is to some extent, restrictive since these values may change during certain tasks. Hence, we need to modify the previous approach to cope with situations where this information is not available. Here, we use the adaptive control framework to find the estimates of the moments of the inertia of the rigid bodies in the network. In this regard, we start by using (3.47), but instead of the values of the moments of inertia, we use the current estimates

$$u_k = -\left[\hat{J}_k \Omega_k\right]^{\wedge} \Omega_k + \hat{J}_k N_k + \mu \left(M_k - \Omega_k + \Omega_d\right), \tag{3.67}$$

where $\hat{J}_k$ denotes the estimate of J_k. In order to fulfill such a design, we modify the Lyapunov function (3.48) as follows:

$$\begin{aligned} V &= \frac{1}{2}\sum_{k=1}^{m}\sum_{j=1}^{m} a_{jk}\left(2-\sqrt{1+tr[R_k^T R_j]}\right) \\ &+ \frac{l}{2}\sum_{k=1}^{m}(\Omega_k^r - G_k)^T J_k(\Omega_k^r - G_k) \\ &+ \sum_{k=1}^{m}\frac{1}{2d_k}\left\|J_k-\hat{J}_k\right\|_F^2 \end{aligned} \tag{3.68}$$

where $\|\cdot\|_F$ denotes the Frobenius norm and $d_k, k \in \{1,\cdots,m\}$ are positive constants. In fact, as we show later, these parameters are the adaptation gains of the update equations and can be adjusted to fine tune the transient behavior of the adaptation task. The generalized time derivative of the Lyapunov function (3.68) is

$$\begin{aligned} \dot{\tilde{V}} &= \frac{1}{2}\sum_{k=1}^{m}\sum_{j=1}^{m}\frac{-a_{jk}tr[\dot{R}_k^T R_j + R_k^T \dot{R}_j]}{2\sqrt{1+tr[R_k^T R_j]}} \\ &+ l\sum_{k=1}^{m}(\Omega_k^r - G_k)^T(J_k\dot{\Omega}_k^r - J_k\dot{G}_k) \\ &+ \sum_{k=1}^{m}\frac{1}{d_k}tr[\bar{J}_k\dot{\bar{J}}_k], \end{aligned} \tag{3.69}$$

where $\bar{J}_k = J_k - \hat{J}_k$. Using (3.3),(3.4),(3.5),(3.67) we reach

$$\begin{aligned} \dot{\tilde{V}} &= \frac{1}{2}\sum_{k=1}^{m}\sum_{j=1}^{m}\frac{-a_{jk}\Omega_j^T\left[R_j^T R_k - R_k^T R_j\right]^\vee}{\sqrt{1+tr[R_k^T R_j]}} + \sum_{k=1}^{m}\frac{1}{d_k}tr[\bar{J}_k\dot{\bar{J}}_k] \\ &+ l\sum_{k=1}^{m}(\Omega_k^r - G_k)^T\left(\left[\bar{J}_k\Omega_k\right]^\wedge\Omega_k + \bar{J}_k N_k + \mu(M_k - \Omega_k + \Omega_d)\right) \end{aligned} \tag{3.70}$$

Next, using the identities $a^T b = tr[ab^T], a, b \in \mathbb{R}^3$ and $a^T(b \times c) = b^T(c \times a) = c^T(a \times b)$, we obtain

$$\dot{\tilde{V}} = \sum_{k=1}^{m} tr\left[\bar{J}_k\left(\frac{1}{d_k}\dot{\bar{J}}_k - \dot{G}_k(\Omega_k^r - G_k)^T - \Omega_k\left((\Omega_k^r - G_k) \times \Omega_k\right)^T\right)\right]$$
$$- \frac{1}{\alpha}\sum_{k=1}^{m} G_k^T \Omega_k - l\mu \sum_{k=1}^{m}(\Omega_k^r - G_k)^T(\Omega_k^r - G_k). \tag{3.71}$$

Here, we can see the main rationale behind using the Frobenius norm in the structure of the Lyapunov function (3.68). This particular norm produces the adequate terms in the generalized time derivative of the Lyapunov function for canceling out the terms involving $\bar{J}_k$. Here, it is clear that by choosing the following adaptation law

$$\dot{\hat{J}}_k = -\dot{\bar{J}}_k = -d_k\left[\dot{G}_k(\Omega_k^r - G_k)^T + \Omega_k((\Omega_k^r - G_k) \times \Omega_k)^T\right] \tag{3.72}$$

we can eliminate the terms involving $\bar{J}_k$. However, here we use the adaptation laws

$$\dot{\hat{J}}_k = -\dot{\bar{J}}_k = -\frac{d_k}{2}\left[\dot{G}_k(\Omega_k^r - G_k)^T + \Omega_k((\Omega_k^r - G_k) \times \Omega_k)^T\right.$$
$$\left. + (\Omega_k^r - G_k)\dot{G}_k^T + ((\Omega_k^r - G_k) \times \Omega_k)\Omega_k^T\right] \tag{3.73}$$

The only difference between (3.72) and (3.73) is that in (3.73) we have used the fact that the inertia matrix estimates of agents must be symmetric. Substituting (3.73) into (3.71), we reach

$$\dot{\tilde{V}} = \frac{-1}{\alpha}\sum_{k=1}^{m} G_k^T \Omega_k - \mu l \sum_{k=1}^{m}(\Omega_k^r - G_k)^T(G_k - \Omega_k + \Omega_d). \tag{3.74}$$

Adding and subtracting the $\sum_{k=1}^{m} G_k^T \Omega_d$ term, we obtain

$$\dot{\tilde{V}} = \sum_{k=1}^{m} -\left(l\mu - \frac{1}{2\alpha}\right)\|\Omega_k^r - G_k\|^2 - \frac{1}{2\alpha}\left(\|\Omega_k^r\|^2 + \|G_k\|^2\right)$$
$$- \frac{1}{\alpha}G_k^T \Omega_d \tag{3.75}$$

Choosing $l\mu \geq \frac{1}{2\alpha}$ and using the fact that $\sum_{k=1}^{m} G_k^T \Omega_d = 0$, we conclude that $\dot{\tilde{V}} \leq 0$, and $\dot{\tilde{V}} < 0$ for $\|\Omega_k^r\| \neq 0$ and $\|G_k\| \neq 0$. Again, using LaSalle-Yoshizawa Theorem for non-smooth systems (Corollary 2 in [88]), we establish that $\Omega_k^r \to 0, G_k \to 0$ as $t \to \infty$.

Theorem 3.2: Consider *Problem 3.2* for a network of rigid body agents with dynamics (3.4) and (3.5). Control law (3.67) together with the adaptation laws (3.73) asymptotically synchronize the attitudes of the agents provided that $\mu l \geq \frac{1}{2\alpha}$.

Remark 3.4: In order to solve the attitude synchronization problem, we did not assume any reference signal for rotation matrix, and the consensus will be achieved on the general manifold of the system. But in many practical situations we need the agents in the network to track a particular path on $SO(3)$. For this case, we can assume a virtual leader with an angular velocity Ω_d and the desired rotation matrix $R_d(t)$ for a tree shaped network communication graph. Following the procedure of this section one can obtain the main stability results.

3.3.5 Robust Adaptive Synchronization

In this section, the main objective is to design a method which can handle the effects of unmodeled dynamics or unknown external disturbances. The main reason for performing this task arises from the practical implementation of synchronization algorithm where a small noise due to atmospheric drag or friction can cause a large amount of error. Here, the robust synchronization task is achieved via manipulating the time derivative of the Lyapunov function, aiming to decrease the virtual disagreement function of the network in the course of time. We assume that the upper bounds on the external disturbances are known a priori. We start by modifying our approach in Section 3.3.4 to make it suitable for robust synchronization. Consider the derivative of the Lyapunov function (3.67) for

the case that (3.4) is affected by the disturbance δ_k:

$$\begin{aligned}\dot{\tilde{V}} &= l\sum_{k=1}^{m}(\Omega_k^r - G_k)^T([J_k\Omega_k]^\wedge \Omega_k + u_k + \delta_k) \\ &- \frac{1}{\alpha}\sum_{k=1}^{m} G_k^T\Omega_k + \sum_{k=1}^{m}\frac{1}{d_k}tr\left[\bar{J}_k\dot{\bar{J}}_k\right]\end{aligned} \tag{3.76}$$

As stated before, the objective is to suppress the effects of unmodeled dynamics, i.e. δ_k. In order to fulfill this task, we assume that the upper bound for each element of the δ_k is known, i.e. $\|\delta_{k,i}\| \leq \Delta_{k,i}$, $i \in \{1,2,3\}$. The modified adaptive control law for this case is selected as

$$u_k = -\left[\hat{J}_k\Omega_k\right]^\wedge \Omega_k + \hat{J}_k N_k + \mu(M_k - \Omega_k + \Omega_d) - P_k, \tag{3.77}$$

$$\dot{\hat{J}}_k = -d_k[\dot{G}_k(\Omega_k^r - G_k)^T + \Omega_k((\Omega_k^r - G_k)\times\Omega_k)^T], \tag{3.78}$$

where the i^{th} element of P_k is chosen as

$$P_{k,i} = -\Delta_{k,i}sign(\Omega_k^r - G_k)_i \tag{3.79}$$

Using (3.77) and (3.78) the generalized time derivative of the Lyapunov function (3.67) results in:

$$\begin{aligned}\dot{\tilde{V}} \leq \sum_{k=1}^{m} &-\left(\mu l - \frac{1}{2\alpha}\right)\|\Omega_k^r - G_k\|^2 - \frac{1}{2\alpha}(\|\Omega_k^r\|^2 + \|G_k\|^2) \\ &+ l\sum_{k=1}^{m}\sum_{i=1}^{3}\left(\delta_{k,i}(\Omega_k^r - G_k)_i - \Delta_{k,i}\|\Omega_k^r - G_k\|_i\right).\end{aligned} \tag{3.80}$$

Since

$$l\sum_{k=1}^{m}\sum_{i=1}^{3}\left(\delta_{k,i}(\Omega_k^r - G_k)_i - \Delta_{k,i}\|\Omega_k^r - G_k\|_i\right) \leq 0,$$

we have

$$\dot{\tilde{V}} \leq \sum_{k=1}^{m} -\left(\mu l - \frac{1}{2\alpha}\right)\|\Omega_k^r - G_k\|^2 - \frac{1}{2\alpha}(\|\Omega_k^r\|^2 + \|G_k\|^2). \tag{3.81}$$

Using LaSalle-Yoshizawa Theorem for nonsmooth systems, we can prove the stability of the synchronization task.

Theorem 3.3: Consider *Problem 3.3*. Control law (3.77) together with adaptation law (3.78) will achieve the robust synchronization task provided that $\mu l \geq \frac{1}{2\alpha}$.

To the best of the authors' knowledge, there is no other *adaptive* control law in the literature for attitude synchronization based on geometric approach. Hence, it is hard to do a comparative analysis for the performance of the proposed robust control law (3.77). Furthermore, the design of (3.77) is based on a constructive Lyapunov analysis leading to an asymptotic convergence result only, as seen above, not providing bounds for transient performance. Yet there exist relevant *non-adaptive* designs in the literature, which may be used to modify (3.77) into a form more suitable for performance analysis, for certain classes of network topologies. One such design is proposed in [84] to reject external disturbances for attitude control of a single robot. This approach can be modified and combined with (3.77) for synchronization of two agents using the control law

$$u_k = -\left[J_k\Omega_k\right]^\wedge \Omega_k + J_k\dot{G}_k + \mu(G_k - \Omega_k + \Omega_d) - \frac{\Delta_k^2(\Omega_k^r - G_k)}{\Delta_k \left\|\Omega_k^r - G_k\right\| + \epsilon_k} \tag{3.82}$$

together with the Lyapunov function (3.48) with $m = 2$ and $a_{12} = a_{21} = 1$. The time derivative of V is found as

$$\begin{aligned}\dot{V} = -\sum_{k=1}^{2}\left(l\mu - \frac{1}{2\alpha}\right)\left\|\Omega_k^r - G_k\right\|^2 - \frac{1}{\alpha}\sum_{k=1}^{2}\left(\left\|\Omega_k^r\right\|^2 + \left\|G_k\right\|^2\right) \\ + \sum_{k=1}^{2}(\Omega_k^r - G_k)^T\left(\delta_k - \frac{\Delta_k^2(\Omega_k^r - G_k)}{\Delta_k \left\|\Omega_k^r - G_k\right\| + \epsilon_k}\right)\end{aligned} \tag{3.83}$$

If we know the upper bounds for δ_k terms, i.e $\left\|\delta_k\right\| \leq \Delta_k$, (3.83) reduces to

$$\dot{V} \leq -\sum_{k=1}^{2}\left(\left(l\mu - \frac{1}{2\alpha}\right)\left\|\Omega_k^r - G_k\right\|^2 + \frac{1}{\alpha}(\left\|\Omega_k^r\right\|^2 + \left\|G_k\right\|^2) - \epsilon_k\right). \tag{3.84}$$

Using the fact

$$G_1 = -G_2 = \frac{1}{2\sqrt{1+tr[R_2^T R_1]}}[R_2^T R_1 - R_1^T R_2]^\vee$$
$$\Rightarrow \ \|G_i\|^2 = \sin^2\frac{\theta_{12}}{2} \Rightarrow \ V_{12} = 2 - \sqrt{1+tr[R_2^T R_1]} \leq 2\|G_i\|^2 \tag{3.85}$$

we can rewrite (3.84) as follows:

$$\dot{V} \leq -\sum_{k=1}^{2}\left(l\mu - \frac{1}{2\alpha}\right)\|\Omega_k^r - G_k\|^2 - \frac{1}{2\alpha}V_{12} + \epsilon_k \leq -\beta V + \epsilon_1 + \epsilon_2 \tag{3.86}$$

Choosing $\mu l \geq \frac{1}{2\alpha}$ and using the Bellman Gronwall Lemma [98], we deduce that ($\beta = \frac{1}{2\alpha} > 0$)

$$V(t) \leq e^{-\beta t}V(0) + \frac{\epsilon_1 + \epsilon_2}{\beta} \tag{3.87}$$

From (3.87), it is clear that trajectories of the system will be trapped inside a neighborhood of the equilibrium of the synchronization task. We can adjust the size of the neighborhood by choosing small values for $\epsilon = \epsilon_1 + \epsilon_2$. However, the latter can increase the control effort and hence there exists a tradeoff between the control cost and the performance of robust control task. The analysis above can be easily extended to networks with more than two agents having line graph topology.

3.4 Geometric Redesign Considering Time-Varying Inertia

3.4.1 Dynamics

In this section we summarize the notation used in this research, and review the attitude kinematics and dynamics properties and typical scenario settings for rigid body rotational

maneuvers. The attitude position of a rigid body is defined as the relative orientation between the global inertial reference frame $\mathcal{I}$ and the rigid body fixed body coordinate frame $\mathcal{B}$ and is expressed by the rotation matrix $R \in SO(3)$, columns of which represent the principle axes of the body fixed coordinate frame $\mathcal{B}$ in the inertial coordinate frame $\mathcal{I}$. The angular velocity vector of the rigid body which is expressed in the body coordinate frame is defined as

$$^{b}\omega = \left[R^T \dot{R}\right]^{\vee} \tag{3.88}$$

where $\vee$ is the inverse of hat map which is defined as follows for $x = [x_1, x_2, x_3]^T \in \mathbb{R}^3$:

$$\overset{\triangle}{x} = \begin{bmatrix} 0 & -x_3 & x_2 \\ x_3 & 0 & -x_1 \\ -x_2 & x_1 & 0 \end{bmatrix}. \tag{3.89}$$

Note here that the estimation of a matrix A is denoted by $\hat{A}$ and the estimation error is represented by $\tilde{A} = \hat{A} - A$.

The attitude dynamics for a spacecraft can be derived by taking the time derivative of the angular momentum in the inertial reference frame as follows:

$$\frac{d}{dt}\left[I(t)\omega\right] = \dot{I}\omega + I\dot{\omega} + \omega \times I\omega = M = \sum \tau_{ext}. \tag{3.90}$$

where $M \in \mathbb{R}^3$ is the total external moment exerted on the spacecraft and $I(t) \in \mathbb{R}^{3\times3}$ represents the inertia tensor expressed in body fixed coordinate frame.

The attitude reference signal is defined in its coordinate frame using the rotation matrix R_r and its kinematics can be obtained using (4.1):

$$\dot{R}_r = R_r \overset{\triangle}{\omega}_r \tag{3.91}$$

where $\omega_r \in \mathbb{R}^3$ is the attitude reference angular velocity vector, and $\overset{\triangle}{\omega}_r$ denotes its hat map.

Remark 3.5 In this section, we consider the following model for the inertia matrix of the spacecraft:

$$I = I_0 + \sum_{i=1}^{n} \psi_i I_i \tag{3.92}$$

where I_0 is the inertia matrix for the rigid part of the spacecraft and it is assumed to be constant. Each term inside the summation in (3.92) contains the effects of the nonrigid parts of the spacecraft on the total inertia of the system. I is required to satisfy the basic properties of an inertia matrix, i.e. it needs to be symmetric positive definite and satisfy the triangle inequalities for the diagonal entries. We assume that the values of $I_i, i \in \{0, 1, \cdots, n\}$ are unknown constant matrices and ψ_i are time varying functions which can be measured at each time instant.

Model (3.92) encompasses many practical situations. For instance, consider the case of a rigid spacecraft which deploys multiple moving bodies. Let $r_i(t)$ denote the position of the center of mass (CM) of the i^{th} moving body with respect to the CM of the main part of the spacecraft and $I_{m,i}$ represent the inertia matrix of the i^{th} body with respect to its principal axis. Then, under the assumptions that attitudes of the moving bodies are fixed within the spacecraft body frame coordinate $\mathcal{B}$ and the position of the CM remains unchanged, i.e. $\sum_{i=1}^{n} r_i(t) m_i = 0$($m_i$ is the mass of i^{th} body.). Using parallel axis theorem, we can write

$$I = \underbrace{\left(I_{main} + \sum_{i=1}^{n} I_{m,i} \right)}_{I_0} + \sum_{i=1}^{n} \left[r_i^T r_i I_{3\times 3} - r_i r_i^T \right] m_i \tag{3.93}$$

where I_{main} represents the inertia matrix for the main body of the spacecraft with respect to the body fixed coordinate $\mathcal{B}$. Using differentiation with respect to time, the time varying model of the inertia of the spacecraft can be computed based on the knowledge of $r_i(t)$.

Another practical scenario with time varying inertial parameters is the case of massive

fuel usage. In general, obtaining an exact mathematical model for such a problem is quite difficult since the fuel expenditure process is subject to complex combustion reactions and sloshing effects, however, based on some simplifications, it is still possible to build a mathematical model for such behaviors. For instance, consider an spacecraft for which the CM of its fuel tank is located at the position r_T with respect to the CM of the spacecraft. Also, assume that the inertial principle axis of the fuel tank is parallel with the body axis of the spacecraft. As a first attempt to model the fuel usage of the spacecraft, it is possible to use the following linear approximation which is first proposed in [99]:

$$\dot{m}_T = -c_1 \|M\|, \quad m_T(0) = m_0 > 0, \ c_1 > 0 \tag{3.94}$$

where c_1 is an unknown constant and m_0 is the initial mass of the fuel tank. The model (3.94) simply expresses the fuel rate as a linear function of the norm of the control moment which is exerted on the spacecraft. Another model which can be used in this regard is as follows

$$\dot{m}_T = -c_1 \|M\| + \sum_{i=2}^{n} c_i \|M\|^i, \qquad \|c_2\|, \cdots, \|c_n\| << c_1 \tag{3.95}$$

where the norm of $c_i, i \geq 2$ are assumed to be small compared with c_1. Note that the r.h.s of (3.95) can become positive for large $\|M\|$, however, since in practice the norm of M always has an upper bound M_{max}, it is possible to use (3.95) to handle small deviation from the linear model (3.94) using sufficiently small values for $c_i, i \geq 2$.

The moment of inertia of the fuel tank, I_T can be calculated based on the mass distribution of the fuel inside the tank. As the next step of simplification, it is assumed that the density of the fuel and its time derivative are uniform within the tank. Using this assumption and the definition of principle moment of inertia, in [99], it is shown that for (3.94), the time derivative of the I_T can be obtained as follows

$$\dot{I}_T = -c_1 diag\{f_1, f_2, f_3\} \|M\|, \quad f_i > 0 \tag{3.96}$$

where the constants f_i are dependent on the geometry of the fuel tank ($f_i = \frac{1}{V}\int x_i^2\, dV$, x_i is measured along the i^{th} principle axis of the tank). As an example, for a spherical tank, all f_i are equal to $\frac{2}{5}R^2$. For model (3.95), (3.96) will be changed as

$$\dot{I}_T = \left(-c_1 \|M\| + \sum_{i=2}^{n} c_i \|M\|^i\right) diag\{f_1, f_2, f_3\}. \tag{3.97}$$

Using the parallel axis theorem, for the inertia matrix $I_{T,C}$ of fuel tank with respect to the CM of the spacecraft, C, we can write

$$\begin{aligned} &I_{T,C} = I_T + m_T\left[r_T^T r_T I_{3\times 3} - r_T r_T^T\right] \\ &\Rightarrow \dot{I}_{T,C} = \dot{I}_T + \left(-c_1 \|M\| + \sum_{i=2}^{n} c_i \|M\|^i\right)\left[r_T^T r_T I_{3\times 3} - r_T r_T^T\right] \\ &= \left(-c_1 \|M\| + \sum_{i=2}^{n} c_i \|M\|^i\right)\left[diag\{f_1, f_2, f_3\} + r_T^T r_T I_{3\times 3} - r_T r_T^T\right] \end{aligned} \tag{3.98}$$

defining $\alpha_1 = diag\{f_1, f_2, f_3\} + r_T^T r_T I_{3\times 3} - r_T r_T^T$, the following linear parametric model is derived from (3.98)

$$\dot{I}_{T,C} = \sum_{i=1}^{n} I_i \dot{\psi}_i,\ I_1 = -\alpha_1 c_1 I_{3\times 3},\ \dot{\psi}_1 = \alpha_1 \|M\| I_{3\times 3},\ I_i = c_i \alpha_1 I_{3\times 3},\ \dot{\psi}_i = I_{3\times 3}\|M\|^i,\ i \geq 2 \tag{3.99}$$

Remark 3.6 The approximation (3.95) is not the Taylor series expansion of $\dot{m}_T$ in terms of the variable $\|M\|$. The purpose of the higher order terms in this model is to enhance the accuracy of the modeling of $\dot{m}_T$. The values of $c_i, i \geq 2$ are assumed to be much smaller than c_1 to ensure negativity of $\dot{m}_T$ for the interval $(0, M_{max}]$. Each of $\dot{\psi}_i$ can be integrated with respect to time to find ψ_i based on the assumption that $\|M\|$ is available for measurement.

3.4.2 Attitude Control for Agents with Time-Varying Inertia

In this section we consider the reference attitude tracking control task for a spacecraft with unknown time varying inertia as modeled by (3.92). Here, the main objective is to design M in (3.90) in a way that ensures $R \to R_r$ and $\omega \to \omega_r$. Since it is more prevalent to express the attitude reference signal in its own coordinate frame, we need to design the angular velocity error vector in such a way that its components are described in body coordinate frame. Such an approach is first proposed in [100] for attitude control of a rigid spacecraft. Consider the following angular velocity error vector:

$$e_\omega = \omega - R^T R_r \omega_r. \tag{3.100}$$

From (3.100) it is clear that ω_r is brought into the body coordinate frame using the orthogonal transformation $R^T R_r$. Next, we need to define the attitude error vector to quantify the differences between the current orientation and attitude reference signal. As in the case of error vectors in $\mathbb{R}^n$, this can be achieved by first constructing the attitude configuration error function and using its derivative as an error vector. Such a function is constructed in [101] as follows:

$$\phi(R_r^T R) = \frac{1}{2} tr\left[K_p(I - R_r^T R)\right] \tag{3.101}$$

where K_p is a symmetric positive definite matrix with three distinct eigenvalues. The error function (3.101) is positive definite for all R and R_r and it becomes zero at $R = R_r$. Using (3.101), the time derivative of $\phi(\cdot)$ is derived as follows:

$$\begin{aligned}\frac{d\phi}{dt} &= \frac{1}{2} tr\left[-K_p \dot{R}_r^T R - K_p R_r^T \dot{R}\right] = \frac{-1}{2} tr\left[K_p \overset{\triangle}{\omega}_r^T R_r^T R + K_p R_r^T R \overset{\triangle}{\omega}\right] \\ &= \frac{-1}{2} tr\left[-K_p \overset{\triangle}{\omega}_r R_r^T R + K_p R_r^T R \overset{\triangle}{\omega}\right]\end{aligned} \tag{3.102}$$

where we have used the fact that $\overset{\triangle}{\omega}_r^T = -\overset{\triangle}{\omega}_r$. Using the identity $R\overset{\triangle}{x}R^T = [Rx]^\wedge$, we obtain

$$\frac{d\phi}{dt} = \frac{-1}{2}\left[K_p R_r^T R\left(\overset{\triangle}{\omega} - R^T R_r \overset{\triangle}{\omega}_r R_r^T R\right)\right] = \frac{-1}{2}\left[K_p R_r^T R \overset{\triangle}{e}_\omega\right]$$
$$= \frac{1}{2}\left(K_p R_r^T R - R^T R_r K_p\right)^\vee \cdot e_\omega \tag{3.103}$$

The last equality in (3.103) resulted from the fact that $tr\left[R\overset{\triangle}{x}\right] = -x^T(R - R^T)^\vee$. (3.103) suggests that attitude error vector can be chosen as

$$e_R = \frac{1}{2}\left[K_p R_r^T R - R^T R_r K_p\right]^\vee \tag{3.104}$$

Also, using the Rodriguez formula the following lemma is proved in [101].

Lemma 3.1 [101] The error function (3.101) satisfies the following:

1. $\phi(R_r^T R) = \phi(R^T R_r) \geq 0$
2. $\phi(\cdot) = 0$ if and only if $R_r^T R = I$, i.e. $R = R_r$
3. $\phi(\cdot)$ is a quadratic function, i.e. there exists c_1 and c_2 where

$$c_1 \|e_R\|^2 \leq \phi(R_r^T R) \leq c_2 \|e_R\|^2 \tag{3.105}$$

In Lemma 3.1, (1) ensures that the error function $\phi(\cdot)$ is always positive semi definite and its values are equal for the two rotation matrices representing the coordinate transformations between the body and angular reference coordinate frames. (2) guarantees that the error function will only vanish at the desired equilibrium point. Based on these characteristics it is possible to use $\phi(\cdot)$ as a part of attitude control Lyapunov function. (3) simply implies that the error function possess the quadratic structure and thus in the context of Lyapunov theory it can be used to find the convergence sets and design the nonlinear robust control

laws.

The attitude control design procedure is started by considering the following Lyapunov function

$$V = \frac{1}{2}e_\omega^T I e_\omega + (b_1 + b_2 d_1)\phi + b_2 \left(I e_\omega\right)^T e_R + \frac{1}{2}b_2^2 e_R^T I e_R + \sum_{i=0}^{n} \frac{1}{2k_i} tr\left[\tilde{I}_i^T \tilde{I}_i\right] \tag{3.106}$$

where b_1, b_2, d_1, k_i are positive constants. The main objective of the attitude control law is to make the time derivative of (3.106) negative semi definite. The fact that (3.106) is a positive definite function can be verified by using (3.105) and the bounds on the eigenvalues of the inertia matrix, i.e. $\sigma_{min} I_{3\times 3} \leq I(t) \leq \sigma_{max} I_{3\times 3}$. We have

$$x^T W x \leq V, W = \begin{bmatrix} c_1(b_1 + b_2 d_1) & -\frac{1}{2}b_2\sigma_{max} & 0 & \cdots & 0 \\ -\frac{1}{2}b_2\sigma_{max} & \frac{1}{2}\sigma_{min} & 0 & \cdots & 0 \\ 0 & 0 & \frac{1}{2k_0} & \cdots & 0 \\ \vdots & \vdots & \vdots & \vdots & \vdots \\ 0 & \cdots & \cdots & \cdots & \frac{1}{2k_n} \end{bmatrix} \tag{3.107}$$

where $x = \left[\|e_R\|, \|e_\omega\|, \left\|\tilde{I}_0\right\|_F, \cdots, \left\|\tilde{I}_n\right\|_F\right]^T \in \mathbb{R}^{n+3}$. Noting that $W > 0$, (3.107) clearly shows the positive definiteness of V. Next, consider the following control law

$$M = -b_1 e_R - d_1 e_\omega + \hat{I}\left[R^T R_r \dot{\omega}_r - \overset{\triangle}{\omega} R^T R_r \omega_r\right] + \omega \times \hat{I}\omega + \nu, \tag{3.108}$$

where the first two terms are proportional controllers which are built on $SO(3)$ using the modified attitude and angular error vectors, the next two terms are added for tracking the reference attitude and dealing with the inherent nonlinear dynamics of rotation. These terms consist of the estimation of the inertia matrix, i.e. $\hat{I} = \hat{I}_0 + \sum_{i=1}^{n} \psi_i \hat{I}_i$, which must be obtained from the Lyapunov design method. The term ν is added to counteract the time variations in inertia and will be designed later. In order to analyze the stability properties

of control law (3.108), we start by taking the derivative of each term in (3.106) with respect to time as follows

$$\begin{aligned}\frac{1}{2}\frac{d}{dt}\left[e_\omega^T I e_\omega\right] &= e_\omega^T I \dot{e}_\omega - \frac{1}{2}e_\omega^T\left(\sum_{i=1}^{n}\dot{\psi}_i I_i\right)e_\omega \\ &= e_\omega^T\left(M - \dot{I}\omega - \omega\times I\omega + I\overset{\triangle}{\omega}R^T R_r\omega_r - IR^T R_r\dot{\omega}_r\right) - \frac{1}{2}e_\omega^T\left(\sum_{i=1}^{n}\dot{\psi}_i I_i\right)e_\omega \end{aligned} \tag{3.109}$$

Using (3.103), the time derivative of the second term on the r.h.s of (3.106) is equal to $(b_1 + b_2 d_1)e_r \cdot e_\omega$. For the third term we have

$$\begin{aligned} b_2\frac{d}{dt}\left[Ie_\omega \cdot e_R\right] &= b_2\left[\left(\dot{I}e_\omega + I\dot{e}_\omega\right)\cdot e_R\right] + b_2\left[Ie_\omega\cdot\dot{e}_R\right] \\ &= b_2 e_R^T\dot{I}e_\omega + b_2 e_R^T\left(M - \dot{I}\omega - \omega\times I\omega + I\overset{\triangle}{\omega}R^T R_r\omega_r - IR^T R_r\dot{\omega}_r\right) + b_2\dot{e}_R^T I e_\omega \end{aligned} \tag{3.110}$$

For the fourth and fifth terms in (3.106) we have

$$\begin{aligned}\frac{d}{dt}\left[\frac{1}{2}b_2^2 e_R^T I e_R\right] &= b_2^2 e_R^T I\dot{e}_R + \frac{1}{2}b_2^2 e_R^T\dot{I}e_R, \\ \frac{d}{dt}\left[\sum_{i=0}^{n}\frac{1}{2k_i}tr\left[\tilde{I}_i^T\tilde{I}_i\right]\right] &= \sum_{i=0}^{n}\frac{1}{k_i}tr\left[\tilde{I}_i^T\dot{\tilde{I}}_i\right] = \sum_{i=0}^{n}\frac{1}{k_i}tr\left[\tilde{I}_i^T\dot{\hat{I}}_i\right]. \end{aligned} \tag{3.111}$$

Hence, the time derivative of (3.106) is

$$\begin{aligned}\dot{V} = (e_\omega + b_2 e_R)^T&\left(M - \dot{I}\omega - \omega\times I\omega + I\overset{\triangle}{\omega}R^T R_r\omega_r - IR^T R_r\dot{\omega}_r\right) - \frac{1}{2}e_\omega^T\left(\sum_{i=1}^{n}\dot{\psi}_i I_i\right)e_\omega \\ &+ b_2 e_R^T\dot{I}e_\omega + b_2\dot{e}_R^T I e_\omega + b_2^2 e_R^T I\dot{e}_R + \frac{1}{2}b_2^2 e_R^T\dot{I}e_R + \sum_{i=0}^{n}\frac{1}{k_i}tr\left[\tilde{I}_i^T\dot{\hat{I}}_i\right] + (b_1 + b_2 d_1)e_r\cdot e_\omega \end{aligned} \tag{3.112}$$

Substituting (3.108) in (3.112), we obtain

$$\dot{V} = (e_\omega + b_2 e_R)^T \left(- \left(\sum_{i=1}^{n} \dot{\psi}_i \tilde{I}_i \right) \omega + \omega \times \tilde{I}\omega - \tilde{I} \overset{\triangle}{\omega} R^T R_r \omega_r + \tilde{I} R^T R_r \dot{\omega}_r \right)$$
$$+ \frac{1}{2}(e_\omega + b_2 e_R)^T \left(\sum_{i=1}^{n} \dot{\psi}_i \tilde{I}_i \right) (e_\omega + b_2 e_R) + \sum_{i=0}^{n} \frac{1}{k_i} tr\left[\tilde{I}_i^T \dot{\hat{I}}_i \right] - d_1 \left\| e_\omega \right\|^2 - b_1 b_2 \left\| e_R \right\|^2$$
$$+ b_2 \dot{e}_R^T I e_\omega + b_2^2 e_R^T I \dot{e}_R \tag{3.113}$$

where we have chosen

$$\nu = \frac{1}{2} \left(\sum_{i=1}^{n} \dot{\psi}_i \hat{I}_i \right) (e_\omega + b_2 e_R) - \sum_{i=1}^{n} \dot{\psi}_i \hat{I}_i \omega \tag{3.114}$$

Next, using the identity $a \cdot (b \times c) = c \cdot (a \times c)$ we can stack the terms containing the adaptation parameters as follows:

$$\dot{V} = \sum_{i=1}^{n} tr \left[\tilde{I}_i (\frac{1}{k_i} \dot{\hat{I}}_i + \frac{1}{2} (e_\omega + b_2 e_R)(e_\omega + b_2 e_R)^T \dot{\psi}_i - R^T R_r \dot{\omega}_r (e_\omega + b_2 e_R)^T \psi_i \right.$$
$$\left. + \overset{\triangle}{\omega} R^T R_r \omega_r (e_\omega + b_2 e_R)^T \psi_i - \omega (e_\omega + b_2 e_R)^T \overset{\triangle}{\omega} \psi_i - \omega (e_\omega + b_2 e_R)^T \dot{\psi}_i) \right]$$
$$+ tr \left[\tilde{I}_0 (\frac{1}{k_0} \dot{\hat{I}}_0 + R^T R_r \dot{\omega}_r (e_\omega + b_2 e_R)^T - \overset{\triangle}{\omega} R^T R_r \omega_r (e_\omega + b_2 e_R)^T + \omega ((e_\omega + b_2 e_R) \times \omega)^T) \right]$$
$$+ b_2 \dot{e}_R^T I e_\omega + b_2^2 e_R^T I \dot{e}_R - d_1 \left\| e_\omega \right\|^2 - b_1 b_2 \left\| e_R \right\|^2 \tag{3.115}$$

Choosing the adaptive control law

$$\dot{\hat{I}}_i = -\frac{k_i}{2} \left(\Lambda_i + \Lambda_i^T \right), \qquad i \in \{0, \cdots, n\} \tag{3.116}$$
$$\Lambda_i = \frac{1}{2} (e_\omega + b_2 e_R)(e_\omega + b_2 e_R)^T \dot{\psi}_i - R^T R_r \dot{\omega}_r (e_\omega + b_2 e_R)^T \psi_i$$
$$+ \overset{\triangle}{\omega} R^T R_r \omega_r (e_\omega + b_2 e_R)^T \psi_i - \omega (e_\omega + b_2 e_R)^T \overset{\triangle}{\omega} \psi_i - \omega (e_\omega + b_2 e_R)^T \dot{\psi}_i \quad i \in \{1, \cdots, n\},$$
$$\Lambda_0 = R^T R_r \dot{\omega}_r (e_\omega + b_2 e_R)^T - \overset{\triangle}{\omega} R^T R_r \omega_r (e_\omega + b_2 e_R)^T + \omega ((e_\omega + b_2 e_R) \times \omega)^T,$$

(3.115) can be rewritten as

$$\dot{V} = b_2 \dot{e}_R^T I e_\omega + b_2^2 e_R^T I \dot{e}_R - d_1 \left\| e_\omega \right\|^2 - b_1 b_2 \left\| e_R \right\|^2 . \tag{3.117}$$

Further analysis of (3.117) leads to Theorem 3.4 below, in proving which, we use the following lemma:

Lemma 3.2 [102] Consider $A, B \in \mathbb{R}^{n\times n}$ where $B = B^T > 0$. Then,

$$\frac{1}{2}\lambda_1(A + A^T)tr(B) \leq tr(AB) \leq \frac{1}{2}\lambda_n(A + A^T)tr(B). \tag{3.118}$$

where $\lambda_i(R)$ denotes the i^{th} largest eigenvalue of the matrix R.

Theorem 3.4 Consider the dynamics (3.90),(3.91) and error variables (3.100),(3.104) together with control law (3.108) and adaptive law (3.116), then the error signals and their time derivatives are bounded i.e. $e_R, \dot{e}_R, e_\omega, \dot{e}_\omega \in \mathcal{L}_\infty$. Moreover, $e_R, e_\omega \in \mathcal{L}_2$ and $e_\omega, e_R \to 0$.

Proof. Differentiating (3.104) with respect to time results in

$$\dot{e}_R = \frac{1}{2}\left[-K_p \overset{\triangle}{\omega}_r R_r^T R + K_p R_r^T R \overset{\triangle}{\omega} + \overset{\triangle}{\omega} R^T R_r K_p - R^T R_r \overset{\triangle}{\omega}_r K_p\right]^\vee . \tag{3.119}$$

using the facts that $R \overset{\triangle}{x} R^T = [Rx]^\wedge$ and $\overset{\triangle}{x} R + R^T \overset{\triangle}{x} = [(tr[R]I - R)x]^\wedge$, (3.119) can be rewritten as

$$\dot{e}_R = \frac{1}{2}\left[tr\left(R^T R_r K_p\right) I - R^T R_r K_p\right] e_\omega. \tag{3.120}$$

To calculate the upper bound for the term $\left[tr\left(R^T R_r K_p\right) I - R^T R_r K_p\right]$, we start by calculating its Frobenious norm as follows

$$\left\| tr\left(R^T R_r K_p\right) I - R^T R_r K_p \right\|_F = \frac{1}{2}\sqrt{tr\left[K_p^2\right] + \left(tr[R^T R_r K_p]\right)^2} \tag{3.121}$$

Since $-3 \leq \lambda_i(R^T R_r + R_r^T R) \leq 3$, choosing $A = R^T R_r$ and $B = K_p$ and invoking Lemma 3.2, we have

$$\begin{aligned} &\left\| \left[tr\left(R^T R_r K_p\right) I - R^T R_r K_p \right] \right\|_2^2 \leq \left\| \left[tr\left(R^T R_r K_p\right) I - R^T R_r K_p \right] \right\|_F^2 \\ &\leq \frac{1}{4}\left(tr\left[K_p^2\right] + b_3 \left(tr[K_p]\right)^2 \right) \end{aligned} \tag{3.122}$$

for ($b_3 = \frac{9}{4}$). Using (3.122) in (3.117), we obtain

$$\begin{aligned} \dot{V} &\leq \left(\frac{b_2 \sigma_{max} \sqrt{tr\left[K_p^2\right] + b_3 \left(tr[K_p]\right)^2}}{2} - d_1 \right) \|e_\omega\|^2 - b_1 b_2 \|e_R\|^2 \\ &+ \frac{b_2^2 \sigma_{max} \sqrt{tr\left[K_p^2\right] + b_3 \left(tr[K_p]\right)^2}}{2} \|e_\omega\| \|e_R\| \\ &\leq - \begin{bmatrix} \|e_\omega\| \\ \|e_R\| \end{bmatrix}^T \begin{bmatrix} b_1 b_2 & \frac{-b_2^2 \sigma_{max} \sqrt{tr\left[K_p^2\right] + b_3 \left(tr[K_p]\right)^2}}{4} \\ \frac{-b_2^2 \sigma_{max} \sqrt{tr\left[K_p^2\right] + b_3 \left(tr[K_p]\right)^2}}{4} & d_1 - \frac{b_2 \sigma_{max} \sqrt{tr\left[K_p^2\right] + b_3 \left(tr[K_p]\right)^2}}{2} \end{bmatrix} \begin{bmatrix} \|e_\omega\| \\ \|e_R\| \end{bmatrix} \end{aligned} \tag{3.123}$$

The parameter b_2 must be chosen in a way that ensures

$$Q = \begin{bmatrix} b_1 b_2 & \frac{-b_2^2 \sigma_{max} \sqrt{S}}{4} \\ \frac{-b_2^2 \sigma_{max} \sqrt{S}}{4} & d_1 - \frac{b_2 \sigma_{max} \sqrt{S}}{2} \end{bmatrix} > 0. \tag{3.124}$$

where $S = tr\left[K_p^2\right] + b_3 \left(tr[K_p]\right)^2$. (3.124) is achieved if

$$\begin{aligned} &b_2 > 0, \quad b_2 \left(b_1 d_1 - \frac{b_1 b_2 \sigma_{max} \sqrt{s}}{2} - \frac{s b_2^3 \sigma_{max}^2}{16} \right) > 0, \\ &d_1 - \frac{b_2 \sigma_{max} \sqrt{s}}{2} \geq 0, \quad \frac{c_1 (b_1 + b_2 d_1) \sigma_{min}}{2} - \frac{1}{4} b_2^2 \sigma_{max}^2 \geq 0. \end{aligned} \tag{3.125}$$

To satisfy (3.125), we can choose b_2 as follows:

$$\begin{aligned} b_2 &= \min \left(\frac{b_1 d_1}{2\gamma}, \sqrt[3]{\frac{b_1 d_1}{2\gamma}}, \frac{2 d_1}{\sigma_{max} \sqrt{s}}, \frac{c_1 d_1 \sigma_{min} + \sqrt{c_1^2 d_1^2 \sigma_{min}^2 + 2 c_1 b_1 \sigma_{min} \sigma_{max}^2}}{\sigma_{max}^2} \right), \\ \gamma &= \max \left(\frac{3 b_1 \sigma_{max}}{\sqrt{2}}, \frac{9 \sigma_{max}^2}{8} \right) \end{aligned} \tag{3.126}$$

(3.126) results in $\dot{V} \leq -z^T Q z \leq 0$ where $z = [\|e_R\|, \|e_\omega\|]^T$. From the fact that the Lyapunov function V is positive definite, the latter implies that V will converge to a limit $V(\infty)$ and hence, e_R,e_ω,$\tilde{I}_i, \hat{I}_i$ $i \in \{0, \cdots, n\}$ belong to $\mathcal{L}_\infty$. Integrating (3.123) from 0 to ∞ results in

$$V(\infty) - V(0) \leq \int_0^\infty -z^T Q z \, dt, \quad \Rightarrow z \in \mathcal{L}_2 \quad \Rightarrow e_R, e_\omega \in \mathcal{L}_2 \tag{3.127}$$

The closed loop system for angular velocity error (3.100), can be rewritten as follows:

$$\begin{aligned} I\dot{e}_\omega = &-b_1 e_R - d_1 e_\omega + \omega \times \tilde{I}\omega - \tilde{I} \overset{\triangle}{\omega} R^T R_r \omega_r + \tilde{I} R^T R_r \dot{\omega}_r + \left(\sum_{i=1}^{n} \dot{\psi}_i I_i \right) (e_\omega + R^T R_r \omega_r) \\ &+ \frac{1}{2} \left(\sum_{i=1}^{n} \dot{\psi}_i \hat{I}_i \right) (e_\omega + b_2 e_R). \end{aligned} \tag{3.128}$$

since e_R,e_ω,$\tilde{I}_i, \hat{I}_i \in \mathcal{L}_\infty$, from (3.128) and (3.120), we deduce that $\dot{e}_\omega, \dot{e}_R \in \mathcal{L}_\infty$. Finally, since $\dot{e}_\omega, \dot{e}_R \in \mathcal{L}_\infty$ and $e_\omega, e_R \in \mathcal{L}_\infty \cap \mathcal{L}_2$, we can conclude that $e_\omega, e_R \to 0$.

Note here that convergence of e_R to zero does not guarantee the convergence of R to R_r. As stated in Preposition 11.31 of [101], there exist three undesired equilibriums at $R_r e^{\pi \overset{\triangle}{\nu}_j}$ where ν_j denotes the j^{th} eigenvector of K_P. In the next step of the analysis, we establish that such equilibrium points are unstable:

For any of the three undesirable equilibrium points we have

$$(e_\omega \to 0, R \to R_r e^{\pi \overset{\triangle}{\nu}_j}) \Rightarrow V_{uns} = (b_1 + d_1 b_2)\phi(R_r e^{\pi \overset{\triangle}{\nu}_j}) + \sum_{i=0}^{n} \frac{1}{2k_i} tr\left[\tilde{I}_i^T \tilde{I}_i\right] = cte \tag{3.129}$$

where the last part results from the fact that $V(\cdot)$ is a positive definite function with negative semi definite derivative. From the Rodriguez formula we can write

$$\phi(R_r e^{\pi \overset{\triangle}{\nu}_j}) = \frac{1}{2} tr\left(K_p \left(I - I - \sin(\pi) \overset{\triangle}{\nu}_j - (1 - \cos(\pi)) \overset{\triangle^2}{\nu}_j \right) \right) = -tr\left(K_p \overset{\triangle^2}{\nu}_j \right) \tag{3.130}$$

Using the identities $R \overset{\triangle}{x} R^T = [Rx]^\wedge$ and $\overset{\triangle}{x} R + R^T \overset{\triangle}{x} = [(tr[R]I - R)\, x]^\wedge$, we have

$$\phi(R_r e^{\pi \overset{\triangle}{\nu}_j}) = -tr((K_p \overset{\triangle}{\nu}_j) \overset{\triangle}{\nu}_j) = \nu_j \cdot \left(K_p \overset{\triangle}{\nu}_j + \overset{\triangle}{\nu}_j K_p \right)^\vee = \nu_j^T (tr(K_p)I - K_p)\nu_j$$

$$= tr(K_p) - \lambda_j(K_p) \tag{3.131}$$

Using (3.131) in (3.129) results in

$$V_{uns} = (b_1 + d_1 b_2)\,(tr(K_p) - \lambda_j(K_p)) + \sum_{i=0}^{n} \frac{1}{2k_i} tr\left[\tilde{I}_i^T \tilde{I}_i\right]$$

$$\geq (b_1 + d_1 b_2)\,(tr(K_p) - \lambda_j(K_p)) > 0 \tag{3.132}$$

For a small neighborhood around the undesired equilibrium, i.e $(e_\omega = 0, R = R_r e^{\pi \overset{\triangle}{\nu}_j})$ the function

$$V' = (b_1 + d_1 b_2)\,(tr(K_p) - \lambda_j(K_p)) - V \tag{3.133}$$

is positive for some R due to the fact that $\phi(R_r^T R)$ is a continuous function. The time derivative of (3.133), clearly satisfies

$$\dot{V}' = -\dot{V} > 0, \quad e_R, e_\omega \neq 0. \tag{3.134}$$

Using Chetaev Theorem [34], instability of the undesired equilibrium follows. The latter indicates that the attitude of the spacecraft will track the reference signal $R_r(t)$ from almost all initial conditions except $R(0) = R_r(0)e^{\pi \overset{\triangle}{\nu}_j}$. This result can be summarized in the following theorem.

Theorem 3.5 The undesired equilibriums of the error systems (3.128) and (3.120) which are located at $R(0) = R_r(0)e^{\pi \overset{\triangle}{\nu}_j}$ are unstable.

Remark 3.7 Compared with [103] where K_p is chosen to be a diagonal positive definite matrix for controlling the attitude of a rigid body, here, by using Lemma.3.2, the only

restriction which we assumed on the structure of the error function $\phi(\cdot)$ is to be symmetric and positive semi definite. This can lead to much less restrictive conditions on the allowable bounds on the control parameters.

Remark 3.8 We can improve the bounds on the term $tr(R^T R_r K_p)$ using the method which is first introduced in [104]. To see this, consider the following relation

$$\begin{aligned} tr(R^T R_r(K_p - \lambda_{min}(K_p))) &= tr(\text{SYM}(R^T R_r)(K_p - \lambda_{min}(K_p))) \\ &\leq \lambda_1(\text{SYM}(R^T R_r))tr(K_p) - 3\lambda_{min}(K_p)\lambda_1(\text{SYM}(R^T R_r)) \end{aligned} \tag{3.135}$$

where $\lambda_1(\cdot)$ denotes the first largest eigenvalue of a matrix and $\text{SYM}(\cdot)$ denotes the symmetric part of a square matrix. We can rewrite (3.135) as follows

$$tr(R^T R_r K_p) \leq \lambda_1(\text{SYM}(R^T R_r))tr(K_p) - \underbrace{\sum_{i=1}^{3}(\lambda_1(\text{SYM}(R^T R_r)) - \lambda_i(R^T R_r))}_{\geq 0} \tag{3.136}$$

Since the second term on the r.h.s of (3.136) is positive semi definite, it represents a tighter upper bound compared with (3.118). It is also possible to find a better lower bound for the l.h.s of (3.118) using the same procedure.

3.4.3 Robust Adaptive Control Using σ-modification

In this section we design a robust adaptive algorithm to enhance the robustness of the adaptive controller designed in Section 3.4.2. We start by modifying the σ-modification method [91] to prove the exponential stability of the system. First, instead of (3.116)

consider the following adaptive laws

$$\dot{\hat{I}}_i = -\frac{k_i}{2}\left(\Lambda_i + \Lambda_i^T\right) - k_i\sigma_{si}\hat{I}_i, \qquad i \in \{0, \cdots, n\} \tag{3.137}$$

$$\sigma_{si} = \begin{cases} 0 & \left\|\hat{I}_i\right\|_F < M_{0i} \\ \sigma_{0i}\left(\frac{\left\|\hat{I}_i\right\|_F}{M_{0i}} - 1\right) & M_{0i} \leq \left\|\hat{I}_i\right\|_F \leq 2M_{0i} \\ \sigma_{0i} & \left\|\hat{I}_i\right\|_F \geq 2M_{0i} \end{cases}$$

Using (3.137) in (3.115), we have

$$\dot{V} = b_2\dot{e}_R^T I e_\omega + b_2^2 e_R^T I \dot{e}_R - d_1\left\|e_\omega\right\|^2 - b_1 b_2\left\|e_R\right\|^2 - \sum_{i=0}^{n}\sigma_{si}tr[\tilde{I}_i\hat{I}_i]. \tag{3.138}$$

Further analysis of (3.138) leads to the following theorem:

Theorem 3.6 Consider the dynamics (3.90),(3.91) and error variables (3.100),(3.104) together with control law (3.108) and adaptive law (3.137), then the error signals and their time derivatives are bounded i.e. $e_R, \dot{e}_R, e_\omega, \dot{e}_\omega \in \mathcal{L}_\infty$. Moreover, $e_R, e_\omega \in \mathcal{L}_2$ and $e_\omega, e_R \to 0$.

Proof. Using the Cauchy-Shwartz inequality for the inner product $< A, B >= tr[A^T B]$, we have

$$\begin{aligned}\sigma_{si}tr[\tilde{I}_i\hat{I}_i] &\geq \sigma_{si}\left\|\hat{I}_i\right\|_F^2 - \sigma_{si}tr[\hat{I}_i I_i] \geq \sigma_{si}\left\|\hat{I}_i\right\|_F^2 - \sigma_{si}\left|tr[\hat{I}_i I_i]\right| \geq \sigma_{si}\left\|\hat{I}_i\right\|_F^2 - \sigma_{si}\left\|\hat{I}_i\right\|_F\left\|I_i\right\|_F \\ &\geq \sigma_{si}\left\|\hat{I}_i\right\|_F\left(\left\|\hat{I}_i\right\|_F - M_{0i}\right) + \sigma_{si}\left\|\tilde{I}_i\right\|_F\left(M_{0i} - \left\|I_i\right\|_F\right)\end{aligned} \tag{3.139}$$

recalling the fact that $M_{0i} \geq \left\|I_i\right\|_F$, $\sigma_{si} \geq 0$ and $\sigma_{si}\left(\left\|\hat{I}_i\right\|_F - M_{0i}\right) \geq 0$ we can conclude that $-\sigma_{si}tr[\tilde{I}_i I_i] \leq 0$ and hence the last term in (3.138) can only make it more negative. Also, using the structure of (3.137), we have

$$-\sigma_{si}tr[\tilde{I}_i\hat{I}_i] \leq -\sigma_{0i}tr[\tilde{I}_i\hat{I}_i] + 6\sigma_{0i}M_{0i}^2 \tag{3.140}$$

using (3.140) in (3.138), we have

$$\dot{V} \leq b_2 \dot{e}_R^T I e_\omega + b_2^2 e_R^T I \dot{e}_R - d_1 \left\| e_\omega \right\|^2 - b_1 b_2 \left\| e_R \right\|^2 - \sum_{i=0}^{n} \sigma_{0i} tr[\tilde{I}_i \hat{I}_i] + \sum_{i=0}^{n} 6\sigma_{0i} M_{0i}^2$$
$$\leq b_2 \dot{e}_R^T I e_\omega + b_2^2 e_R^T I \dot{e}_R - d_1 \left\| e_\omega \right\|^2 - b_1 b_2 \left\| e_R \right\|^2 - \sum_{i=0}^{n} \sigma_{0i} tr[\tilde{I}_i \tilde{I}_i]$$
$$+ \sum_{i=0}^{n} \left| \sigma_{0i} tr[\tilde{I}_i I_i] \right| + \sum_{i=0}^{n} 6\sigma_{0i} M_{0i}^2 \tag{3.141}$$

Next, using the Young inequality of trace [105], i.e. $tr[A^T B] \leq \frac{1}{2} tr[A^T A] + \frac{1}{2} tr[B^T B]$ we have :

$$\dot{V} \leq b_2 \dot{e}_R^T I e_\omega + b_2^2 e_R^T I \dot{e}_R - d_1 \left\| e_\omega \right\|^2 - b_1 b_2 \left\| e_R \right\|^2 - \frac{1}{2} \sum_{i=0}^{n} \sigma_{0i} tr[\tilde{I}_i \tilde{I}_i]$$
$$+ \frac{1}{2} \sum_{i=0}^{n} \sigma_{0i} tr[I_i I_i] + \sum_{i=0}^{n} 6\sigma_{0i} M_{0i}^2 \tag{3.142}$$

defining the vector $\hat{z} = [\left\| e_R \right\|, \left\| e_\omega \right\|, \left\| \tilde{I}_0 \right\|_F, \cdots, \left\| \tilde{I}_n \right\|_F]$ and using the identity $\left\| A \right\|_2 \leq \left\| A \right\|_F \leq \sqrt{r} \left\| A \right\|_2$ for $A \in \mathbb{R}^r$, (3.142) turns into

$$\dot{V} \leq -\hat{z}^T Q' \hat{z} + \frac{3}{2} \sum_{i=0}^{n} \sigma_{0i} \sigma_{max}^2 + \sum_{i=0}^{n} 6\sigma_{0i} M_{0i}^2 \tag{3.143}$$

again, we choose b_2 such that for $Q' \in \mathbb{R}^{n+3 \times n+3}$ we can write

$$Q' = \begin{bmatrix} b_1 b_2 & \frac{-b_2^2 \sigma_{max} \sqrt{S}}{4} & 0 & \cdots & 0 \\ \frac{-b_2^2 \sigma_{max} \sqrt{S}}{4} & d_1 - \frac{b_2 \sigma_{max} \sqrt{S}}{2} & 0 & \cdots & 0 \\ 0 & 0 & \frac{1}{2}\sigma_{00} & \cdots & 0 \\ \vdots & \vdots & \vdots & \vdots & \vdots \\ 0 & 0 & 0 & 0 & \frac{1}{2}\sigma_{0n} \end{bmatrix} > 0 \tag{3.144}$$

for Lyapunov function (3.106) we have

$$x^T W' x \geq V, W' = \begin{bmatrix} c_1(b_1 + b_2 d_1) & \frac{1}{2} b_2 \sigma_{max} & 0 & \cdots & 0 \\ \frac{1}{2} b_2 \sigma_{max} & \frac{1}{2} \sigma_{max} & 0 & \cdots & 0 \\ 0 & 0 & \frac{1}{2k_0} & \cdots & 0 \\ \vdots & \vdots & \vdots & \vdots & \vdots \\ 0 & \cdots & \cdots & \cdots & \frac{1}{2k_n} \end{bmatrix} \tag{3.145}$$

hence, using (3.145), (3.143) can be rewritten as follows

$$\begin{aligned} \dot{V} &\leq -\frac{\lambda_{min}(Q')}{\lambda_{max}(W')} V + \sum_{i=0}^{n} \left(\frac{3}{2} \sigma_{0i} \sigma_{max}^2 + 6 \sigma_{0i} M_{0i}^2 \right) \\ \Rightarrow V &\leq V(0) exp(-\frac{\lambda_{min}(Q')}{\lambda_{max}(W')} t) + \frac{\lambda_{max}(W')}{\lambda_{min}(Q')} \sum_{i=0}^{n} \left(\frac{3}{2} \sigma_{0i} \sigma_{max}^2 + 6 \sigma_{0i} M_{0i}^2 \right) \end{aligned} \tag{3.146}$$

which clearly demonstrates the exponential convergence of V to the set

$$\left\{ V \in \mathbb{R} | V \leq \frac{\lambda_{max}(W')}{\lambda_{min}(Q')} \sum_{i=0}^{n} \left(\frac{3}{2} \sigma_{0i} \sigma_{max}^2 + 6 \sigma_{0i} M_{0i}^2 \right) \right\} \tag{3.147}$$

it is clear that the size of this set can be controlled by choosing small values for σ_{0i}. To complete the boundedness argument for the dynamics (3.90) we need to find the region of attraction for the adaptive control law (3.108) and (3.137). At the desired equilibrium point the value of ϕ becomes zero and at the other equilibrium points of the system it becomes $tr(K_p) - \lambda_i K_p$ for $i \in \{1, 2, 3\}$, this suggests that the for $\phi < \beta < \min_i (tr(K_p) - \lambda_i K_p)$ the following set

$$\left\{ V \in \mathbb{R} | V \leq \frac{\beta}{c_2} \lambda_{min}(W') \right\} \tag{3.148}$$

becomes an invariant set if

$$\frac{\lambda_{max}(W')}{\lambda_{min}(Q')} \sum_{i=0}^{n} \left(\frac{3}{2} \sigma_{0i} \sigma_{max}^2 + 6 \sigma_{0i} M_{0i}^2 \right) \leq \frac{\beta}{c_2} \lambda_{min}(W') \tag{3.149}$$

and hence, we can assure that $\phi < \beta$ for all time. (3.149) can be satisfied by choosing small values for σ_{0i}

Remark 3.9 From (3.137) it is clear that when the norm of the estimated inertia tensors $\hat{I}_i$ are below the previously known upperbound, i.e $\left\|\hat{I}_i\right\|_F \leq M_{0i}$ then there is no need to modify (3.116) with the additive term $-k_i\sigma_{si}\hat{I}_i$ since the objective of the modification term is to prevent the drift of the estimated inertia matrices. In [91] it is shown that in comparison with the fixed modification approach, such a strategy preserves the ideal convergence properties of the adaptive laws.

3.4.4 Geometric Parameter Projection

In this section we design an adaptive projection algorithm which is suited for the geometric adaptive control law (3.137). Compared to the classic projection method we need to replace the 2-norm with the Frobenious norm to perform the algebraic manipulation. we start by considering the convex set $S = \left\{\hat{I} \in \mathbb{R}^{3\times 3} | \left\|\hat{I}\right\|_F^2 \leq \epsilon\right\}$ for which we can express the following Lemma

Lemma 3.3 Consider an arbitrary member $\hat{I}_*$ inside the set S, i.e. $tr(\hat{I}_*^T\hat{I}_*) \leq \epsilon$ together with an arbitrary boundary member $\hat{I}_b$ where $tr(\hat{I}_b^T\hat{I}_b) = \epsilon$, then we can write

$$tr\left[(\hat{I}_* - \hat{I}_b)^T\hat{I}_b\right] \leq 0 \tag{3.150}$$

Proof. For all $0 \leq \lambda \leq 1$, we have

$$\left\|\lambda\hat{I}_* + (1-\lambda)\hat{I}_b\right\|_F^2 \leq \lambda\left\|\hat{I}_*\right\|_F^2 + (1-\lambda)\left\|\hat{I}_b\right\|_F^2, \tag{3.151}$$

which can be rearranged as

$$\left\|\hat{I}_b + \lambda\left(\hat{I}_* - \hat{I}_b\right)\right\|_F^2 \leq \left\|\hat{I}_b\right\|_F^2 + \lambda\left(\left\|\hat{I}_*\right\|_F^2 - \left\|\hat{I}_b\right\|_F^2\right). \tag{3.152}$$

Since (3.152) holds for all $0 < \lambda \leq 1$, we have

$$\lim_{\lambda \to 0} \frac{\left\| \hat{I}_b + \lambda \left(\hat{I}_* - \hat{I}_b \right) \right\|_F^2 - \left\| \hat{I}_b \right\|_F^2}{\lambda} = tr \left[\left(\hat{I}_* - \hat{I}_b \right)^T \hat{I}_b \right] \leq \left\| \hat{I}_* \right\|_F^2 - \epsilon \leq 0, \tag{3.153}$$

where we have used the fact that for $f : \mathbb{R}^{3\times 3} \to \mathbb{R}$ the directional derivative in the direction of $f_1 \in \mathbb{R}^{3\times 3}$ is expressed as $tr\left((\nabla f)^T f_1\right)$ and $\frac{\partial}{\partial X} tr(X^T B X) = BX + B^T X$.

Using the inner product $< A, B >= tr[A^T B]$ the modified projection algorithm can be expressed as follows

$$\begin{aligned} \dot{\hat{I}}_i &= PR\left(\hat{I}_i, \frac{-k_i}{2}(\Lambda_i + \Lambda_i^T) \right) \\ &= \begin{cases} \frac{-k_i}{2}(\Lambda_i + \Lambda_i^T) - \frac{\hat{I}_i tr\left[\hat{I}_i^T \left(\frac{-k_i}{2}(\Lambda_i + \Lambda_i^T)\right)\right]}{tr\left[\hat{I}_i^T \hat{I}_i\right]} & \left(\left\| \hat{I}_i \right\|_F^2 - \epsilon > 0 \wedge tr\left[\hat{I}_i^T \left(\frac{-k_i}{2}(\Lambda_i + \Lambda_i^T) \right) \right] > 0 \right) \\ \frac{-k_i}{2}(\Lambda_i + \Lambda_i^T) & otherwise \end{cases} \end{aligned} \tag{3.154}$$

again as in the case of the projection algorithms which are built based on the norm $\|\cdot\|_2$ we can show that the following lemma holds

Lemma 3.4 The following inequality is true for (3.154)

$$tr\left[\left(\hat{I}_i - \hat{I}_{i,*} \right)^T \left(PR\left(\hat{I}_i, \frac{-k_i}{2}(\Lambda_i + \Lambda_i^T) \right) - \frac{-k_i}{2}(\Lambda_i + \Lambda_i^T) \right) \right] \leq 0 \tag{3.155}$$

to prove Lemma 3.4 first consider the case $\left(\left\| \hat{I}_i \right\|_F^2 - \epsilon > 0 \wedge tr\left[\hat{I}_i^T \left(\frac{-k_i}{2}(\Lambda_i + \Lambda_i^T) \right) \right] > 0 \right)$

$$tr\left[\left(\hat{I}_{i,*} - \hat{I}_i \right)^T \left(\frac{-k_i}{2}(\Lambda_i + \Lambda_i^T) - \left(\frac{-k_i}{2}(\Lambda_i + \Lambda_i^T) - \frac{\hat{I}_i tr\left[\hat{I}_i^T \left(\frac{-k_i}{2}(\Lambda_i + \Lambda_i^T) \right) \right]}{tr\left[\hat{I}_i^T \hat{I}_i \right]} \right) \right) \right] \tag{3.156}$$

which can be rewritten as follows

$$\frac{tr\left[\left(\hat{I}_{i,*} - \hat{I}_i \right)^T \hat{I}_i \right] tr\left[\hat{I}_i^T \left(\frac{-k_i}{2}(\Lambda_i + \Lambda_i^T) \right) \right]}{tr\left[\hat{I}_i^T \hat{I}_i \right]} \leq 0 \tag{3.157}$$

Using the projection algorithm (3.154), $\hat{I}_i(t)$ never leaves the set S_i. This can be seen by taking derivative of the convex function $V_1 = \left\|\hat{I}_i\right\|_F^2 - \epsilon$ as follows

$$\dot{V}_1 = tr\left[\hat{I}_i^T PR\left(\hat{I}_i, \frac{-k_i}{2}(\Lambda_i + \Lambda_i^T)\right)\right] \tag{3.158}$$

which becomes zero if the trajectories of $\hat{I}_i$ leaves S_i

$$\left\|\hat{I}_i\right\|_F^2 - \epsilon \geq 0 \Rightarrow \dot{V}_1 = tr\left[\hat{I}_i^T\left(\frac{-k_i}{2}(\Lambda_i + \Lambda_i^T) - \frac{\hat{I}_i tr\left[\hat{I}_i^T\left(\frac{-k_i}{2}(\Lambda_i + \Lambda_i^T)\right)\right]}{tr\left[\hat{I}_i^T\hat{I}_i\right]}\right)\right] = 0 \tag{3.159}$$

Using the previous results, we can use the projection algorithm with the adaptive law (3.116) to ensure both the stability of the system and the restriction of $\left\|\hat{I}_i\right\|$ to the S_i. This can be shown by taking the time derivative of (3.106) as follows

$$\begin{aligned}\dot{V} \leq\ & b_2 \dot{e}_R^T I e_\omega + b_2^2 e_R^T I \dot{e}_R - d_1 \|e_\omega\|^2 - b_1 b_2 \|e_R\|^2 \\ & + \sum_{i=0}^{n} tr\left[\tilde{I}_i\left(PR\left(\hat{I}_i, \frac{-k_i}{2}(\Lambda_i + \Lambda_i^T)\right) + \frac{k_i}{2}(\Lambda_i + \Lambda_i^T)\right)\right]\end{aligned} \tag{3.160}$$

where using lemma 3.4 and choosing b_2 as in (3.126) results in $\dot{V} \leq -z^T Q z \leq 0$. Using the same argument as in section. 3.4.2 we can prove the stability of the main system.

Remark 3.10 The proof of Lemma 3.4 is obtained based on the convexity of the set S. Using lemma 3.4, we can conclude that the last term on the r.h.s of (3.160) can only makes the $\dot{V}_1$ more negative and therefore the same conclusions regarding the convergence properties of control laws (3.108),(3.116) can be deduced. However, the transient behavior of the signals of the system can be different due to the change in the structure of the estimation laws.

3.4.5 Input Dependent Time Varying Inertia

In this section, we find the conditions under which the adaptive control law (3.108),(3.154) will be extended to the case of an spacecraft with input dependent time varying inertia. For this purpose, consider (3.108) in the following form

$$M = \underbrace{-b_1 e_R - d_1 e_\omega + \hat{I}\left[R^T R_r \dot{\omega}_r - \overset{\triangle}{\omega} R^T R_r \omega_r\right] + \omega \times \hat{I}\omega}_{\alpha_2} + \sum_{i=1}^{n} \dot{\psi}_i \hat{I}_i \left(\omega - \frac{1}{2}(e_\omega + b_2 e_R)\right)$$

$$= \alpha_2 + \sum_{i=1}^{n} \dot{\psi}_i \hat{I}_i \left(\omega - \frac{1}{2}(e_\omega + b_2 e_R)\right) \tag{3.161}$$

First, we start with the simple linear case as in (3.94), i.e. $M = \alpha_2 + \|M\| \alpha_1 \hat{I}_1 \left(\omega - \frac{1}{2}(e_\omega + b_2 e_R)\right)$. Since the value of the α_2 can be calculated at each time, to ensure the existence of M for each α_2 the following equation must have a feasible solution at all time, ($\alpha_3 = \alpha_1 \hat{I}_1 \left(\omega - \frac{1}{2}(e_\omega + b_2 e_R)\right)$)

$$\|M\|^2 \left(1 - \|\alpha_3\|^2\right) - 2\alpha_2^T \alpha_3 \|M\| - \|\alpha_2\|^2 = 0 \tag{3.162}$$

since the last term in (3.162), has the negative sign, if $\|\alpha_3\| < 1$, the (3.162) always has a feasible solution and the adaptive controller (3.108),(3.154) will achieve the control goals. In order to further analyze this condition we can write

$$\|\alpha_3\| < 1 \Rightarrow \left\|\hat{I}_1\right\| \left\|\omega - \frac{1}{2}(e_{\omega + b_2 e_R})\right\| = \left\|\frac{1}{2} e_\omega + R^T R_r \omega_r - \frac{b_2}{2} e_R\right\|$$

$$\left\|\hat{I}_1\right\| \left(\frac{\|e_\omega\|}{2} + \|\omega_r\| + \frac{b_2}{2}\|e_R\|\right) \leq \left\|\hat{I}_1\right\| \left(\frac{\|e_\omega\|}{2} + \hat{\omega}_r + \frac{b_2}{2}\sqrt{\frac{\lambda_{max}(K_p)}{c_1}}\right)$$

$$\leq \left\|\hat{I}_1\right\|_F \left(\frac{\|e_\omega\|}{2} + \hat{\omega}_r + \frac{b_2}{2}\sqrt{\frac{\lambda_{max}(K_p)}{c_1}}\right) \leq \sqrt{\epsilon}\left(\frac{\|e_\omega\|}{2} + \hat{\omega}_r + \frac{b_2}{2}\sqrt{\frac{\lambda_{max}(K_p)}{c_1}}\right) < 1 \tag{3.163}$$

hence, we conclude that if the following condition satisfies at all time $t \geq 0$

$$\|e_\omega(t)\| \leq \frac{2}{\sqrt{\epsilon}} - 2\hat{\omega}_r + b_2\sqrt{\frac{\lambda_{max}(K_p)}{c_1}} \tag{3.164}$$

then (3.162) is guaranteed to have a solution at all time. In order to enforce the condition (3.164), the initial conditions for e_ω must be limited to a set. This can be seen by considering the Lyapunov function (3.106). Since $\dot{V} \leq 0$ we can write

$$\begin{aligned}
V(0) &> \frac{\sigma_{min}}{2}e_\omega^T e_\omega + (b_1 + b_2 d_1)c_1 e_R^T e_R - b_2\sigma_{max}\|e_\omega\|\|e_R\| + \frac{b_2\sigma_{min}}{2}e_R^T e_R + \sum_{i=0}^{1} tr[\tilde{I}_i^T \tilde{I}_i] \\
&> \frac{\sigma_{min}}{2}e_\omega^T e_\omega + (b_1 + b_2 d_1)\frac{c_1}{c_2}\lambda_{min}(K_p) - b_2\sigma_{max}\|e_\omega\|\sqrt{\frac{\lambda_{max}(K_p)}{c_1}} \\
&+ \frac{b_2\sigma_{min}\lambda_{max}(K_p)}{2c_2} + \sum_{i=0}^{1} tr[\tilde{I}_i^T \tilde{I}_i]
\end{aligned}$$

which by completing the squares results in

$$\begin{aligned}
V(0) + \frac{b_2^2\sigma_{max}^2\lambda_{max}(K_p)}{2c_1\sigma_{min}} &> \frac{\sigma_{min}}{2}\left(\left\|e_\omega - \frac{b_2\sigma_{max}}{\sigma_{min}}\sqrt{\frac{\lambda_{max}(K_p)}{c_1}}\right\|\right) \\
&+ \frac{c_1}{c_2}(b_1 + b_2 d_1)\lambda_{min}(K_p) + \frac{b_2\sigma_{min}\lambda_{max}(K_p)}{2c_2}
\end{aligned} \tag{3.165}$$

also, for the upperbound on $V(0)$ we can write

$$\begin{aligned}
V(0) &< \frac{\sigma_{max}}{2}\|e_\omega(0)\|^2 + (b_1 + b_2 d_1)\lambda_{max}(K_p) + b_2\sigma_{max}\|e_\omega(0)\|\sqrt{\frac{\lambda_{max}(K_p)}{c_1}} + \frac{b_2^2\sigma_{max}\lambda_{max}(K_p)}{2c_1} \\
&+ \left(\frac{2\epsilon_0}{k_0} + \frac{2\epsilon}{k_1}\right) < \frac{\sigma_{max}}{2}\left[\left(\|e_\omega(0)\| + b_2\sqrt{\frac{\lambda_{max}(K_p)}{c_1}}\right)^2\right] + (b_1 + b_2 d_1)\lambda_{max}(K_p) + \left(\frac{2\epsilon_0}{k_0} + \frac{2\epsilon}{k_1}\right)
\end{aligned} \tag{3.166}$$

hence if the initial condition for $e_\omega(0)$ is chosen as follows

$$\frac{\sigma_{max}}{2}\left[\left(\|e_\omega(0)\|+b_2\sqrt{\frac{\lambda_{max}(K_p)}{c_1}}\right)^2\right]+\underbrace{(b_1+b_2d_1)\lambda_{max}(K_p)+\left(\frac{2\epsilon_0}{k_0}+\frac{2\epsilon}{k_1}\right)}_{B_1}$$
$$<\underbrace{\frac{-b_2^2\sigma_{max}^2\lambda_{max}(K_p)}{2c_1\sigma_{min}}+\frac{\sigma_{min}}{2}\left(\alpha_4-\frac{b_2\sigma_{max}}{\sigma_{min}}\sqrt{\frac{\lambda_{max}(K_p)}{c_1}}\right)^2}_{B_2} \tag{3.167}$$

where $\alpha_4 > \frac{b_2\sigma_{max}}{\sigma_{min}}\sqrt{\frac{\lambda_{max}(K_p)}{c_1}}$. using (3.167), we can write

$$\frac{\sigma_{min}}{2}\left(\|e_\omega\|-\frac{b_2\sigma_{max}}{\sigma_{min}}\sqrt{\frac{\lambda_{max}(K_p)}{c_1}}\right)^2<\frac{\sigma_{min}}{2}\left(\alpha_4-\frac{b_2\sigma_{max}}{\sigma_{min}}\sqrt{\frac{\lambda_{max}(K_p)}{c_1}}\right)^2 \tag{3.168}$$

which ensures $\|e_\omega\| < \alpha_4$ at all time provided (3.167) holds. Fig. 3.4 illustrates this case A more elegant approach for satisfaction of the condition $\|\alpha_3\| < 1$ is to use the switching σ-modification method which is described in Section. 3.4.3. Using (3.137), the trajectories of the system (3.90) will be confined to the following set

$$\frac{\sigma_{min}}{2}\|e_\omega\|^2+\left(\frac{b_2^2\sigma_{min}^2}{2}+c_1(b_1+b_2d_1)\right)\|e_R\|^2-b_2\sigma_{max}\|e_R\|\|e_\omega\|\leq$$
$$V(0)+\underbrace{\frac{\lambda_{max}(W')}{\lambda_{min}(Q')}\sum_{i=0}^{n}\left(\frac{3}{2}\sigma_{0i}\sigma_{max}^2+6\sigma_{0i}M_{0i}^2\right)}_{\alpha_5}=M_1 \tag{3.169}$$

a better approximation can be achieved by finding M_1 for which the following curves become tangent to each other

$$\underbrace{\frac{\sigma_{min}}{2}}_{a}\|e_\omega\|^2+\underbrace{\left(\frac{b_2^2\sigma_{min}^2}{2}+c_1(b_1+b_2d_1)\right)}_{b}\|e_R\|^2\underbrace{-b_2\sigma_{max}}_{c}\|e_R\|\|e_\omega\|=M_1$$
$$\|e_\omega\|+b_2\|e_R\|=\frac{2}{\sqrt{\epsilon}}-2\hat{\omega}_r=M_2 \tag{3.170}$$

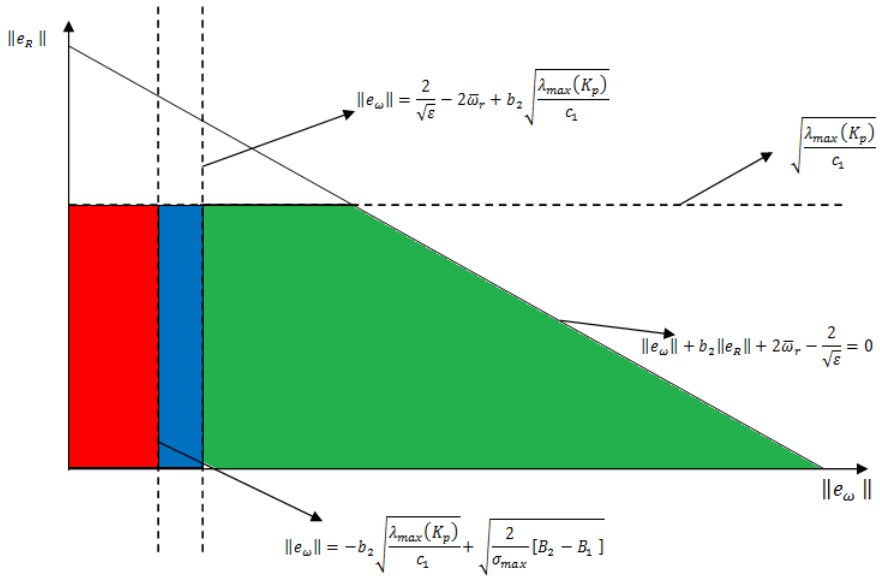

Figure 3.4: Set of allowable initial conditions for (3.168)

To find the location of the intersection, we can write

$$
\begin{aligned}
&2ab_2\|e_\omega\| + cb_2\|e_R\| = 2b\|e_R\| + c\|e_\omega\| \\
&2ab_2(M_2 - b_2\|e_R\|) + cb_2\|e_R\| = 2b\|e_R\| + c(M_2 - b_2\|e_R\|) \\
&\Rightarrow \|e_R\| = \frac{2ab_2M_2 - cM_2}{2ab_2^2 - 2cb_2},\ \|e_\omega\| = M_2 - \frac{2ab_2M_2 - cM_2}{2ab_2 - 2c}
\end{aligned} \tag{3.171}
$$

using (3.171), M_1 can be readily computed. Hence, if the initial conditions for $\|e_\omega\|$ and $\|e_R\|$ satisfies

$$
\begin{aligned}
&\frac{\sigma_{min}}{2}\|e_\omega(0)\|^2 + \left(\frac{b_2^2\sigma_{min}^2}{2} + c_1(b_1 + b_2d_1)\right)\|e_R(0)\|^2 - b_2\sigma_{max}\|e_R(0)\|\,\|e_\omega(0)\| \\
&\leq M_1 - \alpha_5 - \left(\frac{2\epsilon_0}{k_0} + \frac{2\epsilon}{k_1}\right)
\end{aligned}
$$

then the condition $\|\alpha_4\| \leq 1$ will hold.

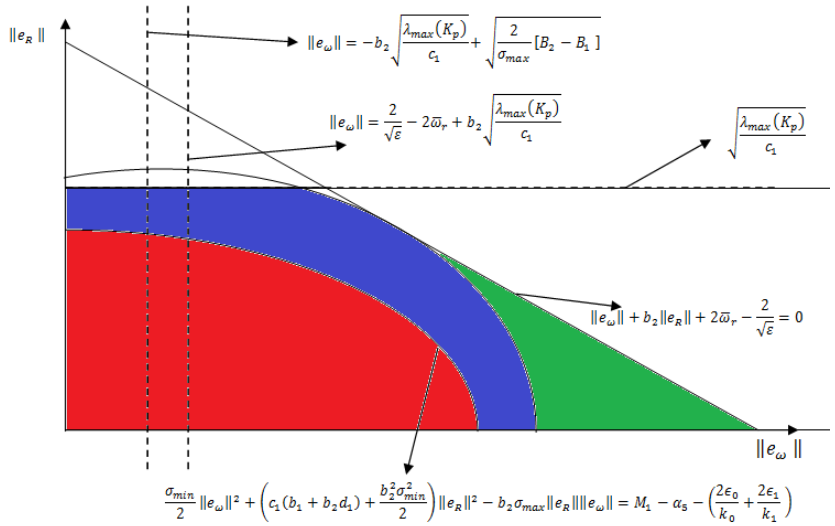

Figure 3.5: Set of allowable initial conditions for (3.169)

Remark 3.11 It should be noted that due to the presence of α_5 and $\sum_{i=0}^{n} \frac{2\epsilon_i}{k_i}$ in the r.h.s of (3.169), it is not possible to use the initial conditions which are located in the blue region which is depicted in Fig. 3.5. By choosing small values for σ_{0i} inside the adaptation laws (3.137) we can increase the size of the allowable set of initial conditions. However, in this case the norm of the estimated inertia matrices may become large and thus leads to loss of performance.

Remark 3.12 Note that if we use second order model for fuel depletion process then the control law (3.161) can be rewritten as follows

$$M = \alpha_2 + \alpha_3 \|M\| + \underbrace{\epsilon\alpha_4'}_{\alpha_4} \|M\|^2 \tag{3.172}$$

Also, we have

$$\|M\|^2 = \|\alpha_2\|^2 + 2\|M\|\alpha_2^T\alpha_3 + \|M\|^2\left(2\alpha_2^T\alpha_4^{'} + \|\alpha_3\|^2\right) + 2\|M\|^3\alpha_3^T\alpha_4^{'} + \|M\|^4\left\|\alpha_4^{'}\right\|^2 \tag{3.173}$$

Next, consider the following solution for (3.173)

$$\|M\| = M_0 + \epsilon M_1 + O(\epsilon^2) \tag{3.174}$$

using (3.174) in (3.173), we reach to the following equalities

$$\begin{aligned} M_0^2 &= \|\alpha_2\|^2 + 2M_0\alpha_2^T\alpha_3 + M_0^2\|\alpha_3\|^2 \\ 2M_0M_1 &= 2M_1\alpha_2^T\alpha_3 + 2M_1M_0\|\alpha_3\|^2 + 2M_0^2\alpha_2^T\alpha_4^{'} + 2M_0^3\alpha_3^T\alpha_4^{'} \end{aligned} \tag{3.175}$$

which results in the following two solutions

$$\|M\| = \frac{-\alpha_2^T\alpha_3 \pm \sqrt{(\alpha_2^T\alpha_3)^2 - \|\alpha_2\|^2\left(\|\alpha_3\|^2 - 1\right)}}{\|\alpha_3\|^2 - 1} + \epsilon\frac{M_0^2\alpha_2^T\alpha_4^{'} + M_0^3\alpha_3^T\alpha_4^{'}}{M_0 - \alpha_2^T\alpha_3 - M_0\|\alpha_3\|^2} + O(\epsilon^2) \tag{3.176}$$

The second term on the r.h.s of (3.176) accounts for the nonlinear second order term inside (3.172). It is interesting to note that since (3.173) is of the fourth order in $\|M\|$, hence, according to the fundamental theorem of algebra it has four roots. These extra solutions can also be computed using the singular perturbation theory. However, in the context of control, ensuring the existence of one real solution for (3.173) is sufficient.

Remark 3.13 If the upperbounds on $\dot{I}$,ω_r and $\dot{\omega}_r$ are known apriori then it is possible to build a hybrid nonlinear robust adaptive control law to push the trajectories of the system to the allowable set of initial conditions (3.169) and then use the adaptive law (3.137) to fulfill the tracking task. This approach provides global stability for the system at the expense of extra control efforts.

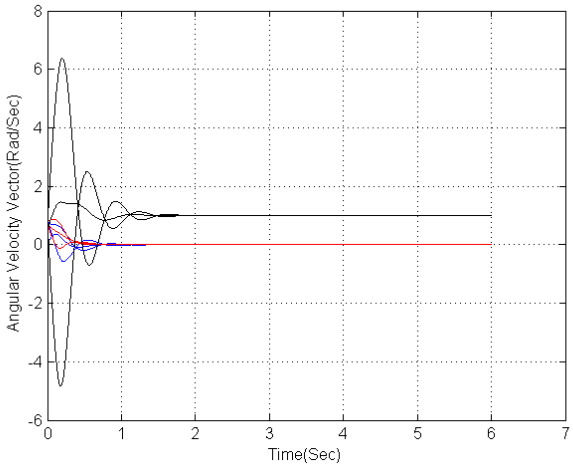

Figure 3.6: Angular velocity vector components versus time

3.5 Simulation Results

In this section, we present the simulation results for the algorithms which are considered in this chapter. First, we consider the simulation results of the control law (3.13) together with adaptation law (3.20) for a network of three agents with a complete communication graph. Fig. 3.6 illustrates the results for the angular velocity of these agents versus time.

The desired angular velocity in this case is $[0, 0, 1]^T \frac{Rad}{Sec}$. As it can be seen from Fig. 3.6, the third component of the angular velocity vector of the agents in network converged to 1 after two seconds. Simulation parameters in this case are chosen as $\mu = 5$ and $\alpha = 1$. From Fig. 3.7, we can deduce that the total disagreement in the network disappeared over time as a result of control law (3.13). The disagreement function of this network will take the following form

$$\Psi = \sum_{i=1}^{3} \sum_{j=1}^{3} tr(I_{3\times 3} - R_i^T R_j) \to 0 \tag{3.177}$$

simulation results for the problem 3.2 with disagreement function (3.36), are presented in

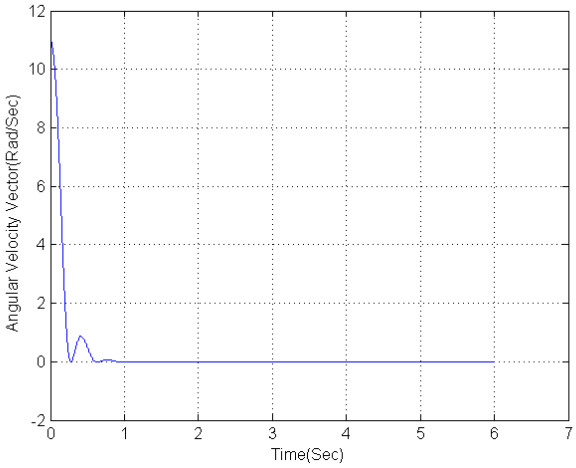

Figure 3.7: Disagreement Function(dimensionless)

Fig. 3.8 and Fig. 3.9. We used $\lambda_{K,M} = 1, \mu = 5, \alpha = 3$ for the control parameters. The considered network consists of three agents with line communication graph. The robust control parameters are chosen to be $\delta = \sqrt{300}$ and $\epsilon = 1$ for all agents in Fig. 3.8. Using the results of the analysis in section 3.2.4, we can deduce that the trajectories of the system eventually reach to the following set:

$$\sum_{k=1}^{3} \left(5 - \frac{1}{3}\right) \|\Omega_k^r - F_k\|^2 + \frac{1}{3}(\|\Omega_k^r\|^2 + \|F_k\|^2) \tag{3.178}$$

$$\frac{\sigma_k}{2} \left\|\tilde{J}_k\right\|_F^2 \leq \sum_{k=1}^{m} \left(\frac{3\sigma_k}{2}\lambda_{K,M}^2 + \epsilon_k\right) \leq \frac{15}{2} \tag{3.179}$$

The norm of disturbance signal is assumed to be less than $10\sqrt{3}$ and the desired angular velocity vector is again $[0, 0, 1]^T \frac{Rad}{Sec}$. As it can be seen from Fig. 3.9, by choosing sufficiently small control parameters($\epsilon_k = 0.01, \sigma_k = 0.01$), we can steer the system trajectories near the desired value for the angular velocity vector. In this case, the system states will be

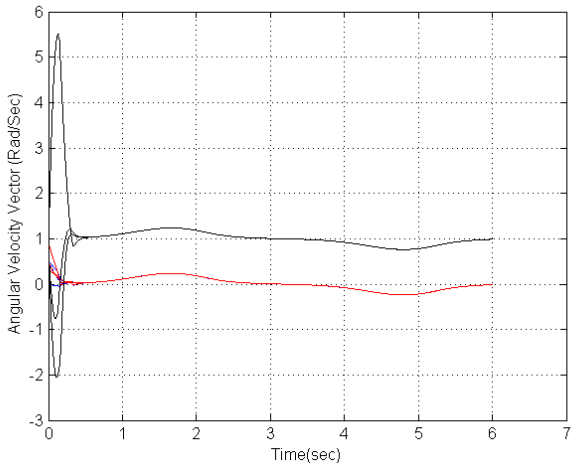

Figure 3.8: Angular velocity vector components(robust adaptive approach with large values for control parameters) $\epsilon_k = 1, \delta_k = \sqrt{300}, \sigma_k = 1$

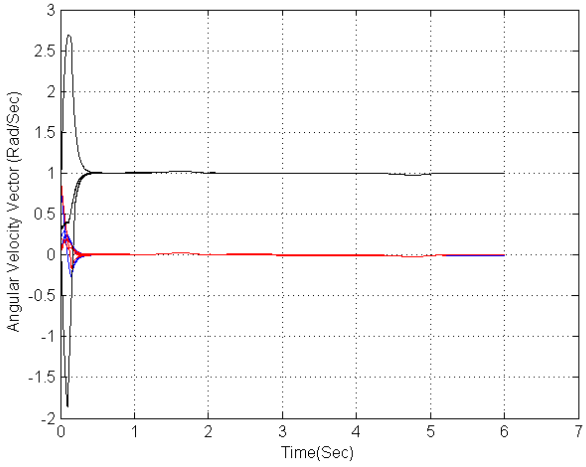

Figure 3.9: Angular velocity vector components(robust adaptive approach with small values for control parameters) $\epsilon_k = 0.01, \delta_k = \sqrt{300}, \sigma_k = 0.01$

confined in the following set

$$\sum_{k=1}^{m}\left(5-\frac{1}{3}\right)\|\Omega_k^r-F_k\|^2+\frac{1}{3}(\|\Omega_k^r\|^2+\|F_k\|^2)+\frac{\sigma_k}{2}\left\|\tilde{J}_k\right\|_F^2$$
$$\leq\sum_{k=1}^{m}\left(\frac{3\sigma_k}{2}\lambda_{K,M}^2+\epsilon_k\right)\leq\frac{0.15}{2} \tag{3.180}$$

The difference between the Fig. 3.8 and Fig. 3.9 stems from the fact that we chose different values for the robust control parameters. This indicates the possibility of controlling the size of the final set at the expense of increasing the control effort.

Next, we present the results of a set of simulations testing the synchronization algorithms proposed in Sections 3.3.2-3.3.5. First, we consider the simulation results for the control law (3.67) together with adaptation law (3.73), for a network of thirteen agents with a tree communication graph depicted in Fig. 3.10(a). Fig. 3.11 shows the time behavior of the angular velocities of these agents.

The desired angular velocity in this case is $\Omega_d=[0\ 0\ 1]^T(\frac{rad}{sec})$. As seen in Fig. 3.11, the components of the angular velocity vectors of the agents in the network converge to a sufficiently small neighborhood of Ω_d after eight seconds. Design parameters in this case are $\mu=5$ and $\alpha=1$. From Fig. 3.12, we deduce that the total disagreement in the network disappeared over time as a result of control law (3.67). The initial value of the disagreement function of this network can be calculated as:

$$\Psi_2(0)=\sum_{i=1}^{13}\sum_{j\in N_i}^{n}2-\sqrt{1+tr\left[R_i^T(0)R_j(0)\right]}=23.1443$$

Simulation results for the robust control algorithm (3.77), (3.78) are presented in Fig. 3.13 for the case that a bounded noise ($r(t)=10\sin(t)[1\ 1\ 1]^T(N\cdot M)$) is affecting the control inputs. The values of the control parameters and the network communication graph are the same as previous case.

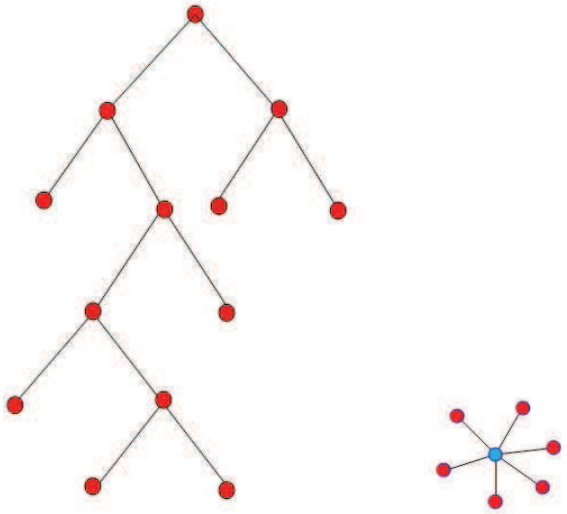

(a) (b)

Figure 3.10: Network communication graph examples.

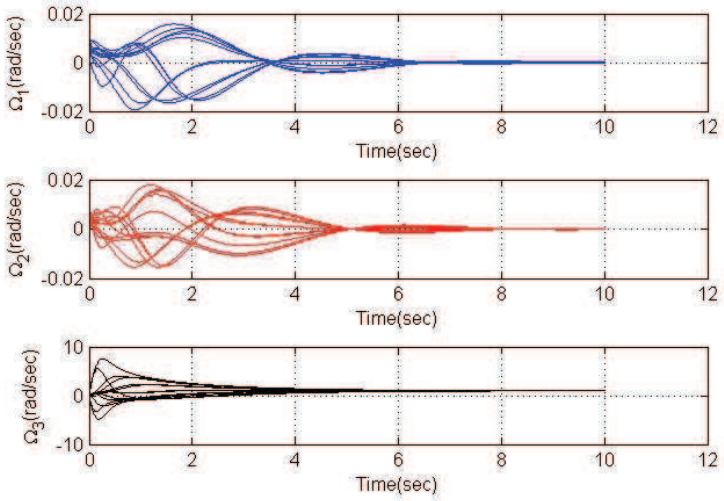

Figure 3.11: Components of the angular velocity vector Ω versus time.

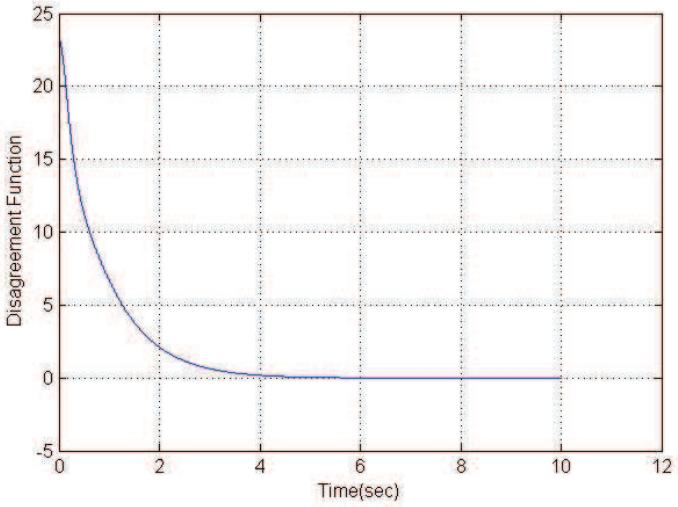

Figure 3.12: Disagreement function.

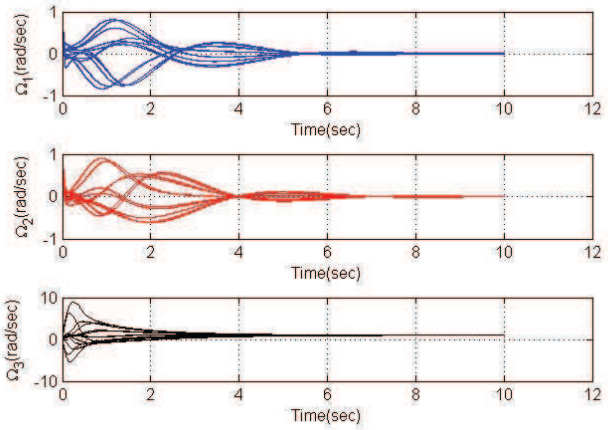

Figure 3.13: Simulation results of the robust adaptive control law (3.77).

Next, we consider a network of six agents with a line communication graph. Fig. 3.14 illustrates the behavior of the third components of angular velocity vectors as result of implementing the robust algorithm (3.82) on this network. The simulation parameters are the same as the previous cases and $\Delta_k = 20$. ϵ_k is set to 1 in case (a) and 0.1 in (b). From (3.84), it is clear that the trajectories of the system will reach to the set

$$\left\{ \Omega_k^r, G_k \mid \sum_{k=1}^{6} 4 \left\| \Omega_k^r - G_k \right\|^2 + \left(\left\| \Omega_k^r \right\|^2 + \left\| G_k \right\|^2 \right) \leq 6\epsilon_k \right\}. \tag{3.181}$$

The simulation results for various other example networks, including the one with a star communication graph depicted in Fig. 3.10(b), show similar behaviors.

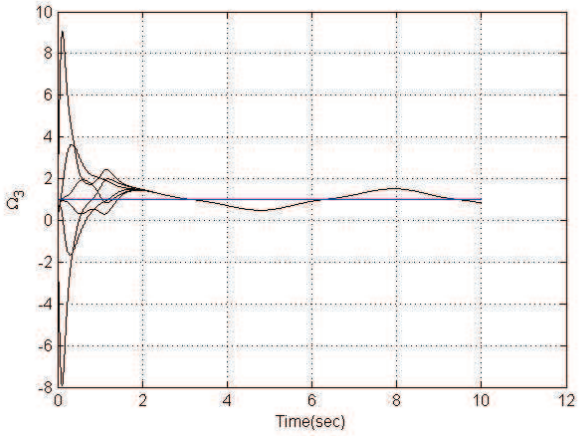

(a)

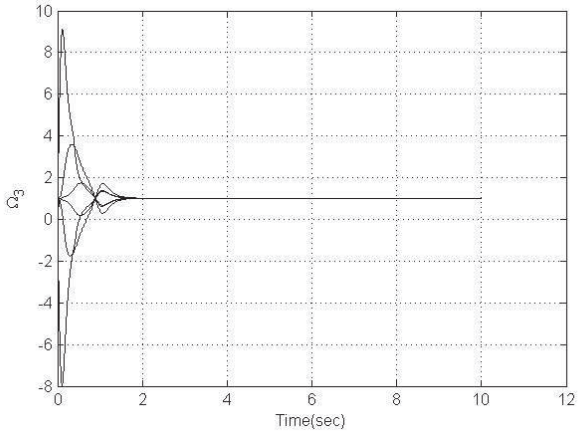

(b)

Figure 3.14: Time behavior of Ω_3 with robust adaptive control law (3.82) with $\Delta_k = 20$ and (a) $\epsilon_k = 1$ and (b) $\epsilon_k = 0.1$.

3.6 Summary

In this chapter, we first considered the adaptive attitude synchronization for a network of rigid bodies and used a geometric approach to solve the problem. Such an approach results in a coordinate independent control and estimation laws which can be used in large rotational maneuvers to handle the singularities which are inherent in the attitude representation of a rigid agent. In the convergence analysis of the proposed method, we used the Frobenius norm as the measure for the estimation error of the inertia matrices of the agents. Comparing to the two norm of a matrix, this norm has a greater value and hence it leads to more conservative convergence results. However, working with such norm is much more simpler in the context of Lyapunov theory. In the next part of this chapter, we used an optimal norm on $SO(3)$ as an error function for measuring the attitude differences in the network. Our proposed control laws act as set of virtual rotational spring and dampers between agents. In the next step, we solved the adaptive version of this problem. We further extend these results to the case of robust adaptive control design for the situations where the network is subjected to external disturbances and unmodeled dynamics. Furthermore, we considered the adaptive attitude control problem in the presence of time varying input dependent inertia matrices. We proposed a modified projection method to solve this problem.

Chapter 4

Distributed Extremum Seeking and Localization

In this chapter, we consider the distributed localization and extremum seeking problems for a network of mobile agents. The main rationale behind using multiple agents in localization of an unknown source is to enhance the identifiably of the network by mixing the information of individual agents through an implementation of a consensus-type algorithm. It will be shown that if certain connectivity conditions are met, then the consensus framework will enable all agents in the network to agree upon the location of the source. This consensus strategy will force the more "informed" agents to share their estimations of the location of the source with others at the expense reducing the convergence rate of their estimation algorithms. However, there are certain cases where none of the agents has access to sufficient information for identification, and all the "informed" agents have equal role in the localization problem. For these cases, if the collective identifiability condition is satisfied by the network of agents then the aforementioned decadence of convergence will

not occur and the network as a whole fulfill the localization task. The main objective in extremum seeking and source localization problems which we consider here, is to find the location of the extremum of a quadratic function $F(\cdot) : \mathbb{R}^m \longrightarrow \mathbb{R}$

$$F(\theta) = (\theta - \theta^*)^T H (\theta - \theta^*) + c_1 \tag{4.1}$$

where c_1 is a constant parameter. This function can represent the measurement of a particular sensor at the state θ [60, 62, 63]. The idea for using a quadratic function as a profile of the field is rooted in the fact that any smooth function can be approximated locally by its Taylor expansion near each extremum point. Since the gradient of such a function will vanish at the extremum point θ^*, for a general nonlinear smooth function $F(\cdot)$, we can write:

$$F(\theta^* + \tilde{\theta}) = F(\theta^*) + \frac{1}{2}\tilde{\theta}^T \nabla^2 F \tilde{\theta} + h.o.t, \quad \tilde{\theta} = \theta - \theta^* \tag{4.2}$$

Noting that $\nabla F(\theta^*) = 0$. Additionally, We use the assumption that the location of the extremum point is time invariant, and treat the localization task as an adaptive parameter identification problem. The approximation (4.2) enables us to extract the gradient of the field using averaging methods [34] and find the location of the extremum point.

4.1 Adaptive Source Localization

In the adaptive source localization problem, where (4.1) corresponds to the strength of the source located at θ^*, we assume that each agent can measure the value of the function (4.1) at its state $\theta_i \in \mathbb{R}^m$,$i = 1, \cdots, n$

$$D_i(t) = F(\theta_i) = \tilde{\theta}_i^T H \tilde{\theta}_i + c_1, \ \tilde{\theta}_i = \theta_i - \theta^* \tag{4.3}$$

where n is the number of agents and we assumed that the Hessian matrix of the field ($\nabla^2 F = H$) is constant. In order to devise a cooperative adaptive localization algorithm, we use the framework proposed in [1] for a single agent and generalize it to a network of agents through embedding a consensus filter in the identification subsystem.

The first step of the design of such an algorithm is to obtain a model which is linear in unknown parameters of the system, i.e., Hessian matrix elements and coordinates of the target. We start by taking derivative of (4.3) as follows:

$$\begin{aligned} 2D_i\dot{D}_i = 2\dot{\tilde{\theta}}_i^T H\tilde{\theta}_i &= 2\sum_l\sum_k \dot{\tilde{\theta}}_{i,l}\tilde{\theta}_{i,k}H_{lk} \\ &= 2\sum_l\sum_k \dot{\theta}_{i,l}\theta_{i,k}H_{lk} - \dot{\theta}_{i,l}\theta_k^* H_{lk} = \sum_l\sum_k \left(\frac{d}{dt}(\theta_{i,l}\theta_{i,k})H_{lk} - 2\frac{d\theta_{i,l}}{dt}H_{lk}\theta_k^*\right) \end{aligned} \tag{4.4}$$

From (4.4), it is clear that we can stack the unknown parameters into the following vectors:

$$\Xi = \left[H_{11},\cdots,H_{1m},\cdots,H_{mm},-2\sum_k \theta_k^* H_{1k},\cdots,-2\sum_k \theta_k^* H_{mk}\right]^T \in \mathbb{R}^{\frac{m(m+3)}{2}} \tag{4.5}$$

Also, by stacking the known signals in model (4.4)

$$\Phi_i = \left[\frac{d}{dt}(\theta_{i,1}\theta_{i,1}),\cdots,2\frac{d}{dt}(\theta_{i,1}\theta_{i,m}),\cdots,\frac{d}{dt}(\theta_{i,m}\theta_{i,m}),\frac{d\theta_{i,1}}{dt},\cdots,\frac{d\theta_{i,m}}{dt}\right]^T \in \mathbb{R}^{\frac{m(m+3)}{2}} \tag{4.6}$$

passing both sides of (4.4) through a low pass filter results in:

$$\frac{s}{s+a}D_i^2 = \frac{1}{s+a}\Phi_i^T\Xi \tag{4.7}$$

The rationale for using such a filtering is to avoid explicit use of differentiation of the available signals. Using (4.7), we can design an adaptive estimation algorithm to identify Ξ.

Remark 4.1 For the case $H_{ij} = 0, i \neq j$ the vectors Φ_i and Ξ can be expressed as follows:

$$\Xi = \left[H_{11}, \cdots, H_{mm}, -2\sum_k \theta_k^* H_{1k}, \cdots, -2\sum_k \theta_k^* H_{mk} \right]^T \in \mathbb{R}^{2m}$$
$$\Phi_i = \left[\frac{d}{dt}(\theta_{i,1}\theta_{i,1}), \cdots, \frac{d}{dt}(\theta_{i,n}\theta_{i,m}), \frac{d\theta_{i,1}}{dt}, \cdots, \frac{d\theta_{i,m}}{dt} \right]^T \in \mathbb{R}^{2m} \tag{4.8}$$

Comparing (4.8) with (4.6), it is clear that the components of the latter do not contain the multiplication of the states of different agents. For a general case, since H is a symmetric matrix with real elements, we can deduce that by choosing appropriate coordinates, we can diagonalize the matrix H and hence, design the identification algorithm based on (4.8). We start the design procedure with an example of a quadratic potential function of the form $f(x, y) = a(x - x^*)^2 + b(y - y^*)^2 + 2c(x - x^*)(y - y^*)$, where $[x^*, y^*]^T$ denotes the position of the source. For each agent, we have:

$$D_i^2 = a(x_i - x^*)^2 + b(y_i - y^*)^2 + 2c(x_i - x^*)(y_i - y^*)$$
$$2D_i\dot{D}_i = 2a\dot{x}_i(x_i - x^*) + 2b\dot{y}_i(y_i - y^*) + 2c\dot{x}_i(y_i - y^*) + 2c\dot{y}_i(x_i - x^*) \tag{4.9}$$

As mentioned before, in order to avoid using explicit differentiation in the structure of the distributed identification algorithm, we pass the both sides of (4.9) through a stable low pass filter which results in ($a > 0$)

$$z_i = \Phi_i^T \eta, \quad z_i = \frac{s}{s+a} D_i^2,$$
$$\eta = [a \ c \ b \ (-2ax* - 2cy^*) \ (-2by^* - 2cx^*)]^T, \ \Phi_i = \frac{s}{s+a}[x_i^2 \ 2x_iy_i \ y_i^2 \ x_i \ y_i]^T \tag{4.10}$$

Using the classical gradient based adaptive parameter identification method [91], the i^{th} agent can use the following " selfish" estimation algorithm to locate the target

$$\dot{\hat{\eta}}_i = \gamma_i \Phi_i \Phi_i^T (\eta - \hat{\eta}_i), \quad \tilde{\eta}_i = \eta - \hat{\eta}_i \tag{4.11}$$

where $\hat{\eta}_i$, denotes the estimation of the i^{th} agent from the parameters of the field.

4.1.1 Persistence of Excitation

The success of the algorithm (4.11) depends on the *Persistence of Excitation* (PE) of the Φ_i term. Note that, although $\Phi_i\Phi_i^T$ is always positive semi definite, the asymptotic convergence of the estimation errors to zero can not be concluded by checking the eigenvalues of $\Phi_i\Phi_i^T$ since (4.11) is a non-autonomous system. The formal definition of a PE signal is as follows

Definition 4.1:[91] The function Φ is said to be persistently exciting (PE), if and only if there exist constants $\epsilon_1, \epsilon_2, T$ such that for all $(\tau \geq 0)$

$$\epsilon_2 I_n \geq \int_{\tau}^{\tau+T} \Phi(t)\Phi(t)^T \, dt \geq \epsilon_1 I_n \tag{4.12}$$

It is shown in [91] that the PE condition is sufficient for ensuring the convergence of the estimation algorithm (4.11). Since the satisfaction of the PE condition is not an straightforward task for one agent, here, we seek for a distributed version of (4.11) which "blends" the information which is a gathered by different agents to enhance the chance of the successful identification of the target's unknown parameters. This objective can be approached through several perspectives. The most common method to achieve this goal is to add a consensus term on the right hand side of (4.11). This extra term will help the network to satisfy the PE condition using a less restrictive condition compared to (4.12).

4.2 Distributed Localization

4.2.1 Problem Definition

In order to formally define and analyze the distributed localization problem, first, we need to present the properties of the Laplacian matrix L of a typical sensing network. We start by assuming that communication graph of the network is undirected. For such a graph the following properties hold:($L \in \mathbb{R}^{n\times n}$)

- $L\mathbf{1}_n = \mathbf{0}_n$, i.e. $\mathbf{1}_n$ is an eigenvector of matrix L which is associated with the zero eigenvalue.
- For a connected graph G, the eigenvalues λ_i, $i \in \{2, \cdots, n\}$ are strictly positive.

Using these properties, we can write any vector $x \in \mathbb{R}^n$ as follows:

$$x = \frac{\mu}{\sqrt{n}}\mathbf{1}_n + \sum_{j=2}^{n} \nu_j v_j, \;\; Lv_i = \lambda_i v_i \tag{4.13}$$

where $\mu^2 + \|\nu\|^2 = \|x\|^2$.
Next, we formally define the localization problem.

Problem 4.1: Consider a network of n agents which are connected through a undirected graph $G = (\mathbb{V}, E, A)$, where $\mathbb{V}$ denotes the set of vertices of the graph G and E is the set of edges of this communication topology. Suppose that each agent has access to the measurement of the target field at its current state which is through appropriate filtering can be modeled as (4.11). Design a distributed identification scheme to find the location of the target and derive the conditions under which the exponential convergence of the identification system is guaranteed.

4.2.2 Distributed Localization Laws

In order to solve *Problem 4.1*, the identification subsystem for each agent in the network which is built based on adding the extra consensus terms to the r.h.s of (4.11) to decrease the disagreement between $\hat{\eta}_i$, can be expressed as follows

$$\dot{\hat{\eta}}_i = \gamma_i \Phi_i \Phi_i^T (\eta - \hat{\eta}_i) + \sum_{j \in N_i} (\hat{\eta}_j - \hat{\eta}_i) \tag{4.14}$$

Using ($\tilde{\eta}_i = \eta - \hat{\eta}_i$), (4.14) can be rewritten as

$$\dot{\tilde{\eta}}_i = -\gamma_i \Phi_i \Phi_i^T \tilde{\eta}_i + \sum_{j \in N_i} (\tilde{\eta}_j - \tilde{\eta}_i) \tag{4.15}$$

Next, using the stack vector of $\tilde{\eta}_i$,($\tilde{\eta} = [\tilde{\eta}_1, \cdots, \tilde{\eta}_n]^T$) and the definition of the Laplacian matrix, we can write

$$\frac{d}{dt}\tilde{\eta} = -(L \otimes I_m)\tilde{\eta} - \Psi\tilde{\eta} \tag{4.16}$$

where Ψ is defined as

$$\Psi = \begin{bmatrix} \gamma_1 \Phi_1 \Phi_1^T & \cdots & 0 \\ \vdots & \cdots & \vdots \\ 0 & \cdots & \gamma_n \Phi_n \Phi_n^T \end{bmatrix} \tag{4.17}$$

In order to analyze the convergence properties of (4.17) we can use the Lyapunov function $V = \frac{1}{2}\tilde{\eta}^T\tilde{\eta}$ and its time derivative which is obtained as follows

$$\dot{V} = -\tilde{\eta}^T((L \otimes I_m + \Psi))\tilde{\eta} \leq 0 \tag{4.18}$$

Since the communication graph of the network is assumed to be undirected, we can conclude that the distributed estimation algorithm will converge to the actual values if the PE condition is satisfied by the network. On the other hand, for a general directed graph,

the same conclusion can not be obtained. However, if we assume that the directed graph of the network is *strongly connected* and *balanced* it is still possible to conclude that $\dot{V} \leq 0$ and hence, guarantee the stability of the system.

4.2.3 Convergence Analysis

The main purpose of this section is to verify the exponential convergence of (4.16) since in [73] only the asymptotic convergence has been proved. Proving the exponential convergence of (4.16) will pave the way for investigating the convergence of (4.16) for cases in which ϕ_i are dependent on the systems state i.e. (η_i).

We start by the following dynamics for each subsystem:$(\tilde{\eta}_i = \hat{\eta}_i - \eta)$

$$\dot{\tilde{\eta}}_i = \dot{\hat{\eta}}_i = -\Gamma \frac{\phi_i \phi_i^T}{m_i^2} \tilde{\eta}_i + \Gamma \sum_{j \in N_i} (\tilde{\eta}_j - \tilde{\eta}_i) \tag{4.19}$$

Next, we consider the Lyapunov function $\frac{1}{2}\sum_{i=1}^{n} \tilde{\eta}_i^T \Gamma^{-1} \tilde{\eta}_i = \frac{1}{2}\tilde{\eta}^T \left(\mathbf{I}_n \otimes \Gamma^{-1}\right) \tilde{\eta}$, where $\tilde{\eta}$ denotes the stack vector of $\tilde{\eta}_i$. Integrating from t to $t+T$ results in:

$$V(t+T) - V(t) = \int_t^{t+T} \dot{V} \, d\tau \tag{4.20}$$

we have:

$$\begin{aligned}
\dot{V} &= \tilde{\eta}^T (\mathbf{I}_n \otimes \Gamma^{-1})(-(\mathbf{I}_n \otimes \Gamma)\Phi\tilde{\eta} - (\mathbf{I}_n \otimes \Gamma)(L \otimes \mathbf{I}_n)\tilde{\eta}) \\
&= -\tilde{\eta}^T \Phi \tilde{\eta} - \tilde{\eta}^T (L \otimes \mathbf{I}_n)\tilde{\eta} \\
&= -\sum_{i=1}^{n} \frac{(\tilde{\eta}_i^T \phi_i)^2}{m_i^2} - 0.5 \sum_{i=1}^{n} \sum_{j \in N(i)} (\eta_i - \eta_j)^T (\eta_i - \eta_j) \leq 0
\end{aligned} \tag{4.21}$$

where the second line is resulted from the identity $((A \otimes B)(C \otimes D) = (AC \otimes BD))$. (4.21) clearly demonstrates the stability of the system (4.19). Further analysis of V results into

the following theorem:

Theorem 4.1 Consider a network of n sensor agents with connected and undirected communication graph topology which is defined in *Problem 4.1*. Suppose that estimation dynamics are designed as (4.14) for which η^* and ϕ_i are defined in (4.5) and (4.6). If there exist $\alpha_0, \beta_0, T_0 > 0$ such that the following condition is satisfied at all time $t > 0$,

$$T_0\beta_0 \geq \int_t^{t+T_0} \sum_{i=1}^{n} \phi_i(\tau)\phi_i(\tau)^T \, d\tau \geq \alpha_0 T_0 \tag{4.22}$$

then the error vector $\tilde{\eta}$ exponentially converges to $\mathbf{1}_n \otimes \eta^*$ with the convergence rate no less than $\gamma = 1 - \gamma_1 > 0$ where $\gamma_1 = \gamma_2\gamma_3\lambda_{min}\Gamma$ and γ_2 and γ_3 are defined as

$$\begin{aligned}
\gamma_2 &= \max\left(\left(\left\|\bar{\tilde{\eta}}\right\|^2 \alpha_0 T_0 - 2n\beta_0 T_0 \left\|\bar{\tilde{\eta}}\right\| \sqrt{1 - n\left\|\bar{\tilde{\eta}}\right\|^2}\right), \lambda_2(1 - n\bar{\tilde{\eta}}^T\bar{\tilde{\eta}})\right), \\
\gamma_3 &= \min\left(\frac{1}{\Delta\left(2m' + 2\beta^4\lambda_{max}^2(\Gamma)T_0^2\right)}, \frac{T_0}{4\Delta(1 + 2\lambda_n^2 T_0^2)}\right)
\end{aligned} \tag{4.23}$$

In (4.23), n is the number of agents, $\beta = \max_i \sup_{\tau \geq 0} |\phi_i(\tau)|$, λ_2 denotes the algebraic connectivity of the network and λ_n is the n^{th} largest eigenvalue of the Laplacian matrix. Δ is defined as

$$\Delta = \max\left(\frac{\lambda_n\lambda_{max}^2(\Gamma)m'^2\beta^2 T_0^2}{(1 + 2\lambda_n^2 T_0^2)}, \frac{2T_0^2\lambda_n}{m' + \beta^4\lambda_{max}^2(\Gamma)T_0^2}\right) \tag{4.24}$$

and $\bar{\tilde{\eta}} = \frac{(\mathbf{1}_n^T \otimes I_m)\tilde{\eta}}{n\|\tilde{\eta}\|}$.

Proof. Using (4.21) in (4.20), we have:

$$\begin{aligned}
V(t+T) - V(t) = \int_t^{t+T} \Bigg[&- \sum_{i=1}^{n} \frac{(\tilde{\eta}_i^T(\tau)\phi_i(\tau))^2}{m_i^2} \\
&- 0.5 \sum_{i=1}^{n} \sum_{j \in N(i)} (\tilde{\eta}_i(\tau) - \tilde{\eta}_j(\tau))^T (\tilde{\eta}_i(\tau) - \tilde{\eta}_j(\tau)) \Bigg] \, d\tau
\end{aligned} \tag{4.25}$$

for each $\tilde{\eta}_i$, we can write:

$$\tilde{\eta}_i^T(\tau)\phi_i(\tau) = \tilde{\eta}_i^T(t)\phi_i(\tau) + (\tilde{\eta}_i^T(\tau) - \tilde{\eta}_i^T(t))\phi_i(\tau)) \tag{4.26}$$

using the fact that $(x+y)^2 \geq 0.5x^2 - y^2$, we can write

$$\begin{aligned} &\frac{1}{m'}\left\{\frac{1}{2}\int_t^{t+T}\sum_{i=1}^{n}(\tilde{\eta}_i^T(t)\phi_i(\tau))^2\ d\tau - \int_t^{t+T}\sum_{i=1}^{n}((\tilde{\eta}_i^T(\tau) - \tilde{\eta}_i^T(t))\phi_i(\tau))^2\ d\tau\right\} \\ &\leq \int_t^{t+T}\sum_{i=1}^{n}\frac{(\tilde{\eta}_i^T(\tau)\phi_i(\tau))^2}{m_i^2(\tau)}\ d\tau \end{aligned} \tag{4.27}$$

Next, consider the quantity $A = \int_t^{t+T}\sum_{i=1}^{n}(\tilde{\eta}_i^T(t)\phi_i(\tau))^2\ d\tau$, we need to find that to what extent A will stabilize the system (4.19). To achieve such a goal, we start by decomposing the $\tilde{\eta}_i$ in to the 'consensus' and 'disagreement' parts as follows:

$$\tilde{\eta}_i = \left(\frac{(\mathbf{1}_n^T \otimes \mathbf{I}_m)\tilde{\eta}}{n\left\|\tilde{\eta}\right\|} + v_i\right)\left\|\tilde{\eta}\right\| = (\bar{\tilde{\eta}} + v_i)\left\|\tilde{\eta}\right\|,\ \sum_{i=1}^{n} v_i = 0 \tag{4.28}$$

based on (4.28), A turns in to

$$\begin{aligned} A &= \sum_{i=1}^{n}\tilde{\eta}_i^T(t)\int_t^{t+T}\phi_i(\tau)\phi_i^T(\tau)\ d\tau\tilde{\eta}_i^T(t) \\ &= \left\|\tilde{\eta}(t)\right\|^2\int_t^{t+T}\sum_{i=1}^{n}(\bar{\tilde{\eta}}^T + v_i^T)\phi_i(\tau)\phi_i^T(\tau)(\bar{\tilde{\eta}} + v_i)\ d\tau \\ &= \left\|\tilde{\eta}(t)\right\|^2\int_t^{t+T}\sum_{i=1}^{n}\bar{\tilde{\eta}}^T\phi_i\phi_i^T\bar{\tilde{\eta}} + 2\bar{\tilde{\eta}}^T\phi_i\phi_i^T v_i + v_i^T\phi_i\phi_i^T v_i\ d\tau \end{aligned} \tag{4.29}$$

for decomposition (4.28), we can also write

$$\left(\sum_{i=1}^{n}\frac{\tilde{\eta}_i^T(t)\tilde{\eta}_i(t)}{\left\|\tilde{\eta}(t)\right\|^2} = 1, \sum_{i=1}^{n} v_i = 0\right) \rightarrow \sum_{i=1}^{n} v_i^T v_i = 1 - n\left\|\bar{\tilde{\eta}}\right\|^2 \tag{4.30}$$

which immediately implies that $\left\|v_i\right\| \leq \sqrt{1 - n\left\|\bar{\tilde{\eta}}\right\|^2}$. Next, suppose that

$$T_0\beta_0 \geq \int_t^{t+T_0}\sum_{i=1}^{n}\phi_i(\tau)\phi_i(\tau)^T\ d\tau \geq \alpha_0 T_0 \tag{4.31}$$

such a condition directly indicates that if the persistency of excitation is satisfied for a collection of agents, then it is possible to reach a conclusion regarding the exponential convergence of the system (4.19). It is interesting to note that (4.31) suggests that even in the case that none of the agents is fully satisfying the PE condition, it is possible to achieve the exponential convergence of the parameters. In another words, the existence of consensus terms inside the estimation laws will help the network to fulfill the robust estimation task.

From (4.31) we can conclude that $\int_t^{t+T_0} \phi_i \phi_i^T \, d\tau \leq \beta_0 T_0$ and hence

$$\sum_{i=1}^{n} \int_t^{t+T_0} 2 v_i^T \phi_i \phi_i^T \bar{\tilde{\eta}} \, d\tau \geq -2n\beta_0 T_0 \left\| \bar{\tilde{\eta}} \right\| \sqrt{1 - n \left\| \bar{\tilde{\eta}} \right\|^2} \tag{4.32}$$

using (4.32), we can rewrite (4.29) as follows:

$$A \geq \left\| \tilde{\eta}(t) \right\|^2 \left[\bar{\tilde{\eta}}^T(t) \sum_{i=1}^{n} \int_t^{t+T_0} \phi_i(\tau) \phi_i^T(\tau) \, d\tau \bar{\tilde{\eta}}(t) - 2n\beta_0 T_0 \left\| \bar{\tilde{\eta}} \right\| \sqrt{1 - n \left\| \bar{\tilde{\eta}} \right\|^2} \right] \tag{4.33}$$

Next, we use (4.31) in (4.33)

$$A \geq \left(\left\| \bar{\tilde{\eta}} \right\|^2 \alpha_0 T_0 - 2n\beta_0 T_0 \left\| \bar{\tilde{\eta}} \right\| \sqrt{1 - n \left\| \bar{\tilde{\eta}} \right\|^2} \right) \left\| \tilde{\eta} \right\|^2 \tag{4.34}$$

we also have:

$$\begin{aligned}
&\tilde{\eta}_i(\tau) - \tilde{\eta}_i(t) = \int_t^{\tau} \dot{\tilde{\eta}}_i(\sigma) \, d\sigma = -\int_t^{\tau} \left(\Gamma \frac{\phi_i \phi_i^T \tilde{\eta}_i}{m_i^2} - \sum_{j \in N_i} (\tilde{\eta}_i(\sigma) - \tilde{\eta}_j(\sigma)) \right) \, d\sigma \\
&\Rightarrow (\tilde{\eta}_i(\tau) - \tilde{\eta}_i(t))^T \phi_i(\tau) = -\int_t^{\tau} \frac{\tilde{\eta}_i^T(\sigma) \phi_i(\sigma)}{m_i(\sigma)} \frac{\phi_i^T(\tau) \Gamma \phi_i(\sigma)}{m_i(\sigma)} \, d\sigma \\
&- \int_t^{\tau} \sum_{j \in N_i} \phi_i^T(\tau) \left(\tilde{\eta}_i(\sigma) - \tilde{\eta}_j(\sigma) \right) \, d\sigma
\end{aligned} \tag{4.35}$$

Next, we consider the second term on the left side of (4.27)

$$\int_t^{t+T_0} \sum_{i=1}^{n} ((\tilde{\eta}_i(\tau) - \tilde{\eta}_i(t))^T \phi_i(\tau))^2 \, d\tau \leq$$
$$\underbrace{2\int_t^{t+T_0} \sum_{i=1}^{n} \left(\int_t^{\tau} \sum_{j \in N_i} \phi_i^T(\tau) \left(\tilde{\eta}_i(\sigma) - \tilde{\eta}_j(\sigma)\right) \, d\sigma \right)^2 d\tau}_{C_1}$$
$$+ \underbrace{\int_t^{t+T_0} 2\sum_{i=1}^{n} \left(\int_t^{\tau} \left(\frac{\tilde{\eta}_i^T(\sigma)\phi_i(\sigma)}{m_i(\sigma)} \right)^2 d\sigma \int_t^{\tau} \left(\frac{\phi_i^T(\tau)\Gamma\phi_i(\sigma)}{m_i(\sigma)} \right)^2 d\sigma \right) d\tau}_{C_2} \tag{4.36}$$

where we have used the following form of Schwartz inequality for the second term

$$\left[\int_a^b \psi_1 \psi_2 \, dx \right]^2 \leq \int_a^b \psi_1^2 \, dx \int_a^b \psi_2^2 \, dx \tag{4.37}$$

since $m_i(\sigma) \geq 1$, we can write the second line in (4.36) as: $(\beta = \max_i \sup_{\tau \geq 0} |\phi_i(\tau)|)$

$$\begin{aligned} C_2 &\leq 2\beta^4 \lambda_{max}(\Gamma)^2 \int_t^{t+T_0} (\tau - t) \int_t^{\tau} \sum_{i=1}^{n} \left(\frac{\tilde{\eta}_i^T(\sigma)\phi_i(\sigma)}{m_i(\sigma)} \right)^2 d\sigma d\tau \\ &\leq 2\beta^4 \lambda_{max}(\Gamma)^2 \int_t^{t+T_0} \sum_{i=1}^{n} \frac{(\tilde{\eta}_i^T(\sigma)\phi_i(\sigma))^2}{m_i^2(\sigma)} \left\{ \frac{T_0^2 - (\sigma - t)^2}{2} \right\} d\sigma \\ &\leq \beta^4 \lambda_{max}(\Gamma)^2 T_0^2 \int_t^{t+T_0} \sum_{i=1}^{n} \frac{(\tilde{\eta}_i^T(\sigma)\phi_i(\sigma))^2}{m_i^2(\sigma)} \, d\sigma \end{aligned} \tag{4.38}$$

Also, for the first term on the r.h.s (4.36), we can write:

$$\begin{aligned} &2\int_t^{t+T_0} \sum_{i=1}^{n} \left(\int_t^{\tau} \sum_{j \in N_i} \phi_i^T(\tau) \left(\tilde{\eta}_i(\sigma) - \tilde{\eta}_j(\sigma)\right) \, d\sigma \right)^2 d\tau \\ &\leq 2\beta^2 \int_t^{t+T_0} (\tau - t) \int_t^{\tau} \sum_{i=1}^{n} \left(\sum_{j \in N_i} (\tilde{\eta}_i - \tilde{\eta}_j) \right)^T \left(\sum_{j \in N_i} (\tilde{\eta}_i - \tilde{\eta}_j) \right) d\sigma d\tau \\ &= 2\beta^2 \int_t^{t+T_0} (\tau - t) \int_t^{\tau} \tilde{\eta}^T (L \otimes \mathbf{I}_n)^2 \tilde{\eta} \, d\sigma d\tau \end{aligned} \tag{4.39}$$

Using the properties of the Laplacian matrix, we can write

$$\tilde{\eta} = \sum_{j=1}^{m} \frac{c_j}{\sqrt{n}} \mathbf{1}_n \otimes \nu_j + \sum_{i=2}^{n} \sum_{j=1}^{m} d_{ij} \alpha_i \otimes \nu_j, \quad \sum_{j=1}^{m} c_j^2 + \sum_{i=2}^{n} \sum_{j=1}^{m} d_{ij}^2 = \|\tilde{\eta}\|^2 \tag{4.40}$$

where e_j denotes the j^{th} unit vector. (4.40) indicates that $\tilde{\eta}$ can be written in terms of the eigenvectors of the Laplacian matrix

$$\tilde{\eta}^T (L \otimes \mathbf{I}_n) \tilde{\eta} = \sum_{i=2}^{n} \sum_{j=1}^{m} \lambda_i d_{ij}^2, \ \tilde{\eta}^T (L \otimes \mathbf{I}_n)^2 \tilde{\eta} = \sum_{i=2}^{n} \sum_{j=1}^{m} \lambda_i^2 d_{ij}^2$$
$$\rightarrow \ \tilde{\eta}^T (L \otimes \mathbf{I}_n)^2 \tilde{\eta} \leq \lambda_n \tilde{\eta}^T (L \otimes \mathbf{I}_n) \tilde{\eta} \tag{4.41}$$

using (4.41) in (4.39),

$$c_1 \leq 2\beta^2 \int_t^{t+T_0} (\tau - t) \int_t^{\tau} \lambda_n \tilde{\eta}^T(\sigma)(L \otimes \mathbf{I}_n)\tilde{\eta}(\sigma) \ d\sigma d\tau \leq$$
$$2\beta^2 \int_t^{t+T_0} \lambda_n \tilde{\eta}^T(\sigma)(L \otimes \mathbf{I}_n)\tilde{\eta}(\sigma) \int_{\sigma}^{t+T_0} (\tau - t) \ d\tau d\sigma$$
$$\leq 2\beta^2 T_0^2 \lambda_n \int_t^{t+T_0} \tilde{\eta}^T(\sigma)(L \otimes \mathbf{I}_n)\tilde{\eta}(\sigma) \ d\sigma \tag{4.42}$$

thus, we have

$$-\int_t^{t+T_0} \sum_{i=1}^{n} \frac{(\tilde{\eta}_i^T(\tau)\phi_i(\tau))^2}{m_i^2(\tau)} \ d\tau \leq \frac{-1}{2m'} \left(\|\bar{\tilde{\eta}}\|^2 \alpha_0 T_0 - 2n\beta_0 T_0 \|\bar{\tilde{\eta}}\| \sqrt{1 - n\|\bar{\tilde{\eta}}\|^2} \right) \|\tilde{\eta}\|^2$$
$$+ \frac{1}{m'} \left[\beta^4 \lambda_{max}(\Gamma)^2 T_0^2 \int_t^{t+T_0} \sum_{i=1}^{n} \frac{(\tilde{\eta}_i^T(\sigma)\phi_i(\sigma))^2}{m_i^2(\sigma)} \ d\sigma + \right.$$
$$\left. 2\beta^2 T_0^2 \lambda_n \int_t^{t+T_0} \tilde{\eta}^T(\sigma)(L \otimes \mathbf{I}_n)\tilde{\eta}(\sigma) \ d\sigma \right] \tag{4.43}$$

which results in

$$
\begin{aligned}
&-\int_t^{t+T_0}\sum_{i=1}^{n}\frac{(\tilde{\eta}_i^T(\tau)\phi_i(\tau))^2}{m_i^2(\tau)}\,d\tau \leq \\
&\frac{-\left(\|\bar{\tilde{\eta}}\|^2\alpha_0T_0-2n\beta_0T_0\|\bar{\tilde{\eta}}\|\sqrt{1-n\|\bar{\tilde{\eta}}\|^2}\right)}{(2m^{'}+2\beta^4\lambda_{max}(\Gamma)^2T_0^2)}\|\tilde{\eta}\|^2 \\
&+\frac{2m^{'}\beta^2T_0^2\lambda_n}{m^{'}+\beta^4\lambda_{max}(\Gamma)^2T_0^2}\int_t^{t+T_0}\tilde{\eta}^T(\sigma)(L\otimes\mathbf{I}_n)\tilde{\eta}(\sigma)\,d\sigma
\end{aligned}
\tag{4.44}
$$

For the second term inside the integral in (4.25), we can write

$$
\begin{aligned}
&\frac{-1}{2}\int_t^{t+T_0}\sum_{i=1}^{n}\sum_{j\in N_i}(\tilde{\eta}_i(\tau)-\tilde{\eta}_j(\tau))^T(\tilde{\eta}_i(\tau)-\tilde{\eta}_j(\tau)) \leq \\
&\frac{-1}{4}\int_t^{t+T_0}\sum_{i=1}^{n}\sum_{j\in N_i}(\tilde{\eta}_i(t)-\tilde{\eta}_j(t))^T(\tilde{\eta}_i(t)-\tilde{\eta}_j(t))\,d\tau \\
&+\frac{1}{2}\int_t^{t+T_0}\sum_{i=1}^{n}\sum_{j\in N_i}(\tilde{\eta}_i^{'}-\tilde{\eta}_j^{'})^T(\tilde{\eta}_i^{'}-\tilde{\eta}_j^{'})\,d\tau
\end{aligned}
\tag{4.45}
$$

where we have used the inequality $(a+b)^2 \geq 0.5a^2 - b^2$ and the following definition

$$
\tilde{\eta}_i(\tau) = \tilde{\eta}_i(t) + \underbrace{(\tilde{\eta}_i(\tau)-\tilde{\eta}_i(t))}_{\tilde{\eta}_i^{'}} = \tilde{\eta}_i(t) + \tilde{\eta}_i^{'} \tag{4.46}
$$

Integrating $\dot{\tilde{\eta}}_i$ from t to τ results in

$$
\tilde{\eta}_i(\tau)-\tilde{\eta}_i(t) = \int_t^{\tau}\dot{\tilde{\eta}}_i(\sigma)\,d\sigma = \tilde{\eta}_i^{'} \rightarrow \tilde{\eta}_i^{'}-\tilde{\eta}_j^{'} = \int_t^{\tau}(\dot{\tilde{\eta}}_i(\sigma)-\dot{\tilde{\eta}}_j(\sigma))\,d\sigma \tag{4.47}
$$

Next, we try to find the upper bound for the second term on the r.h.s of (4.45) by squaring both sides of (4.47) and taking the summation over all agents as follows

$$
\begin{aligned}
&\sum_{i=1}^{n}\sum_{j\in N_i}(\tilde{\eta}_i^{'}-\tilde{\eta}_j^{'})^T(\tilde{\eta}_i^{'}-\tilde{\eta}_j^{'}) \leq \sum_{i=1}^{n}\sum_{j\in N_i}\left(\int_t^{\tau}(\dot{\tilde{\eta}}_i(\sigma)-\dot{\tilde{\eta}}_j(\sigma))\,d\sigma\right)^T\left(\int_t^{\tau}(\dot{\tilde{\eta}}_i(\sigma)-\dot{\tilde{\eta}}_j(\sigma))\,d\sigma\right) \\
&\leq \sum_{i=1}^{n}\sum_{j\in N_i}(\tau-t)\int_t^{\tau}\left((\dot{\tilde{\eta}}_i(\sigma)-\dot{\tilde{\eta}}_j(\sigma))\right)^T\left((\dot{\tilde{\eta}}_i(\sigma)-\dot{\tilde{\eta}}_j(\sigma))\right)\,d\sigma \leq (\tau-t)\int_t^{\tau}\dot{\tilde{\eta}}^T(L\otimes\mathbf{I}_n)\dot{\tilde{\eta}}\,d\sigma
\end{aligned}
\tag{4.48}
$$

using (4.40) we have

$$\dot{\tilde{\eta}}^T(L\otimes \mathbf{I}_n)\dot{\tilde{\eta}} \leq \sum_{i=2}^{n}\sum_{j=1}^{m}\lambda_i d_{ij}^2 \leq \lambda_n \dot{\tilde{\eta}}^T\dot{\tilde{\eta}} = \lambda_n \sum_{i=1}^{n}\dot{\tilde{\eta}}_i^T\dot{\tilde{\eta}}_i \tag{4.49}$$

which results in

$$\sum_{i=1}^{n}\sum_{j\in N_i}(\tilde{\eta}_i^{'}-\tilde{\eta}_j^{'})^T(\tilde{\eta}_i^{'}-\tilde{\eta}_j^{'}) \leq (\tau-t)\int_t^{\tau}\lambda_n\sum_{i=1}^{n}\dot{\tilde{\eta}}_i^T\dot{\tilde{\eta}}_i\ d\sigma \tag{4.50}$$

using $(a+b)^2 \leq 2a^2+2b^2$ for $\sum_{i=1}^{n}\dot{\tilde{\eta}}_i^T\dot{\tilde{\eta}}_i$, we can write

$$\begin{aligned}\sum_{i=1}^{n}\dot{\tilde{\eta}}_i^T\dot{\tilde{\eta}}_i &\leq 2\sum_{i=1}^{n}(\tilde{\eta}_i^T\phi_i)^2\phi_i^T\Gamma^T\Gamma\Phi_i + 2\sum_{i=1}^{n}\left(\sum_{j\in N_i}(\tilde{\eta}_i-\tilde{\eta}_j)\right)^T\left(\sum_{j\in N_i}(\tilde{\eta}_i-\tilde{\eta}_j)\right)\\ &\leq 2\lambda_{max}^2(\Gamma)\beta^2\sum_{i=1}^{n}(\tilde{\eta}_i^T\phi_i)^2 + 2\sum_{i=1}^{n}\left(\sum_{j\in N_i}(\tilde{\eta}_i-\tilde{\eta}_j)\right)^T\left(\sum_{j\in N_i}(\tilde{\eta}_i-\tilde{\eta}_j)\right)\end{aligned} \tag{4.51}$$

hence, for (4.48) the following holds

$$\begin{aligned}\int_t^{t+T_0}\sum_{i=1}^{n}\sum_{j\in N_i}(\tilde{\eta}_i^{'}-\tilde{\eta}_j^{'})^T(\tilde{\eta}_i^{'}-\tilde{\eta}_j^{'})\ d\tau &\leq \int_t^{t+T_0}(\tau-t)\int_t^{\tau}2\lambda_n\lambda_{max}^2(\Gamma)\beta^2\sum_{i=1}^{n}(\tilde{\eta}_i^T\phi_i)^2\ d\sigma d\tau\\ +\int_t^{t+T_0}(\tau-t)2\lambda_n^2\int_t^{\tau}\tilde{\eta}^T(\sigma)(L\otimes\mathbf{I}_n)\tilde{\eta}(\sigma)\ d\sigma d\tau\end{aligned} \tag{4.52}$$

changing the order of integrations results in

$$\begin{aligned}\int_t^{t+T_0}\sum_{i=1}^{n}\sum_{j\in N_i}(\tilde{\eta}_i^{'}-\tilde{\eta}_j^{'})^T(\tilde{\eta}_i^{'}-\tilde{\eta}_j^{'})\ d\tau &\leq 2\lambda_n\lambda_{max}(\Gamma)\beta^2T_0^2\int_t^{t+T_0}\sum_{i=1}^{n}(\tilde{\eta}_i^T\phi_i)^2\ d\sigma\\ &+2\lambda_n^2T_0^2\int_t^{t+T_0}\tilde{\eta}^T(\sigma)(L\otimes\mathbf{I}_n)\tilde{\eta}(\sigma)\ d\sigma\end{aligned} \tag{4.53}$$

Next, using (4.53), we can find the following upperbound

$$\frac{-1}{2}\int_t^{t+T_0}\sum_{i=1}^{n}\sum_{j\in N_i}(\tilde{\eta}_i(\tau)-\tilde{\eta}_j(\tau))^T(\tilde{\eta}_i(\tau)-\tilde{\eta}_j(\tau))\;d\tau \leq$$
$$\frac{-1}{4(1+2\lambda_n^2T_0^2)}\int_t^{t+T_0}\sum_{i=1}^{n}\sum_{j\in N_i}(\tilde{\eta}_i(t)-\tilde{\eta}_j(t))^T(\tilde{\eta}_i(t)-\tilde{\eta}_j(t))\;d\tau$$
$$+\frac{\lambda_n\lambda_{max}^2(\Gamma)\beta^2T_0^2}{(1+2\lambda_n^2T_0^2)}\int_t^{t+T_0}\sum_{i=1}^{n}(\tilde{\eta}_i^T\phi_i)^2\;d\sigma \tag{4.54}$$

Using the definition of the Laplacian matrix and $\bar{\tilde{\eta}}$, we have

$$\tilde{\eta}^T(L\otimes\mathbf{I}_n)\tilde{\eta}=\sum_{i=2}^{n}\sum_{j=1}^{m}\lambda_i d_{ij}^2\geq\sum_{i=2}^{n}\sum_{j=1}^{m}\lambda_2 d_{ij}^2\geq\lambda_2(1-n\bar{\tilde{\eta}}^T\bar{\tilde{\eta}})\left\|\tilde{\eta}\right\|^2 \tag{4.55}$$

using (4.55), (4.54) turns into

$$\frac{-1}{2}\int_t^{t+T_0}\sum_{i=1}^{n}\sum_{j\in N_i}(\tilde{\eta}_i(\tau)-\tilde{\eta}_j(\tau))^T(\tilde{\eta}_i(\tau)-\tilde{\eta}_j(\tau))\;d\tau \leq$$
$$\frac{-T_0\lambda_2(1-n\bar{\tilde{\eta}}^T\bar{\tilde{\eta}})}{4(1+2\lambda_n^2T_0^2)}\left\|\tilde{\eta}\right\|^2+\frac{\lambda_n\lambda_{max}^2(\Gamma)\beta^2T_0^2}{(1+2\lambda_n^2T_0^2)}\int_t^{t+T_0}\sum_{i=1}^{n}(\tilde{\eta}_i^T\phi_i)^2\;d\sigma$$

hence, we can write

$$V(t+T_0)-V(t)\leq-\left(\frac{\left(\left\|\bar{\tilde{\eta}}\right\|^2\alpha_0T_0-2n\beta_0T_0\left\|\bar{\tilde{\eta}}\right\|\sqrt{1-n\left\|\bar{\tilde{\eta}}\right\|^2}\right)}{(2m'+2\beta^4\lambda_{max}(\Gamma)^2T_0^2)}+\frac{T_0\lambda_2(1-n\bar{\tilde{\eta}}^T\bar{\tilde{\eta}})}{4(1+2\lambda_n^2T_0^2)}\right)\left\|\tilde{\eta}\right\|^2$$
$$+\frac{2T_0^2\lambda_n}{m'+\beta^4\lambda_{max}^2(\Gamma)T_0^2}\int_t^{t+T_0}\tilde{\eta}^T(\sigma)(L\otimes\mathbf{I}_n)\tilde{\eta}(\sigma)\;d\sigma$$
$$+\frac{\lambda_n\lambda_{max}^2(\Gamma)m'^2\beta^2T_0^2}{(1+2\lambda_n^2T_0^2)}\int_t^{t+T_0}\sum_{i=1}^{n}\left(\frac{\tilde{\eta}_i^T\phi_i}{m_i}\right)^2\;d\sigma \tag{4.56}$$

since $-\dot{V}(\sigma)=\sum_{i=1}^{n}\frac{(\tilde{\eta}_i(\sigma)^T\phi_i(\sigma))^2}{m_i^2}+\tilde{\eta}^T(\sigma)(L\otimes\mathbf{I}_n)\tilde{\eta}(\sigma)$, based on the following definition

$$\Delta=\max\left(\frac{\lambda_n\lambda_{max}^2(\Gamma)m'^2\beta^2T_0^2}{(1+2\lambda_n^2T_0^2)},\frac{2T_0^2\lambda_n}{m'+\beta^4\lambda_{max}^2(\Gamma)T_0^2}\right) \tag{4.57}$$

we can write

$$V(t+T_0)-V(t)\leq-\left(\frac{\left(\left\|\bar{\tilde{\eta}}\right\|^2\alpha_0T_0-2n\beta_0T_0\left\|\bar{\tilde{\eta}}\right\|\sqrt{1-n\left\|\bar{\tilde{\eta}}\right\|^2}\right)}{\Delta\left(2m'+2\beta^4\lambda_{max}^2(\Gamma)T_0^2\right)}+\frac{T_0\lambda_2(1-n\bar{\tilde{\eta}}^T\bar{\tilde{\eta}})}{4\Delta(1+2\lambda_n^2T_0^2)}\right)\left\|\tilde{\eta}\right\|^2 \tag{4.58}$$

hence, if the following condition holds

$$\gamma_1^{'}=\lambda_{min}(\Gamma)\left(\frac{\left(\left\|\bar{\tilde{\eta}}\right\|^2\alpha_0T_0-2n\beta_0T_0\left\|\bar{\tilde{\eta}}\right\|\sqrt{1-n\left\|\bar{\tilde{\eta}}\right\|^2}\right)}{\Delta\left(2m'+2\beta^4\lambda_{max}^2(\Gamma)T_0^2\right)}+\frac{T_0\lambda_2(1-n\bar{\tilde{\eta}}^T\bar{\tilde{\eta}})}{4\Delta(1+2\lambda_n^2T_0^2)}\right)>0 \tag{4.59}$$

from (4.58), we can assure that $\gamma_1^{'}\leq 1$ and $V(t+T_0)=\gamma^{'}V(t)\leq V(t).(\gamma^{'}=1-\gamma_1^{'})$
As it is clear from (4.59), $\gamma_1^{'}$ can also become negative which does not represent the real situations since according to (4.21), $\dot{V}\leq 0$. A more realistic bound for the stability of (4.19) can be derived by noting the fact that the r.h.s of (4.34) must be changed as follows

$$A\geq\max\left(\left(\left\|\bar{\tilde{\eta}}\right\|^2\alpha_0T_0-2n\beta_0T_0\left\|\bar{\tilde{\eta}}\right\|\sqrt{1-n\left\|\bar{\tilde{\eta}}\right\|^2}\right),0\right)\left\|\bar{\tilde{\eta}}\right\|^2 \tag{4.60}$$

Therefore, from the fact that $\lambda_2(1-n\bar{\tilde{\eta}}^T\bar{\tilde{\eta}})\geq 0$, we can calculate a conservative bound for the convergence of (4.19) as follows

$$\begin{aligned}
&V(t+T_0)-V(t)=-\gamma_2\gamma_3\lambda_{min}(\Gamma)V(t)=-\gamma_1V(t),\quad\rightarrow\ V(t+T_0)=\gamma V(t)\\
&\gamma_2=\max\left(\left(\left\|\bar{\tilde{\eta}}\right\|^2\alpha_0T_0-2n\beta_0T_0\left\|\bar{\tilde{\eta}}\right\|\sqrt{1-n\left\|\bar{\tilde{\eta}}\right\|^2}\right),\lambda_2(1-n\bar{\tilde{\eta}}^T\bar{\tilde{\eta}})\right),\\
&\gamma_3=\min\left(\frac{1}{\Delta\left(2m'+2\beta^4\lambda_{max}^2(\Gamma)T_0^2\right)},\frac{T_0}{4\Delta(1+2\lambda_n^2T_0^2)}\right)
\end{aligned} \tag{4.61}$$

where $\gamma_1=\gamma_2\gamma_3\lambda_{min}(\Gamma)$ and $\gamma=1-\gamma_1$. Next, if we divide the domain $[0,t]$ with the sub domains of length T_0, for $t=(n-1)T_0$, we can conclude $V(t)\leq V(nT_0)\leq\gamma^nV(0)$ which proves the exponential stability of the identification system.

4.2.4 Analysis of Convergence Rates

In this section, we analyze the L_2 gain of the identification system and study the effects of changing the parameters such as the level of the satisfaction of the persistency excitation α_0 in (4.31) on the convergence of the algorithm (4.19). From (4.59) and (4.61), it is clear that the performance of (4.19) also depends on the state of the "consensus" in the network. In other words, if we consider $x^2 = n \left\|\bar{\tilde{\eta}}\right\|^2$ as a measure of consensus in the system (4.19), it is clear that the exponential decadence of (4.61) has a nonlinear relation with x. We can rewrite the $\gamma_1^{'}$ as follows

$$\gamma_1^{'} = \frac{T_0\lambda_2\lambda_{min}(\Gamma)}{4\Delta(1+2\lambda_n^2T_0^2)} + \left(\frac{\alpha_0 T_0\lambda_{min}(\Gamma)}{n\Delta\left(2m^{'}+2\beta^4\lambda_{max}^2(\Gamma)T_0^2\right)} - \frac{T_0\lambda_2\lambda_{min}(\Gamma)}{4\Delta(1+2\lambda_n^2T_0^2)}\right)x^2 - \frac{2\sqrt{n}\beta_0 T_0\lambda_{min}(\Gamma)}{\Delta\left(2m^{'}+2\beta^4\lambda_{max}^2(\Gamma)T_0^2\right)}\sqrt{x^2-x^4} \tag{4.62}$$

For the purpose of simplification, consider the parameters a, b, c with the following definitions

$$a = \frac{T_0\lambda_2\lambda_{min}(\Gamma)}{4\Delta(1+2\lambda_n^2T_0^2)},\ b = \left(\frac{\alpha_0 T_0\lambda_{min}(\Gamma)}{n\Delta\left(2m^{'}+2\beta^4\lambda_{max}^2(\Gamma)T_0^2\right)} - \frac{T_0\lambda_2\lambda_{min}(\Gamma)}{4\Delta(1+2\lambda_n^2T_0^2)}\right),$$
$$c = \frac{2\sqrt{n}\beta_0 T_0\lambda_{min}(\Gamma)}{\Delta\left(2m^{'}+2\beta^4\lambda_{max}^2(\Gamma)T_0^2\right)}$$

first, note that c is at least two times greater than b, this is due to the fact that $\beta_0 \geq \alpha_0$ and $\lambda_2 \geq 0$ for a connected graph. It is also clear that if the level of the satisfaction of the PE condition is high i.e. $\alpha_0 >> 1$, then the network performs the identification process much faster regarding (4.21), however, b can be either negative or positive and hence, we divide the analysis in to two parts depending on the sign of b. The effects of changing b and c are depicted in Fig. 4.1

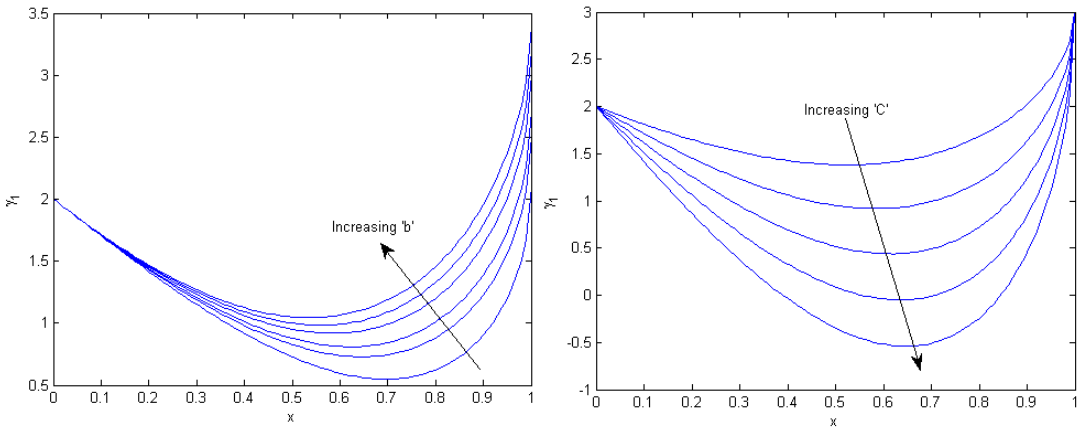

Figure 4.1: Effects of changing b and c in $\gamma_1^{'}$ (Case 1), $(b \geq 0)$

Case 1: $(b \geq 0)$

For this case, we can calculate the minimum of the $\gamma_1^{'}$ by computing the derivative of $\gamma_1^{'}$ with respect to x as follows:

$$\frac{d\gamma_1^{'}}{dx} = 2bx - \frac{c(x - 2x^3)}{\sqrt{x^2 - x^4}} = 0 \;\Rightarrow\; 2b\sqrt{x^2 - x^4} = c(1 - 2x^2)b > 0 \;\Rightarrow 1 - 2x_{min}^2 > 0$$

$$\Rightarrow 4(b^2 + c^2)x^4 - 4(b^2 + c^2)x^2 + c^2 = 0 \Rightarrow x_{min} = \sqrt{\frac{1 - \sqrt{\frac{b^2}{b^2+c^2}}}{2}} \tag{4.63}$$

where the other solution is disregarded since $(1 - 2x_{min}^2 > 0)$. Calculating the second derivative of $\gamma_1^{'}$ with respect to x, we have:

$$\frac{d^2\gamma_1^{'}}{dx^2} = 2b + \frac{c(12x^2 - 2)}{2\sqrt{x^2 - x^4}} + \frac{c(-4x^3 + 2x)^2}{4\sqrt{x^2 - x^4}}$$
$$= 2b + \frac{2c(2b^2 - 3bd + 2c^2)}{cd} + \frac{4b^2c(b^4 - bd^3 + c^4 + 2b^2c^2)}{c^3d^3} > 0,\; d^2 = b^2 + c^2 \tag{4.64}$$

which demonstrates that the x_{min} is indeed a minimizer of γ_1. The minimum value of γ_1 is as follows:

$$\gamma_1^{'}(x_{min}) = a + \frac{b}{2} - \frac{\sqrt{b^2 + c^2}}{2} \tag{4.65}$$

γ_{min} represents the worst gain of the system which is positive definite. In fact, (4.65) suggests a criteria for designing the network communication graph to ensure the convergence of the estimates of the unknown parameters. However, it should be noted that such an approach is quite conservative as the first term in $\gamma_1^{'}$ must be replaced with a better approximation.

Case 2: $(b < 0)$

The effect of changing b and c for this case is shown in Fig. 4.2. It is clear that we need to choose the other solution of (4.63) for this case as $1 - 2x_{min}^2 < 0$ must hold. Calculating the second derivative of γ_1 in this case results in:

$$\frac{d^2\gamma_1}{dx^2} = 8b + 4d + \frac{4b^2c(b+d)}{c^3}, \; d^2 = b^2 + c^2 \tag{4.66}$$

which is positive definite since $(b < 2c)$. Next, we try to get a better bound for the L_2 gain of the estimation system.

We can also find a better approximation on the bound for γ_1. This can be done by noticing that the r.h.s of (4.34) can be better approximated by a positive semi definite function, in fact, since the first term on the l.h.s of (4.27) is always positive semi definite, this can be done by replacing the summation with the max function of the two terms.

$$\gamma_2 = \max\left(\left(\left\|\bar{\tilde{\eta}}\right\|^2 \alpha_0 T_0 - 2n\beta_0 T_0 \left\|\bar{\tilde{\eta}}\right\| \sqrt{1 - n\left\|\bar{\tilde{\eta}}\right\|^2}\right), \lambda_2(1 - n\bar{\tilde{\eta}}^T\bar{\tilde{\eta}})\right), \tag{4.67}$$

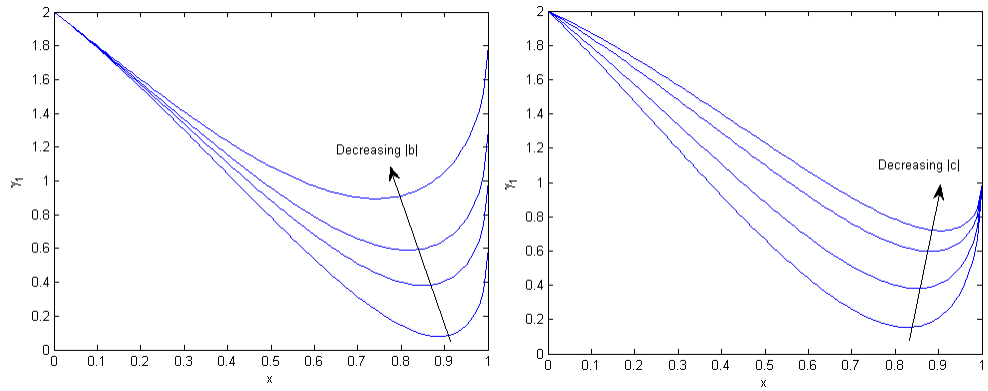

Figure 4.2: Effects of changing b and c in $\gamma_1^{'}$ (Case 2), $(b < 0)$

It is clear that even for any small α_0, γ_1 is positive semi definite. The latter comes from the fact that the first term in the argument of the max function only becomes zero where $1 - n\left\|\bar{\tilde{\eta}}\right\|^2 = 0$ and at this point the second argument is positive definite based on (4.31). Fig. 4.3 illustrates the effect of changing parameters for γ_1 for two cases depending on the value of the algebraic connectivity of the network λ_2. (a) depicts the case that (λ_2) is high compared to b and c. The figure on the right, suggests that for this case the better convergence behavior can be achieved by enforcing the network to reach to the consensus state on a faster time scale. On the other hand, for the figure on the left, the maximum of γ_1 occurs at the boundaries, i.e. $x = \pm 1$, and this suggest that achieving the consensus task will decrease the performance of the estimation task. Anther interesting fact which can be deduced from Fig. 4.3 is that the convergence behavior of the network is not just dependent on the lower bound in (4.31). It is clear that by increasing the upper bound in (4.31), the worst γ_1 of the network will be decreased. This case will occur at

$$x = \pm\sqrt{\frac{2ab + c\sqrt{c^2 + 4ab} + 2a^2 + c^2}{2(a^2 + 2ab + b^2 + c^2)}} \tag{4.68}$$

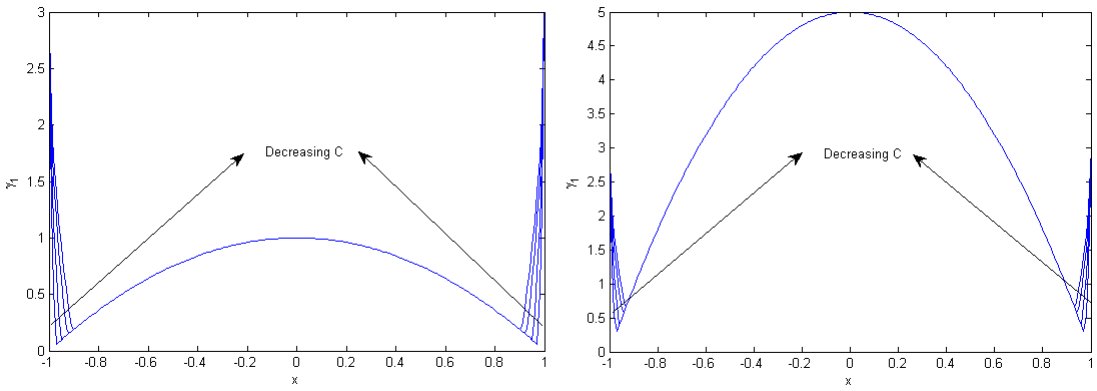

Figure 4.3: Effects of changing b and c in γ_2,

which suggests that increasing the algebraic connectivity will push the minimum toward $x \pm 1$. This shows that increasing λ_2 will improve the worst convergence gain.

4.2.5 Two time Scales Approach Toward Consensus Estimation

In this section, we devise another approach for distributed estimation problem. In the previous section, we discussed the case that the maximum of γ_1 will happen around the consensus equilibrium. Inspired by such cases, here, we design an algorithm which takes the consensus task as the main priority. We address this issue using a singular perturbation consensus method which is described in [106],[107]. The main idea is to achieve the consensus task on the fast time scale and the estimation task on the slower time scale. We start by introducing the following lemmas from [107].

Lemma 4.1: [107] Consider a network of agents with Laplacian matrix L with the constant

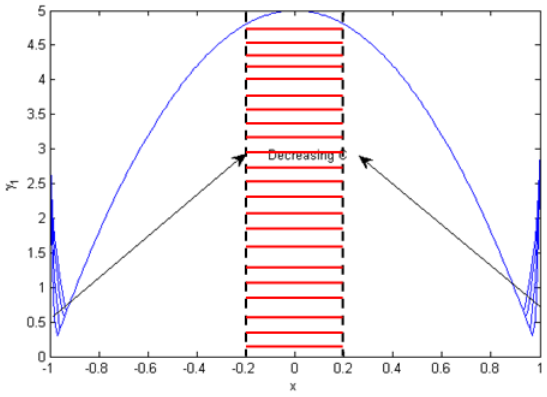

Figure 4.4: A particular case for which the consensus is the priority

inputs $u_i \in \mathbb{R}^n$, then the system:

$$\begin{aligned} \dot{z}_i &= -(z_i - u_i) - \sum_{i=1}^{n} L_{ij}(z_j + \nu_j) \\ \dot{\nu}_i &= \sum_{i=1}^{n} L_{ij} z_j \end{aligned} \tag{4.69}$$

will converge to the average of u_i, i.e. $\frac{1}{n}\sum_{i=1}^{n} u_i$.

Lemma 4.2 [106] Consider a network of agents with Laplacian matrix L with the inputs u_i and small $\epsilon > 0$, then the following system

$$\begin{aligned} \epsilon \dot{z}_i &= -(z_i + \beta u_i + \dot{u}_i) - \sum_{i=1}^{n} L_{ij}(z_j + \nu_j) \\ \epsilon \dot{\nu}_i &= \sum_{i=1}^{n} L_{ij} z_j, \quad \dot{x}_i = -\beta x_i - z_i, \ \beta > 0 \end{aligned} \tag{4.70}$$

will ensure that $\left\| x_i(t) - \frac{1}{n}\sum_{i=1}^{n} u_i(t) \right\| < O(\epsilon)$.

We can formulate the consensus estimation problem using *Lemma 4.2*. Consider $u = \hat{\theta}, u_i = \hat{\theta}_i, i \in \{1, \cdots, n\}$. Then, consider the filter (4.70) together with the following

system

$$\dot{\hat{\theta}}_i = -\beta\epsilon_i\phi_i = -\beta\phi_i\phi_i^T(\theta^* - x_i) \tag{4.71}$$

where $\epsilon_i = \phi_i(\theta^* - x_i)$. From Lemma 4.2, we can conclude that there exist k such that, $x_i(t) \to \frac{1}{n}\sum_{i=1}^{n}\hat{\theta}_i + k_i\epsilon$, we have

$$\dot{\hat{\theta}}_i = -\beta\phi_i\phi_i^T\left(\frac{1}{n}\sum_{i=1}^{n}(\hat{\theta}_i - \theta^*) + k_i\epsilon\right),\ \beta > 0 \tag{4.72}$$

Next, using the change of variables $\tilde{\theta}_i = \hat{\theta}_i - \theta^*$ and $S = \frac{\sum_{i=1}^{n}\tilde{\theta}_i}{n}$, and summing (4.72) over all agents, we can write

$$\dot{S} = -\beta\left(\sum_{i=1}^{n}\phi_i\phi_i^T\right)S + G\epsilon \tag{4.73}$$

assuming that (4.48) is satisfied here, i.e there exists α_0 such that $\left(\sum_{i=1}^{n}\phi_i\phi_i^T\right) > \alpha_0$, then the first order approximation of (4.73) in terms of ϵ, $(\dot{S}_1 = -\beta\left(\sum_{i=1}^{n}\phi_i\phi_i^T\right)S_1)$, is exponentially stable and using Theorem 8.3 in [34], we can conclude that the trajectories of the main system (4.73) remain in the ϵ-neighborhood of origin on the infinite time intervals.

Remark 4.1 In [105], authors have shown that it is possible for the estimation subsystem to converge to actual values of the parameters provided that it uses the previously recorded information which is sufficiently rich to ensure the stability of the estimation subsystem. This approach can be used to reduce the oscillation in the inputs which are needed to ensure that the PE condition is satisfied for the estimation system. Using the results of this section, it is easy to add the consensus term inside the main estimation laws. This way we can ensure the convergence of estimation subsystems provided that the recorded data for all agents satisfy the PE condition which is much less restrictive than satisfying the PE condition for the recorded data of a single agent. In order to show this, consider a network of n agents with a connected topology graph and suppose that each agents has

access to p data from previous measurements. Consider the estimation system of (4.19) without the denominator term. The consensus estimation algorithm can be expressed as follows

$$\dot{\hat{\eta}}_i = \phi_i \epsilon_i - \sum_{k=1}^{p} \phi(x_k)\epsilon_k - \sum_{j\in N_i} (\hat{\eta}_i - \hat{\eta}_j) \tag{4.74}$$
$$\epsilon_i = \phi_i^T(\hat{\eta}_i - \eta^*),\ \epsilon_k = \phi(x_k)^T(\hat{\eta}_i - \eta^*) = \phi(x_k)^T\hat{\eta}_i - \phi(x_j)^T\eta^*$$

where $\phi(x_k)$ represents the previous data at x_k which could be the states of a mobile robot. It should be noted that ϵ_k can be computed since all $\phi(x_k)^T$ and $\hat{\eta}_i$ and $\phi(x_j)^T\eta^*$ are measurable. Using the same procedure in this section, we can reach to a similar gain as in (4.61)

$$\gamma_1 = \max\left(2\lambda_2(1 - n\bar{\bar{\eta}}^2), \frac{(\bar{\bar{\eta}}^2\alpha_1 T_0 - 2\beta_1 T_0 \|\bar{\bar{\eta}}\| \sqrt{1 - n\bar{\bar{\eta}}})}{m' + \beta^4\Gamma^2 T^2}\right) \tag{4.75}$$

where α_1 and β_1 are as follows

$$T_0\beta_1 \geq \sum_{i=1}^{n}\sum_{k=1}^{p} \phi(x_{ki})\phi(x_{ki})^T + \int_t^{t+T} \sum_{i=1}^{n} \|\phi_i(\tau)\|^2\ d\tau \geq \alpha_1 T_0 \tag{4.76}$$

which suggests that we can choose higher values for α_1 to satisfy the PE condition for the estimation network. We can summarize the result of this section in to the following lemma:

Lemma 4.3 Consider a network of estimator as in (4.73) and suppose that the recorded data for all agents contain m linearly independent vectors $\phi(x_{ik})$, i.e

$$Z = [\phi(x_{11}), \cdots, \phi(x_{1p}), \cdots, \phi(x_{n1}), \cdots, \phi(x_{1p})],\ Rank(Z) = m \tag{4.77}$$

Then condition (4.76) will be satisfied and the exponential convergence of the network is followed.

Remark 4.2 we can also study the stability of the network (4.19) for the situations which

the parameters are slowly varying, i.e. $\left\|\dot{\theta}_i^*\right\| \leq \epsilon_i$ and $|\theta_i| \leq \delta_i$. It is possible to show that the system is enjoying nice robustness properties with respect to the variation of the parameters with respect to time. To see this, consider a network of multi agent systems which each agent can measure the following function at its location

$$f_i = \sum_{k=1}^{m} (x_{ik} - \theta_k^*)^2 \tag{4.78}$$

using differentiation, we have

$$\begin{aligned} &\frac{d}{dt}\left(f - \sum_{k=1}^{m} x_{ik}^2\right) = -2\sum_{k=1}^{m} \dot{x}_{ik}\theta_k^* - 2\sum_{k=1}^{m} \dot{\theta}_k^*(x_{ik} - \theta_k^*) \\ &\rightarrow \;\; z_i = \phi_i^T \theta^* + \alpha_i \end{aligned} \tag{4.79}$$

Next, suppose that the trajectories of agents are bounded i.e. $|x_{ik}| \leq M_i$ which results in

$$\alpha(\epsilon) = 2\sum_{k=1}^{m} \dot{\theta}_k^*(x_{ik} - \theta_k^*) \leq |2m\epsilon_i(\delta_i + M_i)| \leq |2m\epsilon(\delta_i + M_i)|\,, \;\; \epsilon = \max_i(\epsilon_i) \tag{4.80}$$

and for estimation network we can write

$$\begin{aligned} &\dot{\tilde{\eta}}_i = \gamma\phi_i\phi_i^T\tilde{\eta}_i + \sum_{j\in N_i}(\hat{\eta}_j - \hat{\eta}_i) + \alpha(\epsilon) \\ &\rightarrow \;\; \dot{\tilde{\eta}}_i = \gamma\phi_i\phi_i^T\tilde{\eta}_i + \sum_{j\in N_i}(\hat{\eta}_j - \hat{\eta}_i) + \alpha(\epsilon) - \dot{\eta}^* \end{aligned} \tag{4.81}$$

using the fact

$$|\alpha(\epsilon) - \dot{\eta}^*| \leq 2m\epsilon(\delta_i + M_i) + \epsilon_i \leq \epsilon(2m(\delta_i + M_i) + 1) \leq K\epsilon \rightarrow (\alpha(\epsilon) - \dot{\eta}^*) \in O(\epsilon) \tag{4.82}$$

and assuming the collective PE condition is satisfied, we can conclude that the main system is stable and using Theorem 8.3 in [34], it is easy to conclude that the trajectories of the perturbed system will remain in the ϵ-neighborhood of the main system on an infinite time interval.

4.3 Extremum Seeking Using Adaptive Localization

4.3.1 Single Agent

In this section, we design an adaptive extremum seeking algorithm based on [1] for a single agent. In general, we are trying to add the concept of "control" to the localization problem of previous sections. The main difficulty toward this goal comes from the fact that the robot needs to simultaneously satisfy the PE condition and reaching the target which are in contradiction. From practical point of view, if the robot reaches to a neighborhood of the target and stays in that neighborhood for the future time, it would be sufficient. This can be attained by embedding oscillatory signals in to the inputs of the vehicle to ensure that the PE condition is satisfied at least locally in the vicinity of the target. Since studying the stability of the resulting system is very difficult due to the system nonlinearities and the presence of time-varying signals, we focus on the stability of the averaged system which is time invariant and can be approached by classic techniques. In the next step, we extend the results to infinite interval based on the local exponential convergence of the main subsystem and Theorem 8.3 in [34]. We start by considering the kinematics of a single holonomic robot with the adaptive extremum seeking algorithm which is depicted in Fig. 4.5. Suppose that the robot is moving in $\mathbb{R}^2$ and it can measure its distance to an unknown target, i.e. $(d^2 = (x - x^*)^2 + (y - y^*)^2)$, we can write

$$\frac{d}{dt}[d^2(t)] = 2[\dot{x}\ \dot{y}] \begin{bmatrix} x - x^* \\ y - y^* \end{bmatrix} \tag{4.83}$$

An interesting feature of (4.83) is that it has a linear in parameter structure and thus the classical adaptive parameter estimation techniques can be easily used to construct the identification subsystem. Also, notice that if we consider a general quadratic function

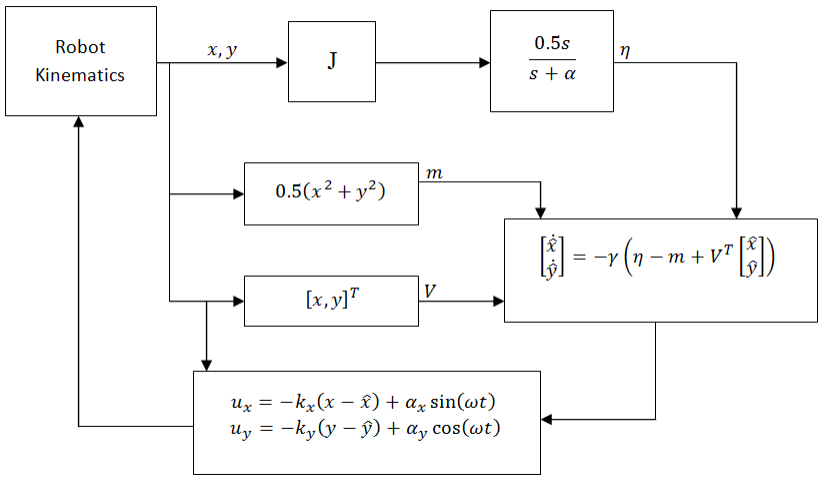

Figure 4.5: Extremum seeking loop for a single vehicle based on [1]

which has elliptical level curves as opposed to (4.83) where the level curves are assumed to be circular, two additional terms will be added to the r.h.s of (4.83) which contain the parameters regarding the shape of the field. It is also possible to derive the linear in parameter model of the location of the extremum without differentiation. To see this consider the following equations

$$\int_0^t d^2\ dt = \int_0^t (x^2 + y^2)\ dt - 2x^* \int_0^t x\ dt - 2y^* \int_0^t y\ dt + (x^{*2} + y^{*2})t$$
$$d^2 t = (x^2 + y^2)t - 2xx^* t - 2yy^* t + (x^{*2} + y^{*2})t \tag{4.84}$$

where the second equation in (4.84) is obtained via multiplying the square of the measurement of the distance by the value of the current measurement of time. Subtracting the

two equations in (4.84), we can write

$$\left(\int_0^t d^2\ dt - td^2\right) - \left(\int_0^t (x^2+y^2)\ dt - (x^2+y^2)t\right)$$
$$= 2x^*\left(\int_0^t x\ dt - tx\right) + 2y^*\left(\int_0^t y\ dt - ty\right) \tag{4.85}$$

The l.h.s of (4.85) can be measured at each time instants and it is clear that the r.h.s contains the linear in parameter model of the coordinates of the extremum point. Both of (4.83) and (4.85) can be used for building the extremum seeking algorithm, however, here, we use (4.83) to facilitate the convergence proofs. Since using the differential of signals in the design might not be practical due to the external noises, we introduce the following low pass filters from [1]

$$\begin{aligned}
\dot{z}_1 &= -\alpha z_1 + 0.5d^2(t)\\
\eta &= -\alpha z_1 + 0.5d^2(t)\\
\dot{z}_2 &= -\alpha z_2 + 0.5(x^2+y^2)\\
m &= -\alpha z_2 + 0.5(x^2+y^2)\\
\dot{z}_3 &= -\alpha z_3 + [x\ y]^T\\
V &= -\alpha z_3 + [x\ y]^T
\end{aligned}$$

using previous definitions, it is easy to verify that

$$\eta(t) = m(t) - V^T[x^*, y^*]^T \tag{4.86}$$

Then adaptive localization algorithm for this problem can be written as

$$\begin{bmatrix} \dot{\hat{x}} \\ \dot{\hat{y}} \end{bmatrix} = -\gamma(\eta - m + V^T[\hat{x}\ \hat{y}]^T) \tag{4.87}$$

Using the change of variables $[\tilde{x}\ \tilde{y}]^T = [\hat{x} - x^*\ \hat{y} - y^*]^T$, our proposed extremum seeking algorithm for this case can be expressed as follows:

$$\begin{aligned}
\dot{x} &= -k_x(x - \hat{x}) + \alpha_x \sin(\omega t) \\
\dot{y} &= -k_y(y - \hat{y}) + \alpha_y \cos(\omega t) \\
\begin{bmatrix} \dot{\tilde{x}} \\ \dot{\tilde{y}} \end{bmatrix} &= -\gamma V V^T \begin{bmatrix} \tilde{x} \\ \tilde{y} \end{bmatrix}
\end{aligned} \tag{4.88}$$

here, we show that the equilibrium of the averaged system of (4.88) is locally exponentially stable. Consider the additional change of variables

$$\begin{aligned}
\bar{x} &= x - \alpha_x \sin(\omega t) \\
\bar{y} &= y - \alpha_y \cos(\omega t)
\end{aligned} \tag{4.89}$$

since $V = [V_1, V_2]^T = \frac{s}{s+\alpha} \begin{bmatrix} x \\ y \end{bmatrix}$, we have

$$V_1 = \frac{s}{s+\alpha}[\bar{x} + \alpha_x \sin(\omega t)] = \bar{V}_1 + \frac{s}{s+\alpha}(\alpha_x \sin(\omega t)) \tag{4.90}$$

Also, we can observe that

$$\begin{aligned}
\frac{s}{s+\alpha}(\alpha_x \sin(\omega t)) &= \frac{\omega s}{(s+\alpha)(s^2+\omega^2)} \\
\xrightarrow{time\ \ domain} \frac{\omega^2 \sin(\omega t) + \alpha\omega \cos(\omega t)}{\alpha^2 + \omega^2} &- \frac{\alpha\omega e^{-\alpha t}}{\alpha^2 + \omega^2}
\end{aligned} \tag{4.91}$$

The second term in (4.91) will vanish quickly because of the presence of the exponential term and the fact that the value of ω is high. For V_2, we can write

$$V_2 = \frac{s}{s+\alpha}[\bar{y} + \alpha_y \cos(\omega t)] = \bar{V}_2 + \frac{s}{s+\alpha}(\alpha_y \cos(\omega t)) \tag{4.92}$$

again, as in the case of V_1, we have

$$\begin{aligned}\frac{s}{s+\alpha}(\alpha_y \cos(\omega t)) &= \frac{s^2}{(s+\alpha)(s^2+\omega^2)} \\ \xrightarrow{time\ domain} \frac{\omega^2\cos(\omega t) - \alpha\omega\sin(\omega t)}{\alpha^2+\omega^2} &+ \frac{\alpha^2 e^{-\alpha t}}{\alpha^2+\omega^2}\end{aligned} \tag{4.93}$$

therefore, the estimation subsystem becomes

$$\begin{aligned}\dot{\tilde{x}} = -\gamma \Bigg(&\left[\bar{V}_1^2 + \frac{\alpha_x^2}{(\alpha^2+\omega^2)^2}[\omega^2\sin(\omega t) + \alpha\omega\cos(\omega t)]^2 + \frac{2\bar{V}_1}{\alpha^2+\omega^2}[\omega^2\sin(\omega t) + \alpha\omega\cos(\omega t)]\right]\tilde{x} \\ &+ \left[\bar{V}_1\bar{V}_2 + \bar{V}_1\frac{\omega^2\cos(\omega t) - \alpha\omega\sin(\omega t)}{\alpha^2+\omega^2} + \bar{V}_2\frac{\omega^2\sin(\omega t) + \alpha\omega\cos(\omega t)}{\alpha^2+\omega^2}\right] \\ &+ \frac{\omega^2\cos(\omega t) - \alpha\omega\sin(\omega t)}{\alpha^2+\omega^2}\frac{\omega^2\sin(\omega t) + \alpha\omega\cos(\omega t)}{\alpha^2+\omega^2}\Bigg)\tilde{y}\end{aligned} \tag{4.94}$$

using the facts

$$\begin{aligned}&\int_0^{\frac{2\pi}{\omega}} \sin(\omega t)\cos(\omega t) = 0 \\ &\frac{\alpha_x^2}{\omega^2+\alpha^2}\int_0^{\frac{2\pi}{\omega}} \sin^2(\omega t)\ dt = \frac{\alpha_x^2}{\omega^2+\alpha^2}\int_0^{\frac{2\pi}{\omega}} \cos^2(\omega t)\ dt = \frac{\pi\alpha_x^2}{\omega(\omega^2+\alpha^2)}\end{aligned} \tag{4.95}$$

we can obtain the averaged system of (4.88) as follows

$$\dot{x}_{ave} = -\gamma\left(\bar{V}_{1,ave}^2 + \frac{\omega\pi\alpha_x^2(1+\alpha^2)}{\alpha^2+\omega^2}\right)\tilde{x}_{ave} - \gamma(\bar{V}_{1,ave}\bar{V}_{2,ave})\tilde{y}_{ave} \tag{4.96}$$

for $\tilde{y}$ we have

$$\dot{\tilde{y}} = -\gamma(V_2^2\tilde{y} + V_1V_2\tilde{x}) \tag{4.97}$$

$$\begin{aligned}\dot{\tilde{y}} = -\gamma \Bigg(&\left[\bar{V}_2^2 + \frac{\alpha_y^2}{(\alpha^2+\omega^2)^2}[\omega^2\cos(\omega t) - \alpha\omega\sin(\omega t)]^2 - \frac{2\bar{V}_2}{\alpha^2+\omega^2}[\omega^2\cos(\omega t) - \alpha\omega\sin(\omega t)]\right]\tilde{y} \\ &+ \left[\bar{V}_1\bar{V}_2 + \bar{V}_1\frac{\omega^2\cos(\omega t) - \alpha\omega\sin(\omega t)}{\alpha^2+\omega^2} + \bar{V}_2\frac{\omega^2\sin(\omega t) + \alpha\omega\cos(\omega t)}{\alpha^2+\omega^2}\right] \\ &+ \frac{\omega^2\cos(\omega t) - \alpha\omega\sin(\omega t)}{\alpha^2+\omega^2}\frac{\omega^2\sin(\omega t) + \alpha\omega\cos(\omega t)}{\alpha^2+\omega^2}\Bigg)\tilde{x}\end{aligned} \tag{4.98}$$

which results in

$$\dot{y}_{ave} = -\gamma \left(\bar{V}_{2,ave}^2 + \frac{\omega\pi\alpha_y^2(1+\alpha^2)}{\alpha^2+\omega^2} \right) \tilde{y}_{ave} - \gamma(\bar{V}_{1,ave}\bar{V}_{2,ave})\tilde{x}_{ave} \tag{4.99}$$

thus, the linearized system is as follows

$$\begin{bmatrix} \dot{\tilde{x}}_{ave} \\ \dot{\tilde{y}}_{ave} \end{bmatrix} = -\frac{\gamma\pi(1+\alpha^2)}{\alpha^2\omega^2} \begin{bmatrix} \alpha_x^2 & 0 \\ 0 & \alpha_y^2 \end{bmatrix} \begin{bmatrix} \tilde{x}_{ave} \\ \tilde{y}_{ave} \end{bmatrix} \tag{4.100}$$

and for the kinematics of the robot we have

$$\begin{aligned} \dot{\tilde{x}} &= -k_x(\bar{x} + \alpha_x \sin(\omega t) - x^* - \tilde{x}) + \alpha_x \sin(\omega t) - \alpha_x\omega \cos(\omega t) \\ \dot{\tilde{y}} &= -k_y(\bar{y} + \alpha_y \cos(\omega t) - y^* - \tilde{y}) + \alpha_y \cos(\omega t) + \alpha_y\omega \sin(\omega t) \end{aligned} \tag{4.101}$$

and the averaged trajectories can be computed by

$$\begin{aligned} \dot{\tilde{x}}_{ave} &= -k_x(\bar{x}_{ave} - x^* - \tilde{x}_{ave}) \\ \dot{\tilde{y}}_{ave} &= -k_y(\bar{y}_{ave} - y^* - \tilde{y}_{ave}) \end{aligned} \tag{4.102}$$

system (4.102), together with (4.100) composed the averaged system of the extremum seeking problem and since it is locally exponentially stable we can conclude that the trajectories of the main system remains in a neighborhood of the origin with the size of $O\left(\frac{1}{\omega}\right)$.

Remark 4.3 In (4.91) and (4.93) we did not consider the effects of exponential decaying terms which are produced by filtering the agents velocities. Since these transient behaviors can be considered as the vanishing perturbation terms, it is possible to show that the exponential stability of the system (4.100)-(4.102) will not be affected [34] and therefore, the convergence to a $O\left(\frac{1}{\omega}\right)$ neighborhood of $[x^*, y^*]$ is guaranteed.

Remark 4.4 For the linearization of (4.96) and (4.99), we only used the equations regarding the robot states, however, the complete linearized system should be written based on the states of the high-pass filters which are used for the coordinates of the mobile robot. It

is easy to deduce that the linearized version of the filters equations are also exponential stable and decoupled.

4.3.2 Multi Agent Case

In this section, we consider the adaptive extremum seeking problem for a network of agents. Again, we consider a quadratic potential for the field with circular level curves and for the sake of simplicity, we assume that the Hessian matrix of this field is diagonal and it is equal to $\mathbf{I}_m$. The extension for the case which the Hessian matrix is a general symmetrix positive definite matrix can be obtained easily using the framework which is proposed in section 4.3.3.

For this case, the measurements of the agents can be expressed by

$$d_i^2 = \sum_{j=1}^{m} \left(x_j^i - x_j^*\right)^2, \quad i = \{1, \cdots, n\} \tag{4.103}$$

where $[x_1^*, \cdots, x_m^*]$ denotes the location of the extremum of the field. Differentiating (4.103) with respect to time, we have:

$$z_i = \frac{1}{2}\frac{d}{dt}\left(\sum_{j=1}^{m}\left(x_j^i\right)^2 - d_i^2\right) = \sum_{j=1}^{m} \dot{x}_j^i x_j^* \tag{4.104}$$

Consider the following definitions

$$\phi_i = [\dot{x}_1^i, \cdots, \dot{x}_m^i]^T, \quad \theta = [x_1^*, \cdots, x_m^*]^T, \tag{4.105}$$

Next, consider the following consensus parameter identification law which is inspired by (4.19)

$$\dot{\tilde{x}}_i = \dot{\hat{x}}_i = -\gamma \phi_i \phi_i^T \tilde{x}_i - \sum_{j \in N_i} (\hat{x}_i - \hat{x}_j) \tag{4.106}$$

together, with the following extremum seeking law

$$\dot{x}_i = -(x_i - \hat{x}_i) + \zeta_i, \quad \zeta_i = [\zeta_1^i, \cdots, \zeta_m^i]^T \tag{4.107}$$

where ζ_j^i are either orthogonal $2k\pi$-periodic functions or equal to zero. The identification subsystem for each agent can be expressed as follows

$$\dot{\hat{x}}_i = -\gamma(x_i - \hat{x}_i)(x_i - \hat{x}_i)^T - \gamma(x_i - \hat{x}_i)\zeta_i^T - \gamma\zeta_i(x_i - \hat{x}_i)^T - \gamma\zeta_i\zeta_i^T - \sum_{j\in N_i}(\hat{x}_i - \hat{x}_j) \tag{4.108}$$

Next, we compute the average of the identification subsystems

$$\dot{\hat{x}}_{i,ave} = -\left[\gamma(x_{i,ave} - \hat{x}_{i,ave})(x_{i,ave} - \hat{x}_{i,ave})^T - \frac{\gamma}{2k\pi}\int_0^{2k\pi}\zeta_i\zeta_i^T\, dt\right]\tilde{x}_{i,ave} - \sum_{j\in N_i}(\hat{x}_{i,ave} - \hat{x}_{j,ave}) \tag{4.109}$$

Using the following identities for periodic ζ_k^i and ζ_l^i

$$\begin{aligned}\frac{1}{2k\pi}\int_0^{2k\pi}\zeta_k^i\zeta_l^i &= 0,\ for\ k \neq l \\ \frac{1}{2k\pi}\int_0^{2k\pi}\zeta_k^i\zeta_l^i &= 1,\ otherwise\end{aligned} \tag{4.110}$$

thus, $\chi_i = \frac{1}{2k\pi}\int_0^{2k\pi}\zeta_i\zeta_i^T\, dt$ is a diagonal matrix whose diagonal elements are either zero or one. We can write

$$\dot{\hat{x}}_{i,ave} = -\left[\gamma(x_{i,ave} - \hat{x}_{i,ave})(x_{i,ave} - \hat{x}_{i,ave})^T - \gamma\chi_i\right]\tilde{x}_{i,ave} - \sum_{j\in N_i}(\tilde{x}_{i,ave} - \tilde{x}_{j,ave}) \tag{4.111}$$

finally, the linearized identification subsystem is as follows

$$\dot{\tilde{x}}_{i,ave} = -\gamma\chi_i\tilde{x}_{i,ave} - \sum_{j\in N_i}(\tilde{x}_{i,ave} - \tilde{x}_{j,ave}) \tag{4.112}$$

Using the results of the previous section, we can conclude that the averaged trajectories of the identification subsystem will converge if $\sum_{i=1}^n \chi_i > 0$. This condition clearly shows the benefit of using a consensus filter inside the extremum seeking identification subsystem since according to this condition none of agents is required to satisfy the PE condition. For

example a subset of m agents for which each agent only has one dither signal with respect to a distinct coordinate is sufficient for the satisfaction of the PE condition (4.48) for the whole network.

Remark 4.5 In this section, we applied an extra consensus term to the estimation subsystem to enhance the identification process of the extremum point coordinates. It is also interesting to point out that the consensus terms can also be added to the kinematic controller of the agents. In this context, the consensus filter acts as a "rendezvous" filter. In another words, instead of sharing the information regarding the position of the target, the agents tries to reach to a common trajectory while reaching to the extremum point. This can be useful in the situations where there exist a well-informed agent in the network which can take the role of the leader.

4.3.3 Extremum Seeking for General Hessian Matrix

It is also possible to extend the previous results to the case of quadratic fields with general positive definite symmetric Hessian matrix. Here, we use the framework which is first proposed in [60] for ES task. We show that the idea of using a consensus filter for the network will give the extra freedom for choosing the extremum seeking dither signals. To describe the method, consider a quadratic cost function $f(\theta^i) = f^* + (\theta^i - \theta^*)^T H(\theta^i - \theta^*)$. The identification subsystem can be described by

$$\begin{aligned}
\dot{\hat{\theta}}^i &= KM_i(t)[f^* + (\hat{\theta}^i + S_i(t) - \theta^*)^T H(\hat{\theta}^i + S_i(t) - \theta^*)] - \sum_{j\in N_i}\left(\hat{\theta}^i - \hat{\theta}^j\right) \\
S_i(t) &= [a_{1i}\sin(\omega_{1i}t), \cdots, a_{mi}\sin(\omega_{mi}t)]^T, \\
M_i(t) &= [\frac{2}{a_{1i}}\sin(\omega_{1i}t), \cdots, \frac{2}{a_{mi}}\sin(\omega_{mi}t)]^T
\end{aligned} \tag{4.113}$$

where ω_{mi} are either distinct positive integers or zero, defining $\tilde{\theta}^i = \hat{\theta}^i - \theta^*$ we can rewrite (4.113) as follows

$$\begin{aligned}\dot{\hat{\theta}}^i &= Kf^* M_i(t) + \frac{1}{2} K M_i(t) \left[(\tilde{\theta}^i)^T H \tilde{\theta}^i + 2(\tilde{\theta}^i)^T H S_i(t) + S_i^T(t) H S_i(t) \right] \\ &- \sum_{j \in N_i} \left(\hat{\theta}^i - \hat{\theta}^j \right)\end{aligned} \tag{4.114}$$

computing the average of the system (4.114) from 0 to $2k\pi$, we have

$$\dot{\hat{\theta}} = \dot{\tilde{\theta}}^i_{ave} = K \Pi_i H \tilde{\theta}^i_{ave} - \sum_{j \in N_i} \left(\tilde{\theta}^i_{ave} - \tilde{\theta}^j_{ave} \right) \tag{4.115}$$

where $\Pi_i = \frac{1}{2k\pi} \int_0^{2k\pi} M_i(t) S_i^T(t)\ dt$ and we have used the facts

$$\begin{aligned}&\frac{1}{2k\pi} \int_0^{2k\pi} M_i(t)\ dt = \frac{1}{2k\pi} \int_0^{2k\pi} S_i(t)\ dt = 0, \\ &\begin{cases} \frac{1}{2k\pi} \int_0^{2k\pi} m_{ik}(t) s_{il}(t)\ dt = 0\ for\ l \neq 0, \\ \frac{1}{2k\pi} \int_0^{2k\pi} m_{ik}(t) s_{il}(t)\ dt = 1\ otherwise \end{cases}\end{aligned} \tag{4.116}$$

(4.115) suggests that Π_i is a diagonal matrix whose diagonal elements are either zero or one. Again, using the results of the previous sections, we can conclude that if the following condition is met

$$\sum_{i=1}^{n} \Pi_i > 0 \tag{4.117}$$

then the local convergence of the extremum seeking algorithm will be followed. This implicates that even if a subset of m-agents for which each agent contains a distinct frequency for a distinct coordinate, and the dither signals of the other $n - m$ agents are equal to zero, we can still guarantee the convergence of the estimates to the extremum value of the function of the field.

Remark 4.6 Note that (4.115) represents a gradient-based extremum seeking algorithm

since the convergence of the method is directly dependent on the Hessian matrix of the field. This might force the seeking agent to move in the direction of the gradient of the field to reach to the extremum state which might not be the shortest path to that point. As in Newton-based optimization method, it is possible to extend the current results in a way that the convergence of (4.115) does not depend on the Hessian matrix of the field. One way to achieve this is to use the method in [63] to estimate the Hessian matrix using additional filtering. Using the filtered version of its inverse, it is possible to design a Newton-based distributed ES method.

4.4 Cooperative Extremum Seeking with Multiple Dubin's Vehicles

In this section, we consider the cooperative extremum seeking task for multiple nonholonomic agents with fixed forward velocities. This problem is first considered in [65],[66] and in [108], it is extended to a network of unicycles. Here, we assume that the agents can only measure the function of the field at their respective locations together with a convex function of the relative distances to their respective neighbors. We employ a modified ES method to solve this problem. As in the previous sections, the main idea is to add several dithering signals at the inputs of the vehicles to find the gradient of the field and the relative formation errors. Then, such information will be used to steer the network toward the extremum point while, simultaneously, it fulfills the formation goals. Fig. 4.6 depicts the framework which we use in this section. Compared to the methods which are used in [65] and [66], here, we can see that each agent can obtain the local formation cost from its neighbors and adds it to the value of the measured signal of the field. In the next

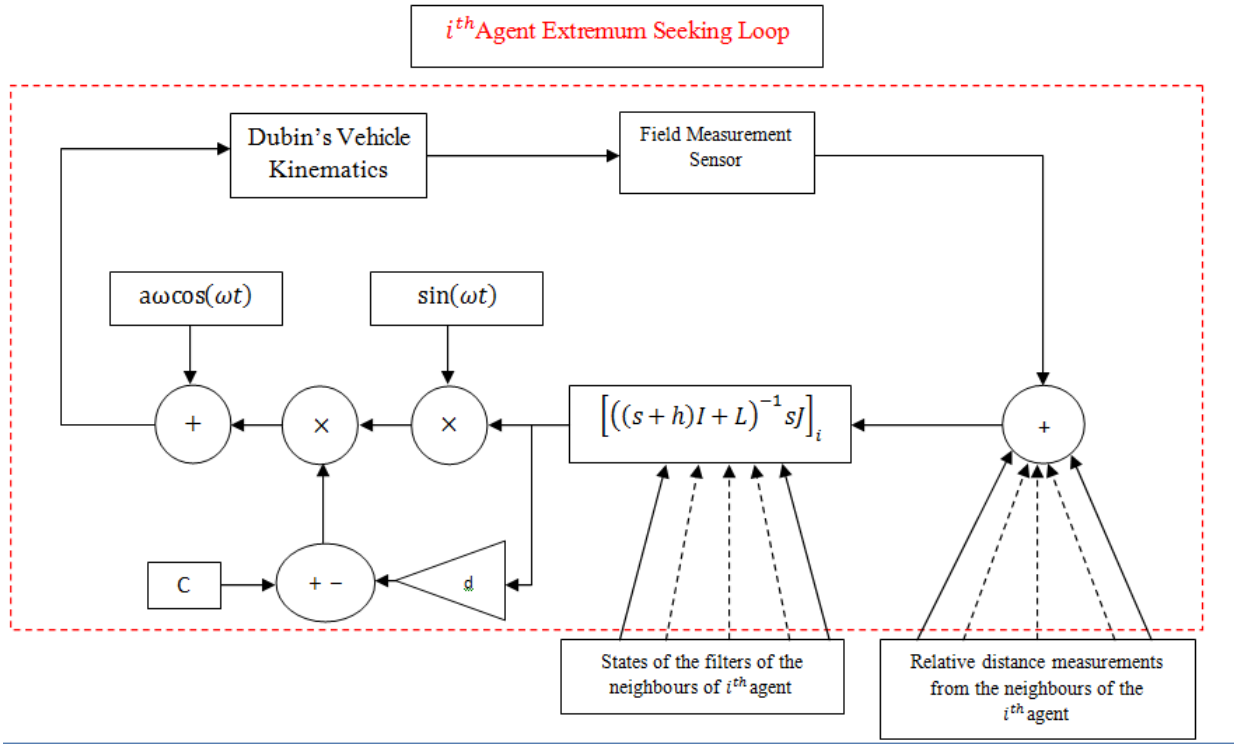

Figure 4.6: Distributed extremum seeking loop

part of the algorithm, the gradient of the collected signals are computed using the distributed filtering which is built based on the states of the high pass filters of the neighbors of each agent. The network will be steered to the location of the extremum by adjusting the angular velocities of the vehicles using the acquired gradient. Assuming that the field sensors are located at the distance of q in front of the agents, the dynamical system which

represents Fig. 4.6 can be expressed as follows:

$$\dot{r}_i = Ue^{j\theta_i}$$
$$\dot{\theta}_i = a\omega\cos(\omega t) + c\xi_i\sin(\omega t) - d\xi_i^2\sin(\omega t)$$
$$\dot{e}_i = h\xi_i + \sum_{j\in N_i}(\xi_i - \xi_j), \quad e = [e_1, \cdots, e_n]^T$$
$$\xi_i = -(\alpha\left\|r_i + qe^{j\theta_i} + r^{ext}\right\|^2 + \beta\sum_{j\in N_i}\|r_i - r_j\|^2 + e_i), \quad \xi = [\xi_1, \cdots, \xi_n]^T \tag{4.118}$$
$$j_1 = f^{ext} - \alpha\left\|r_i + qe^{j\theta_i} - r^{ext}\right\|^2 - \beta\sum_{j\in N_i}\|r_i - r_j\|^2, \quad J = [j_1, \cdots, j_n]^T \tag{4.119}$$

where r_i, θ_i denotes the position vector and heading angle of the i^{th} agent. e_i can be computed as follows

$$e = (sI + hI + L)^{-1}(hI + L)(J) - f^{ext}\mathbf{1}_n$$
$$\rightarrow \xi = (sI + hI + L)^{-1}sJ = J - (sI + hI + L)^{-1}(hI + L)J = J - e - f^{ext}\mathbf{1}_n \tag{4.120}$$

From (4.120), it is clear that ξ_i denotes the state of the filter of the i^{th} agent and e_i contains the difference between the low-pass filtered version of the obtained signals and the extremum of the field which is assumed to be unknown. It should be noted that e_i does not appear explicitly in the extremum seeking control loop and it is defined for the purpose of stability analysis. Also, (4.120) indicates that a consensus term is added to "Blend" the information of the nearby agents to enhance the identifiably of the network. Furthermore, (4.118) suggests that the rendezvous cost is added to the measured signal of the field. This can be easily extended to the formation case by considering the offsets between the agents position vectors and the center of formation in the relative costs.

In order to analyze the algorithm (4.118)-(4.119), we use the methodology which is pro-

posed in [65] by considering the following change of variables

$$\begin{aligned}\hat{r}_i &= r_i - r^{ext} \\ \hat{\theta}_i &= \theta_i - a\sin(\omega t)\end{aligned} \tag{4.121}$$

using (4.121), we can write ($\tau = \omega t$)

$$\begin{aligned}\frac{d\hat{r}_i}{d\tau} &= \frac{U}{\omega} e^{j(\hat{\theta}_i + a\sin(\tau))} \\ \frac{d\hat{\theta}_i}{d\tau} &= \frac{1}{\omega}\left(c - d\xi_i\right)\xi_i \sin(\tau) \\ \frac{de_i}{d\tau} &= \frac{1}{\omega}\left[h\xi_i + \sum_{j\in N_i}(\xi_i - \xi_j)\right]\end{aligned} \tag{4.122}$$

The first set of equations in (4.122) describes the evolution of the positions of the agents while the second set represents the evolution of the angular directions of the vehicles. The third set is related to the dynamics of the differences between the current measurements of the sensors which are added to the local formation costs with the value of the field at the extremum point. From (4.122), it is also clear that by changing the time scale to τ, the system (4.118)-(4.119) turns into the canonical form of the averaging theory. in order to facilitate the analysis, consider the new quantity θ_i^*

$$\begin{aligned}&\theta_i^* = arg\left(r^{ext} - r_i\right) \\ &\Rightarrow \xi_i = \left[\alpha\left(q^2 + \left\|\hat{r}_i^2\right\| - 2q\left\|\hat{r}_i\right\|\cos(\hat{\theta}_i - \theta_i^* + a\sin(\tau))\right) + \beta\sum_{j\in N_i}\left\|\hat{r}_i - \hat{r}_j\right\|^2 + e_i\right]\end{aligned} \tag{4.123}$$

these variables are shown in Fig. 4.7. It is clear that (4.123) results from writing the cosine formula for the triangle which is constructed by the center of the i^{th} agent, its field sensor and the location of the extremum of the field. To further continue the stability analysis,

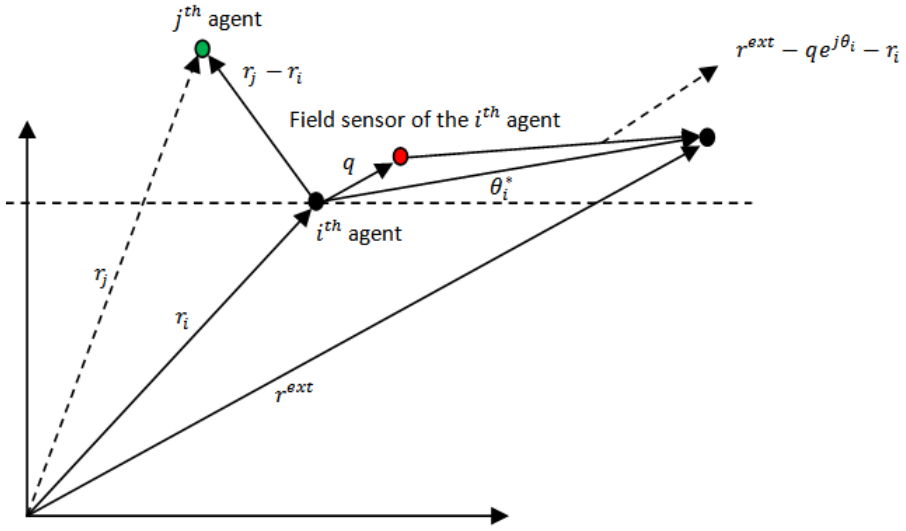

Figure 4.7: Definition of the relative vectors

we consider the following error variables

$$\begin{aligned} \rho_i &= \|\hat{r}_i\| \\ \tilde{\theta}_i &= \hat{\theta}_i - \theta_i^* \end{aligned} \tag{4.124}$$

using (4.124), the dynamics of the error variables $\rho_i, \tilde{\theta}_i$ can be obtained as follows

$$\begin{aligned} \frac{d\rho_i}{d\tau} &= -\frac{U}{\omega}\cos(\tilde{\theta}_i + a\sin(\tau)) \\ \frac{d\tilde{\theta}_i}{d\tau} &= \frac{1}{\omega}(c - d\xi_i)\xi_i \sin(\tau) + \frac{U}{\rho_i \omega}\sin(\tilde{\theta}_i + a\sin(\tau)) \\ \frac{de_i}{d\tau} &= \frac{1}{\omega}\left[h\xi_i + \sum_{j\in N_i}(\xi_i - \xi_j)\right] \end{aligned} \tag{4.125}$$

where ξ_i is computed using (4.118). We continue the convergence analysis using (4.125) instead of (4.122) since with the help of the new error variables (4.124), it is possible to

perform the analysis with the scalar variables. Our main strategy for achieving this goal is to find out that to what extent the filtered version of the measured signals will help the agents to reach to the extremum point. In this regard, we substitute (4.118) in (4.125). Using the facts that (4.125) is periodic and in canonical form of the averaging theory, integrating (4.125) from 0 to 2π, results in

$$
\begin{aligned}
&\frac{1}{2\pi}\int_0^{2\pi}\left(\frac{-U}{\omega}\right)\cos(\tilde{\theta}_i+a\sin(\tau))\ d\tau\\
&=\frac{-U}{2\omega\pi}\int_0^{2\pi}\cos(\tilde{\theta}_i)\cos(a\sin(\tau))-\sin(\tilde{\theta}_i)\sin(a\sin(\tau))\ d\tau=\frac{-U}{\omega}\cos(\tilde{\theta}_{i,ave})J_0(a)\\
&\frac{1}{2\pi}\int_0^{2\pi}\sin(\tilde{\theta}_i+a\sin(\tau))=\\
&\frac{1}{2\pi}\int_0^{2\pi}\sin(\tilde{\theta}_i)\cos(a\sin(\tau))+\cos(\tilde{\theta}_i)\sin(a\sin(\tau))\ d\tau=\sin(\tilde{\theta}_{i,ave})J_0(a)\\
&\frac{1}{2\pi}\int_0^{2\pi}\sin(\tau)\cos(\tilde{\theta}_i+a\sin(\tau))\ d\tau=\\
&\frac{1}{2\pi}\int_0^{2\pi}\sin(\tau)\cos(\tilde{\theta}_i)\cos(a\sin(\tau))-\sin(\tau)\sin(\tilde{\theta}_i)\sin(a\sin(\tau))\ d\tau=-J_1(a)\\
&=\frac{1}{2\pi}\int_0^{2\pi}\sin(\tau)\left(\cos(\tilde{\theta}_i+a\sin(\tau))\right)^2\ d\tau=\frac{-1}{2\pi}\int_0^{4\pi}\sin(\tau)\sin(2\tilde{\theta}_i)\sin(2a\sin(\tau))\ d\tau\\
&=\frac{-1}{2}J_1(2a)\sin(2\tilde{\theta}_i)
\end{aligned}
\tag{4.126}
$$

using the subscript "ave" for the averaged variables, we can write the average system as follows for the case that $\beta=0$

$$
\begin{aligned}
&\frac{d\rho_{i,ave}}{d\tau}=-\frac{UJ_0(a)}{\omega}\cos(\tilde{\theta}_{i,ave})\\
&\frac{d\tilde{\theta}_{i,ave}}{d\tau}=\left[\frac{UJ_0(a)}{\rho_{i,ave}}-2\alpha qJ_1(a)\rho_{i,ave}\left(c+2d\left(\alpha(q^2+\rho_{i,ave}^2)\right)+e_{i,ave}\right)\right]\frac{\sin\tilde{\theta}_{i,ave}}{\omega}\\
&+\frac{1}{\omega}2d\alpha^2q^2\rho_{i,ave}^2J_1(2a)\sin(2\tilde{\theta}_{i,ave})\\
&\frac{de_{i,ave}}{d\tau}=\frac{1}{\omega}\left(2h\alpha q\rho_{i,ave}J_0(a)\cos(\tilde{\theta}_{i,ave})-\alpha(q^2+\rho_{i,ave}^2)-e_{i,ave}\right)\\
&+\frac{1}{\omega}\sum_{j\in N_i}\Big[\left(2h\alpha q\rho_{i,ave}J_0(a)\cos(\tilde{\theta}_{i,ave})-\alpha(q^2+\rho_{i,ave}^2)-e_{i,ave}\right)\\
&-\left(2h\alpha q\rho_{j,ave}J_0(a)\cos(\tilde{\theta}_{j,ave})-\alpha(q^2+\rho_{j,ave}^2)-e_{j,ave}\right)\Big]
\end{aligned}
\tag{4.127}
$$

one of the equilibrium point of the system (4.127) can be expressed as follows

$$\begin{aligned}
\rho_{1,ave} = \cdots = \rho_{n,ave} &= \sqrt{\frac{UJ_0(a)}{2c\alpha q J_1(a)}} \\
\tilde{\theta}_{1,ave} = \cdots = \tilde{\theta}_{n,ave} &= \frac{\pi}{2} \\
e_{1,ave} = \cdots = e_{n,ave} &= -\frac{\alpha\left(UJ_0(a) + 2c\alpha q^3 J_1(a)\right)}{2c\alpha q J_1(a)}
\end{aligned} \tag{4.128}$$

using linearization, it is straightforward to show that (4.128) is exponentially stable under the following conditions:

$$2UJ_0(a)J_1(a) + hRJ_1(2a) - 2hRJ_0(a)J_1(a) > 0 \tag{4.129}$$

Note that a better stability condition can be derived based on the properties of the Laplacian matrix of the network. This is the subject of our ongoing research. Also, using Theorem 8.3 in [34] we can find that the exponential stability of (4.127) indicates that the trajectory of the main system (4.118)-(4.119) will reach to a $O\left(\frac{1}{\omega}\right)$ neighborhood of the equilibrium points (4.128).

4.5 Simulation Results

In this section, we present the simulation results of the previous algorithms. Fig. 4.8 illustrates the results for the cooperative extremum seeking method of section 4.4. The forward velocities of the agents are assumed to be $0.1\frac{m}{s}$ and the dither signal is chosen to be $\sin(60t)$. The field sensors of the agents are are located at the distance of $0.1m$ in front of the center of each vehicle. The values of the constants of the high-pass filters are chosen to be the same and equal to one. The function of the field is $z = 1-(x_i-1)^2-1.2(y_i-1)^2$. The desired relative distance between the agents is 0 and as it can be seen from Fig. 4.8, In

the first stage of the motion, the agents try to reach to each other and in the second phase, together, they move toward the extremum location. In Fig. 4.9, the relative position of the agents is chosen to be $1m$. Furthermore, it is assumed that one of the agents does not have the capability of measuring the aforementioned field. The trajectory of this vehicle is depicted with solid line. It is clear that by sharing the consensus cost, this agent also fulfills the extremum seeking objective. Fig. 4.10 shows the components of the position of each vehicle versus time. In Fig. 4.11, it is assumed that the field sensors are located at the center of each vehicle. In this case, instead of the high-pass filter, a derivative block is used inside the extremum seeking loop(Fig. 4.6). The simulation results for the case that both agents have the field sensors and the desired relative position is equal to $1m$ is depicted in Fig. 4.12. Fig. 4.13 shows the results of same problem with a network of three agents. The communication graph of the network is assumed to be a line. These results suggests that the extremum seeking algorithm can be used to fulfill the formation control objectives. This can also be extended to three dimensions. Fig. 4.14-4.15 illustrates this situation where the desired relative distance is chosen to be $1m$.

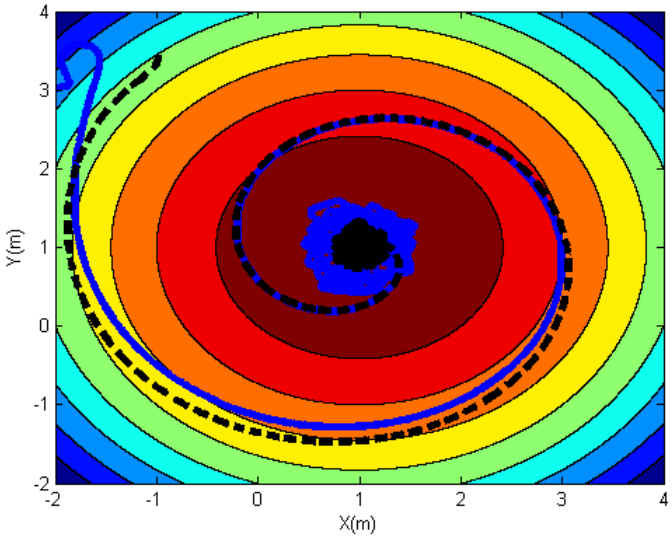

Figure 4.8: Trajectories of vehicles for cooperative extremum seeking setting of Section 4.4

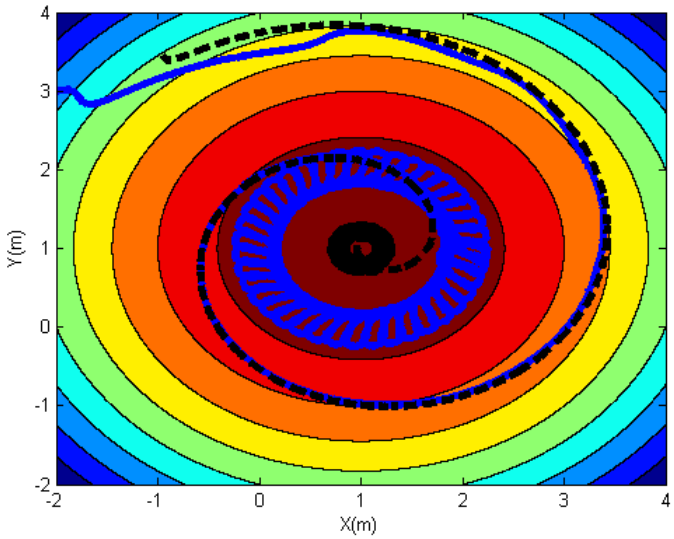

Figure 4.9: Trajectories of the agents for the case in which one of the vehicles(solid line) can not measure the value of the field while performing the cooperative extremum seeking setting of Section 4.4

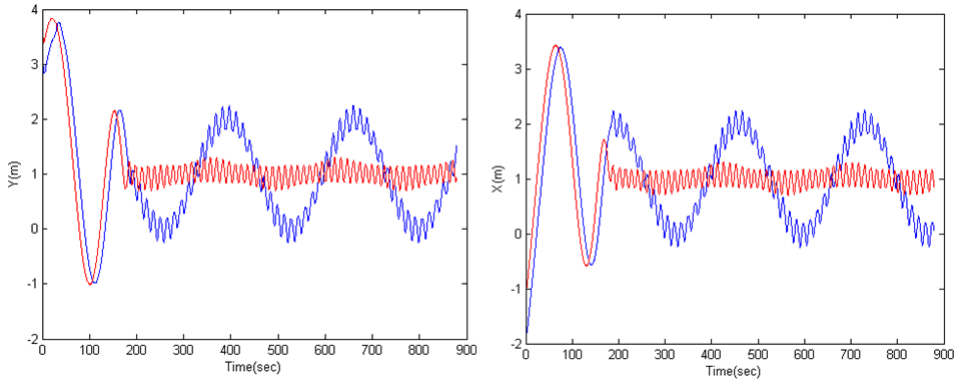

Figure 4.10: Components of the positions of the vehicles versus time for cooperative extremum seeking setting of Section 4.4

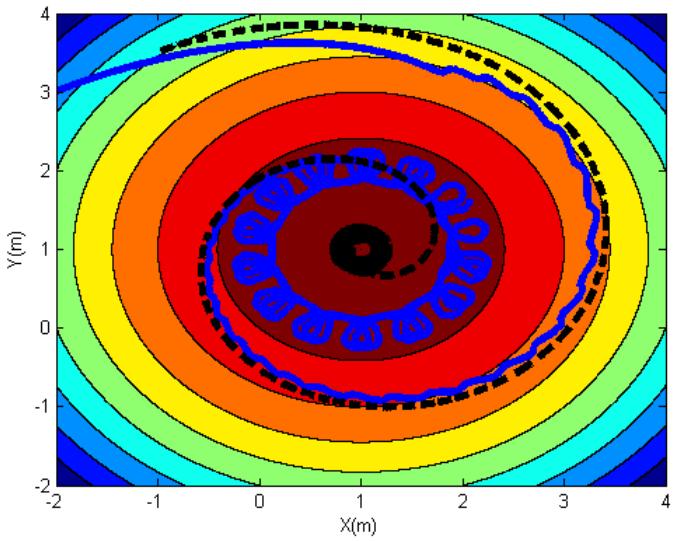

Figure 4.11: Trajectories of the vehicles for the case that the field sensors are located at the center of the agents

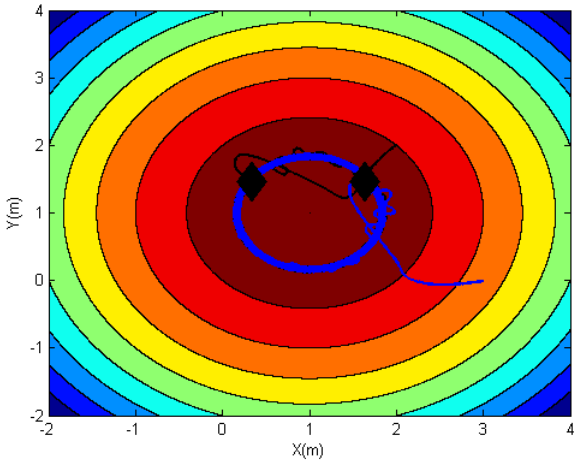

Figure 4.12: Simultaneous extremum seeking and formation control with two agents

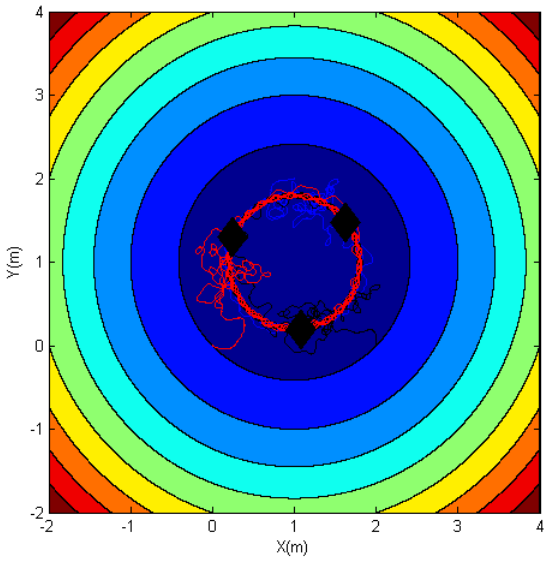

Figure 4.13: Simultaneous extremum seeking and formation control using a network of three agents with line communication graph

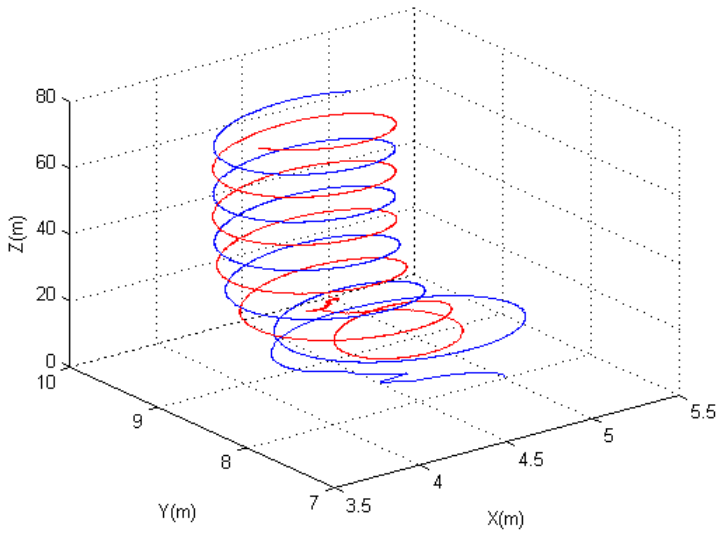

Figure 4.14: Formation control in three dimension using extremum seeking method

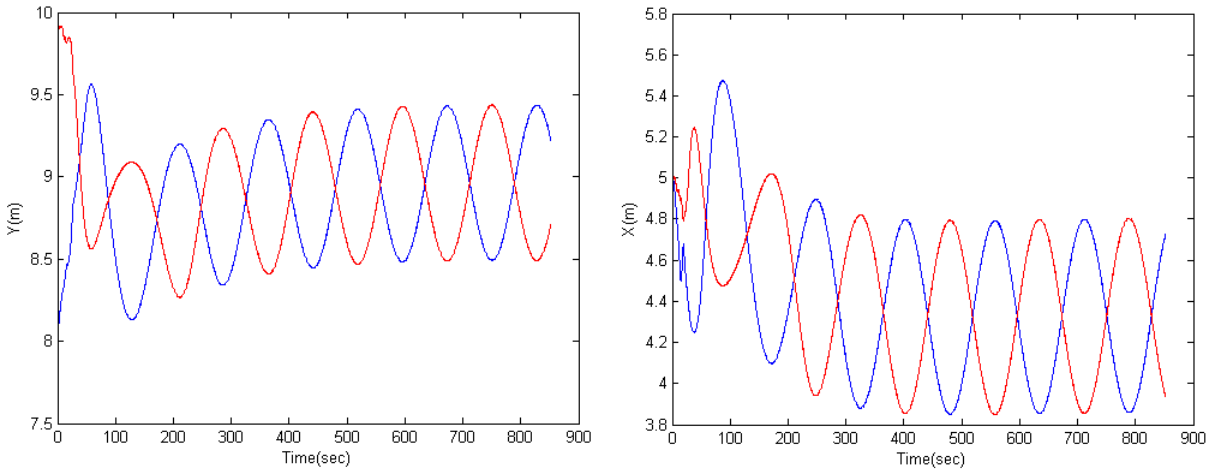

Figure 4.15: X and Y components of the agent positions versus time

4.6 Motion Camouflage

In the previous sections we studied the cooperative localization and extremum seeking problems. The extremum seeking problem can also be defined for situations where the agents are not sharing their data with each other and the amount of information which the agents can elicit from each other is limited. One example is the motion camouflage problem [109],[110]. The main purpose of this task is to capture an specific evader with a chaser agent. This agent must camouflage its motion toward the evader in a way that the angular velocity of the line which connects these two agents, remains zero. This objective is inspired by observing the behavior of the natural predator-prey systems in nature. For instance, in [111], it is mentioned that many predator animals are using this tactic to minimize the deviation in their apparent position which is viewed from the line of sight(LOS) of the prey. This will help the predators to decrease the amount of information which the prey can elicit from their relative motion. In addition, in [112], it is reported that the insects which their eyes are consist of arrays of visual units, e.g. flies,bees,etc. are far more susceptible to the component of the relative velocity which is orthogonal to the LOS of the predator-prey system compared to the component which is along in this direction. Here, we analyze this problem in detail and propose several control strategy to fulfill this task. We start the mathematical modeling by considering the two dimensional case in which the dynamics of both chaser and evader agent can be represented by the following kinematics($\alpha \in \{c, e\}$ where 'c' and 'e' denote the chaser and evader agents):

$$\begin{aligned} \dot{x}_\alpha &= v_\alpha \cos\theta_\alpha \\ \dot{y}_\alpha &= v_\alpha \sin\theta_\alpha \\ \dot{\theta}_\alpha &= u_\alpha \end{aligned} \tag{4.130}$$

where v_α and u_α denote the linear and angular velocities of the agents, respectively and $v_c > v_e$. The position vectors of these two agents are defined as $r_c = [x_c, y_c]^T$ and $r_e = [x_e, y_e]^T$. During the motion camouflage period, the direction of the $r_c - r_e$ must be fixed. In this regard, we can define two different motion camouflage situations. In the first case, the chaser agent increases its distance to perform the motion camouflage task $\frac{\frac{d}{dt}|r_c - r_e|}{\left|\frac{d}{dt}(r_c - r_e)\right|} = 1$ and in the second scenario, the chaser agent tries to reach to evader $\frac{\frac{d}{dt}|r_c - r_e|}{\left|\frac{d}{dt}(r_c - r_e)\right|} = -1$. Fig. 4.16 illustrates these two situations. In the context of control theory, the second task

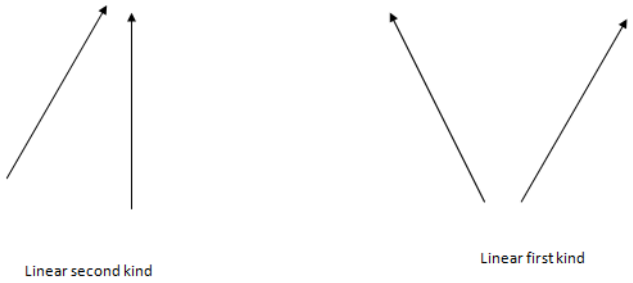

Figure 4.16: Two different kinds of motion camouflage state

is more important since we usually need to capture the evader. In the second step of the modeling, there is a need for a mathematical measure to quantify the deviation from motion camouflage state. We use the method which is first introduced in [109]. This approach is based on comparing the time derivative of the relative measurements which can be obtained easily by using image processing or other devices. Consider the following performance index:

$$I = 1 - \left(\frac{\frac{d}{dt}|r_c - r_e|}{\left|\frac{d}{dt}(r_c - r_e)\right|} \right)^2 \tag{4.131}$$

It is obvious that the minimums of the function (4.131) are related to the two states of motion camouflage. The main problem which we want to solve in this section can be

formally expressed as follows:

Problem 4.3 Considering the dynamics (4.130) for the evader and chaser agents, design a control method to minimize the cost function (4.131) without the knowledge of the evader's plan i.e. u_e.

The first method which we use in this section is based on the dynamics of the variable.($\hat{r} = r_c - r_e$)

$$P = \frac{\frac{d}{dt}\|\hat{r}\|}{\frac{d\hat{r}}{dt}} \tag{4.132}$$

Next, we express the kinematics of the agents in the Frenet Serret frame as follows

$$\begin{aligned} \dot{r}_c &= t_c & \dot{r}_e &= t_c \\ \dot{t}_c &= u_c n_c & \dot{t}_e &= v_e u_e n_c \\ \dot{n}_c &= -u_c t_c & \dot{n}_e &= -v_e u_e t_c \end{aligned} \tag{4.133}$$

where t_i is the unit vector which is along the velocities of the agents. n_i is the unit vector which is together with t_i and z forms the right handed orthonormal basis. Since $\|\hat{r}\|^2 = \hat{r}^T\hat{r}$ we can rewrite (4.132) as follows

$$P = \frac{\hat{r}^T\dot{\hat{r}}}{\|\hat{r}\|\,||\dot{\hat{r}}||} \tag{4.134}$$

using (4.133), we start the control design procedure by taking the time derivative of (4.134) as in [109]

$$\dot{P} = \frac{||\dot{\hat{r}}||}{\|\hat{r}\|}\left[1 - P^2\right] + \frac{\ddot{\hat{r}}^T}{||\dot{\hat{r}}||}\left[\frac{\hat{r}}{\|\hat{r}\|} - P\frac{\dot{\hat{r}}}{||\dot{\hat{r}}||}\right]\|\hat{r}\| \tag{4.135}$$

for the bracket of the second term on the r.h.s of (4.135), we have

$$\frac{\hat{r}}{\|\hat{r}\|} - P\frac{\dot{\hat{r}}}{||\dot{\hat{r}}||} = \left(\frac{\hat{r}^T R\dot{\hat{r}}}{\|\hat{r}\|\,||\dot{\hat{r}}||}\right)\frac{R\dot{\hat{r}}}{||\dot{\hat{r}}||} = \frac{1}{||\dot{\hat{r}}||^2}\left(\frac{\hat{r}^T R\dot{\hat{r}}}{\|\hat{r}\|}\right)R\dot{\hat{r}} \tag{4.136}$$

hence, the time derivative of P changes into

$$\dot{P} = \frac{||\dot{\hat{r}}||}{\|\hat{r}\|}\left[\frac{1}{||\dot{\hat{r}}||^2}\left(\frac{\hat{r}^T R\dot{\hat{r}}}{\|\hat{r}\|}\right)^2\right] + \frac{1}{||\dot{\hat{r}}||^3}\left(\frac{\hat{r}^T R\dot{\hat{r}}}{\|\hat{r}\|}\right)\dot{\hat{r}}^T R^T\left(u_c n_c - v^2 u_e n_e\right) \tag{4.137}$$

Using the definitions of n_i and t_i, (4.137) becomes

$$\dot{P} = \frac{||\dot{\hat{r}}||}{\|\hat{r}\|}\left[\frac{1}{||\dot{\hat{r}}||^2}\left(\frac{\hat{r}^T R\dot{\hat{r}}}{\|\hat{r}\|}\right)^2\right] + \frac{u_c}{||\dot{\hat{r}}||^3}\left(\frac{\hat{r}^T R\dot{\hat{r}}}{\|\hat{r}\|}\right)\left(1 - v t_c^T t_e\right) + \frac{v^2 u_e}{||\dot{\hat{r}}||^3}\left(\frac{\hat{r}^T R\dot{\hat{r}}}{\|\hat{r}\|}\right)\left(v - t_c^T t_e\right) \tag{4.138}$$

Consider the following control law for the chaser agent

$$u_c = -k_1\left(\frac{\hat{r}^T R\dot{\hat{r}}}{\|\hat{r}\|}\right) - k_2 sgn\left(\hat{r}^T R\dot{\hat{r}}\right) v^2(1+v)\bar{u}_e \tag{4.139}$$

Using (4.139) in (4.138), we can write

$$\begin{aligned}\dot{P} = &-\left[\frac{k_1}{\left\|\dot{\hat{r}}\right\|}\left(1 - v t_c^T t_e\right) - \frac{\left\|\dot{\hat{r}}\right\|}{\|\hat{r}\|}\right]\left[\frac{1}{\left\|\dot{\hat{r}}\right\|}\left(\frac{\hat{r}^T R\dot{\hat{r}}}{\|\hat{r}\|}\right)\right]^2 \\ &- k_2 v^2(1+v)\left|\frac{1}{||\dot{\hat{r}}||}\left[\frac{1}{||\dot{\hat{r}}||^2}\left(\frac{\hat{r}^T R\dot{\hat{r}}}{\|\hat{r}\|}\right)\right]\right|\bar{u}_e\left(1 - v t_c^T t_e\right) + \frac{v^2 u_e}{||\dot{\hat{r}}||^3}\left(\frac{\hat{r}^T R\dot{\hat{r}}}{\|\hat{r}\|}\right)\left(v - t_c^T t_e\right)\end{aligned} \tag{4.140}$$

where $\bar{u}_e = \max\|u_e\|$. Since $1 - v t_c^T t_e \geq 1 - v > 0$, choosing $k_2 \geq \frac{1}{1-v}$ results in

$$\begin{aligned}\dot{P} &\leq -\left[\frac{k_1}{\left\|\dot{\hat{r}}\right\|}\left(1 - v t_c^T t_e\right) - \frac{\left\|\dot{\hat{r}}\right\|}{\|\hat{r}\|}\right]\left[\frac{1}{\left\|\dot{\hat{r}}\right\|}\left(\frac{\hat{r}^T R\dot{\hat{r}}}{\|\hat{r}\|}\right)\right]^2 \\ &\quad - v^2(1+v)\left|\frac{1}{||\dot{\hat{r}}||}\left[\frac{1}{||\dot{\hat{r}}||^2}\left(\frac{\hat{r}^T R\dot{\hat{r}}}{\|\hat{r}\|}\right)\right]\right|\bar{u}_e + \frac{v^2 u_e}{||\dot{\hat{r}}||^3}\left(\frac{\hat{r}^T R\dot{\hat{r}}}{\|\hat{r}\|}\right)(v+1) \\ &\leq -\left[\frac{k_1}{\left\|\dot{\hat{r}}\right\|}\left(1 - v t_c^T t_e\right) - \frac{\left\|\dot{\hat{r}}\right\|}{\|\hat{r}\|}\right]\left[\frac{1}{\left\|\dot{\hat{r}}\right\|}\left(\frac{\hat{r}^T R\dot{\hat{r}}}{\|\hat{r}\|}\right)\right]^2\end{aligned} \tag{4.141}$$

from the fact that $1 - v \leq \left\|\dot{\hat{r}}\right\| \leq 1 + v$, we can conclude that there exist ρ^* such that for $\|\hat{r}\| > \rho^*$ we have $\dot{P} \leq 0$. On the other hand, if we use the following control law for the pursuer agent

$$u_c = -k_1 \left(\frac{\hat{r}^T R \dot{\hat{r}}}{\|\hat{r}\|}\right) - \left(\frac{v^2\left(v - t_c^T t_e\right)}{1 - v t_c^T t_e}\right)\left(\frac{\alpha \bar{u}}{\bar{u}\,\|\alpha\| + \epsilon}\right) \tag{4.142}$$

$$\alpha = \frac{1}{||\dot{\hat{r}}||}\left[\frac{1}{||\dot{\hat{r}}||^2}\left(\frac{\hat{r}^T R \dot{\hat{r}}}{\|\hat{r}\|}\right)\right]\left(v - t_c^T t_e\right) v^2 \tag{4.143}$$

we have

$$\begin{aligned}
\dot{P} &\leq -\left[\frac{k_1}{\left\|\dot{\hat{r}}\right\|}\left(1 - v t_c^T t_e\right) - \frac{\left\|\dot{\hat{r}}\right\|}{\|\hat{r}\|}\right]\left[\frac{1}{\left\|\dot{\hat{r}}\right\|}\left(\frac{\hat{r}^T R \dot{\hat{r}}}{\|\hat{r}\|}\right)\right]^2 + \alpha\left(u_e - \frac{\alpha \bar{u}}{\alpha \bar{u} + \epsilon}\right) \\
&\leq -(1 - P^2)\left[\frac{k_1}{\left\|\dot{\hat{r}}\right\|}\left(1 - v t_c^T t_e\right) - \frac{\left\|\dot{\hat{r}}\right\|}{\|\hat{r}\|}\right] + \bar{u}\,\|\alpha\| - \frac{\bar{u}\alpha^2}{\bar{u}\,\|\alpha\| + \epsilon} \\
&\leq -(1 - P^2)\left[\frac{k_1}{\left\|\dot{\hat{r}}\right\|}\left(1 - v t_c^T t_e\right) - \frac{\left\|\dot{\hat{r}}\right\|}{\|\hat{r}\|}\right] + \epsilon
\end{aligned} \tag{4.144}$$

Next, we study the performance of the previous algorithms. Using (4.144), we can write

$$\dot{P} \leq -(1 - P^2)\left[\frac{k_1(1 - v)}{(1 + v)} - \frac{(1 + v)}{\|\hat{r}\|}\right] + \epsilon \tag{4.145}$$

suppose that we choose k_1 as follows

$$k_1 = \frac{1 + v}{1 - v}\left(\frac{1 + v}{\bar{r}} + \bar{c}\right) \tag{4.146}$$

then for $\|\hat{r}(t)\| > \bar{r}$ we have

$$\dot{P} \leq -\bar{c}(1 - P^2) + \epsilon \tag{4.147}$$

integrating from P_0 to $P(t)$ results in

$$\int_{P_0}^{P(t)} \frac{1}{-\epsilon + \bar{c}(1-P^2)}\, dP = -\int_0^t t\, dt$$
$$\Rightarrow \frac{1}{\sqrt{\bar{c}(\bar{c}-\epsilon)}}\left[\tanh^{-1}\left(\frac{\sqrt{\bar{c}}P}{\sqrt{\bar{c}-\epsilon}}\right) - \tanh^{-1}\left(\frac{\sqrt{\bar{c}}P_0}{\sqrt{\bar{c}-\epsilon}}\right)\right] \leq -t \tag{4.148}$$

thus

$$P(t) \leq \frac{\sqrt{\bar{c}-\epsilon}}{\sqrt{\bar{c}}} \tanh\left(\tanh^{-1}\left(\frac{\sqrt{\bar{c}}P_0}{\sqrt{\bar{c}-\epsilon}}\right) - \sqrt{\bar{c}(\bar{c}-\epsilon)}t\right) = f \tag{4.149}$$

Also, from (4.149), we can show that if $\|\hat{r}(0)\| > \bar{r}$ then $\|\hat{r}(t)\|$ will remain outside the $\bar{r}$-neighborhood of the origin for

$$t \leq \frac{\|\hat{r}(0)\| - \bar{r}}{1+v} = T_1 \tag{4.150}$$

therefore, in order to ensure that $P(T) \leq -1 + \epsilon_1$, the following must hold

$$\tanh^{-1}\left(\frac{\sqrt{\bar{c}}P_0}{\sqrt{\bar{c}-\epsilon}}\right) - \sqrt{\bar{c}(\bar{c}-\epsilon)}T \leq \frac{1}{2} ln\left[\frac{1+\frac{\sqrt{\bar{c}}}{\sqrt{\bar{c}-\epsilon}}(-1+\epsilon_1)}{1-\frac{\sqrt{\bar{c}}}{\sqrt{\bar{c}-\epsilon}}(-1+\epsilon_1)}\right] \tag{4.151}$$

which can be achieved since ϵ can become arbitrary small. Fig. 4.17 shows this situation.

4.6.1 Motion Camouflage Using Extremum Seeking Methods

The next tool which we use here is the extremum seeking approach in [60]. In fact, we try to solve the motion camouflage task as a real time optimization problem. In this regard, we consider the control algorithm which is depicted in Fig. 4.18 The main purpose of the high pass filter in Fig. 4.18 is to extract the local information regarding the gradient of the cost function associated with (4.131) from its measurement at each time instants. Passing this signal through an integrator, we can design a local adaptation law which helps the agents

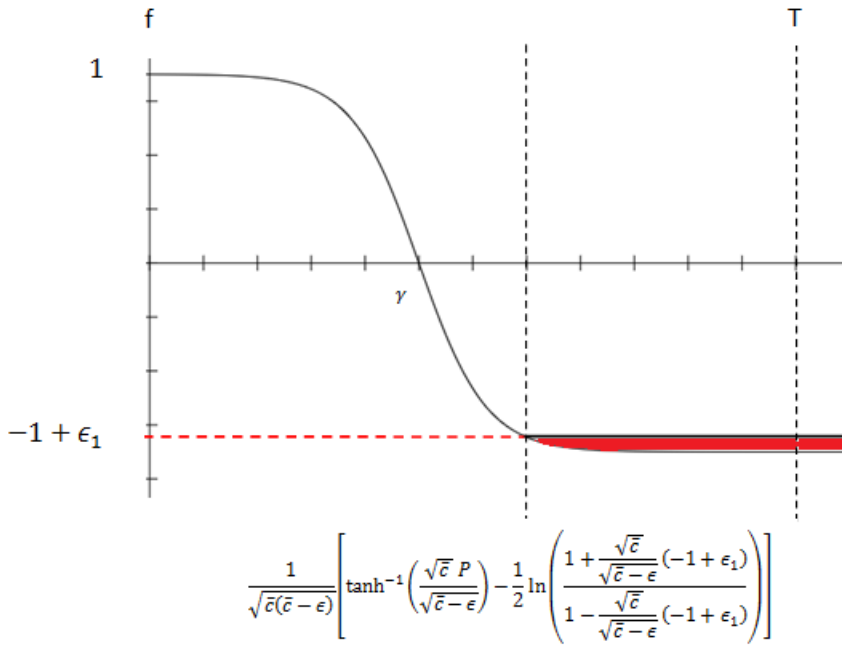

Figure 4.17: Behavior of function f

to find the better estimation of the field. The simulation results for this case are shown in Fig. 4.19-4.21 As it can be seen from the simulation results, the chaser agents captured the target after 900 (sec). Fig. 4.19 suggests that the trajectories of the system has reached to a neighborhood of the optimal state. As mentioned before, the chaser agent did not have any access to the evader plan which is in this case, chosen to be $u_e = \sin(0.001t)$. From Fig. 4.19, we can also see that after capturing the evader the performance index abruptly changes to 1, the main reason for this behavior is stemming from the fact that we assumed a constant linear velocity for the agents. In another word, this is a numerical issue since the simulation must be stopped after capturing the target by the chaser. Fig. 4.21 shows that the chaser agent has captured the target and the relative distance between the chaser and evader agents monotonically decreased.

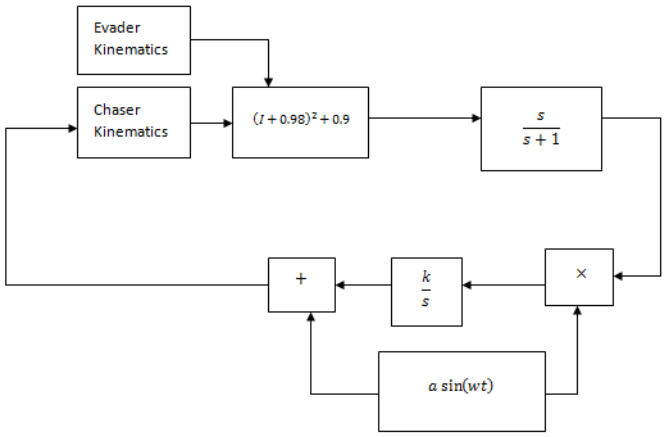

Figure 4.18: Extremum seeking loop for motion camouflage(First method)

Next, we consider the motion camouflage task in three dimensions. For this purpose, we use the model (4.46)-(4.48) for representing the path of both evader and pursuer agents. Our proposed strategy for fulfilling this task is depicted in Fig. 4.22. As it is depicted in Fig. 4.22, we have used two different frequency in the structure of the extermum seeking scheme, in fact, by using this approach we can acquire more date about the position of the evader. The latter is to some extent related to the persistency of the excitation of adaptation algorithm which is hidden in the structure of the search algorithm. The simulation results for this section are depicted in Fig. 4.23 through 4.25. The evader and pursuer forward velocities in this case are assumed to be 0.1 and 0.2, receptively.

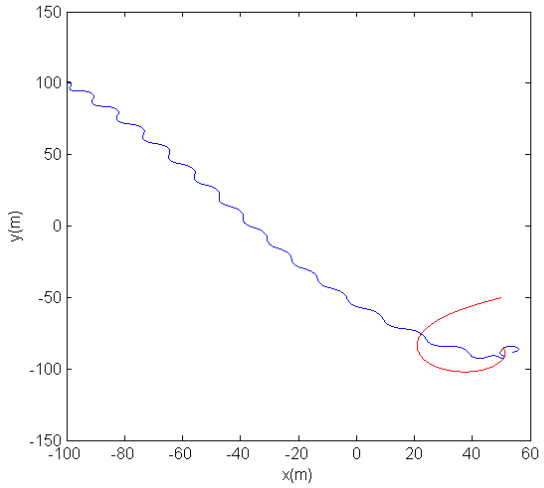

Figure 4.19: Paths of evader and chaser agents

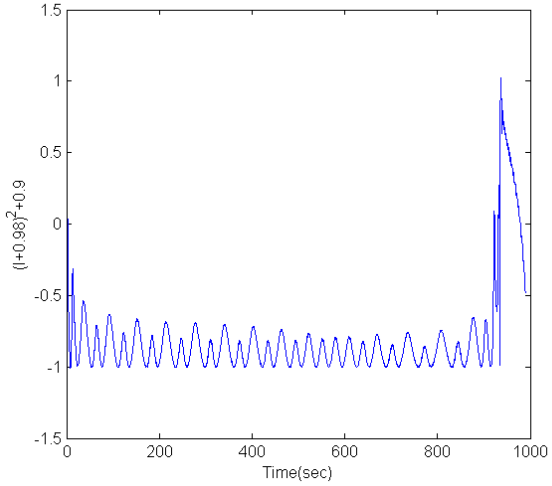

Figure 4.20: The value of the cost function I versus time for motion camouflage

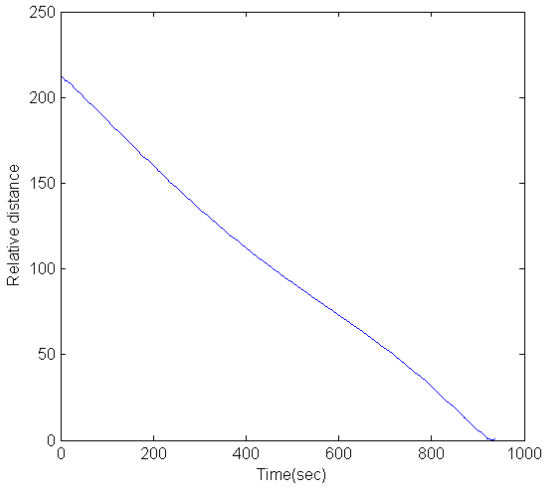

Figure 4.21: Distance between two agents versus time for motion camouflage

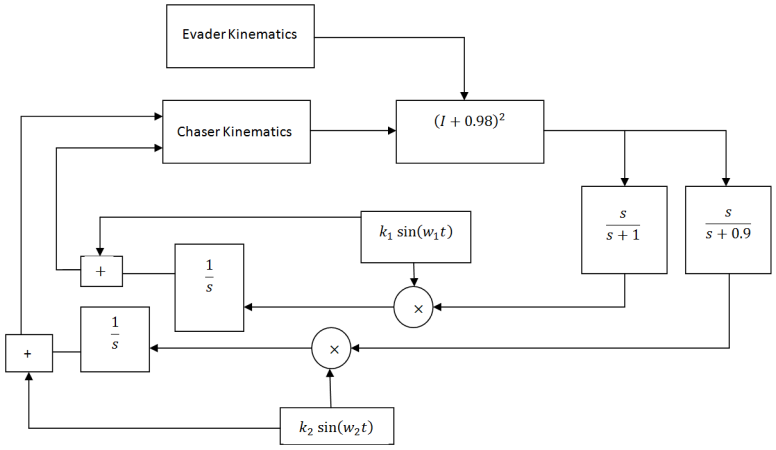

Figure 4.22: Extremum seeking loop for motion camouflage in 3D

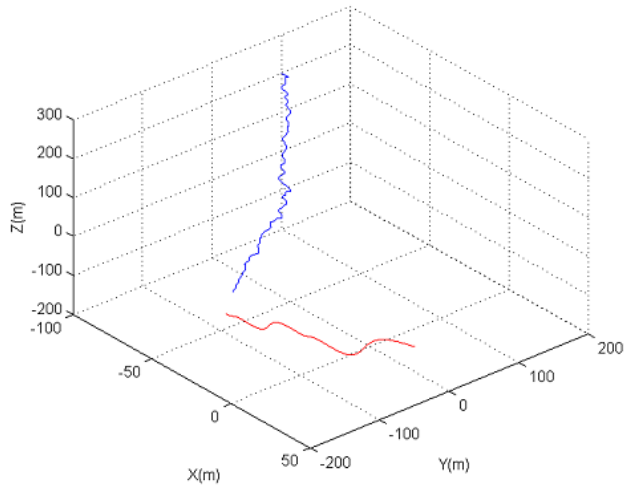

Figure 4.23: Simulation results for motion camouflage in 3D

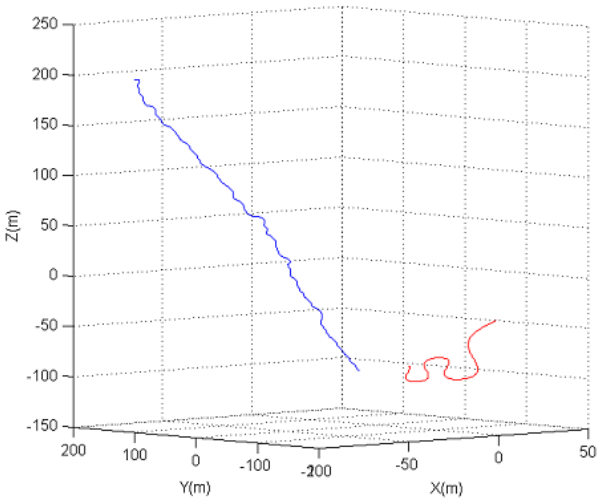

Figure 4.24: Simulation results for motion camouflage(side view)

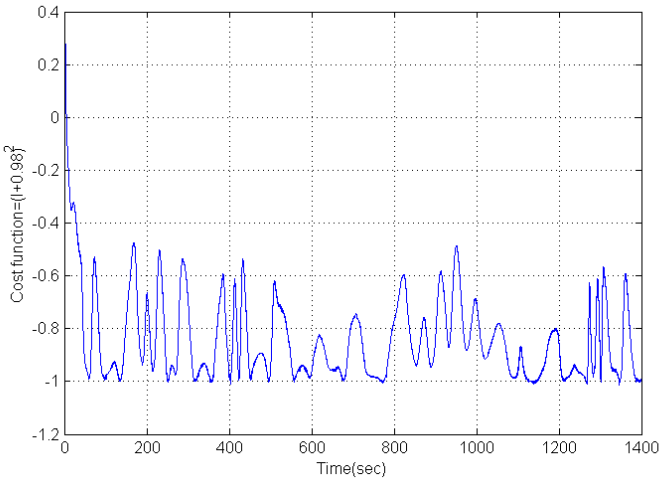

Figure 4.25: The value of the cost function I versus time for motion camouflage

4.7 Summary

In this chapter, we first studied the distributed localization problem for finding the extremum point of the unknown quadratic function. It is assumed that the value of such function can be measured at each instant. Using high pass filtering of the measured signals an identification model is obtained which is linear in unknown parameters. In the next step of the design procedure, we added a consensus term to modify the identification subsystem and proved the exponential convergence of the proposed estimation scheme. In the next part of this chapter, we used the localization results such as distributed identifiably condition for the extremum seeking problem. In particular, we showed that for a network of connected agents, if each agent contains a portion of the dithering signals, it is still possible to drive the system states to the extremum point provided that the distributed identifiably condition is satisfied. In the next section, we tackled the distributed source seeking problem. We considered a network of Dubin's vehicles with fixed forward velocities and showed that it is feasible to steer the robots to the extremum point of a field in the presence of partial availability of the information about the field. In addition, the formation control problem is formulated as an extremum seeking task where the formation pattern correspond to the extremum of formation costs. In the final part of this chapter we studied the motion camouflage problem. Two control algorithms were designed to solve this problem for the situations where the plan of evader is not available for chaser agent. The first approach has better performance compared to the second one, however, it needs extra control effort. Finally, we consider the motion camouflage task as an extremum seeking problem.

Chapter 5

Robust Formation Control

In this chapter, we consider several robust control problems for MASs with general linear time invariant dynamics. Compared to previous chapters, here, we assume that in addition to the external norm bounded uncertainties, the internal dynamics of each agent belongs to a known polytope. In general, studying the robustness of control algorithms for a network can be divided into the two main branches. In the first category, the robustness can be defined as assessing the stability of the network with respect to the uncertainties which are present in the dynamics of each agent. In the second class, the robustness can be characterized as the measure of stability for different types of communication topologies. These switching topologies can be resulted from communication failure, packet-dropping, etc. In the first part of this chapter, we consider two robust control problems for a network of mobile agents with undirected communication topology in the presence of polytopic uncertainties and Lipschitz nonlinear dynamics. The former can be caused by unmodeled dynamics and the latter is the result of lack of knowledge regarding the agents parameters such as mass, inertia tensor, etc. Furthermore, we consider the two time scale formation

control problem which is a result of analyzing the robustness of the algorithms for MASs.

5.1 Robust Consensus Problems

In this section, we consider a network of n identical agents whit dynamics

$$\dot{x}_i = A(\rho)x_i + Bu_i + B_1 f(x_i) \tag{5.1}$$

for each agent i with state $x_i \in \mathbb{R}^m$ and input $u_i \in \mathbb{R}^{m_1}$. $f(\cdot)$ is a Lipschitz continuous function that satisfies ($k_1 > 0$)

$$\|f(x) - f(y)\| \leq k_1 \|x - y\| \tag{5.2}$$

and $A(\rho)$ belongs to the set

$$A = \left\{ A(\rho) = \sum_{k=1}^{p} \rho_k A_k, \sum_{k=1}^{p} \rho_k = 1, \rho_k \geq 0 \right\} \tag{5.3}$$

ρ is an unknown constant vector which represents the uncertainty in the model (5.1), and as seen from (5.3) it belongs to a polytope with A_k as its vertices. The robust consensus problems which we consider in this section are formally defined as follows:

Problem 5.1 Consider a connected network of agents with dynamics (5.1)-(5.3). Furthermore, assume that the communication graph topology of the network is undirected. Design a set of distributed control laws for the network such that $x_1 = \cdots = x_n$ as $t \to \infty$.

Problem 5.2 Consider Problem 5.1, but, in addition, assume that the dynamics of each agent is also subject to an external norm and energy bounded disturbance ω_i, i.e., let the agent dynamics be in the form

$$\dot{x}_i = A(\rho)x_i + Bu_i + B_1 f(x_i) + D\omega_i. \tag{5.4}$$

Design a set of distributed control laws which guarantee the desired level of H_∞ performance $\gamma > 0$ for the consensus task, i.e.

$$\int_0^\infty Z^T Z \, dt \leq \gamma^2 \int_0^\infty \Omega^T \Omega \, dt \tag{5.5}$$

where Z and Ω are the stack vectors of performance variables and external disturbances of the agents defined as

$$z_i = C\left(x_i - \frac{1}{n}\sum_{j=1}^{n} x_j\right), \quad \Omega = [\omega_1, \cdots, \omega_n]^T, \; Z = [z_1, \cdots, z_n]^T \tag{5.6}$$

where C is a constant matrix and ω_i belongs to the space of square integrable functions, $\mathcal{L}_2$.

5.1.1 Polytopic Uncertainties

In this section, we consider Problem 5.1 with the following formation control law:

$$u_i = k_2 K \sum_{i=1}^{n} a_{ij}(x_i - x_j), i = 1, \cdots, n \tag{5.7}$$

where $k_2 \in \mathbb{R}$ and $K \in \mathbb{R}^{m_1 \times m}$ are control gains to be designed in a way to ensure the convergence of the error system. a_{ij} is the element of adjacency matrix which is defined in Chapter 3 and L denotes the Laplacian matrix of the network which is introduced in Chapter 4. (5.7) can be written in compact form as

$$\begin{aligned} U &= k_2(L \otimes I_m)KX \\ X &= [x_1^T, \cdots, x_n^T]^T, \quad U = [u_1^T, \cdots, u_n^T]^T \end{aligned} \tag{5.8}$$

The control law (5.7) has similar structure with the one proposed in [85] and [113]. However, in this case, the control gains k_2 and K must be designed in a way that ensures the stability

of the network inside the uncertainty polytope (5.3). Since the communication topology of the network is undirected, it is easy to show that $\mathbf{1}_n^T L = \mathbf{0}_n$ and hence, $\mathbf{1}_n$ is a left eigenvector of the Laplacian L. Considering the new error variables $e_i = x_i - \frac{1}{n}\sum_{j=1}^{n} x_j$, which represent the deviation of x_i from the average state of the network, the stack vector of the errors can be expressed as follows:

$$E = \left(\left(I_n - \frac{\mathbf{1}_n \mathbf{1}_n^T}{n}\right) \otimes I_m\right) X, \quad E = [e_1^T, \cdots, e_n^T]^T \tag{5.9}$$

The error dynamics of the agents can be computed by taking derivative of (5.9) with respect to time and using (5.7) in (5.1) results in:

$$\begin{aligned}
\dot{e}_i &= A(\rho)e_i + B_1\left(f(x_i) - \frac{1}{n}\sum_{j=1}^{n} f(x_j)\right) + B\left(u_i - \frac{1}{n}\sum_{j=1}^{n} u_j\right) \\
&= A(\rho)e_i + B_1\left(f(x_i) - \frac{1}{n}\sum_{j=1}^{n} f(x_j)\right) \\
&+ k_2\left[\sum_{j=1}^{n} a_{ij}BK(x_i - x_j) - \frac{1}{n}\underbrace{\sum_{j=1}^{n}\sum_{s=1}^{n} a_{js}BK(x_j - x_s)}_{=0,}\right] \\
&= A(\rho)e_i + B_1\left(f(x_i) - \frac{1}{n}\sum_{j=1}^{n} f(x_j)\right) + k_2\sum_{j=1}^{n} L_{ij}BKe_j \\
&\Rightarrow \dot{E} = (I_n \otimes A(\rho))E + k_2(L \otimes BK)E + \nu
\end{aligned} \tag{5.10}$$

where ν is the stack vector of all $\nu_i = B_1\left(f(x_i) - \frac{1}{n}\sum_{j=1}^{n} f(x_j)\right)$. The second term on on the third line of (5.10) is equal to zero due to the fact that $\mathbf{1}_n$ is both the right and left eigenvectors of the Laplacian matrix which is associated with the zero eigenvalue. In order to analyze the stability properties of (5.10), consider the following Lyapunov function

$$V = \frac{1}{n}\sum_{i=1}^{n} e_i^T P^{-1} e_i = \frac{1}{n}E^T(I_n \otimes P^{-1})E \tag{5.11}$$

where P is the positive definite matrix which must be calculated. The time derivative of (5.11) is

$$\dot{V} = \frac{1}{n}\left[E^T(I_n \otimes A^T(\rho)) + k_2 E^T(L \otimes K^T B^T) + \nu^T\right](I_n \otimes P^{-1})E$$
$$+ \frac{1}{n}E^T(I_n \otimes P^{-1})\left[(I_n \otimes A(\rho))E + k_2(L \otimes BK)E + \nu\right]. \tag{5.12}$$

Using the identity $(A \otimes B)(C \otimes D) = (AC \otimes BD)$ we have

$$\dot{V} = \frac{1}{n}E^T\left[(I_n \otimes A^T(\rho)P^{-1}) + (I_n \otimes P^{-1}A(\rho)) + k_2(L \otimes K^T B^T P^{-1}) + k_2(L \otimes P^{-1}BK)\right]E$$
$$\frac{2}{n}\nu^T(I_n \otimes P^{-1})E. \tag{5.13}$$

Choosing $K = -\frac{1}{2}B^T P^{-1}$, (5.13) can be rewritten as

$$\dot{V} = \frac{1}{n}E^T\left[(I_n \otimes A^T(\rho)P^{-1}) + (I_n \otimes P^{-1}A(\rho)) - k_2(L \otimes P^{-1}BB^T P^{-1})\right]E$$
$$\frac{2}{n}\nu^T(I_n \otimes P^{-1})E. \tag{5.14}$$

The last term on the r.h.s of (5.14) satisfies

$$\frac{2}{n}\nu^T(I_n \otimes P^{-1})E = \frac{2}{n}\sum_{i=1}^{n} e_i^T P^{-1}\nu_i = \frac{2}{n}\sum_{i=1}^{n} e_i^T P^{-1}B_1\left(f(x_i) - f\left(\frac{1}{n}\sum_{j=1}^{n} x_j\right)\right)$$
$$+ \underbrace{\frac{2}{n}\sum_{i=1}^{n} e_i^T P^{-1}B_1\left(f\left(\frac{1}{n}\sum_{j=1}^{n} x_j\right) - \frac{1}{n}\sum_{j=1}^{n} f(x_j)\right)}_{=0,\ since \sum_{i=1}^{n} e_i = 0}. \tag{5.15}$$

Hence,

$$\frac{2}{n}\nu^T(I_n \otimes P^{-1})E \leq \frac{2k_1}{n}\sum_{i=1}^{n}\left\|e_i^T P^{-1}B_1\right\|\|e_i\| \leq \frac{1}{n}\sum_{i=1}^{n}\left[k_1^2 e_i^T P^{-1}B_1 B_1^T P^{-1}e_i + e_i^T e_i\right]$$
$$\leq \frac{1}{n}E^T\left(I_n \otimes \left(\left(k_1^2 P^{-1}B_1 B_1^T P^{-1}\right) + I\right)\right)E. \tag{5.16}$$

Defining $Y = (I_n \otimes P^{-1})E$, we can rewrite (5.16) as follows:

$$\dot{V} \leq \frac{1}{n} Y^T (I_n \otimes P) \left[(I_n \otimes A^T(\rho) P^{-1}) + (I_n \otimes P^{-1} A(\rho)) - k_2 (L \otimes P^{-1} B B^T P^{-1}) \right] (I_n \otimes P) Y$$
$$+ \frac{1}{n} Y^T (I_n \otimes P) \left(I_n \otimes \left((k_1^2 P^{-1} B_1 B_1^T P^{-1}) + I \right) \right) (I_n \otimes P) Y. \tag{5.17}$$

Using the properties of the Kronecker product we have

$$\begin{aligned} \dot{V} &\leq \frac{1}{n} Y^T \left(I_n \otimes \left(P A^T(\rho) + A(\rho) P + k_1^2 B_1 B_1^T + P^2 \right) - k_2 \left(L \otimes B B^T \right) \right) Y \\ &\leq \frac{1}{n} Y^T \left(I_n \otimes \left(P A^T(\rho) + A(\rho) P + k_1^2 B_1 B_1^T + P^2 - k_2 \lambda_2 B B^T \right) \right) Y \end{aligned} \tag{5.18}$$

Note that we have used Fiedler eigenvalue theorem [12] for the second line in (5.18). Therefore, if the conditions

$$\begin{bmatrix} P A^T(\rho) + A(\rho) P + k_1^2 B_1 B_1^T - k_3 B B^T & P \\ P & -I \end{bmatrix} < 0, \quad k_2 \geq \frac{k_3}{\lambda_2} \tag{5.19}$$

is satisfied, we can conclude that the consensus will be achieved. Since $A(\rho)$ belongs to the polytope (5.3), condition (5.16) can be turned into the following set of conditions,

$$\begin{bmatrix} P A_i^T + A_i P + k_1^2 B_1 B_1^T - k_3 B B^T & P \\ P & -I \end{bmatrix} < 0,$$
$$i \in \{1, \cdots, p\}, \quad k_2 \geq \frac{k_3}{\lambda_2} \tag{5.20}$$

Remark 5.1: Compared with the results in [85], here, there exist p LMIs which must be checked at the vertices of the uncertainty polytope to ensure the stability of the consensus task.

5.1.2 H_∞ Consensus in the Presence of Polytopic Uncertainties

In the previous section, the consensus task achieved in the presence of the polytopic uncertainties, in this section, we study the Problem 5.2 in detail and consider the effects of the

external disturbances on the dynamics (5.1). It should be noted that each element of ω_i belongs to the space of square integrable functions over $[0, \infty)$. In other words, the disturbance ω_i is assumed to be energy bounded. The assumptions on network communication graph are considered to be the same as in the previous section. Defining e_i and E as in (5.9), we have ($\Omega = [\omega_1, \cdots, \omega_n]^T$)

$$\dot{e}_i = A(\rho)e_i + B_1\left(f(x_i) - \frac{1}{n}\sum_{j=1}^{n} f(x_j)\right) + B\left(u_i - \frac{1}{n}\sum_{j=1}^{n} u_j\right) + D\left(\omega_i - \frac{1}{n}\sum_{j=1}^{n}\omega_j\right)$$
$$\Longrightarrow \dot{E} = (I_n \otimes A(\rho))E + k_2(L \otimes BK)E + (I_n \otimes D)(F \otimes I)\Omega, \tag{5.21}$$

Where we have assumed that the control laws have the same structure as in (5.7).The performance for each agent is defined as follows

$$z_i = C\left(x_i - \frac{1}{n}\sum_{j=1}^{n} x_j\right) \tag{5.22}$$

The main objective of this section is to achieve asymptotic consensus while under the zero initial condition the H_∞ performance is assured to be less than γ i.e.($Z = [z_1, \cdots, z_n]^T$)

$$J = \int_0^\infty Z^T Z \; dt \leq \gamma^2 \int_0^\infty \Omega^T \Omega \; dt \tag{5.23}$$

In order to design the gain K in a way that achieves the consensus task and guarantees the H_∞ performance γ in the presence of polytopic uncertainties, consider the following Lyapunov function

$$V = \sum_{i=1}^{n}\sum_{l=1}^{p} e_i^T(\rho_l Q_l^{-1})e_i = \sum_{i=1}^{n} e_i^T\left(\sum_{l=1}^{p}\rho_l Q_l^{-1}\right)e_i$$
$$= \sum_{i=1}^{n} e_i^T Q^{-1}(\rho)e_i = E^T(I_n \otimes Q^{-1})E \tag{5.24}$$

taking the derivative of (5.24) with respect to time results in

$$\begin{aligned}\dot{V} = E^T \big[&\big((I_n \otimes A^T(\rho)) + k_2(L \otimes K^T B^T)\big)(I_n \otimes Q^{-1}) \\ &+(I_n \otimes Q^{-1})\left((I_n \otimes A(\rho)) + k_2(L \otimes BK)\right)\big] E \\ &+ 2E^T(I_n \otimes Q^{-1})\nu + 2E^T(I_n \otimes Q^{-1})(I_n \otimes D)(F \otimes I)\Omega \end{aligned} \tag{5.25}$$

using (5.15), we have

$$\begin{aligned}\dot{V} \leq E^T \big[&\big((I_n \otimes A^T(\rho)) + k_2(L \otimes K^T B^T)\big)(I_n \otimes Q^{-1}) \\ &+(I_n \otimes Q^{-1})\left((I_n \otimes A(\rho)) + k_2(L \otimes BK)\right)\big] E \\ &+ E^T\left(I_n \otimes \left(\left(k_1^2 Q^{-1} B_1 B_1^T Q^{-1}\right) + I\right)\right) E + 2E^T(F \otimes Q^{-1}D)\Omega \end{aligned} \tag{5.26}$$

Next, using the change of variable $\bar{E} = (I_n \otimes Q^{-1})E$, (5.26) turns into

$$\begin{aligned}\dot{V} \leq \bar{E}^T \big[&(I_n \otimes Q)\left((I_n \otimes A^T(\rho)) + k_2(L \otimes K^T B^T)\right) \\ &+ \left((I_n \otimes A(\rho)) + k_2(L \otimes BK)\right)(I_n \otimes Q)\big] \bar{E} \\ &+ \bar{E}^T\left(I_n \otimes \left(\left(k_1^2 B_1 B_1^T\right) + Q^2\right)\right) \bar{E} + 2\bar{E}^T(F \otimes D)\Omega \end{aligned} \tag{5.27}$$

under the zero initial condition assumption, we can conclude that (5.23) satisfies if $\dot{V} + Z^T Z - \gamma^2 \Omega^T \Omega < 0$. Using the fact

$$\begin{aligned}2\bar{E}^T(F \otimes D)\Omega - \gamma^2 \Omega^T \Omega = \gamma^{-2}\bar{E}^T(F^2 \otimes DD^T)\bar{E} \\ - \gamma^2\left(\Omega - \gamma^{-2}(F \otimes D^T)\bar{E}\right)^T\left(\Omega - \gamma^{-2}(F \otimes D^T)\bar{E}\right) \end{aligned} \tag{5.28}$$

we can write

$$\begin{aligned}\dot{V} + Z^T Z - \gamma^2 \Omega^T \Omega \leq \bar{E}^T(I_n \otimes (QC^T CQ))\bar{E} + \gamma^{-2}\bar{E}^T(F^2 \otimes DD^T)\bar{E} \\ + \bar{E}^T\big[(I_n \otimes Q)\left((I_n \otimes A^T(\rho)) + k_2(L \otimes K^T B^T)\right) \\ + \left((I_n \otimes A(\rho)) + k_2(L \otimes BK)\right)(I_n \otimes Q)\big]\bar{E} \\ + \bar{E}^T\left(I_n \otimes \left(\left(k_1^2 B_1 B_1^T\right) + Q^2\right)\right)\bar{E} \end{aligned} \tag{5.29}$$

since the multiplication of F and L is commutative, they can be simultaneously diagonalized using a single orthogonal matrix U. This can be proved using Schur decomposition. Also, From the fact that $\mathbf{1}_n$ is the right and left eigen vector for both matrices, we can choose a unitary matrix $U = [\frac{\mathbf{1}_n}{\sqrt{n}}\ M]$ such that $U^T F U = diag(0, I_{n-1})$ and $\bar{L} = U^T L U = diag(0, \lambda_2, \cdots, \lambda_n)$. Hence, using the change of variable $\bar{\bar{E}} = (U^T \otimes I_n)\bar{E}$ we can write

$$\begin{aligned}
&\dot{V} + Z^T Z - \gamma^2 \Omega^T \Omega \leq \bar{\bar{E}}^T (I_n \otimes (QC^T CQ))\bar{\bar{E}} + \gamma^{-2} \bar{\bar{E}}^T (U^T F^2 U \otimes DD^T)\bar{\bar{E}} \\
&+ \bar{\bar{E}}^T \left[(I_n \otimes Q) \left((I_n \otimes A^T(\rho)) + k_2 (U^T L U \otimes K^T B^T) \right) \right. \\
&\left. + \left((I_n \otimes A(\rho)) + k_2 (U^T L U \otimes BK) \right) (I_n \otimes Q) \right] \bar{\bar{E}} \\
&+ \bar{\bar{E}}^T \left(I_n \otimes \left(\left(k_1^2 B_1 B_1^T \right) + Q^2 \right) \right) \bar{\bar{E}}
\end{aligned} \tag{5.30}$$

for F^2, we can write

$$F^2 = \left(I_n - \frac{\mathbf{1}_n \mathbf{1}_n^T}{n} \right) \left(I_n - \frac{\mathbf{1}_n \mathbf{1}_n^T}{n} \right) = I_n - \frac{2}{n} \mathbf{1}_n \mathbf{1}_n^T + \frac{1}{n^2} \mathbf{1}_n \mathbf{1}_n^T \mathbf{1}_n \mathbf{1}_n^T = F \tag{5.31}$$

from (5.31), we can conclude that $U^T F^2 U = diag\,(0, I_{n-1})$. Since the first element of $\bar{\bar{E}}$ is equal to zero, defining $\bar{\bar{E}}_r = \left[\bar{\bar{E}}_2, \cdots, \bar{\bar{E}}_n \right]^T$ and $\bar{L}_r = diag(\lambda_2, \cdots, \lambda_n) > 0$ we can write

$$\begin{aligned}
&\dot{V} + Z^T Z - \gamma^2 \Omega^T \Omega \leq \bar{\bar{E}}_r^T (I_{n-1} \otimes (QC^T CQ))\bar{\bar{E}}_r + \gamma^{-2} \bar{\bar{E}}_r^T (I_{n-1} \otimes DD^T)\bar{\bar{E}}_r \\
&+ \bar{\bar{E}}_r^T \left[(I_{n-1} \otimes Q) \underbrace{\left((I_{n-1} \otimes A^T(\rho)) + k_2 (\bar{L}_r \otimes K^T B^T) \right)}_{\bar{A}^T} \right. \\
&\left. + \underbrace{\left((I_{n-1} \otimes A(\rho)) + k_2 (\bar{L}_r \otimes BK) \right)}_{\bar{A}} (I_{n-1} \otimes Q) \right] \bar{\bar{E}}_r \\
&+ \bar{\bar{E}}_r^T \left(I_{n-1} \otimes \left(\left(k_1^2 B_1 B_1^T \right) + Q^2 \right) \right) \bar{\bar{E}}_r
\end{aligned} \tag{5.32}$$

thus, to achieve H_∞ performance, we need to design K such that the following holds

$$(I_{n-1}\otimes Q)\bar{A}^T+\bar{A}(I_{n-1}\otimes Q)+(I_{n-1}\otimes Q)(I_{n-1}\otimes C^TC)(I_{n-1}\otimes Q)+\gamma^{-2}(I_{n-1}\otimes DD^T)$$
$$+(I_{n-1}\otimes(k_1^2B_1B_1^T)+Q^2)<0 \tag{5.33}$$

using the facts

$$\begin{aligned}\epsilon\Bigg[&(I_{n-1}\otimes Q)\underbrace{\big((I_{n-1}\otimes A^T(\rho))+k_2(\bar{L}_r\otimes K^TB^T)\big)}_{\bar{A}^T}\\&+\underbrace{\big((I_{n-1}\otimes A(\rho))+k_2(\bar{L}_r\otimes BK)\big)}_{\bar{A}}(I_{n-1}\otimes Q)\Bigg]\\&=-(I_{n-1}\otimes Q)+(I+\epsilon\bar{A})(I_{n-1}\otimes Q)(I+\epsilon\bar{A}^T)-\epsilon^2\bar{A}(I_{n-1}\otimes Q)\bar{A}^T\end{aligned} \tag{5.34}$$

and

$$\epsilon(I_{n-1}\otimes Q)(I_{n-1}\otimes C^TC)(I_{n-1}\otimes Q)=$$
$$\epsilon(I_{n-1}\otimes QC^T)(I-\epsilon\left(I_{n-1}\otimes(CQC^T)\right)^{-1})(I_{n-1}\otimes CQ)+\mathcal{O}(\epsilon^2)$$

(5.34) turns into the following inequality

$$\begin{bmatrix} -(I_{n-1}\otimes Q)^{-1} & I+\epsilon\left((I_{n-1}\otimes A^T(\rho))+k_2(\bar{L}_r\otimes K^TB^T)\right) & 0 \\ I+\epsilon\left((I_{n-1}\otimes A(\rho))+k_2(\bar{L}_r\otimes BK)\right) & -(I_{n-1}\otimes Q) & I_{n-1}\otimes D \\ 0 & (I_{n-1}\otimes D^T) & -\gamma^2\epsilon^{-1}I \\ 0 & I_{n-1}\otimes Q & 0 \\ 0 & I_{n-1}\otimes B_1^T & 0 \\ I_{n-1}\otimes C & 0 & 0 \end{bmatrix}$$

$$\begin{bmatrix} 0 & 0 & I_{n-1}\otimes C^T \\ I_{n-1}\otimes Q & I_{n-1}\otimes B_1 & 0 \\ 0 & 0 & 0 \\ \epsilon^{-1}I & 0 & 0 \\ 0 & \epsilon^{-1}k_1^2I & 0 \\ 0 & 0 & \epsilon^{-1}I \end{bmatrix} < 0 \tag{5.35}$$

choosing $K = VM^{-1}$ and using corollary 2.4 in [114], we can show that the H_∞ consensus problem has a solution, if and only if the following set of LMIs have a feasible solutions.

$$\begin{bmatrix} (I_{n-1}\otimes(Q_i-M^T-M)) & ((I_{n-1}\otimes M^T)+\epsilon\left((I_{n-1}\otimes M^TA_i^T)+k_2(\bar{L}_r\otimes V^TB_i^T)\right) \\ (I_{n-1}\otimes M)+\epsilon\left((I_{n-1}\otimes A_iM)+k_2(\bar{L}_r\otimes BV)\right) & -(I_{n-1}\otimes Q_i) \\ 0 & (I_{n-1}\otimes D^T) \\ 0 & I_{n-1}\otimes Q \\ 0 & I_{n-1}\otimes B_1^T \\ I_{n-1}\otimes CM & 0 \end{bmatrix}$$

$$\begin{bmatrix} 0 & 0 & 0 & I_{n-1}\otimes M^TC^T \\ I_{n-1}\otimes D & I_{n-1}\otimes Q & I_{n-1}\otimes B_1 & 0 \\ -\gamma^2\epsilon^{-1}I & 0 & 0 & 0 \\ 0 & \epsilon^{-1}I & 0 & 0 \\ 0 & 0 & \epsilon^{-1}k_1^2I & 0 \\ 0 & 0 & 0 & \epsilon^{-1}I \end{bmatrix} < 0 \tag{5.36}$$

Remark 5.2 The convergence results in [85] can not be directly extended to the H_∞ consensus problem in the presence of polytopic uncertainties as in the section 5.1.1. The main difficulty here is stemming from the structure of the Lyapunov function which is used for the control design task. This function depends on the uncertainty parameters and hence,

it should be chosen in a way that satisfies the convexity properties. In this regard, here, we used the method in [114] to solve this problem.

5.2 Two Time Scale Formation Control

In this section, we consider the two time scales behavior for multi agent systems, we start our analysis by considering a simple network of two mechanical agents whose dynamics are expressed as follows

$$M_i(r_i)\ddot{r}_i + C_i(r_i, \dot{r}_i)\dot{r}_i = f_i + \omega_i, i = 1, 2 \tag{5.37}$$

where $r_i \in \mathbb{R}^{n_1}$ are coordinates of each agent in physical workspace. $\omega_i \in \mathbb{R}^{n_1}$ denotes the summation of external disturbance or modeled dynamics which are affecting the i^{th} agent and it is assumed to be upper bounded, i.e. $\|\omega_i\| \leq \bar{\omega}_i$. From (5.37), it is clear that M_1 and M_2 are time varying inertia matrices which are only dependent on r_i. The latter is due to the fact that (5.37) is the result of Lagrange's equation of motion with quadratic energy functions. The term involving C_i contains the Coriolis and damping effects. In general, for C_i and M_i we can assume the followings

$$\underline{M} \leq \|M_i(r_i)\| \leq \bar{M}, \quad \|C_i(r_i, \dot{r}_i)\| \leq C \|\dot{r}_i\| \tag{5.38}$$

where $C, \underline{M}, \bar{M} \in \mathbb{R}$ are positive constants. As the main formation control objective, the center of mass of all the agents are required to follow the desired path on the slow time scale while the agents maintain a particular distance from each other. In order to design a set of control laws for agents such that they exhibit such a two time scales behavior, we use the strategy which is first proposed in [50] by considering the following change of

coordinates

$$R = \frac{r_1 + r_2}{2}, \quad E = \frac{r_1 - r_2}{2} \tag{5.39}$$

It is clear that R represents the center of mass of the two agents and E denotes the respective relative position vector. Using (5.39) and (5.37), we can write

$$\ddot{R} = \underbrace{\frac{(M_1^{-1} f_1 + M_2^{-1} f_2)}{2}}_{f_R} + \underbrace{\frac{(M_1^{-1}\omega_1 + M_2^{-1}\omega_2)}{2}}_{\omega_R} - \underbrace{\frac{(M_1^{-1}C_1 - M_2^{-1}C_2)}{2}}_{M_b}\dot{E} - \underbrace{\frac{(M_1^{-1}C_2 + M_2^{-1}C_2)}{2}}_{M_a}\dot{R}$$
$$\ddot{E} = \underbrace{\frac{(M_1^{-1} f_1 - M_2^{-1} f_2)}{2}}_{f_E} + \underbrace{\frac{(M_1^{-1}\omega_1 - M_2^{-1}\omega_2)}{2}}_{\omega_E} - \underbrace{\frac{(M_1^{-1}C_1 - M_2^{-1}C_2)}{2}}_{M_b}\dot{R} - \underbrace{\frac{(M_1^{-1}C_1 + M_2^{-1}C_2)}{2}}_{M_a}\dot{E}$$

or in matrix form

$$\begin{bmatrix} \ddot{R} \\ \ddot{E} \end{bmatrix} = \begin{bmatrix} f_R \\ f_E \end{bmatrix} + \begin{bmatrix} \omega_R \\ \omega_E \end{bmatrix} - \begin{bmatrix} M_a & M_b \\ M_b & M_a \end{bmatrix} \begin{bmatrix} \dot{R} \\ \dot{E} \end{bmatrix} \tag{5.40}$$

Notice that the matrix M_b makes the dynamics of R and E coupled. The error system can be written as follows

$$\begin{bmatrix} \ddot{e}_R \\ \ddot{e}_E \end{bmatrix} = \begin{bmatrix} f_R \\ f_E \end{bmatrix} + \begin{bmatrix} \omega_R \\ \omega_E \end{bmatrix} - \begin{bmatrix} M_a & M_b \\ M_b & M_a \end{bmatrix} \begin{bmatrix} \dot{e}_R \\ \dot{e}_E \end{bmatrix} - \begin{bmatrix} M_a & M_b \\ M_b & M_a \end{bmatrix} \begin{bmatrix} \dot{R}_r \\ 0 \end{bmatrix} - \begin{bmatrix} \ddot{R}_r \\ 0 \end{bmatrix} \tag{5.41}$$

Next, consider the following control laws

$$\begin{aligned} f_R &= M_a \dot{R}_r + \ddot{R}_r + f_{r1}(e_R) + f_{r2}(\dot{e}_R) \\ f_E &= M_b \dot{R}_r + \frac{1}{\epsilon^2} f_{e1}(e_E) + \frac{1}{\epsilon} f_{e2}(\dot{e}_E) \end{aligned} \tag{5.42}$$

where ϵ is the small constant which represent the time dilation and needs to be chosen later. Using (5.42), the control law for agents can be obtained as follows

$$\begin{aligned} f_1 &= C_1 \dot{R}_r + M_1(\ddot{R}_r + f_{r1}(e_R) + f_{r2}(\dot{e}_R) + \frac{1}{\epsilon^2} f_{e1}(e_E) + \frac{1}{\epsilon} f_{e2}(\dot{e}_E)) \\ f_2 &= C_2 \dot{R}_r + M_2(\ddot{R}_r + f_{r1}(e_R) + f_{r2}(\dot{e}_R) - \frac{1}{\epsilon^2} f_{e1}(e_E) - \frac{1}{\epsilon} f_{e2}(\dot{e}_E)) \end{aligned} \tag{5.43}$$

and the closed loop system for (5.41) becomes

$$\begin{aligned}\ddot{e}_R &= -M_a\dot{e}_R - M_b\dot{e}_E + f_{r1}(e_R) + f_{r2}(\dot{e}_R)\\ \ddot{e}_E &= -M_a\dot{e}_E - M_b\dot{e}_R + \frac{1}{\epsilon^2}f_{e1}(e_E) + \frac{1}{\epsilon}(\dot{e}_E)\end{aligned} \tag{5.44}$$

before studying the stability properties of (5.44), first we need to bring the equation to the canonical form of the singular perturbation theory using the following definitions

$$X_R = \begin{bmatrix} e_R \\ \dot{e}_R \end{bmatrix}, \quad X_E = \begin{bmatrix} \frac{1}{\epsilon}e_E \\ \dot{e}_E \end{bmatrix} \tag{5.45}$$

as follows

$$\begin{aligned}\dot{X}_R &= \begin{bmatrix} 0 & I \\ 0 & -M_a \end{bmatrix} X_R + \begin{bmatrix} 0 & 0 \\ 0 & -M_b \end{bmatrix} X_E + \begin{bmatrix} 0 \\ f_{r1}(X_{R1}) + f_{r2}(X_{R2}) \end{bmatrix}\\ \dot{X}_E &= \begin{bmatrix} 0 & \frac{I}{\epsilon} \\ 0 & 0 \end{bmatrix} X_E + \begin{bmatrix} 0 \\ \frac{1}{\epsilon^2}f_{e1}(\epsilon X_{E1}) + \frac{1}{\epsilon}(X_{E2}) \end{bmatrix} + \begin{bmatrix} 0 & 0 \\ 0 & -M_a \end{bmatrix} X_E + \begin{bmatrix} 0 & 0 \\ 0 & -M_b \end{bmatrix} X_R\end{aligned} \tag{5.46}$$

or, in canonical form as

$$\begin{aligned}\dot{X}_R &= \begin{bmatrix} 0 & I \\ 0 & -M_a \end{bmatrix} X_R + \begin{bmatrix} 0 & 0 \\ 0 & -M_b \end{bmatrix} X_E + \begin{bmatrix} 0 \\ f_{r1}(X_{R1}) + f_{r2}(X_{R2}) \end{bmatrix}\\ \epsilon\dot{X}_E &= \left(\begin{bmatrix} 0 & I \\ 0 & 0 \end{bmatrix} X_E + \begin{bmatrix} 0 \\ \frac{1}{\epsilon}f_{e1}(\epsilon X_{E1}) + f_{e2}(X_{E2}) \end{bmatrix} \right)\\ &+ \epsilon \left(\begin{bmatrix} 0 & 0 \\ 0 & -M_a \end{bmatrix} X_E + \begin{bmatrix} 0 & 0 \\ 0 & -M_b \end{bmatrix} X_R \right)\end{aligned} \tag{5.47}$$

In order to ensure that for $\epsilon = 0$, the second line in (5.47) only has isolated solution, the function $f_{e1}(\cdot)$ must be a homogenous function to cancel $\frac{1}{\epsilon}$. Hence, we can choose $f_{e1}(\epsilon X_{E1}) = k_1\epsilon X_{E1}$. Also f_{e2} must vanish at zero, i.e. $(f_{e2}(0) = 0)$. In order to use

Theorem 8.3 in [34], first we need to show that the origin of boundary layer system

$$\dot{X}_E = \begin{bmatrix} 0 & I \\ 0 & 0 \end{bmatrix} X_E + \begin{bmatrix} 0 \\ k_1 X_{E1} + f_{e2}(X_{E2}) \end{bmatrix} \tag{5.48}$$

is exponentially stable. This can be investigated by using the time derivative of the Lyapunov function $V = \frac{1}{2} X_E^T X_E$ as follows (Q is a symmetric positive definite matrix.)

$$\begin{aligned} \dot{V} &= \frac{1}{2}\left(2\dot{X}_{E1}^T X_{E1} + 2\dot{X}_{E2}^T X_{E2} + 2(\dot{X}_{E1}^T X_{E2} + X_{E1}^T \dot{X}_{E2})\right) \\ &= \frac{1}{2}\left(2X_{E2}^T X_{E1} + 2(k_1 X_{E1} + f_{e2}(X_{E2}))^T X_{E2}\right. \\ &\left. +2(X_{E2}^T X_{E2} + X_{E1}^T (k_1 X_{E1} + f_{e2}(X_{E2})))\right) \end{aligned} \tag{5.49}$$

if the function $f_{e2}(\cdot)$ is designed to satisfy the following conditions

$$X_{E2}^T f_{e2}(X_{E2}) \leq -a_1 X_{E2}^T X_{E2}, \quad \|f_{e2}(X_{E2})\| \leq a_1^{'} \|X_{E2}\| \tag{5.50}$$

then (5.49) turns in to

$$\begin{aligned} \dot{V} &\leq -\frac{1}{2} \begin{bmatrix} \|X_{E1}\| \\ \|X_{E2}\| \end{bmatrix}^T \underbrace{\begin{bmatrix} -2k_1 & -(1+k_1+a_1^{'}) \\ -(1+k_1+a_1^{'}) & 2a_1 - 2 \end{bmatrix}}_{W_1 > 0} \begin{bmatrix} \|X_{E1}\| \\ \|X_{E2}\| \end{bmatrix} \\ &\leq -\lambda_{min}(W_1) V < 0 \end{aligned} \tag{5.51}$$

which clearly demonstrates the exponential stability of the system (5.44).

Next, we study the stability of the reduced system

$$\dot{X}_R = \begin{bmatrix} 0 & I \\ 0 & -M_a \end{bmatrix} X_R + \begin{bmatrix} 0 \\ f_{r1}(X_{R1}) + f_{r2}(X_{R2}) \end{bmatrix} \tag{5.52}$$

Using the Lyapunov function $V_2 = \frac{1}{2} X_R^T P X_R$, we have

$$\begin{aligned} &\dot{V} = 2X_{R2}^T P_{11} X_{R1} + (-M_a X_{R2} + f_{r1} + f_{r2})^T P_{22} X_{R2} + X_{R2}^T P_{22}(-M_a X_{R2} + f_{r1} + f_{r2}) \\ &2X_{R2}^T P_{12} X_{R2} + X_{R1}^T P_{12}(-M_a X_{R2} + f_{r1} + f_{r2}) + (-M_a X_{R2} + f_{r1} + f_{r2})^T P_{12} X_{R1} \end{aligned} \tag{5.53}$$

choosing $f_{r1} = -K_{r1}X_{R1}$ and $f_{r2} = -K_{r2}X_{R2}$, (5.53) turns into

$$\dot{V} = \begin{bmatrix} X_{R1} \\ X_{R2} \end{bmatrix}^T \overbrace{\begin{bmatrix} -P_{12}k_{r1} - K_{r1}P_{12} & -K_{r1}P_{22} + P_{11} - P_{12}K_{r2} \\ -P_{22}K_{r1} + P_{11} - K_{r2}P_{12} & 2P_{12} - K_{r2}P_{22} - P_{22}K_{r2} \end{bmatrix}}^{-W_2} \begin{bmatrix} X_{R1} \\ X_{R2} \end{bmatrix}$$
$$+ 2 \begin{bmatrix} X_{R1} \\ X_{R2} \end{bmatrix}^T \underbrace{\begin{bmatrix} 0 & 0 \\ 0 & -M_a \end{bmatrix}}_{Q} \begin{bmatrix} P_{11} & P_{12} \\ P_{12} & P_{22} \end{bmatrix} \begin{bmatrix} X_{R1} \\ X_{R2} \end{bmatrix} \tag{5.54}$$

The matrix P can be chosen in a way that W_2 becomes negative definite. Hence, we can write

$$\dot{V} \leq -\lambda_{min}(W_2) \left\| X_R \right\|^2 + 2X_R^T Q P X_R \tag{5.55}$$

for M_a we have

$$\|M_a\| = \left\| \frac{M_1^{-1}C_1 + M_2^{-1}C_2}{2} \right\| \leq \underbrace{M^{-1}C}_{\gamma_1} \left\| X_{R2} + \dot{R}_r \right\| \leq \gamma_1 \left\| X_{R2} \right\| + \gamma_1 \bar{V}_r \tag{5.56}$$

where $\left\| \dot{R}_r \right\| = \|V_r\| \leq \bar{V}_r$. Using (5.56), (5.55) can be rewritten as follows

$$\dot{V} \leq -\lambda_{min}(W_2) \left\| X_R \right\|^2 + 2\gamma_1 \lambda_{max}(P)(\left\| X_{R2} \right\| + \bar{V}_r) \left\| X_R \right\|^2 \tag{5.57}$$

Therefore, if $\|X_{R2}\| \leq l_1$, then $\dot{V} \leq -(\lambda_{min}(W_2) - 2\gamma_1\lambda_{max}(P)(l_1 + \bar{V}_r)) \left\| X_R \right\|^2$. The latter suggests that if the condition $\lambda_{min}(W_2) \geq 2\gamma_1\lambda_{max}(P)(l_1 + \bar{V}_r)$ is satisfied then the exponential stability of the origin will be guaranteed for the trajectories which are starting inside the set $V \leq \frac{\lambda_{min}(P)l_1^2}{2}$. Next, we consider the interconnection conditions as follows

$$\left(\frac{\partial V_2}{\partial X_R} \right)^T \begin{bmatrix} 0 & 0 \\ 0 & -M_b \end{bmatrix} X_E \leq \gamma_1(\left\| X_{R2} \right\| + \bar{V}_r) X_R^T P X_E$$
$$\leq \gamma_1 \lambda_{max}(P)(\left\| X_{R2} \right\| + \bar{V}_r) \left\| X_R \right\| \left\| X_E \right\| \tag{5.58}$$

which for trajectories inside the set $V \leq \frac{\lambda_{min}(P)l_1^2}{2}$ can be rewritten as follows

$$\left(\frac{\partial V_2}{\partial X_R}\right)^T \begin{bmatrix} 0 & 0 \\ 0 & -M_b \end{bmatrix} X_E \leq \gamma_1 \lambda_{max}(P)(l_1 + \bar{V}_r) \|X_R\| \|X_E\| \tag{5.59}$$

Also, we can write

$$\epsilon \left(\frac{\partial V_1}{\partial X_E}\right)^T \left(\begin{bmatrix} 0 & 0 \\ 0 & -M_a \end{bmatrix} X_E + \begin{bmatrix} 0 & 0 \\ 0 & -M_b \end{bmatrix} X_R \right) \leq \epsilon(l_1 + \bar{V}_r) \left(\|X_E\|^2 + \|X_E\| \|X_R\| \right) \tag{5.60}$$

thus, for the following Lyapunov function

$$\nu = (1-d)V_2 + dV_1 \tag{5.61}$$

we can find that $\dot{\nu} = z^T W_3 z, z = [\|X_R\| \ \ \|X_E\|]^T$ where

$$W_3 = \begin{bmatrix} (1-d)(\lambda_{min}(W_2) - 2\gamma_1 \lambda_{max}(P)(l_1 + \bar{V}_r))) & \frac{-1}{2}(1-d)\gamma_1 \lambda_{max}(P)(l_1 + \bar{V}_r) - \frac{1}{2}d(l_1 + \bar{V}_r) \\ \frac{-1}{2}(1-d)\gamma_1 \lambda_{max}(P)(l_1 + \bar{V}_r) - \frac{1}{2}d(l_1 + \bar{V}_r) & \frac{d}{\epsilon}\lambda_{min}(W_1) - \epsilon(l_1 + \bar{V}_r) \end{bmatrix}$$

hence, if the following condition

$$\epsilon \leq \frac{\lambda_{min}(W_1)(\lambda_{min}(W_2) - 2\gamma_1 \lambda_{max}(P)(l_1 + \bar{V}_r))}{\lambda_{min}(W_2)(l_1 + \bar{V}_r) - 2\gamma_1 \lambda_{max}(P)(l_1 + \bar{V}_r)^2 + \frac{1}{4(1-d)d}[(1-d)\gamma_1 \lambda_{max}(P)(l_1 + \bar{V}_r) + d(l_1 + \bar{V}_r)]^2} \tag{5.62}$$

holds, the exponential stability of the whole system will be guaranteed.

Remark 5.3 From (5.43), it is clear that compared with [50], here, we used general nonlinear feedback control laws for each subsystem to find less restrictive bound on the perturbation parameter ϵ.

5.2.1 Complete Graph Topology

In order to generalize the previous results to the case of n agents with complete communication graph, consider the following transformations

$$R = \frac{1}{n}\sum_{i=1}^{n} r_i, \qquad E_j = r_j - \frac{1}{n}\sum_{i=1}^{n} r_i,\ j \in \{1, \cdots, n-1\} \tag{5.63}$$

which represents the location of the center of agents R (not center of mass) and the relative vector of position of agents from R. Fig.5.1 illustrates the vectors R and E_j. Using (5.63),

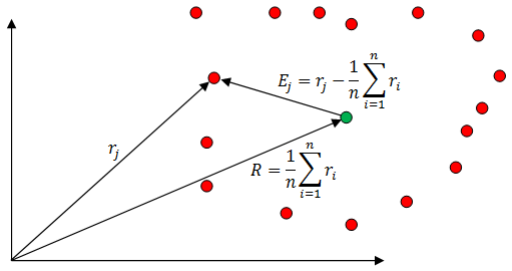

Figure 5.1: Illustration of the vectors R and E_j

the modified error dynamics can be obtained as follows

$$\ddot{e}_R = -\left(\underbrace{\frac{1}{n}\sum_{i=1}^{n} M_i^{-1}C_i}_{M_a}\right)\dot{e}_R - \frac{1}{n}\sum_{i=1}^{n-1}\left(\underbrace{M_i^{-1}C_i - M_n^{-1}C_n}_{nM_{bi}}\right)\dot{e}_{Ej}$$
$$-\left(\frac{1}{n}\sum_{i=1}^{n} M_i^{-1}C_i\right)\dot{R}_r + \underbrace{\frac{1}{n}\sum_{i=1}^{n} M_i^{-1}f_i}_{f_R}$$
$$\ddot{e}_{Ej} = -\left(\underbrace{M_j^{-1}C_j - \frac{1}{n}\sum_{i=1}^{n} M_i^{-1}C_i}_{M_{cj}}\right)\dot{e}_R - \underbrace{\left(\frac{n-1}{n}\right)M_j^{-1}C_j}_{M_{dj}}\dot{e}_{Ej} + \frac{1}{n}\sum_{i=1,i\neq j}^{n-1}\left(M_i^{-1}C_i - M_n^{-1}C_n\right)\dot{e}_{Ei}$$
$$-\left(M_j^{-1}C_j - \frac{1}{n}\sum_{i=1}^{n} M_i^{-1}C_i\right)\dot{R}_r + \underbrace{M_j^{-1}f_j - \frac{1}{n}\sum_{i=1}^{n} M_i^{-1}f_i}_{f_{Ej}}, \quad j = 1, \cdots, n-1 \tag{5.64}$$

following the similar steps as in the case of two agents, we choose the following control laws

$$f_R = \left(\frac{1}{n}\sum_{i=1}^{n} M_i^{-1}C_i\right)\dot{R}_r + f_{r1}(e_R) + f_{r2}(\dot{e}_R)$$
$$f_{Ej} = \left[M_j^{-1}C_j - \frac{1}{n}\sum_{i=1}^{n} M_i^{-1}C_i\right]\dot{R}_r + \frac{1}{\epsilon^2}f_{e1j}(e_{Ej}) + \frac{1}{\epsilon}f_{e2j}(\dot{e}_{Ej}) \tag{5.65}$$

As in the case of two agents, consider the following definitions

$$X_R = \begin{bmatrix} e_R \\ \dot{e}_R \end{bmatrix}, \quad X_{Ej} = \begin{bmatrix} \frac{1}{\epsilon}e_{Ej} \\ \dot{e}_{Ej} \end{bmatrix} \tag{5.66}$$

using (5.66), we can write

$$\dot{X}_R = \begin{bmatrix} 0 & I \\ 0 & -M_a \end{bmatrix} X_R + \sum_{i=1}^{n-1} \begin{bmatrix} 0 & 0 \\ 0 & -M_{bi} \end{bmatrix} X_{Ei} + \begin{bmatrix} 0 \\ f_{r1}(e_R) + f_{r2}(\dot{e}_R) \end{bmatrix}$$
$$\epsilon \dot{X}_{Ej} = \epsilon \left(\begin{bmatrix} 0 & 0 \\ 0 & -M_{dj} \end{bmatrix} X_{Ej} + \begin{bmatrix} 0 & 0 \\ 0 & -M_{cj} \end{bmatrix} X_R \right) + \begin{bmatrix} 0 & 0 \\ 0 & I \end{bmatrix} X_{Ej}$$
$$+ \epsilon \left(\sum_{i=1, i\neq j}^{n-1} \begin{bmatrix} 0 & 0 \\ 0 & -M_{bi} \end{bmatrix} \right) + \begin{bmatrix} 0 \\ \frac{1}{\epsilon} f_{e1j}(\epsilon X_{Ej1}) + f_{e2j}(X_{Ej2}) \end{bmatrix} \tag{5.67}$$

using the homogeneity assumption for the function, i.e. $f_{e1j}(\epsilon X_{Ej1}) = \epsilon k_{e1j} X_{Ej1}$, the boundary layer equations can be written as follows

$$\dot{X}_{Ej} = \begin{bmatrix} 0 & 0 \\ 0 & I \end{bmatrix} X_{Ej} + \begin{bmatrix} 0 \\ k_{e1j} X_{Ej1} + f_{e2j}(X_{Ej2}) \end{bmatrix}, \quad j \in \{1, \cdots, n-1\} \tag{5.68}$$

If the function $f_{e2j}(\cdot)$ satisfies

$$X_{Ej2}^T f_{e2j}(X_{Ej2}) \leq -a_{1j} X_{Ej2}^T X_{Ej2}, \quad \|f_{e2j}(X_{Ej2})\| \leq a_{1j}^{'} \|X_{Ej2}\| \tag{5.69}$$

using the Lyapunov function $V_{1j} = \frac{1}{2} X_{Ej}^T X_{Ej}$, we can show that $\dot{V}_{1j} \leq -\lambda_{min}(W_{1j}) V_{1j}$. For reduced system the following holds

$$\dot{V}_2 \leq \alpha_1 \|X_R\|^2, \quad \text{for} \quad \|X_{R2}\| \leq l_1^{'} \tag{5.70}$$

Checking the interconnection conditions, it is easy to drive the upperbound on ϵ.

Remark 5.4 Compared with the results of [50], The nonlinear functions $f_{e2j}(\cdot)$ provides extra freedom for control design of the fast and slow subsystems.

5.2.2 General Balanced Graph

In the previous section, we used the complete graph topology to design a two time scale control law for agents since the transformation (5.63), requires that the j^{th} agent gather

information from all agents which are existing in the network. In order to generalize the previous results to a larger class of communication graphs, first, we need to modify (5.63) to incorporate the structure of the communication graph of the network. This can be attained by using the following transformation from [47],[49]

$$w = \begin{bmatrix} R \\ E \end{bmatrix} = Ur, \quad U = \begin{bmatrix} \frac{\mathbf{1}_n^T \mathbf{M}}{\sum_{i=1}^{n} M_i} \\ L_g \ a_1 \end{bmatrix} \otimes I_3 \tag{5.71}$$

where L_g denotes the grounded Laplacian matrix of the network which can be obtained from

$$L = \begin{bmatrix} L_g & a_1 \\ a_2^T & a_3 \end{bmatrix} \tag{5.72}$$

It is possible to show that the rank of $L_{g1} = [L_g \ a_1]$ is equal to $n-1$, this can be seen from the following theorem.

Theorem 5.1 [86]: Suppose that $L_g \in \mathbb{R}^{(n-1)\times(n-1)}$ denotes the submatrix of the original Laplacian matrix of network which is obtained by deleting its i^{th} row and j^{th} column, then the number of spanning tree in the communication graph of the network is equal to $(-1)^{i+j} \det(L_g)$.

Since it is assumed that the communication graph of the network is connected, it has at least one spanning tree, hence, from Theorem 5.1 we can conclude that $\det(L_g) \neq 0$ and hence $[L_g \ a_1]$ is of full row rank. In addition, it is easy to show that $\mathbf{1}_n^T \mathbf{M}$ does not belong to the row space of $[L_g \ a_1]$ based on the fact the $L\mathbf{1}_n = \mathbf{0}$. This shows that the transformation U is not singular and has an inverse which can be computed based on the following lemma.

Lemma 5.1 [115] For any two matrices X_1, X_2 where $[X_1 \ X_2]$ is nonsingular and $X_1^T S X_2 =$

$X_1^T S^T X_2 = 0$ with $\det S \neq 0$, then the following holds

$$[X_1 \ X_2] \begin{bmatrix} (X_1^T S X_1)^{-1} X_1^T \\ (X_2^T S X_2)^{-1} X_2^T \end{bmatrix} S = I \tag{5.73}$$

hence, with $S = M^{-1}$ for (5.73) we can write

$$\begin{bmatrix} \frac{\mathbf{M1}_n}{\sum_{i=1}^n M_i} & L_{g1}^T \end{bmatrix} \begin{bmatrix} \left(\frac{\mathbf{1}_n^T \mathbf{M}}{\sum_{i=1}^n M_i} M^{-1} \frac{\mathbf{M1}_n}{\sum_{i=1}^n M_i}\right)^{-1} \left(\frac{\mathbf{1}_n^T \mathbf{M}}{\sum_{i=1}^n M_i}\right) M^{-1} \\ \left(L_{g1} M^{-1} L_{g1}^T\right)^{-1} L_{g1} M^{-1} \end{bmatrix} = I \tag{5.74}$$

which proves that the inverse of the transformation U can be expressed as follows

$$U^{-1} = \begin{bmatrix} \mathbf{1}_n & M^{-1} L_{g1}^T (L_{g1} M^{-1} L_{g1}^T)^{-1} \end{bmatrix} \otimes I_3 = \begin{bmatrix} \mathbf{1}_n & L_{g1}^+ \end{bmatrix} \otimes I_3 \tag{5.75}$$

Next, consider the following control laws for agents

$$f_i = -\frac{k_1}{\epsilon} \sum_{j \in N_i} \dot{x}_{ij} - \frac{k_2}{\epsilon^2} \sum_{j \in N_i} x_{ij} - \underbrace{(M_i(k_3(\dot{x}_i - \dot{R}_r) + k_4(x_i - R_r) - \ddot{R}_r) - K_1 C_i \dot{R}_r)}_{b_i} \tag{5.76}$$

using (5.76) as the control inputs of the agents, we have

$$(M \otimes I_3)\ddot{X} + \frac{k_1}{\epsilon}((L + C) \otimes I_3)\dot{X} + \frac{k_2}{\epsilon^2}(L \otimes I_3)X + B = 0 \tag{5.77}$$

Using the transformation $P = UX$, (5.77) turns into

$$(M \otimes I_3)U^{-1}\ddot{P} + \frac{k_1}{\epsilon}((L + C) \otimes I_3)U^{-1}\dot{P} + \frac{k_2}{\epsilon^2}(L \otimes I_3)U^{-1}P + B = 0 \tag{5.78}$$

post multiplying (5.78) by U^{-T} results in

$$\begin{aligned} &U^{-T}(M \otimes I_3)U^{-1}\ddot{P} + \frac{k_1}{\epsilon}U^{-T}((L + C) \otimes I_3)U^{-1}\dot{P} \\ &+ \frac{k_2}{\epsilon^2}U^{-T}(L \otimes I_3)U^{-1}P + U^{-T}B = 0 \end{aligned} \tag{5.79}$$

for $U^{-T}(M \otimes I_3)U^{-1}$ we can write

$$U^{-T}(M \otimes I_3)U^{-1} = \begin{bmatrix} \mathbf{1}_n^T \otimes I_3 \\ (L_{g1}^+)^T \otimes I_3 \end{bmatrix} (M \otimes I_3) \begin{bmatrix} \mathbf{1}_n & L_{g1}^+ \end{bmatrix}$$

$$= \begin{bmatrix} \mathbf{1}_n^T M \mathbf{1}_n & \mathbf{1}_n^T M L_{g1}^+ \\ (L_{g1}^+)^T M \mathbf{1}_n & (L_{g1}^+)^T M L_{g1}^+ \end{bmatrix} \otimes I_3 = \text{diag}(\sum_{i=1}^{n} M_i, (L_{g1}^+)^T M L_{g1}^+) \otimes I_3 \tag{5.80}$$

where we have used the fact that $\mathbf{1}_n^T M L_{g1}^+ = 0$. For $U^{-T}(L \otimes I_3)U^{-1}$, we have

$$U^{-T}(L \otimes I_3)U^{-1} = \begin{bmatrix} \mathbf{1}_n^T L \mathbf{1}_n & \mathbf{1}_n^T L L_{g1}^+ \\ (L_{g1}^+)^T L \mathbf{1}_n & (L_{g1}^+)^T L L_{g1}^+ \end{bmatrix} \otimes I_3 = \text{diag}(\mathbf{0}, (L_{g1}^+)^T M L_{g1}^+) \otimes I_3 \tag{5.81}$$

where the last line resulted from $L\mathbf{1}_n = \mathbf{1}_n^T L = \mathbf{0}$. For $U^{-T}(C \otimes I_3)U^{-1}$,

$$U^{-T}(C \otimes I_3)U^{-1} = \begin{bmatrix} \mathbf{1}_n^T C \mathbf{1}_n & \mathbf{1}_n^T C L_{g1}^+ \\ (L_{g1}^+)^T C \mathbf{1}_n & (L_{g1}^+)^T C L_{g1}^+ \end{bmatrix} \otimes I_3 \tag{5.82}$$

using (5.80)-(5.82), (5.79) becomes

$$\sum_{i=1}^{n} M_i \ddot{P}_1 + k_1(\mathbf{1}_n^T C \mathbf{1}_n)\dot{P}_1 + k_1[(\mathbf{1}_n^T C L_{g1}^+) \otimes I_3]\dot{P}_2 + (\mathbf{1}_n^T \otimes I_3)B = 0$$

$$\underbrace{[((L_{g1}^+)^T M L_{g1}^+) \otimes I_3]}_{M^+} \ddot{P}_2 + \frac{k_1}{\epsilon} \underbrace{[((L_{g1}^+)^T L L_{g1}^+) \otimes I_3]}_{L^+} \dot{P}_2 + \frac{k_2}{\epsilon^2} \underbrace{[((L_{g1}^+)^T L L_{g1}^+) \otimes I_3]}_{L^+} P_2$$

$$+ [(L_{g1}^+)^T \otimes I_3]B + k_1[((L_{g1}^+)^T C \mathbf{1}_n) \otimes I_3]\dot{P}_1 + k_1[((L_{g1}^+)^T C L_{g1}^+) \otimes I_3]\dot{P}_2 = 0$$

Also, we have

$$(\mathbf{1}_n^T \otimes I_3)B = \sum_{i=1}^{n} M_i(k_3(\dot{x}_i - \dot{R}_r) + k_4(x_i - R_r) - \ddot{R}_r) - K_1 C_i \dot{R}_r$$

$$= \left(\sum_{i=1}^{n} M_i\right)(k_3(\dot{P}_1 - \dot{R}_r) + k_4(P_1 - R_r)) - k_1(\mathbf{1}_n^T C \mathbf{1}_n)\dot{R}_r \tag{5.83}$$

and

$$
\begin{aligned}
&((L_{g1}^{+})^{T} \otimes I_3)B = [((L_{g1}M^{-1}L_{g1}^{T})^{-1}L_{g1}M^{-1}) \otimes I_3](M \otimes I_3)(k_3\dot{X} + k_4X) \\
&- k_1((L_{g1}^{+})^{T} \otimes I_3)(C \otimes I_3)(\mathbf{1}_n \otimes I_3)\dot{R}_r \\
&= ((L_{g1}M^{-1}L_{g1}^{T})^{-1} \otimes I_3)(L_{g1} \otimes I_3)(M^{-1} \otimes I_3)(M \otimes I_3)(k_3\dot{X} + k_4X) \\
&- k_1((L_{g1}^{+})^{T} \otimes I_3)(C \otimes I_3)(\mathbf{1}_n \otimes I_3)\dot{R}_r \\
&= \underbrace{((L_{g1}M^{-1}L_{g1}^{T})^{-1} \otimes I_3)}_{\alpha}(k_3\dot{P}_2 + k_4P_2) - k_1((L_{g1}^{+})^{T} \otimes I_3)(C \otimes I_3)(\mathbf{1}_n \otimes I_3)\dot{R}_r
\end{aligned} \tag{5.84}
$$

using (5.83) and (5.84), we have

$$
\begin{aligned}
&\left(\sum_{i=1}^{n} M_i\right)(\ddot{P}_1 - \ddot{R}_r) + \left(k_1(\mathbf{1}_n^{T}C\mathbf{1}_n) + k_3\sum_{i=1}^{n} M_i\right)(\dot{P}_1 - \dot{R}_r) \\
&+ \left(k_4\sum_{i=1}^{n} M_i\right)(P_1 - R_r) + k_1[(\mathbf{1}_n^{T}CL_{g1}^{+}) \otimes I_3]\dot{P}_2 = 0 \\
&M^{+}\ddot{P}_2 + \left(\frac{k_1}{\epsilon}L^{+} + k_3\alpha + k_1[((L_{g1}^{+})^{T}CL_{g1}^{+}) \otimes I_3]\right)\dot{P}_2 + \left(\frac{k_2}{\epsilon^2}L^{+} + k_4\alpha\right)P_2 \\
&+ k_1[((L_{g1}^{+})^{T}C\mathbf{1}_n) \otimes I_3]\dot{P}_1 - k_1((L_{g1}^{+})^{T} \otimes I_3)(C \otimes I_3)(\mathbf{1}_n \otimes I_3)\dot{R}_r = 0
\end{aligned} \tag{5.85}
$$

based on the following transformations

$$
\eta = \begin{bmatrix} P_1 - R_r \\ \dot{P}_1 - \dot{R}_r \end{bmatrix}, \quad \zeta = \begin{bmatrix} \frac{P_2}{\epsilon} \\ \dot{P}_2 \end{bmatrix} \tag{5.86}
$$

(5.85) turns into

$$\dot{\eta} = \begin{bmatrix} 0 & 1 \\ k_4 & k_3 + k_1 \left(\sum_{i=1}^{n} M_i\right)^{-1} (\mathbf{1}_n^T C \mathbf{1}_n) \end{bmatrix} \eta + \begin{bmatrix} 0 & 0 \\ 0 & k_1 \left(\sum_{i=1}^{n} M_i\right)^{-1} [(\mathbf{1}_n^T C L_{g1}^+) \otimes I_3] \end{bmatrix} \zeta$$

$$\dot{\zeta} = \begin{bmatrix} 0 & \frac{I}{\epsilon} \\ (M^+)^{-1} \left(\frac{k_2}{\epsilon} L^+ + \epsilon k_4 \alpha\right) & (M^+)^{-1} \left(\frac{k_1}{\epsilon} L^+ + k_3 \alpha + k_1 [((L_{g1}^+)^T C L_{g1}^+) \otimes I_3]\right) \end{bmatrix} \zeta$$

$$+ \begin{bmatrix} 0 & 0 \\ 0 & k_1 (M^+)^{-1} [((L_{g1}^+)^T C \mathbf{1}_n) \otimes I_3] \end{bmatrix} \eta \tag{5.87}$$

which can be rewritten as follows

$$\dot{\eta} = \begin{bmatrix} 0 & 1 \\ k_4 & k_3 + k_1 \left(\sum_{i=1}^{n} M_i\right)^{-1} (\mathbf{1}_n^T C \mathbf{1}_n) \end{bmatrix} \eta + \begin{bmatrix} 0 & 0 \\ 0 & k_1 \left(\sum_{i=1}^{n} M_i\right)^{-1} [(\mathbf{1}_n^T C L_{g1}^+) \otimes I_3] \end{bmatrix} \zeta$$

$$\epsilon \dot{\zeta} = \begin{bmatrix} 0 & I \\ (M^+)^{-1} k_2 L^+ & (M^+)^{-1} k_1 L^+ \end{bmatrix} \zeta +$$

$$\epsilon \left(\begin{bmatrix} 0 & 0 \\ (M^+)^{-1} (\epsilon k_4 \alpha) & (M^+)^{-1} \left(k_3 \alpha + k_1 [((L_{g1}^+)^T C L_{g1}^+) \otimes I_3]\right) \end{bmatrix} \zeta \right.$$

$$\left. + \begin{bmatrix} 0 & 0 \\ 0 & k_1 (M^+)^{-1} [((L_{g1}^+)^T C \mathbf{1}_n) \otimes I_3] \end{bmatrix} \eta \right) \tag{5.88}$$

From (5.88), it is clear that the boundary layer system can be written as follows

$$\dot{\zeta} = \begin{bmatrix} 0 & I \\ -(M^+)^{-1} k_2 L^+ & -(M^+)^{-1} k_1 L^+ \end{bmatrix} \zeta \tag{5.89}$$

to study the stability properties of (5.89), consider the following Lyapunov function

$$V_1 = \frac{1}{2} \zeta^T \begin{bmatrix} (k_2 + \delta k_1) \left(\frac{L^+ + (L^+)^T}{2}\right) & \delta M^+ \\ \delta M^+ & M^+ \end{bmatrix} \zeta \tag{5.90}$$

differentiating (5.90) with respect to time, we can prove the stability of the system.

5.3 Simulation Results

In this section, we present the simulation results of the control algorithm (5.76) for two different graph topologies. Fig. 5.2, shows the result for a network of six agents with diamond-shaped communication graph. The components of the initial positions of agents are chosen to be random numbers between $0 - 30m$ and the initial velocities are assumed to be zero. Also, for the control parameters, we have

$$k_1 = k_2 = 1, \quad \epsilon = 0.1 \quad k_3 = k_4 = 0.3$$

The desired relative offset between agents are chosen based on the following matrix

$$\begin{bmatrix} 1 & 5 & 5 & 1 & 3 & 3 \\ 1 & 1 & 5 & 5 & 3 & 3 \\ 3 & 3 & 3 & 3 & -2 & 8 \end{bmatrix}$$

Fig. 5.3 illustrates the results for a cubic-shaped communication graph where the offset matrix is chosen as follows

$$\begin{bmatrix} 1 & 5 & 5 & 1 & 5 & 5 & 1 & 1 \\ 1 & 1 & 5 & 5 & 1 & 5 & 5 & 1 \\ 3 & 3 & 3 & 3 & 7 & 7 & 7 & 7 \end{bmatrix}$$

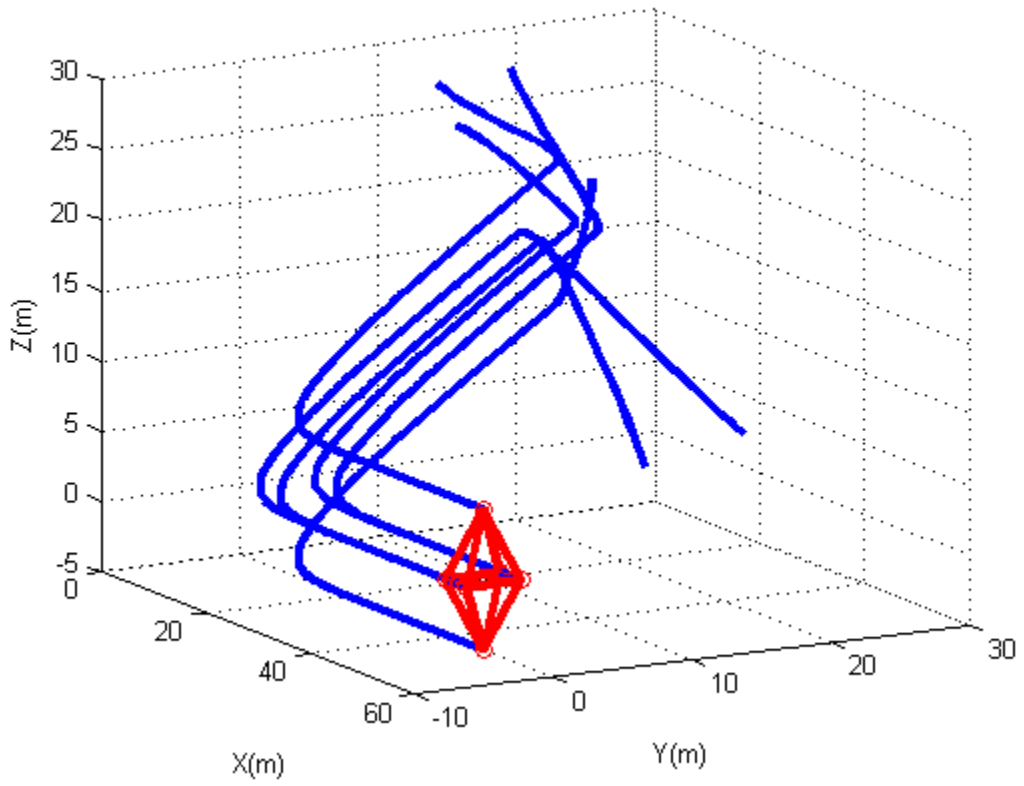

Figure 5.2: Diamond-shaped two time scaled formation control

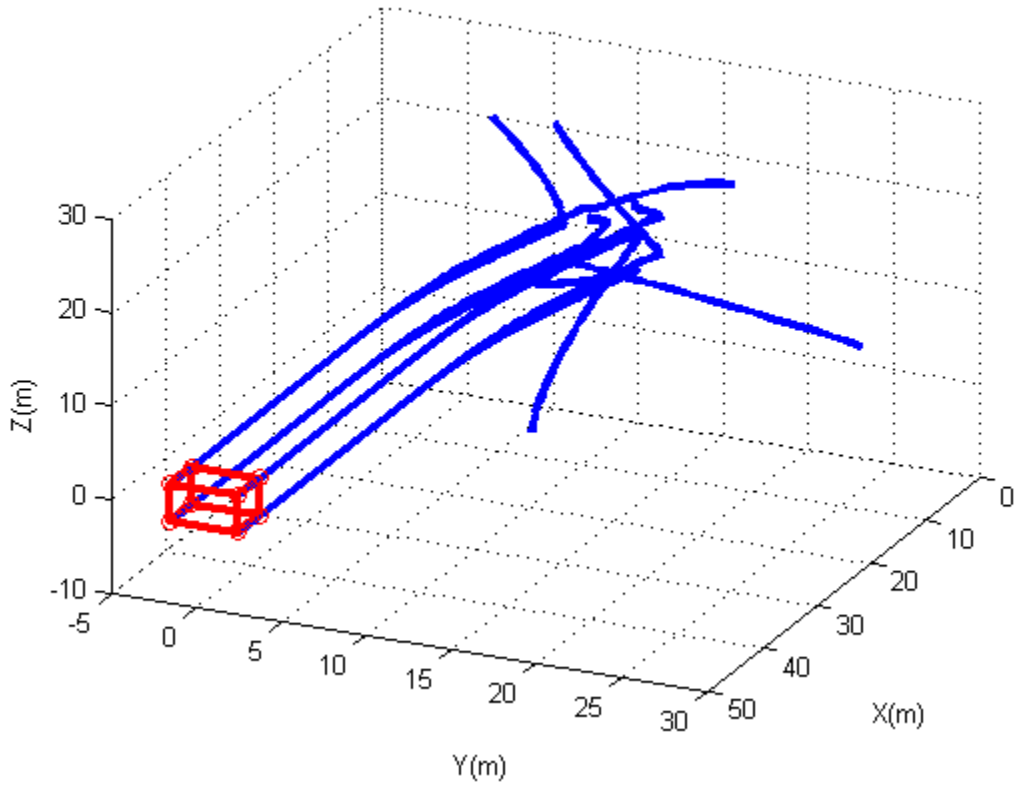

Figure 5.3: Cubic-shaped two time scaled formation control

5.4 Summary

In this chapter, we considered several robust control problems for multi agent system. In the first section , we consider the robust consensus problem in the presence of unknown Lipschitz nonlinearities and ploytopic uncertainties in the model of each agent. These types of uncertainties are ubiquitous in mechanical and electrical systems. For instance, many unmodeled dynamics satisfy the Lipschitz condition. Also, the lack of information regarding the agents parameters such as mass, inertia tensor, electrical properties, can be seen as polytopic uncertainties since in many practical situations an approximation of the convex sets containing these parameters are known apriori. In the next section, this problem is solved in the presence of external disturbances. A set of control laws is proposed for the network to attain the consensus task and under the zero initial condition, achieves the desired H_∞ performance. It is widely known that the exponential stability concept provides certain level of robustness for the systems. In the next part of this chapter, we designed distributed control laws to satisfy such a strong notion of stability. We showed that by implementing these control laws, it is possible to perform two time scales formation control.

Chapter 6

Conclusion and Future Directions

In this research, we studied multiple spatial formation control problems for a network of moving agents. Several distributed control and estimation laws are proposed to solve attitude synchronization, extremum seeking and formation tracking problems in the presence of modeling uncertainties and external disturbances. Based on these distributed robust algorithms, we study the convergence properties of the aforementioned tasks under the effects of local (e.g. inertia tensors) and global (e.g. location of the source) uncertainties. Here, we summarize the results of this work and propose some future research directions. Several distributed robust and adaptive control laws to solve the attitude synchronization problem have been proposed. The uncertainties which affect the agents are assumed to be local, and hence the robust adaptive laws are also designed locally based on the dynamical states of each agent and its respective neighbors. Since the uncertainties within the dynamics of each agent do not directly affect the neighbors, the adaptive estimation laws do not depend on the estimation states of the neighboring agents. We first considered the adaptive attitude synchronization for a network of rigid bodies and used a geometric

approach to solve the problem. Such an approach results in a coordinate independent control and estimation law which can be used in large rotational maneuvers to handle the singularities which are inherent in the attitude representation of a rigid agent. In the convergence analysis of the proposed method, we used the Frobenius norm as the measure of the error in estimation of the inertia matrices of the agents. Compared to the 2-norm of a matrix, the Frobenius norm has a greater value and hence, it leads to more conservative convergence results. However, working with such a norm is simpler in the context of Lyapunov analysis. The main strategy used for deriving the adaptive control and estimation laws is based on constructive control design methods. A single Lyapunov function is used for measuring the deviation of the network from the synchronized state and the estimation error. The distributed robust adaptive laws are then designed to make the time derivative of such a function negative semi definite. Later, we used an optimal norm on $SO(3)$ as an error function for measuring the attitude differences in the network. Our proposed control laws act as a set of virtual rotational spring and dampers between agents. In the next step, we solved the adaptive version of this problem. We further extended these results to robust adaptive control designs for situations where the network is subject to external disturbances and unmodeled dynamics, and for the cases where the inertia matrices are time varying and input dependent, using a modified projection method. Finally, we proved that based on this modified approach it is possible to increase the region of attraction of the tracking error subsystem. This indicates that compared to the previous methods, our proposed approach can fulfill the attitude tracking problem from a wide range of initial conditions.

Using similar adaptive approaches, we next studied the distributed localization problem for finding the extremum point of the unknown quadratic function which can be regarded as a local model for smooth and analytic convex cost functions. Compared to the atti-

tude synchronization problem, the uncertainties (location of the source) are assumed to be global and therefore the local adaptive estimation laws are designed based on the states of each agent and its neighbors' estimators. For solving this problem, it is assumed that the value of the cost function can be measured at each instant. Using high pass filtering of the measured signals, an identification model is obtained which is linear in unknown parameters (the coordinates of the extremum point). In the next step of the design procedure, we added a consensus term to modify the identification subsystem and proved the exponential convergence of the proposed estimation scheme. Such a term plays as a local averaging filter which mixes the information of each agent and its neighbors from the global unknown parameters.

We later used the localization results including a distributed identifiability condition for the extremum seeking problem. In extremum seeking problems, in addition to successful identification of the extremum location, it is required that the physical states of the seeking agents reach the extremum position. In order to solve this problem with a single agent, a dithering signal must be added to the dynamics of the agent to ensure the satisfaction of the persistency of excitation condition during the control period. Next, we extend this task to the case of a network of seeking agents. In particular, we showed that for a network of connected agents, if each agent contains a portion of the dithering signals, it is still possible to drive the system states to the extremum point, provided that the distributed identifiability condition is satisfied. For the distributed source seeking problem with a network of Dubin's vehicles with fixed forward velocities, we showed that it is feasible to steer the robots to the extremum point of a field in the presence of partial availability of the information about the field. In addition, the formation control problem is formulated as an extremum seeking task where the formation pattern corresponds to the extremum of formation costs. Defining as an extremum seeking problem, we also studied the motion

camouflage problem without explicit knowledge of agent positions. Two control algorithms were designed to solve this problem for the situations where the plan of the evader is not available to the chaser agent. The first approach has better performance compared to the second, however, it needs extra control effort.

Finally, we studied robust re-design of the proposed schemes assuming that the uncertainties belong to certain sets of convex polytopes. This additional information is exploited to obtain less conservative robust control laws. We considered the robust consensus problem in the presence of unknown Lipschitz nonlinearities and polytopic uncertainties in the model of each agent. Later, this problem is solved in the presence of external disturbances. A set of control laws is proposed for the network to attain the consensus task and under zero initial conditions, achieves the desired H_∞ performance.

The results of this research can be extended in the following directions.

1. For the attitude synchronization problem, we assumed that the network consists of rigid agents. One possible future direction is to consider this problem for a network of non-rigid agents. This situation can arise in the case of spacecraft with flexible or moving rigid appendages. For the case of spacecraft with flexible parts, the equations of motion can be derived as follows[116]

$$J_k\dot{\Omega}_k = -[\Omega_k]^\wedge J_k\Omega_k - [\Omega_k]^\wedge + \delta_k^T\dot{\eta}_k - \delta_k^T\ddot{\eta}_k + u_k \tag{6.1}$$

$$\ddot{\eta}_k + C_k\dot{\eta}_k + K_k\eta_k = \delta_k\dot{\Omega}_k \tag{6.2}$$

From (6.1) and (6.2), it is clear that the interconnection between the rigid body and the flexible appendages is modeled with the use of the coupling matrix δ_k for the k^{th} agent. η_k is the vector of modal coordinates for this agent. C_k and K_k denote the

damping and stiffness matrices, respectively. The first step of design can be carried out by modifying the control law (3.13) with the help of the Lyapunov function

$$V = \frac{-1}{2}\sum_{k=1}^{m}\sum_{j=1}^{m} a_{jk} tr\left(R_k^T R_j\right) + \sum_{k=1}^{m}\frac{1}{2d_k}\left\|J_k - \hat{J}_k\right\|_F^2 + \frac{l}{2}\sum_{k=1}^{m}\left(\Omega_k^r - F_k\right)^T J_k\left(\Omega_k^r - F_k\right) + \sum_{k=1}^{m}\left(\eta_k^T\eta_k + \dot{\eta}_k^T\dot{\eta}_k\right). \tag{6.3}$$

However, it should be noted that the estimation subsystem in this case will also contain the η_k terms and hence, they should be designed in a way to ensure the stability of the whole network dynamics. Another possible extension in this regard is to solve the attitude synchronization task with agents whose inertia tensors are time varying. In practice, this situation happens as the fuel is depleted. Furthermore, this problem can be solved in the presence of unknown elasticity coefficients such as Young modulus, structural damping ratio, etc.

2. A second potential research direction is to tackle the distributed extremum seeking problem, using receding horizon control methodology. This point of view can be used to design a distributed online optimization scheme which does not contain the dithering signals explicitly. The required level of excitation of the input signals can be satisfied by embedding the PE condition as an additional constraint for a model predictive control problem definition and thus the amount of agitation in the input terminals of agents can be reduced. More formally, we can represent the dynamics of the seeking agents by the following dynamics ($x_k^i \in \mathbb{R}^{n_1}, u_k^i \in \mathbb{R}^{n_2}, \theta \in \mathbb{R}^{n_3}$)

$$x_{k+1}^i = f(x_k^i, u_k^i(x_k^i - \hat{\theta}^i), \theta) \tag{6.4}$$

$$y_k^i = h(x_k^i, u_k^i, \theta), \quad i \in \{1, \cdots, n\} \tag{6.5}$$

where θ denotes the vectors of unknowns such as the coordinates of the extremum point and $\hat{\theta}^i$ is the estimation of the unknown parameters by the i^{th} agent. Next,

following the control sequence vector for the prediction horizon of length N as

$$\bar{u}_k^i = \left[u_k^{i,k^T}, u_{k+1}^{i,k\ T}, \cdots, u_{k+N-1}^{i,k\ T} \right]^T \tag{6.6}$$

the distributed model predictive control problem will be formulated as

$$\min_{\bar{u}^1,\cdots,\bar{u}^n} J(k, \bar{u}^1, \cdots, \bar{u}^n) = \sum_{i=1}^{n} \left(F(\hat{x}_{k+N}^i - \hat{\theta}_{k+N}^i) + \sum_{s=0}^{N-1} g(\hat{x}_{k+s}^i - \hat{\theta}_{k+s}^i, u_{k+s}^{i,k}) \right)$$

$$\text{subject to} \quad \hat{x}_{k+s+1}^i = f(\hat{x}_{k+s}^i, u_{k+s}^{i,k}, \hat{\theta}^i), \quad u_{k+s}^{i,k} \in \mathcal{U}$$

$$s = 0, \cdots, N-1, \quad i = 1, \cdots, n$$

$$\hat{x}_{k+s}^i \in \mathcal{X}, \quad s = 0 \cdots, N$$

$$\sum_{j\in\mathcal{N}_i} \sum_{s=0}^{N-1} \begin{bmatrix} u_{k-s}^j \\ u_{k-1-s}^j \\ \vdots \\ u_{k-N+1-s}^j \end{bmatrix} \begin{bmatrix} u_{k-s}^j \\ u_{k-1-s}^j \\ \vdots \\ u_{k-N+1-s}^j \end{bmatrix}^T > \alpha I, i \in \{1, \cdots, n\} \tag{6.7}$$

where $\mathcal{X}$ and $\mathcal{U}$ denote the set of allowable domains for states and input vectors. α represents the local level of satisfaction of the PE condition which must be attained by the agents in the network. Such a distributed optimization problem can be solved using methods which are introduced in [117]. Also, note that using the optimization framework for satisfaction of the PE condition, it is possible to choose time varying values for α which depend on the distance between the states of each agent and its neighbors with the location of the extremum point i.e. $\sum_{j\in\mathcal{N}_i} \left\| \hat{x}_k^i - \hat{\theta}_k^i \right\|$. This can significantly decrease the agitation in the inputs of the agents near the location of the extremum and therefore leads to a smoother approach towards the extremum seeking problem.

3. As another future research direction, the distributed localization problem can be analyzed further in the context of distributed optimization methods. In this regard,

it is feasible to use distributed total least squares (TLS) to find the location of the extremum. In TLS problems, it is assumed that both dependent and independent variables are subject to disturbances. For instance, in source seeking, it is common that in addition to the noise affecting the measurement of the field, the dynamics of each robot also are subject to the external disturbances from the environment, e.g. wind and friction. To model such a distributed optimization problem, we can start by considering the modified version of (4.7) as

$$Z_i + \delta Z_i = (\Phi_i + \delta\Phi_i)\,\Xi \tag{6.8}$$

where $Z_i + \delta Z_i$ corresponds to the vector of measurements which are available to the i^{th} agent through communication with its neighbors. The matrix $\Phi_i + \delta\Phi_i$ is constructed based on the states of the dynamics of each agent and its neighbors. The distributed localization problem can be formulated as follows

$$\begin{aligned} &\min_{\delta Z_1,\cdots,\delta Z_n,\delta\Phi_1,\cdots,\delta\Phi_n} \sum_{i=1}^{n} \|\delta\Phi_i\|_F^2 + \|\delta Z_i\|_2^2 \\ &\text{subject to } Z_i + \delta Z_i = (\Phi_i + \delta\Phi_i)\,\Xi,\ i = 1,\cdots,n \end{aligned} \tag{6.9}$$

where the Frobenius norm is used to measure the error in the matrix Φ_i. The solution to the program (6.9) can be obtained using Alternating Direction Methods of Multipliers [118].

4. In robust consensus design, we assumed that the polytopic uncertainties which affect the dynamics of each agent are time invariant. One possible extension is to consider a linear parameter varying model for the dynamics of the agents and find a set of consensus gains to ensure that the $\mathcal{L}_2$ gain of the network will remain below a pre-specified value. Furthermore, it is possible to add the effects of uncertainties in the communication graph of the network to the stability analysis. For instance, for the

case that the Laplacian matrix of the network belongs to a known polytope $\bar{L}$ and the agents' dynamics are as (5.1) with $B_1 = 0$ and $\omega = 0$, we can write

$$\dot{E} = (I_n \otimes A(\rho(t)) + k_2(L(\rho(t)) \otimes BK))E \tag{6.10}$$

The dynamics (6.10) is robustly stable if the time derivative of the Lyapunov function

$$V = E^T \left(I_n \otimes \left(\sum_{l=1}^{p} \rho_l P_l \right) \right) E = E^T \left(\sum_{l=1}^{p} \rho_l \underbrace{(I_n \otimes P_l)}_{P_l'} \right) E \tag{6.11}$$

is negative definite, i.e.

$$\begin{aligned} &(I_n \otimes A(\rho(t)) + k_2(L(\rho(t)) \otimes BK))^T \left(\sum_{l=1}^{p} \rho_l P_l' \right) \\ &+ \left(\sum_{l=1}^{p} \rho_l P_l' \right) (I_n \otimes A(\rho(t)) + k_2(L(\rho(t)) \otimes BK)) + \left(\sum_{l=1}^{p} \dot{\rho}_l P_l' \right) < 0 \end{aligned} \tag{6.12}$$

Unfortunately, (6.12) does not possess convexity and hence, by checking it at vertices of uncertainty polytopes we can not prove stability. One simple approach to address this problem is to use the method in [119] based on verifying the feasibility of the following conservative conditions for sufficiently large $a > 0$:

$$\begin{bmatrix} -X^T + X & P_i' + X^T(I_n \otimes A_l + k_2 L_l \otimes BK)) & X^T \\ \star & -aP_i' + \sum_{l=1}^{p} P_l' \theta_l & 0 \\ \star & \star & -a^{-1} P_i' \end{bmatrix} < 0, \ i = 1, \cdots, n \tag{6.13}$$

where θ_l denotes the vertices of the polytope which contain the time derivative of the parameters. The LMI conditions (6.13) must be solved for fixed $a > 0$ to find $X \in \mathbb{R}^{n \times n}$ and symmetric positive definite matrices P_l'. Also, the sum of squares techniques [120] can be used in this context for both the design and stability analysis.

References

[1] S.H. Dandach, B. Fidan, S. Dasgupta, B.D.O. Anderson. A continuous time linear adaptive source localization algorithm, robust to persistent drift. *Systems & Control Letters*, 58(1):7–16, 2009.

[2] E. Lavretsky. F/a-18 autonomous formation flight control system design. *AIAA paper*, 4757, 2002.

[3] W. Kang, H. Yeh. Co-ordinated attitude control of multi-satellite systems. *International Journal of Robust and Nonlinear control*, 12(2-3):185–205, 2002.

[4] H. Min, S. Wang, F. Sun, Z. Gao, J. Zhang. Decentralized adaptive attitude synchronization of spacecraft formation. *Systems & Control Letters*, 61(1):238–246, 2012.

[5] S. Nair, N.E. Leonard. Stable synchronization of rigid body networks. *Networks and Heterogeneous Media*, 2(4):597, 2007.

[6] I. Fadakar, B. Fidan, and J. Huissoon. Robust adaptive attitude synchronization of rigid body networks with unknown inertias. In *Proc. 9th Asian Control Conference*, pages 1–6, June 2013.

[7] I. Fadakar, B. Fidan, J. Huissoon. Robust adaptive attitude synchronisation of rigid body networks on SO(3). *IET Control Theory & Applications*, 9(1):52–61, 2014.

[8] C. Reynolds. Flocks, herds and schools: a distributed behavioral model. In *ACM Siggraph Computer Graphics*, volume 21, pages 25–34, 1987.

[9] T. Vicsek, A. Czirók, E. Ben-Jacob, I. Cohen, O. Shochet. Novel type of phase transition in a system of self-driven particles. *Phys. Rev. Lett.*, 75:1226–1229, Aug 1995.

[10] D. Helbing, I. Farkas, T. Vicsek. Simulating dynamical features of escape panic. *Nature*, 407(6803):487–490, 2000.

[11] R. Olfati-Saber. Flocking for multi-agent dynamic systems: algorithms and theory. *IEEE Transactions on Automatic Control*, 51(3):401–420, 2006.

[12] R. Olfati-Saber, R.M. Murray. Consensus problems in networks of agents with switching topology and time-delays. *IEEE Transactions on Automatic Control*, 49(9):1520–1533, Sept 2004.

[13] R.A. Horn, C.R. Johnson. *Matrix Analysis*. Cambridge University Press, 2012.

[14] L. Xiao, S. Boyd. Fast linear iterations for distributed averaging. *Systems and Control Letters*, 53(1):65 – 78, 2004.

[15] Y. Kim, M. Mesbahi. On maximizing the second smallest eigenvalue of a state-dependent graph laplacian. *IEEE Transactions on Automatic Control*, 51(1):116–120, Jan 2006.

[16] W. Ren, R.W. Beard. Consensus seeking in multiagent systems under dynamically changing interaction topologies. *IEEE Transactions on Automatic Control*, 50(5):655–661, May 2005.

[17] Y. Hatano, M. Mesbahi. Agreement over random networks. *IEEE Transactions on Automatic Control*, 50(11):1867–1872, Nov 2005.

[18] P.R. Kumar, P. Varaiya. *Stochastic Systems: Estimation, Identification and Adaptive Control*. Prentice-Hall, Inc., Upper Saddle River, NJ, USA, 1986.

[19] R. Olfati-Saber. Ultrafast consensus in small-world networks. In *Proc. American Control Conference*, pages 2371–2378, 2005.

[20] F. Borrelli, T. Keviczky. Distributed LQR design for identical dynamically decoupled systems. *IEEE Transactions on Automatic Control*, 53(8):1901–1912, Sept 2008.

[21] Y. Cao, W. Ren. Optimal linear-consensus algorithms: an lqr perspective. *IEEE Transactions on Systems, Man, and Cybernetics, Part B: Cybernetics*, 40(3):819–830, June 2010.

[22] W.B. Dunbar, R.M. Murray. Distributed receding horizon control for multi-vehicle formation stabilization. *Automatica*, 42(4):549 – 558, 2006.

[23] E. Semsar-Kazerooni, K. Khorasani. Optimal consensus algorithms for cooperative team of agents subject to partial information. *Automatica*, 44(11):2766 – 2777, 2008.

[24] E. Semsar-Kazerooni, K. Khorasani. Multi-agent team cooperation: a game theory approach. *Automatica*, 45(10):2205 – 2213, 2009.

[25] H. Li, W. Yan. Receding horizon control based consensus scheme in general linear multi-agent systems. *Automatica*, 56(C):12–18, June 2015.

[26] K.H. Movric, F.L. Lewis. Cooperative optimal control for multi-agent systems on directed graph topologies. *IEEE Transactions on Automatic Control*, 59(3):769–774, March 2014.

[27] A. Nedic, A. Ozdaglar, P.A. Parrilo. Constrained consensus and optimization in multi-agent networks. *IEEE Transactions on Automatic Control*, 55(4):922–938, April 2010.

[28] H.G. Tanner. On the controllability of nearest neighbor interconnections. In *Proc. IEEE Conference on Decision and Control*, volume 3, pages 2467–2472, Dec 2004.

[29] A. Rahmani, M. Ji, M. Mesbahi, M. Egerstedt. Controllability of multi-agent systems from a graph-theoretic perspective. *SIAM Journal on Control and Optimization*, 48(1):162–186, 2009.

[30] R. Olfati-Saber, R.M. Murray. Distributed cooperative control of multiple vehicle formations using structural potential functions. In *Proc. IFAC World Congress*, pages 346–352, 2002.

[31] A. Jadbabaie, J. Lin. Coordination of groups of mobile autonomous agents using nearest neighbor rules. *IEEE Transactions on Automatic Control*, 48(6):988–1001, 2003.

[32] J.A Fax, R.M. Murray. Information flow and cooperative control of vehicle formations. *IEEE Transactions on Automatic Control*, 49(9):1465–1476, 2004.

[33] H.G. Tanner, G. Pappas, V. Kumar. Leader-to-formation stability. *IEEE Transactions on Robotics and Automation*, 20(3):443–455, 2004.

[34] H.K. Khalil. *Nonlinear Systems*. Prentice Hall New Jersey, 2002.

[35] J.P. Ostrowski, J. Spletzer, C.J. Taylor A.K. Das, A. Fierro, V. Kumar. A vision-based formation control framework. *IEEE Transactions on Robotics and Automation*, 18(5):813–825, 2002.

[36] N.E. Leonard, E. Fiorelli. Virtual leaders, artificial potentials and coordinated control of groups. In *Proc. IEEE Conference on Decision and Control*, volume 3, pages 2968–2973 vol.3, 2001.

[37] R. Olfati-Saber, P. Jalalkamali. Coupled distributed estimation and control for mobile sensor networks. *IEEE Transactions on Automatic Control*, 57(10):2609–2614, 2012.

[38] E.W. Justh, P.S. Krishnaprasad. Equilibria and steering laws for planar formations. *Systems and Control Letters*, 52(1):25 – 38, 2004.

[39] J. Marshall, M.E. Broucke, B. Francis. Formations of vehicles in cyclic pursuit. *IEEE Transactions on Automatic Control*, 49(11):1963–1974, 2004.

[40] Z. Lin, B. Francis, M. Maggiore. Necessary and sufficient graphical conditions for formation control of unicycles. *IEEE Transactions on Automatic Control*, 50(1):121–127, 2005.

[41] D.V. Dimarogonas, K.J. Kyriakopoulos. On the rendezvous problem for multiple nonholonomic agents. *IEEE Transactions on Automatic Control*, 52(5):916–922, May 2007.

[42] R.L. Raffard, C.J.Tomlin, S. Boyd. Distributed optimization for cooperative agents: application to formation flight. In *Proc. IEEE Conference on Decision and Control*, volume 3, pages 2453–2459 Vol.3, Dec 2004.

[43] J.H. Hours, C.N. Jones. A parametric non-convex decomposition algorithm for real-time and distributed NMPC. *IEEE Transactions on Automatic Control*, PP(99):1–1, 2015.

[44] D. Morgan, S.J. Chung, F.Y. Hadaegh. Model predictive control of swarms of spacecraft using sequential convex programming. *AIAA Journal of Guidance, Control, and Dynamics*, 37(6):1725–1740, 2014.

[45] J. Qi, R. Vazquez, M. Krstic. Multi-agent deployment in 3-D via PDE control. *IEEE Transactions on Automatic Control*, 60(4):891–906, April 2015.

[46] X. Cai, M. De Queiroz. Multi-agent formation maintenance and target tracking. In *Proc. American Control Conference*, pages 2521–2526, 2013.

[47] D. Lee, P.Y. Li. Passive decomposition approach to formation and maneuver control of multiple rigid bodies. *ASME Journal of Dynamic Systems, Measurement, and Control*, 129(5):662–677, 2007.

[48] D. Lee, M.W. Spong. Stable flocking of multiple inertial agents on balanced graphs. *IEEE Transactions on Automatic Control*, 52(8):1469–1475, 2007.

[49] D. Lee. Distributed backstepping control of multiple thrust-propelled vehicles on a balanced graph. *Automatica*, 48(11):2971–2977, 2012.

[50] S. Mastellone, J.S. Meja, D.M. Stipanovic, M.W. Spong. Formation control and coordinated tracking via asymptotic decoupling for lagrangian multi-agent systems. *Automatica*, 47(11):2355 – 2363, 2011.

[51] D.M. Stipanović, P.F. Hokayem, M.W. Spong, D. Šiljak. Cooperative avoidance control for multiagent systems. *ASME Journal of Dynamic Systems, Measurement, and Control*, 129(5):699–707, 2007.

[52] J. Cortés. Global and robust formation-shape stabilization of relative sensing networks. *Automatica*, 45(12):2754–2762, 2009.

[53] S. Hosseini, A. Chapman, M. Mesbahi. Online distributed optimization on dynamic networks. *arXiv preprint arXiv:1412.7215*, 2014.

[54] J. Cortes, S. Martinez, T. Karatas, F. Bullo. Coverage control for mobile sensing networks. In *Proc. IEEE International Conference on Robotics and Automation*, volume 2, pages 1327–1332, 2002.

[55] J. Cortés. Coverage optimization and spatial load balancing by robotic sensor networks. *IEEE Transactions on Automatic Control*, 55(3):749–754, 2010.

[56] V.M. Guibout, D.J. Scheeres. Spacecraft formation dynamics and design. *AIAA Journal of Guidance, Control, and Dynamics*, 29(1):121–133, 2006.

[57] H.J. Pernicka, B.A. Carlson, S.N. Balakrishnan. Spacecraft formation flight about libration points using impulsive maneuvering. *AIAA Journal of Guidance, Control, and Dynamics*, 29(5):1122–1130, 2006.

[58] M. Bando, A. Ichikawa. Active formation flying along an elliptic orbit. *AIAA Journal of Guidance, Control, and Dynamics*, 36(1):324–332, 2012.

[59] D. Morgan, S.J. Chung, L. Blackmore, B. Acikmese, D. Bayard, F.Y. Hadaegh. Swarm-keeping strategies for spacecraft under J2 and atmospheric drag perturbations. *AIAA Journal of Guidance, Control, and Dynamics*, 35(5):1492–1506, 2012.

[60] M. Krstić, H. Wang. Stability of extremum seeking feedback for general nonlinear dynamic systems. *Automatica*, 36(4):595–601, 2000.

[61] D. Nešić, Y. Tan, W.H. Moase, C. Manzie. A unifying approach to extremum seeking: Adaptive schemes based on estimation of derivatives. In *Proc. IEEE Conference on Decision and Control*, pages 4625–4630. IEEE, 2010.

[62] A. Ghaffari, M. Krstić, D. Nešić. Multivariable newton-based extremum seeking. *Automatica*, 48(8):1759–1767, 2012.

[63] S.J. Liu, M. Krstic. Newton-based stochastic extremum seeking. *Automatica*, 50(3):952–961, 2014.

[64] Y. Tan, D. Nešić, I. Mareels. On the choice of dither in extremum seeking systems: a case study. *Automatica*, 44(5):1446–1450, 2008.

[65] J. Cochran, M. Krstic. Nonholonomic source seeking with tuning of angular velocity. *IEEE Transactions on Automatic Control*, 54(4):717–731, 2009.

[66] J. Cochran, A. Siranosian, N. Ghods, M. Krstic. 3-D source seeking for underactuated vehicles without position measurement. *IEEE Transactions on Robotics*, 25(1):117–129, 2009.

[67] N. Ghods, M. Krstic. Multiagent deployment over a source. *IEEE Transactions on Control Systems Technology*, 20(1):277–285, 2012.

[68] M.S. Stankovic, K.H. Johansson, D.M. Stipanovic. Distributed seeking of nash equilibria in mobile sensor networks. In *Proc. IEEE Conference on Decision and Control*, pages 5598–5603, Dec 2010.

[69] J. Choi, O. Songhwai, R. Horowitz. Distributed learning and cooperative control for multi-agent systems. *Automatica*, 45(12):2802 – 2814, 2009.

[70] V. Ugrinovskii. Conditions for detectability in distributed consensus-based observer networks. In *Proc. IEEE Conference on Decision and Control*, pages 4171–4174, Dec 2012.

[71] V. Ugrinovskii. Distributed robust filtering with consensus of estimates. *Automatica*, 47(1):1 – 13, 2011.

[72] R. Olfati-Saber. Distributed kalman filtering for sensor networks. In *Proc. IEEE Conference on Decision and Control*, pages 5492–5498, 2007.

[73] I. Papusha, E. Lavretsky, R.M. Murray. Collaborative system identification via parameter consensus. In *Proc. American Control Conference*, pages 13–19, June 2014.

[74] J. Wen, K. Kreutz-Delgado. The attitude control problem. *IEEE Transactions on Automatic Control*, 36(10):1148–1162, 1991.

[75] J.B. Aldrich. Attitude control with analytic disturbance-rejection guarantee. *AIAA Journal of Guidance, Control, and Dynamics*, 37(6):1791–1807, 2014.

[76] C.G. Mayhew, R.G. Sanfelice, A.R. Teel. quaternion-based hybrid control for robust global attitude tracking. *IEEE Transactions on Automatic Control*, 56(11):2555–2566, Nov 2011.

[77] S. Bertrand, N. Gunard, T. Hamel, H. Piet-Lahanier, L. Eck. A hierarchical controller for miniature vtol uavs: Design and stability analysis using singular perturbation theory. *Control Engineering Practice*, 19(10):1099 – 1108, 2011.

[78] P. Pounds, R. Mahony, P. Corke. Modelling and control of a quad-rotor robot. In *Proc. Australasian Conference on Robotics and Automation 2006*. Australian Robotics and Automation Association Inc., 2006.

[79] T.J. Koo, S. Sastry. Output tracking control design of a helicopter model based on approximate linearization. In *Proc. IEEE Conference on Decision and Control*, volume 4, pages 3635–3640, 1998.

[80] R. Mahony, T. Hamel. Robust trajectory tracking for a scale model autonomous helicopter. *International Journal of Robust and Nonlinear Control*, 14(12):1035–1059, 2004.

[81] A. Abdessameud, A. Tayebi. Global trajectory tracking control of vtol-uavs without linear velocity measurements. *Automatica*, 46(6):1053–1059, 2010.

[82] A. Abdessameud, A. Tayebi. Formation control of VTOL UAVs. In *Motion Coordination for VTOL Unmanned Aerial Vehicles*, pages 105–127. Springer, 2013.

[83] A. Sarlette, R. Sepulchre, N.E. Leonard. Autonomous rigid body attitude synchronization. *Automatica*, 45(2):572–577, 2009.

[84] T. Lee. Exponential stability of an attitude tracking control system on SO(3) for large-angle rotational maneuvers. *Systems & Control Letters*, 61(1):231–237, 2012.

[85] Z. Li, X. Liu, M. Fu, L. Xie. Global H_∞ consensus of multi-agent systems with lipschitz non-linear dynamics. *IET Control Theory Applications*, 6(13):2041–2048, September 2012.

[86] C. Godsil, G.F. Royle. *Algebraic Graph Theory*. Springer, 2013.

[87] A. Sarlette. *Geometry and Symmetries in Coordination Control*. PhD Thesis, 2009.

[88] N. Fischer, R. Kamalapurkar, W.E. Dixon. Lasalle-yoshizawa corollaries for nonsmooth systems. *IEEE Transactions on Automatic Control*, 9(58):2333–2338, 2013.

[89] A. Sarlette, R. Sepulchre. Consensus optimization on manifolds. *SIAM Journal on Control and Optimization*, 48(1):56–76, 2009.

[90] J. Cortés. Finite-time convergent gradient flows with applications to network consensus. *Automatica*, 42(11):1993–2000, 2006.

[91] P.A. Ioannou, J. Sun. *Robust Adaptive Control*. Prentice Hall, 1996.

[92] T. Fernando, J. Chandiramani, T. Lee, H. Gutierrez. Robust adaptive geometric tracking controls on SO(3) with an application to the attitude dynamics of a quadrotor UAV. In *Proc. IEEE Conference on Decision and Control*, pages 7380–7385, 2011.

[93] A. Saccon, J. Hauser, A.P. Aguiar. Exploration of kinematic optimal control on the lie group SO(3). In *Proc. Eighth IFAC Symp. on Nonlinear Control Systems, Bologna, Italy*, pages 1302–1307, 2010.

[94] S.Y. Chang, C.R. Carlson, J.C. Gerdes. A Lyapunov function approach to energy based model reduction. In *Proc. ASME Dynamics Systems and Control Divison*, 2001.

[95] R. Olfati Saber, R.M. Murray. Consensus protocols for networks of dynamic agents. In *Proc. American Control Conference*, 2003.

[96] C.G. Mayhew, R.G. Sanfelice, J. Sheng, M. Arcak, A.R. Teel. Quaternion-based hybrid feedback for robust global attitude synchronization. *IEEE Transactions on Automatic Control*, 57(8):2122–2127, 2012.

[97] B. Wu, D. Wang, E.K. Poh. Decentralized sliding-mode control for attitude synchronization in spacecraft formation. *International Journal of Robust and Nonlinear Control*, 23(11):1183–1197, 2013.

[98] M. Krstic, P.V. Kokotovic, I. Kanellakopoulos. *Nonlinear and Adaptive Control Design*. John Wiley & Sons, Inc., 1995.

[99] D. Thakur, S. Srikant, M.R. Akella. Adaptive attitude-tracking control of spacecraft with uncertain time-varying inertia parameters. *AIAA Journal of Guidance, Control, and Dynamics*, 38(1):41–52, 2014.

[100] F. Bullo, R. Murray. Tracking for fully actuated mechanical systems: a geometric framework. *Automatica*, 35(1):17–34, 1999.

[101] F. Bullo. *Geometric Control of Mechanical Systems*, volume 49. Springer, 2005.

[102] T. Mori. Comments on" a matrix inequality associated with bounds on solutions of algebraic riccati and lyapunov equation" by J. Saniuk and I. Rhodes. *IEEE Transactions on Automatic Control*, 33(11):1088, 1988.

[103] T. Lee. Robust adaptive attitude tracking on SO(3) with an application to a quadrotor uav. *IEEE Transactions on Control Systems Technology*, 21(5):1924–1930, 2013.

[104] Y. Fang, K. Loparo, X. Feng. Inequalities for the trace of matrix product. *IEEE Transactions on Automatic Control*, 39(12):2489–2490, 1994.

[105] G. Chowdhary, E. Johnson. Concurrent learning for convergence in adaptive control without persistency of excitation. In *Proc. IEEE Conference on Decision and Control*, pages 3674–3679. IEEE, 2010.

[106] R.A. Freeman, P. Yang, K. Lynch. Stability and convergence properties of dynamic average consensus estimators. In *Proc. IEEE Conference on Decision and Control*, pages 398–403, 2006.

[107] S. Kia, J. Cortés, S. Martínez. Singularly perturbed algorithms for dynamic average consensus. In *Proc. European Control Conference*, pages 1758–1763, 2013.

[108] P. Frihauf, S. J. Liu, M. Krstic. A single forward-velocity control signal for stochastic source seeking with multiple nonholonomic vehicles. *ASME Journal of Dynamic Systems, Measurement, and Control*, 136(5):051024, 2014.

[109] E.W. Justh, P.S. Krishnaprasad. Steering laws for motion camouflage. In *Proceedings of the Royal Society of London A: Mathematical, Physical and Engineering Sciences*, volume 462, pages 3629–3643. The Royal Society, 2006.

[110] P. V. Reddy, E. W. Justh, P. S. Krishnaprasad. Motion camouflage in three dimensions. In *Proc. IEEE Conference on Decision and Control*, pages 3327–3332, 2006.

[111] M.V. Srinivasan, M. Davey. Strategies for active camouflage of motion. *Proceedings of the Royal Society of London B: Biological Sciences*, 259(1354):19–25, 1995.

[112] T.S. Collett, M.F. Land. Visual control of flight behaviour in the hoverfly, syritta pipiens l. *Journal of Comparative Physiology*, 99(1):1–66, 1975.

[113] Z. Li, Z. Duan, G. Chen. On H_∞ and H_2 performance regions of multi-agent systems. *Automatica*, 47(4):797–803, 2011.

[114] U. Shaked. Improved lmi representations for the analysis and the design of continuous-time systems with polytopic type uncertainty. *IEEE Transactions on Automatic Control*, 46(4):652–656, 2001.

[115] S. Banerjee, A. Roy. *Linear Algebra and Matrix Analysis for Statistics*. CRC Press, 2014.

[116] S.D. Gennaro. Output stabilization of flexible spacecraft with active vibration suppression. *IEEE Transactions on Aerospace and Electronic Systems*, 39(3):747–759, 2003.

[117] S. Boyd, N. Parikh, E. Chu, B. Peleato, J. Eckstein. Distributed optimization and statistical learning via the alternating direction method of multipliers. *Foundations and Trends in Machine Learning*, 3(1):1–122, 2011.

[118] A. Bertrand, M. Moonen. Low-complexity distributed total least squares estimation in ad hoc sensor networks. *IEEE Transactions on Signal Processing*, 60(8):4321–4333, 2012.

[119] C. Briat. *Linear Parameter-varying and Time-delay Systems*. Springer, 2014.

[120] P.A. Parrilo S. Prajna, A. Papachristodoulou, P. Seiler. Sum of squares optimization toolbox for matlab users guide, 2004.

[121] N. Lynch. *Distributed Algorithms*. Morgan Kaufmann Publishers Inc., San Francisco, CA, USA, 1996.

[122] R.M. Murray, Z. Li, S.S. Sastry. *A Mathematical Introduction to Robotic Manipulation*. CRC press, 1994.

[123] H. Goldstein. *Classical Mechanics*. Pearson Education, 1965.

[124] E. Lavretsky, T. E. Gibson, A. M. Annaswamy. Projection operator in adaptive systems. *ArXiv preprint arXiv:1112.4232*, 2011.

[125] B. Wie. *Space Vehicle Dynamics and Control*. AIAA, 1998.

[126] R. Brockett. The early days of geometric nonlinear control. *Automatica*, 50(9):2203–2224, 2014.

[127] J. Wen, K.D. Kenneth. The attitude control problem. *IEEE Transactions on Automatic Control*, 36(10):1148–1162, 1991.

[128] S.P. Bhat, D.S. Bernstein. A topological obstruction to continuous global stabilization of rotational motion and the unwinding phenomenon. *Systems & Control Letters*, 39(1):63–70, 2000.

[129] T. Lee. Robust global exponential attitude tracking controls on SO(3). In *Proc. American Control Conference*, pages 2103–2108, 2013.

[130] A. Van der Schaft. *L2-gain and Passivity Techniques in Nonlinear Control*. Springer, 2012.

[131] O. Egeland, J.M. Godhavn. Passivity-based adaptive attitude control of a rigid spacecraft. *IEEE Transactions on Automatic Control*, 39(4):842–846, 1994.

[132] W. Luo, Y.C. Chu, K.V. Ling. Inverse optimal adaptive control for attitude tracking of spacecraft. *IEEE Transactions on Automatic Control*, 50(11):1639–1654, 2005.

[133] M. Krstic, J.W. Modestino, H. Deng, A. Fettweis, J.L. Massey, M. Thoma, E.D. Sontag, B.W. Dickinson. *Stabilization of Nonlinear Uncertain Systems*. Springer-Verlag New York, Inc., 1998.

[134] P. Pisu, A. Serrani. Attitude tracking with adaptive rejection of rate gyro disturbances. In *Proc. American Control Conference*, pages 4839–4844, 2008.

[135] Z. Chen, J. Huang. Attitude tracking and disturbance rejection of rigid spacecraft by adaptive control. *IEEE Transactions on Automatic Control*, 54(3):600–605, 2009.

[136] J. Ahmed, V.T. Coppola, D.S. Bernstein. Adaptive asymptotic tracking of spacecraft attitude motion with inertia matrix identification. *AIAA Journal of Guidance, Control, and Dynamics*, 21(5):684–691, 1998.

[137] T. Yucelen, A.J. Calise. Robustness of a derivative-free adaptive control law. *AIAA Journal of Guidance, Control, and Dynamics*, 37(5):1583–1594, 2014.

[138] H. Yoon, P. Tsiotras. Adaptive spacecraft attitude tracking control with actuator uncertainties. *The Journal of the Astronautical Sciences*, 56(2):251–268, 2008.